SOME ASPECTS OF THE DISTRIBUTION AND FATE OF POLYCYCLIC AROMATIC HYDROCARBON CONTAMINATION IN THE KITIMAT FJORD SYSTEM

by

CHRISTOPHER DAVID SIMPSON

B.Sc., University of Waikato, New Zealand, 1990

M.Sc. (Hons.), University of Waikato, New Zealand, 1992

A THESIS SUBMITTED IN PARTIAL FULFILLMENT OF

THE REQUIREMENTS FOR THE DEGREE OF

DOCTOR OF PHILOSOPHY

in

THE FACULTY OF GRADUATE STUDIES

(Department of Chemistry)

We accept this thesis as conforming to the required standard

THE UNIVERSITY OF BRITISH COLUMBIA

September 1997

In presenting this thesis in partial fulfilment of the requirements for an advanced degree at the University of British Columbia, I agree that the Library shall make it freely available for reference and study. I further agree that permission for extensive copying of this thesis for scholarly purposes may be granted by the head of my department or by his or her representatives. It is understood that copying or publication of this thesis for financial gain shall not be allowed without my written permission.

Department of CHEMISTRY

The University of British Columbia
Vancouver, Canada

Date 14 - October - 1997

DE-6 (2/88)

Abstract

The presence of polycyclic aromatic hydrocarbons (PAHs) in the environment is of concern because many PAHs are carcinogens, and PAHs are very persistent. In this thesis the distribution of PAHs has been investigated in the Kitimat fjord system, British Columbia, Canada. Total PAHs in the range 1-500 mg/kg were detected in sediments from the fjord system. Sediments with the highest PAH levels were collected from sites in close proximity to the aluminum smelter, and PAH levels in sediments declined with increasing distance from the smelter. The PAH composition in all samples was typical of combustion generated PAH mixtures.

PAH composition and distribution as a function of sediment particle size was investigated. Sediments from two sites close to the aluminum smelter (CD2, CD3) showed a differential distribution of PAHs amongst various sediment particle size fractions (PSFs). At all other sites PAHs were uniformly distributed amongst the various sediment PSFs. At one site (CD3), the distribution of perylene and retene amongst PSFs was different from the distribution of the other PAHs examined.

Total PAH levels were elevated in the upper sections of a sediment core, but declined to constant low levels (~30 ng/g) in the lower sections of the sediment core. The PAH composition in the upper part of the core was typical of combustion generated PAH mixtures. In contrast, perylene accounted for ~70-80% of total (unsubstituted) PAHs in sections from the lower part of the core, pre-dating the operation of the aluminum smelter.

The accumulation of PAHs by soft-shelled clams (*Mya arenaria*) collected from four beaches in the Kitimat fjord system was investigated. PAHs were detected in clams (0.8-5.7 mg/kg) and

sediments (0.02-125 mg/kg) from all four beaches. The PAH composition was similar in both clams and sediments at each site. Biota-sediment accumulation factors (BSAFs) at Hospital Beach were significantly lower than predicted by the equilibrium partitioning (EP) theory, but BSAFs at the other three sites were within an order of magnitude of the EP predictions.

Metabolism of pyrene and 1-hydroxypyrene by two species of bivalve mollusk, *Mya arenaria* and *Protothaca staminea* was studied under laboratory conditions. The metabolites identified included an hydroxypyrene isomer, pyrene-1-sulfate, and a sulfate conjugate of dihydroxypyrene. The metabolites formed indicate that the metabolic pathways used by the two mollusk species to metabolize pyrene are similar to the pathways vertebrates use to metabolize PAHs.

Table of Contents

List of Tables

List of Figures

List of Abbreviations

AHD	alkyl homologue distribution
BCF	bioconcentration factor
BCMOE	British Columbia Ministry of the Environment
BSAF	biota-sediment accumulation factor
CCME	Canadian Council of Ministers of the Environment
C_B	concentration of contaminant in biota
CE	capillary electrophoresis
CEPA	Canadian Environmental Protection Act
CI-MS	chemical ionization-mass spectrometry
C_S	concentration of contaminant in sediment
C_W	concentration of contaminant in water
DOM	dissolved organic matter
EP	equilibrium partition
ER-L	effects range-low
ER-M	effects range-median
ESI-MS	electrospray ionization-mass spectrometry
FA	factor analysis
FID	flame ionization detector
f_L	weight of lipid as fraction of total dry weight of an organism
f_{OC}	weight of organic carbon as fraction of total dry weight of sediment
f_{SC}	weight of soot carbon as fraction of total dry weight of sediment
GC	gas chromatograph(y)
GC-MS	gas chromatography-mass spectrometry
HOC(s)	hydrophobic organic compound(s)
HPAH	high molecular weight PAHs (MW ≥202)
HPLC	high pressure liquid chromatography
K_{OC}	organic-carbon-normalized sediment-water partition coefficient
K_{OW}	octanol-water partition coefficient
K_{SC}	soot-carbon-normalized sediment-water partition coefficient
LPAH	low molecular weight PAHs (MW <202)

MFO	mixed function oxidase
MS	mass spectrometry
MW	molecular weight
PAC(s)	polycyclic aromatic compound(s), or polynuclear aromatic compound(s)
PAD	photo-diode array detector
PAH(s)	polycyclic aromatic hydrocarbon(s)
PCA	principal components analysis
PCB(s)	polychlorinated biphenyl(s)
PCDDs	polychlorinated dibenzodioxins
PCDFs	polychlorinated dibenzofurans
PNAs	polynuclear aromatics
QSTD	Quantitation standard
RSTD	Recovery standard
SEC	size exclusion chromatography
SFE	supercritical fluid extraction
SPE	solid phase extraction
SPMD	semi permeable membrane device
TLC	thin layer chromatography
USE	ultra sonic extraction
US EPA	United States Environmental Protection Agency
UV	ultra violet

Acknowledgements

I wish to express my sincere thanks to my research supervisors, Drs. W. R. Cullen and K. J. Reimer for their guidance, encouragement and support during my Ph.D. program at UBC. I would also like to thank the members of my supervisory committee, Drs. G. Eigendorf, K. Orians and T. Carefoot, for their advice and assistance.

This thesis has benefited from collaborations with esteemed colleagues including Dr. D. Bright, Dr. C. Harrington and Mr. A. Mosi. I am especially grateful to Dr. W. Cretney for allocating me space on the Canadian Department of Fisheries and Oceans research vessel R.V. Vector during several expeditions to Kitimat in order to collect samples. I am grateful to Dr. M. Ikonomou from the Institute of Ocean Sciences, Sidney, for providing the ESI-MS analyses in Chapter 5. Dr. S. Serves assisted with interpretation of the ^{1}H-NMR data presented in Chapter 5. D. Minife of Alcan smelters and Chemicals (Kitimat) Ltd. was most helpful in facilitating access to the smelter property at Kitimat, and providing samples of coke, pitch and effluent from the smelter.

Thanks to members of the Cullen Group (past and present) both for their intellectual stimulation, and their friendship over the last five years. Thanks also to the summer students who assisted on this project: Charmaine Chang, Nadia Zalunardo, and Kris Quinlan.

Finally I wish to acknowledge the contributions of those closest to me, my family and Iris Koch. Their friendship, love, support and encouragement has provided me with the confidence, energy and motivation necessary to persevere through the inevitable hurdles encountered along the road to the completion of this Ph.D. Thesis.

1. Introduction

1.1 General

The limitations of our knowledge and our understanding of environmental processes have increasingly become apparent through the unforeseen and deleterious consequences of human actions upon the environment. The field of environmental chemistry, therefore, has recently assumed greater importance as we seek to develop a deeper understanding of the environment, and to mitigate or prevent damage to the environment. Environmental chemistry is the study of the distribution, transport, transformation, ultimate fate and biological effects of chemicals (both natural and anthropogenic) in the environment. It is a broad discipline, combining aspects of chemistry, biology, toxicology, physics and medicine.

This thesis will focus on one important class of environmental contaminants known as polycyclic aromatic hydrocarbons (PAHs). PAHs are carcinogenic, persistent, and widespread throughout the environment. PAHs have been present in the environment for millennia. High levels of PAHs can often be found in the environment as the result of natural agents, from oil seeps or forest fires, for example. However these PAHs are usually tied up in forms that restrict their availability to biota. In recent times, humans have added greatly to the environmental PAH burden, largely as a result of the combustion of fossil fuels. These anthropogenically generated PAHs are often widely dispersed, and are available to biota. Of particular significance to humans is the observation that ambient PAH levels are typically highest in urban settings. Because PAHs are toxic, exposure of both humans and the environment as a whole, to PAHs, is a matter for concern. Hence, understanding the environmental chemistry of PAHs should be considered a priority.

1.2 Properties of PAHs

1.2.1 Structure of PAHs

The term polycyclic aromatic compound (PAC) refers to a diverse class of chemicals, which all possess the common structural element of an extended multi-cyclic aromatic ring system. The simplest PACs contain only carbon and hydrogen atoms arranged in two or more linked aromatic rings, and these are typically referred to as polycyclic aromatic hydrocarbons (PAHs) or polynuclear aromatics (PNAs). Typical examples are illustrated in Figure 1-1. These compounds are generally referred to as unsubstituted, or parent, PAHs.

The hydrogen atoms attached to the aromatic rings of PAHs may be replaced with a number of different chemical functional groups (e.g. alkyl, alkoxy, Cl, Br, NH_2, NO_2, OH, SO_3) to create a huge variety of substituted PAHs. Several examples of these substituted PAHs are included in Figure 1-2.

Another class of PACs, the hetero-atom substituted PACs, are formed by replacement of one or more of the ring carbon atoms with a hetero atom, typically nitrogen, oxygen or sulfur. Some examples are illustrated in Figure 1-2.

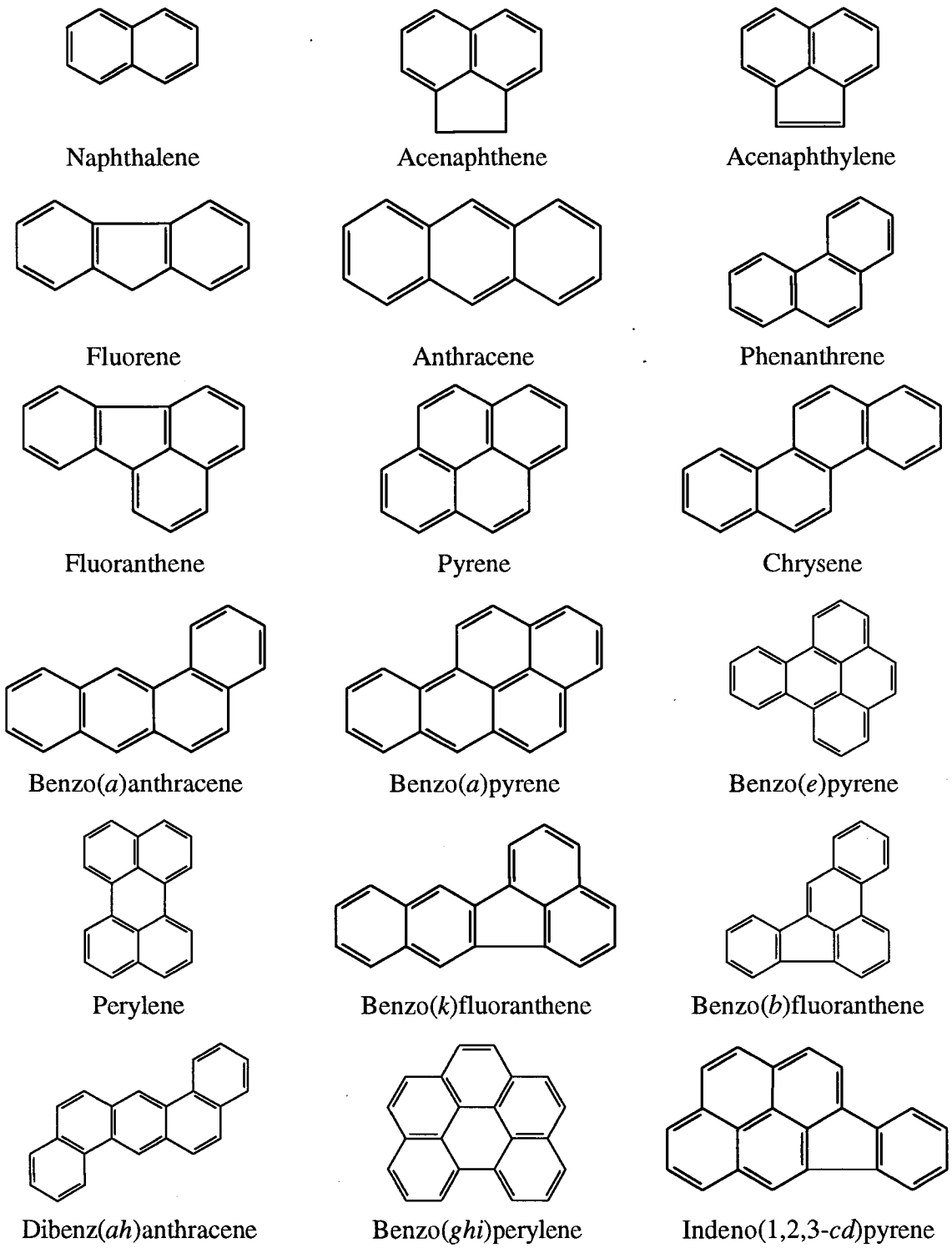

Figure 1-1 Chemical structures of some unsubstituted PAHs.

This figure includes the 16 US EPA designated priority pollutant PAHs (see section 1.6), *plus benzo(e)pyrene and perylene*

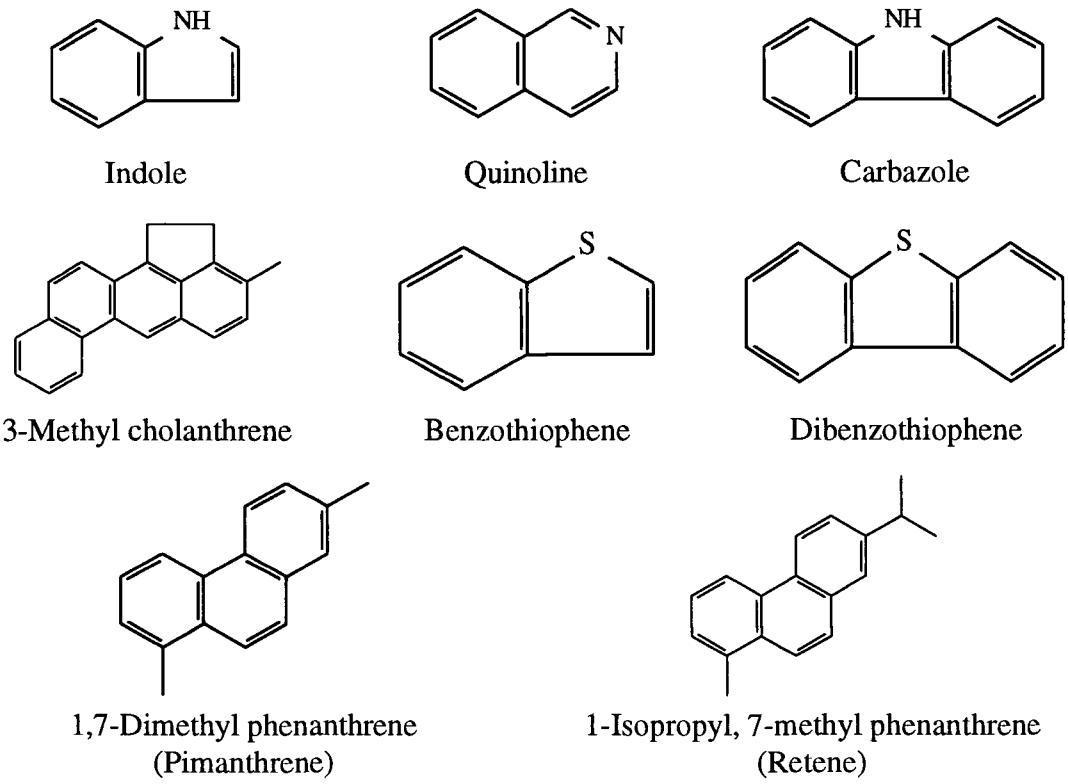

Figure 1-2 Chemical structures of some important alkyl- and hetero-atom-substituted PAHs.

Many important physical and chemical properties of PAHs (e.g. aqueous solubility, volatility, biodegradability) are correlated with molecular weight. Thus, there are great differences in physical and chemicals properties between, for example, naphthalene (MW 128) and coronene (MW 302). It has occasionally been useful to subdivide PAHs into high molecular weight PAHs (HPAH, MW ≥202) and low molecular weight PAHs (LPAH, MW <202).

PAHs may also be classified as linear (where all rings are in a straight line, e.g. anthracene), angular (where there is one or more 120° angles in the chain of aromatic rings, e.g. phenanthrene) or pericondensed (where at least one carbon atom is shared by three rings, e.g. pyrene)

This thesis will focus primarily on parent (unsubstituted) PAHs - specifically the 16 compounds listed as priority pollutants by the United States Environmental Protection Agency (US EPA), as

shown in Figure 1-1. PAHs with alkyl side-chain substituents will be considered where necessary when their presence aids in identification of specific PAH sources or environmental processes affecting PAH fate (see chapters two and three). Oxygen substituted PAH will be considered only in the context of metabolism of the parent compounds by indigenous biota. Chlorinated PAHs, which may be considered to include polychlorinated dibenzodioxins (PCDDs), polychlorinated dibenzofurans (PCDFs) and polychlorinated biphenyls (PCBs), or brominated and fluorinated analogues of these three classes, are not considered in this thesis.

1.2.2 Physical and Chemical Properties

The defining feature of PAH chemistry is the high thermodynamic stability of these compounds (3-5). This stability arises not only from the delocalized aromatic system, but also from the low H/C ratios which increase the entropy of the system (4). In their chemical reactions, therefore, PAHs show a tendency to retain their aromaticity, and substitution reactions are usually favored over addition reactions (6). For isomeric PAHs, the linear configuration (e.g. anthracene) has the lowest thermodynamic stability, while angular configurations (e.g. phenanthrene) are the most stable (3).

The extended π-electron systems give rise to the characteristic spectroscopic properties of PAHs, which have been utilized by analytical chemists to detect PAHs extracted from environmental samples (see section 1.7). The π-electron systems also provide a means by which PAHs may be excited into a reactive state. Thus photo-catalyzed reactions are important, both in the degradation of PAHs in the environment, and in the generation of reactive species that are toxic to biota (7-10).

A compilation of some important physical-chemical properties of selected parent and alkylated PAHs is presented in Table 1-1. All unsubstituted PAHs are solids at room temperature. PAHs are typically insoluble in water and have a low vapor pressure. Both these properties are inversely correlated with molecular weight. Increasing alkyl substitution also decreases water solubility, and for isomeric PAHs, the linear isomers are less soluble than angular or pericondensed structures (cf. anthracene and phenanthrene, Table 1-1).

Table 1-1 Some physical-chemical properties of selected parent and alkylated PAHs.

Compound	MW (g/mol)	log K_{ow}	m.p. (°C)	b.p. (°C)	H (Pa m^3/mol)	S (25°C g/m^3)
naphthalene	128	3.37	80.5	178	43.01	31
1-methyl	142	3.87	-22	245	44.90	28
2-methyl	142	3.86	34.6	242	51.19	25
1,4-dimethyl	156	4.37	7.7	262	31.11	11.4
acenaphthene	154	3.92	96.2	277.5	12.17	3.8
acenaphthylene	152	4.00	92	265-275	8.40	16.1
fluorene	166	4.18	116	295	7.87	1.9
phenanthrene	178	4.57	101	339	3.24	1.1
anthracene	178	4.54	216	340	3.96	0.045
9-methyl	192	5.07	82	355	-	0.261
9,10-dimethyl	206	5.25	182	-	-	0.056
pyrene	202	5.18	156	360	0.92	0.132
fluoranthene	202	5.22	111	375	1.037	0.26
benzo(*a*)anthracene	228	5.91	160	435	0.581	0.011
7,12-dimethyl	256	6.00	122	-	-	0.050
chrysene	228	5.86	255	448	0.065	0.002

Table 1-1 (continued)

Compound	MW (g/mol)	log K_{OW}	m.p. (°C)	b.p. (°C)	H (Pa m^3/mol)	S (25°C g/m^3)
benzo(*a*)pyrene	252	6.04	175	495	0.046	0.0038
benzo(*e*)pyrene	252	6.44	178	493	0.020	0.004
perylene	252	6.25	277	495	0.003	0.0004
benzo(*b*)fluoranthene	252	5.80	168	481	0.0054	0.0015
benzo(*k*)fluoranthene	252	6.00	217	481	0.016	0.0008
indeno(1,2,3-*cd*)pyrene	276	6.40	164	-	-	0.00053
dibenz(*ah*)anthracene	278	6.75	267	524	0.0075	0.0006
benzo(*ghi*)perylene	276	6.50	277	525	0.075	0.00026
3-methyl cholanthrene	268	6.42	178	-	0.145	0.0019

Abbreviations: MW, molecular weight; log K_{OW}, octanol-water partition coefficient; m.p., melting point; b.p., boiling point; H, Henry's Law constant; S, aqueous solubility.
All data from Mackay et al. (11), *except for the indeno(1,2,3-cd)pyrene data which was obtained from reference (8).*

Water solubility increases with increasing temperature, and decreases (slightly) with increasing ionic strength. It should be noted that the extreme insolubility of the HPAHs makes the direct determination of aqueous solubility and related parameters such as log K_{OW} very difficult and prone to error. For example, while Mackay *et al.* quote the aqueous solubility and log K_{OW} of pyrene as being 0.132 g/m^3 and 5.18, respectively, in the summary table of their Handbook of Environmental Data (11), values ranging between 0.03-1.56 g/m^3 for aqueous solubility and 4.45-6.70 for log K_{OW} have been published.

1.3 Metabolism of PAHs

As a compound class, PAHs are fairly readily metabolized by higher organisms, but only selectively so by micro-organisms. In general, prokaryotes oxidize PAHs as a prelude to ring fission and carbon assimilation (1, 12). PAHs of low molecular weight are readily metabolized by prokaryotes, but higher molecular weight PAHs are metabolized less readily, if at all (1, 12, 13). In contrast, eucaryotes metabolize PAHs by initial oxidation, then conjugating them to polar moieties in order to facilitate excretion (2, 12, 14). PAH metabolism involving both ring fission and conjugation has been shown to occur in fungi (15, 16).

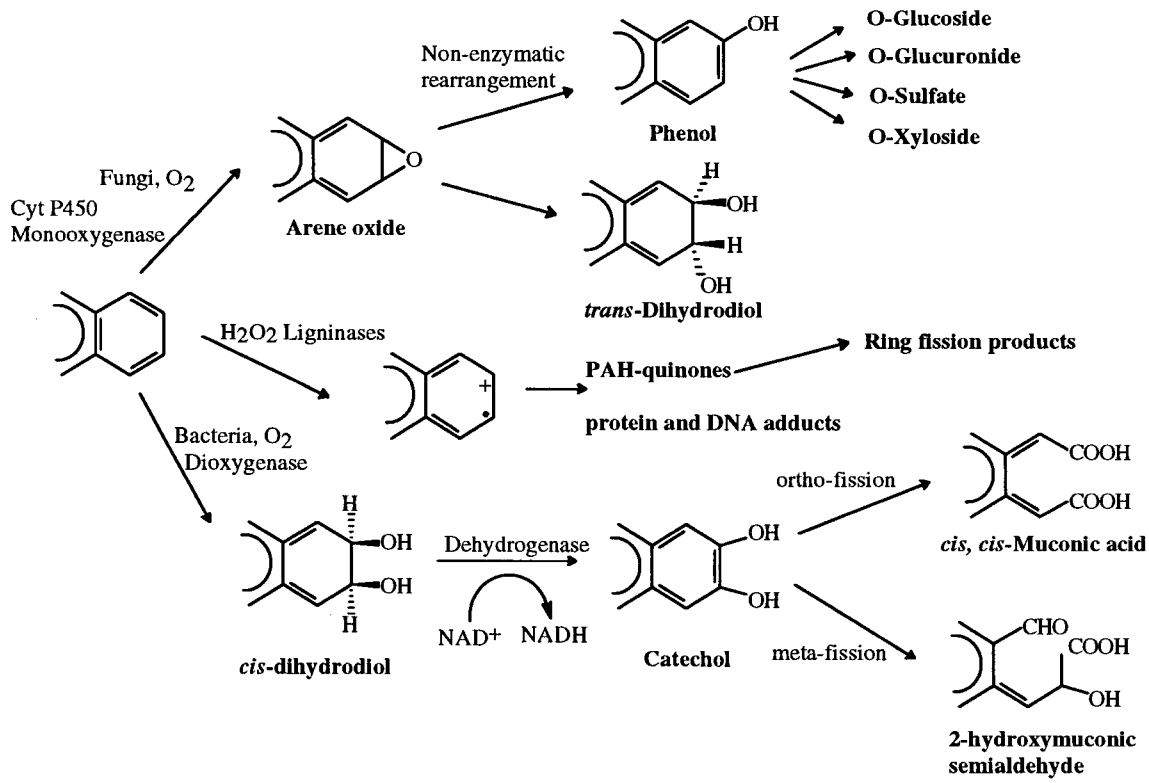

Figure 1-3 Typical oxidation pathways for PAHs (adapted from (1)).

1.3.1 Microbial metabolism

The metabolism of PAHs by pure cultures of micro-organisms, and co-metabolic transformations by microbial consortia have been studied for almost 80 years (1, 12). Microbial degradation of

PAHs proceeds initially by one of two pathways that involve either monooxygenase or dioxygenase enzymes. Monooxygenase enzymes are present in bacteria and fungi; however, bacterial degradation of PAHs usually involves dioxygenases, and both atoms from molecular oxygen are incorporated into the aromatic compound (1, 12, 13). The two pathways are illustrated in Figure 1-3.

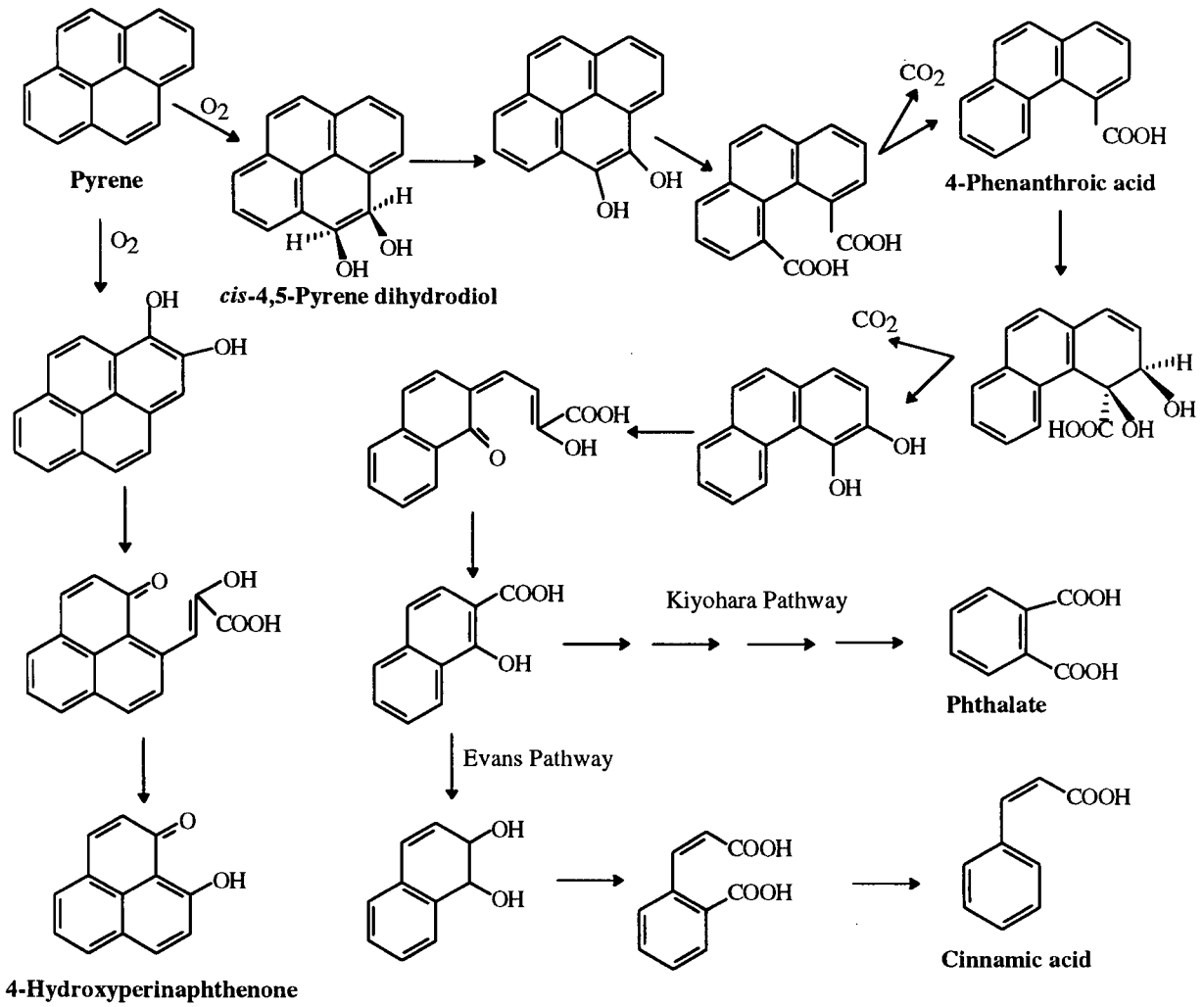

Figure 1-4 Partial pathways for the degradation of pyrene by Mycobacterium sp. PYR-1 (adapted from (1)).

Pathways of microbial degradation of a typical PAH (pyrene) are illustrated in Figure 1-4. The initial step of oxidation utilizes dioxygenases to incorporate molecular oxygen to form a

cis-dihydrodiol. The dihydrodiol is re-aromatized by a dehydrogenase, then oxidative ring cleavage either between (ortho fission), or adjacent to (meta fission) the two hydroxyl groups takes place. Further ring cleavage and oxidation steps occur as shown in Figure 1-4. Mineralization of PAHs to produce CO_2, and incorporation of PAH-derived carbon into bacterial biomass has been demonstrated using ^{14}C-labelled PAHs (17, 18).

The rate at which micro-organisms degrade PAH is inversely proportional to the number of aromatic rings (12, 13), and decreases as the number of attached alkyl carbons increases (12). The rate of biodegradation is proportional to the aqueous solubility of the PAHs (12, 13, 19).

Molecular oxygen is essential for PAH biodegradation by aerobic micro-organisms (12), so PAH biodegradation is severely restricted under oxygen-limited conditions. A few studies have indicated that degradation of PAHs can take place under anaerobic conditions (12, 20, 21). This process may be important for removal of PAHs from anaerobic ecosystems.

1.3.2 Metabolism in higher organisms

In contrast to micro-organisms, most higher species (including vertebrates and crustacea) metabolize PAHs by monooxygenase (rather than dioxygenase) mediated pathways (2, 14). Mixed function oxidase (MFO) enzyme systems, especially cytochrome P450 1A1, introduce a single atom from molecular oxygen to form an arene oxide, which either rearranges to form a phenol, or is stereospecifically hydrated by epoxide hydratase to form a *trans*-dihydrodiol (Figure 1-3). An important contrast with microbial metabolism is that metabolic pathways in higher organisms typically do not lead to ring cleavage. The metabolic pathways for benzo(*a*)pyrene in the rat are illustrated in Figure 1-5. Most other higher organisms metabolize benzo(*a*)pyrene (and other PAHs) by similar pathways.

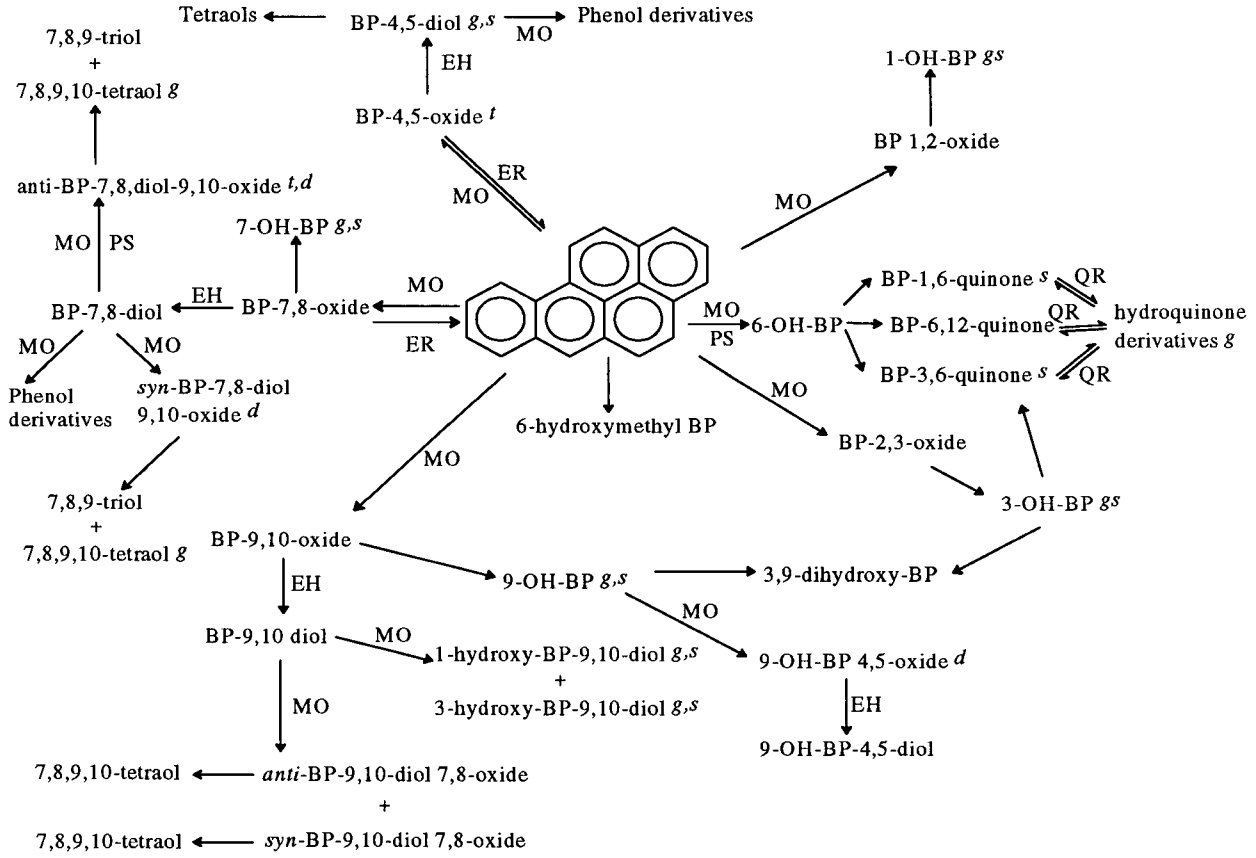

Figure 1-5 Metabolic pathways of benzo(a)pyrene in the rat (adapted from (2)).

Abbreviations: MO, monooxygenase; EH, epoxide hydrolase; ER, epoxide reductase; QR, quinone reductase; PS, prostaglandin synthetase.
The superscripts indicate metabolites that: [t], can be converted into a glutathione conjugate; [s], can be converted into a sulfuric acid conjugate; [g], can be converted into a glucuronic acid conjugate; and [d], can contribute to covalent binding of hydrocarbon to nucleic acids in cells or tissues that have been treated with benzo(a)pyrene.

The products from initial oxidation can undergo several subsequent reactions. Phenols and quinones are substrates for glucuronide and sulfate conjugation, or they can be further oxidized to phenol-oxides (2, 14, 22). As an example of the complex interrelationships between metabolism, activation and detoxification, it is generally thought that conjugation to sulfate (in the liver), which facilitates excretion, is a mechanism for detoxification of PAHs. However, the gut flora in many organisms possess sulfatase activity, thus hydrolysis of the sulfate-PAH conjugate may occur, releasing potentially mutagenic PAH metabolites (23). The PAH dihydrodiols can also be further oxidized to diol-epoxides, some of which are especially reactive towards DNA and

proteins (24), and are thought to be ultimately responsible for PAH carcinogenesis. The epoxides can be conjugated to glutathione and excreted.

In addition to the diol-epoxides, some authors have suggested that radical cations produced from one-electron oxidation of PAHs (25, 26), or benzylic electrophillic PAH esters (27) are also important DNA-reactive metabolites. As a secondary effect, futile redox-cycling of PAH-quinones which exhausts the protective supply of cellular anti-oxidants may leave cells susceptible to DNA damage from reactive oxidizing species, including by-products of lipid peroxidation (28).

1.3.3 Metabolism of PAHs by fungi

Filamentous fungi generally oxidize PAHs as a prelude to detoxification (excretion) (12). Several different oxidation pathways are represented amongst the fungi, and some species may utilize multiple pathways (1). The non-lignolytic fungus *Cunninghamella elegans,* which has been well studied, uses cytochrome P450 monooxygenase enzymes to oxidize PAHs (e.g. naphthalene, pyrene) to *trans*-dihyrodiols, phenols or quinones (15). The phenols can be conjugated with sulfate, glucose or glucuronic acid (15, 29). Similarly, the non-basidiomycete soil fungus *Penicillium janthinellum* metabolized pyrene to phenols and di-phenols (30).

In contrast, the white rot fungi, *Phanerochaete chrysosporium* produces extracellular lignin peroxidases that catalyze the 1-electron oxidation of PAHs including pyrene, perylene, anthracene and benzo(*a*)anthracene to quinones (1, 16). This pathway is also illustrated in Figure 1-3. Lignolytic fungi have been shown to degrade high molecular weight PAHs, which are essentially resistant to degradation by normal mono- or dioxygenase pathways (13). It has been suggested that this may be because the lignin peroxidases are extra-cellular, and the PAHs therefore do not have to cross the fungal cell wall, a process which may not be possible for the larger PAHs.

1.3.4 Metabolism of PAHs by mollusks

Because the isolation and identification of PAH metabolites from mollusks forms a major part of this thesis, the literature on this subject is extensively reviewed in the following sections.

1.3.4.1 Biochemical Studies

The major pathways of unsubstituted PAH metabolism in mollusks are similar to those in mammals, as illustrated in Figure 1-5. Although initial studies implied an absence of cytochrome P450 MFO activity in mollusks (31-33), more recent work confirms that P450 activity is widespread in mollusks, albeit at levels substantially lower than those typical for vertebrates (34-38).

Table 1-2 Comparison of selected PAH-metabolizing enzyme activities in mollusks and other phyla.

Enzyme	Mollusks	Crustaceans	Fish
cytochrome P450 (nmol/mg protein)	0.07	0.33	0.32
benzo(a)pyrene hydroxylase (nmol/min/mg protein)	0.02	0.04	0.31
UDP-glucuronyl transferase (nmol/min/mg protein)	8-30	0.01	0.08
UDP-glucosyl transferase (nmol/min/mg protein)	>0.002	0.2-1	nd

Data from Livingstone, (37, 38) and Foureman, (39).
nd; not determined

Other enzyme activities relevant to the metabolism of PAHs that have been identified in mollusks include: epoxide hydratase, superoxide dismutase, catalase, glutathione-*s*-transferase, UDP-glucuronosyl transferase, UDP-glucosyl transferase, sulfotransferase (37, 38, 40, 41). A comparison of the activities of several important Phase I and Phase II enzymes in different phyla is

shown in Table 1-2. It can be seen that the activity of the phase II (conjugating) enzymes compared to cytochrome P450 is much higher in mollusks than in the other phyla. Thus, whilst phenol and dihydrodiol metabolites may accumulate in fish or mammals, in mollusks they would probably be conjugated and excreted more readily. Sulfate and glycoside conjugates probably predominate over glucuronidation in mollusks (sulfate and glycosyl conjugates have been detected whereas glucuronides have not), but the experimental evidence for this is limited (37, 38).

In addition to the 2-electron cytochrome P450 mediated oxidation of PAHs, there is evidence to suggest that a 1-electron oxidation, catalyzed either by cytochrome P450 or peroxidases, may also be important for some PAHs in mollusks (37, 42). Specifically, the predominance of quinone metabolites over phenols and dihydrodiols (see section 1.3.4.2) is indicative of initial 1-electron oxidation reactions (25, 26). A major fate of the cation radical initially formed via 1-electron oxidation could be the formation of macromolecular adducts to DNA and protein (25, 26, 37). Both oxidation mechanisms are summarized in Figure 1-3.

1.3.4.2 Identification of PAH metabolites from mollusks

In spite of the widespread evidence of the potential for PAH metabolism in mollusks from biochemical studies, few reports have been able to identify or characterize metabolites of unsubstituted PAHs generated by mollusks, and many authors have failed to find evidence for the generation of PAH metabolites by mollusks in feeding studies under controlled laboratory conditions (31-33, 43). Thus, the topic remains controversial.

Benzo(*a*)pyrene is the most intensively studied PAH. Stegeman (42) studied metabolism of ^{3}H-benzo(*a*)pyrene in microsomes isolated from the digestive gland of the blue mussel (*Mytilus edulis)*. Benzo(*a*)pyrene quinones (3 isomers, 65% of total metabolites), phenols (2 isomers,

30%) and dihydrodiols (3 isomers, 3%) were identified by comparing their migration distances on thin layer chromatography (TLC) plates, and their ultra-violet absorption spectra, with authentic standards. Digestive gland microsomes from the oyster (*Cryptochiton stelleri*) and mussel (*Mytilus edulis*) also converted benzo(*a*)pyrene predominantly to quinones (44, 45). In contrast, Anderson (46) identified only ^{14}C-benzo(*a*)pyrene dihydrodiols as benzo(*a*)pyrene metabolites generated by digestive gland microsomes from the hard-shell clam (*Mercenaria mercenaria*), and both dihydrodiols and phenols from the atlantic oyster (*Crassostrea virginica*). Pre-exposure of both species to the PCB mixture Arochlor 1254 (a potent MFO inducer) led to the formation of various quinones, and changes in both the absolute and the relative amounts of the dihydrodiol and phenol isomers. The amount of Arochlor 1254 added also seemed to alter the metabolite profiles. All metabolites were identified by comparing HPLC retention times to those of authentic standards.

In studies using intact mollusks, Augenfeld *et al.* (47) exposed *Macoma inquinata* to ^{14}C-phenanthrene. Radioactivity was detected in the insoluble tissue fraction, and it was suggested that this indicated the presence of PAH adducts to macro molecules (e.g. to protein and DNA). Water soluble metabolites were also indicated by progressive loss of radioactivity from sediments and clam tissue; however, it was suggested that these were probably bacterial metabolites. The oyster (*Ostrea edulis*), after metabolic stimulation with glucose, was able to convert ^{14}C-naphthalene to 1- and 2-naphthols (48). The naphthols were identified by comparing migration distances on TLC to authentic standards. A spot at the origin of the TLC was indicative of polar conjugates. Lu *et al.* investigated uptake of ^{14}C-benzo(a)pyrene in an aquatic snail (*Physa sp.*) (49). Snail tissue was homogenized with acetone, and a TLC of the resulting extract revealed

several unidentified metabolites including polar compounds. Unextractable radioactivity in the tissue indicated possible adducts to DNA and/or protein.

The possible formation of PAH adducts to macromolecules has been suggested as a consequence of 1-electron oxidations (25, 26, 37), and invoked to explain the frequent failure to detect oxidized PAH metabolites (phenols and dihydrodiols) in mollusks (37). In addition to the reports above, PAH-protein and PAH-DNA adducts are indicated in several recent studies (40, 50, 51). Radioactivity was detected in protein and DNA isolates from *Mytilus edulis* 2 and 5 days after exposure to ^{3}H-benzo(*a*)pyrene (51). Bulky, hydrophobic DNA-adducts were detected in digestive gland tissue from mussels (*Mytius edulis*) collected from several PAH contaminated sites; however, the adducts were not identified (40). Using a sensitive ^{32}P-postlabeling assay Venier and Canova detected a benzo(*a*)pyrene adduct to gill DNA from *Mytilus galloprovincialis* (50). The amount of adduct increased with increasing dose of benzo(*a*)pyrene. However, a study by Kurelec indicated very weak or no adduct formation when digestive gland homogenates from *Mytilus galloprovincialis* were treated with benzo(*a*)pyrene (52).

1.4 PAHs as Environmental Contaminants

1.4.1 Sources

PAHs are generated by three different types of processes: high temperature combustion, low to moderate temperature diagenesis of sediment organic matter, and biosynthesis (3, 8, 53, 54). The most significant source of PAH contamination in the environment is incomplete combustion of organic material (8, 54-56). This includes natural combustion events such as forest and grassland fires, and possibly volcanism, and anthropogenic sources such as industry, transportation, thermal power generation, and burning of fuel for domestic heating and cooking (6, 8, 57, 58). A risk

assessment for PAHs performed under the Canadian Environmental Protection Act (CEPA) estimated 4300 tonnes of PAHs were discharged into the Canadian atmosphere in 1990, of which 53% was attributed to industrial sources. Aluminum smelting alone produced 925 tonnes of PAH (8). Because Canada has a high land to population ratio, the fraction of total atmospheric PAH emissions due to forest and prairie fires (47%) is higher in Canada than is typical for other industrialized nations (e.g. 17% for USA (59)).

1.4.1.1 Combustion generated PAHs

The mechanisms by which PAH are formed during combustion have been extensively studied, but are still far from being understood completely. Both pyrolysis (the thermal cracking of organic compounds to form smaller fragments, many of which are radicals) and pyrosynthesis (recombination of the radical species to yield more stable aromatic fragments) are thought to be important (6, 59). In addition, some "combustion" processes undoubtedly release large amounts of PAH simply due to volatilization of PAH from PAH-containing feedstocks (e.g. aluminum smelters which utilize Söderberg electrodes) (60).

The complex PAH mixtures produced by combustion have been shown to be more strongly dependent on the combustion temperature than on the fuel itself (3, 59). High temperature processes produce almost exclusively unsubstituted PAH, while lower temperature processes (e.g. oil production) produce many alkyl-substituted compounds, as illustrated in Figure 1-6. High temperature formation processes also favor condensed ring structures (e.g. pyrene, benzopyrenes, benzo(*ghi*)perylene) over linear or angular structures (3). Bjorseth and Ramdahl suggest that high combustion temperature favors the formation of the thermodynamically more stable PAH isomers

(59); however, rapid quenching of the formation reaction enables less stable isomers to persist in combustion generated PAH mixtures (3).

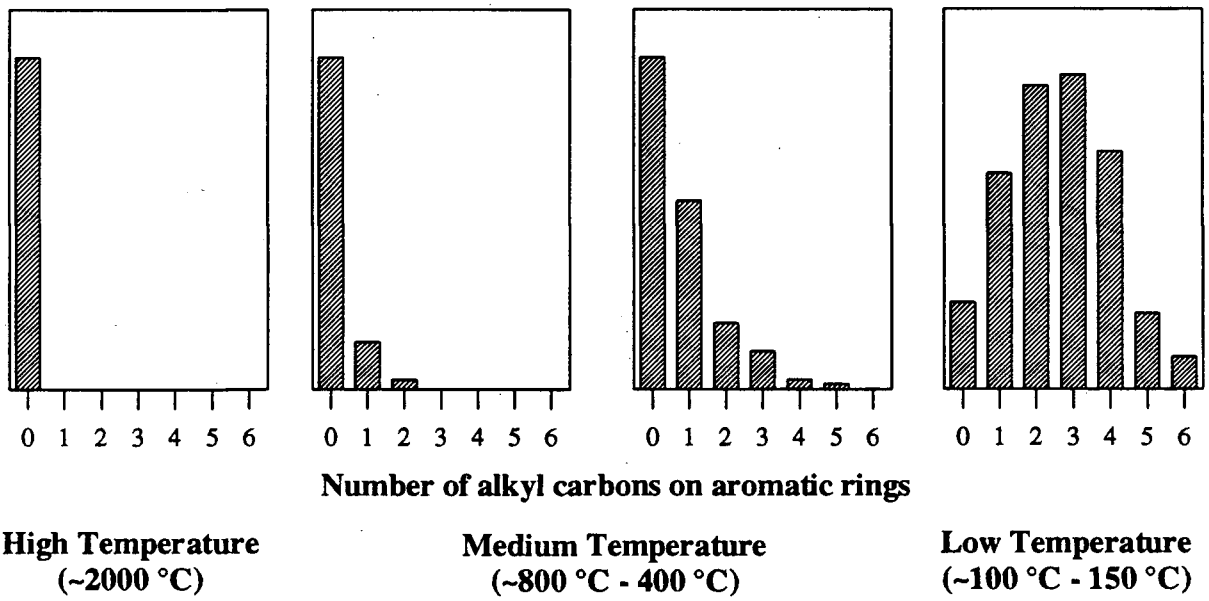

Figure 1-6 Graphs showing inverse relationship between the degree of alkyl substitution of PAHs and formation temperature (adapted from Blumer, (3)).

1.4.1.2 PAHs in fossil fuels

PAH are also present in substantial amounts in fossil fuels (8, 54, 61), thus fuel spillage or effluent from fuel-processing industries represents important local sources of PAH contamination. In contrast to combustion generated PAHs, petrogenic PAH mixtures consist mainly of alkyl-substituted compounds (3, 62, 63); two or three ring structures (naphthalenes, phenanthrenes) are present in greater abundance than four or five ring structures (62, 64-66), and compounds containing multiple 5-membered rings are common (3). The aromatic fraction of crude oils often exhibits a broad hump (an unresolved complex mixture) when analyzed by using capillary GC (66-68). This feature is typical of weathered or degraded bitumens (69).

The processes controlling the formation of petrogenic PAH are complex and poorly understood. PAH production is postulated to begin during early diagenesis of plant material due to

fragmentation and progressive aromatization of organic chemicals derived from the plants. Possible plant precursors have been suggested for a number of PAH (6, 70), but for many of the other PAHs no likely plant precursors are known. With increasing thermal maturation of the forming oil deposit, the degree of aromaticity increases, and reactions involving methylation, demethylation and methyl transfer become important (61, 71, 72). In coalification (late catagenesis), condensation of polycyclic aromatic compounds takes place to form ashphaltenes and other graphite-like oligomers (73). PAHs can be generated due to fragmentation of these polymeric compounds.

1.4.1.3 Biosynthesis and short term diagenesis

Micro-organisms, plants and animals are all capable of producing compounds containing fused-ring polyaromatic systems, and these compounds often contain oxygen, nitrogen or sulfur hetero-atoms (3, 54). Included among these compounds are perylene quinones, and it has been postulated that high levels of perylene found in some sediments may arise from reduction of the (perylene) quinones (53, 54). *de novo* biosynthesis of unsubstituted PAHs has not been demonstrated conclusively (54).

PAHs can be formed via diagenesis of organic matter in soils and sediments (8, 53, 74). Unlike combustion or petrogenic PAHs, diagenesis usually forms simple mixtures of PAHs with 1 or 2 compounds being dominant. Perylene is usually the most important diagenic PAH, although sediments near coniferous forests often have high levels of retene and pimanthrene (55). Alkylated naphthalenes, phenanthrenes, picenes and chrysenes are other PAH with probable diagenic origins found in some soils and sediments (6, 55, 70). Lee *et al.* postulated that alkylated naphthalenes may be formed by degradation of plant-derived sesquiterpenoids (6). It has been

proposed that alkylated phenanthrenes (e.g. retene, pimanthrene) are derived from resin acids (55, 70), and that alkylated chrysenes and picenes are generated from pentacyclic triterpenoids (70). Usually, diagenic PAHs are only present in trace amounts, and their presence in contaminated sediments is often masked by the more abundant combustion generated or petrogenic PAHs. Under some circumstances, diagenic PAHs can be present in substantial quantities (53, 75) (see also Chapters 3 and 4, this thesis).

1.4.2 Distribution

PAHs are both stable and ubiquitous in the environment. PAHs have been detected in ice and snow on Ellesmere Island in the arctic (76), and in water, sediments and biota in the antarctic (77, 78). PAHs have even been detected in meteorites (79), and their presence in interstellar matter has been indicated by using infra red spectroscopy (80, 81). Laflamme and Hites analyzed twenty soils and sediments from around the world for unsubstituted and alkylated PAHs (55). They concluded that PAHs are widespread, that the PAH composition is similar for most of the locations studied, and that absolute levels of PAHs increase with proximity to urban centers.

A number of studies have examined the historical deposition of PAHs by examining ice and sediment cores (58, 76, 82-84). Worldwide, there has been a substantial increase in PAH levels in sediments since the late 19th century (58, 62, 84). Youngblood and Blumer suggested that the PAHs were generated by forest fires (3, 58), however this hypothesis doesn't account for the observation that PAH concentrations from a number of sediment cores maximized in the period 1950-1960 (84), and have declined since then (although PAH levels are still elevated in comparison to pre-1900 levels (62, 83, 84)). The elevated PAH levels in recent sediments are usually attributed to anthropogenic sources (56, 83, 84). Supporting evidence for this theory

includes the co-variance of PAH concentration with other anthropogenic pollutants such as Zn, Cu and Pb (82), and in at least one core, the similarity of the PAH composition to urban street dust (83).

1.4.3 PAHs and source apportionment

As described in previous sections, different PAH sources produce characteristic mixtures of PAHs. Thus, it is often possible to ascribe the PAHs in unknown environmental samples to a particular source, based on the PAH composition in the unknown samples.

The ratio of the concentration of an unsubstituted PAH to the concentration of its alkylated homologs (the Alkyl Homologue Distribution, AHD) is often used to distinguish between combustion derived PAHs and petrogenic PAHs in sediments (64, 65, 85). Ratios of thermodynamically-more-stable : thermodynamically-less-stable PAH isomers can also be used to differentiate sources (62, 64, 84). For example the ratio phenanthrene:anthracene is typically ~3-4 in urban street dust, but is closer to ~30-40 in PAH mixtures from remote locations (84).

In some cases, individual PAHs may be characteristic of a certain source. For example, retene appears to be associated exclusively with either PAH formed through early diagenesis or coniferous wood combustion (70, 86). More often PAHs have multiple possible sources, and multivariate statistical techniques are used (e.g. principle components analysis (PCA), factor analysis (FA), cluster analysis) to examine subtle differences in PAH composition (64, 87, 88). Thus, using PCA, Naes and Oug were able to distinguish two combustion sources (aluminum smelters, Mn alloy smelters) based upon PAH composition in marine sediments (87).

If the source of PAH contamination is known and its composition well characterized, measurement of changes in PAH composition over time or space can give information on the fate of PAH contamination. Changes in the AHD for spilled oils have been used to monitor weathering and biodegradation of the spilled oil (89, 90), and to differentiate oil types (91). For the monomethylphenanthrene isomers, 9-methylphenanthrene is the isomer most resistant to biodegradation (68), whereas it is the isomer most susceptible to photodegradation (92). Thus changes in the ratios of monomethylphenanthrene isomers may provide insight into the relative importance of different degradation pathways.

1.4.4 PAHs as biogeochemical markers

Systematic changes in several parent/alkylated PAH ratios, and in ratios of specific alkyl PAH isomers, have been used as indices of oil and coal maturity (e.g. methyl and dimethyl naphthalenes, methyl and dimethyl phenanthrenes, methyl pyrenes (61, 71, 93, 94)). One example is the methylphenanthrene index MPI_3, defined by Garrigues *et al.* (93) as shown in equation 1.

$$MPI_3 = \frac{(2\text{-methyl}) + (3\text{-methylphenanthrene})}{(1\text{-methyl}) + (4\text{-methyl}) + (9\text{-methylphenanthrene})} \qquad \text{eqn. (1)}$$

This ratio increases with increasing thermal maturation of coal (within the oil window). The increase has been ascribed to a greater thermodynamic stability of the 2-methyl and 3-methylphenanthrenes compared to the sterically crowded 1-methyl, 9-methyl and 4-methyl phenanthrenes (61, 71).

1.4.5 Effects of PAHs on biota

This section provides a general review of the effects of exposure to PAHs on biota. Detailed reviews of the effects of exposure to PAHs on humans and mollusks are included in subsequent sections.

PAHs are acutely toxic to aquatic organisms at low levels. Typical 96 hour LC_{50} values for aquatic invertebrates are on the order of 1-0.01 mg/kg (ppm) (8, 54), and HPAHs are considered to be more acutely toxic than LPAH (8, 54). In contrast, sediment quality criteria proposed by Long *et al.* are more stringent for LPAH than for HPAH (95).

Laboratory based bioassays that utilize benthic invertebrates (e.g. echinoderms, amphipods, polychaetes, mollusks, crustacea) and larval forms of fish are widely used to test PAH contaminated sediments and overlying water for toxicity (8, 95, 96). Toxicity end-points include mortality/survival, emergence and reburial, cellular abnormalities, growth abnormalities, and altered respiration (8, 95, 96). Field studies based on ecological parameters such as species abundance and richness are also used to evaluate the toxicity of PAH contaminated sediments (96).

PAHs have been shown to induce tumors and cellular abnormalities in fish (54, 97), and a number of studies have demonstrated a higher prevalence of neoplasia in flatfish inhabiting PAH contaminated sediments compared to control fish from pristine sites (98-100). Krahn *et al.* found a positive correlation between PAH metabolite concentrations in the bile of english sole *(Parophrys vetulus)* and the incidence of hepatic tumors in the same fish (99). PAH-DNA adducts have been detected in fish collected from PAH-contaminated environments (101, 102). PAHs have also been shown to induce MFO activity in fish (74, 103).

The major toxic concern for higher animals associated with PAH exposure is cancer. The mechanisms by which PAHs cause cancer are not completely understood, and a thorough critique of the various theories of PAH carcinogenesis (25, 27, 104, 105) is beyond the scope of this thesis. It is generally accepted that alkylated and unsubstituted PAHs are not direct acting

carcinogens and require metabolic activation to reactive species, and the reactive PAH metabolites have been shown to bind to DNA and protein (14, 27). Non-neoplastic effects of PAHs in mammals include: altered enzyme activity (e.g. cytochrome P450, glutathione-s-transferase, uridine 5'-diphosphoglucuronyl transferase), endocrine disruption and immunosupression (106-111).

PAHs have been shown to be photo-toxic to a variety of organisms including fish, plants and benthic invertebrates (e.g. oligochaetes, amphipods) (7, 9, 112, 113). The photo-toxicity may be due to either generation of reactive PAH photo-transformation products, or generation of singlet oxygen via PAH-mediated photo-sensitization (7, 9). Photo-toxic effects include mortality in benthic invertebrates (7) and growth inhibition in plants (9).

1.4.6 Toxic effects of PAHs in mollusks

Given that sediments are the ultimate sink for PAHs in the marine environment, one might expect sediment dwelling organisms to accumulate especially high levels of PAHs in their tissues, and hence to be particularly susceptible to any acute or chronic toxic effects arising from PAH exposure. Indeed, as discussed in section 1.4.5, a number of studies have demonstrated a higher prevalence of neoplasia in flatfish inhabiting PAH contaminated sediments compared to control fish from pristine sites (98-100), and benthic invertebrates are routinely used in toxicity bioassays of PAH contaminated sediments (96).

The limited ability of mollusks to metabolize PAHs almost certainly prevents the accumulation of carcinogenic metabolites, and some authors suggest that mollusks would be unlikely to develop cancers as a result of exposure to PAHs (111). However, neoplasms or genetic damage have been detected in shellfish populations from contaminated sites (114-116), and disseminated

neoplasia have been identified in at least 15 species of bivalve. Body burdens of PCBs have been correlated with neoplasia in *Mya arenaria* (115), and Mix described a relationship between elevated PAH levels and neoplasia in *Mytilus edulis* from Yaquina Bay, Oregon (116). Preliminary results from Brand *et al.* (*pers. comm.*) indicate that prevalence of leukemic cells and reactivity with a leukemia cell specific polyclonal antibody are both significantly higher in *Mya arenaria* collected from a site heavily contaminated with PAHs (Hospital Beach, Kitimat, BC), than in specimens collected from a reference site.

These studies are certainly suggestive of a link between increased prevalence of neoplasia in bivalves and elevated levels of PAHs or other toxicants in sediments. No causal relationship has been established, however, and many studies have failed to demonstrate any link between shellfish diseases and PAH contamination ((116) and references therein). A recent review, concluded that *"evidence in support of the pollution-neoplasia hypothesis is not impressive"* (116).

PAHs are responsible for a number of potentially toxic effects, other than cancer, in mollusks. Several PAHs are potent inducers of cytochrome P450 in mammals, and this effect has been documented in mollusks also (35, 38, 117). Potentially hazardous consequences of P450 induction include: mutagenesis due to increased oxidative stress and free radical formation, carcinogenesis due to increased activation of pro-carcinogens, and attenuation of endogenous cellular processes because of increased metabolism of steroid-type hormones and other endogenous P450 substrates (103, 118). These effects may be responsible for observations of reproductive impairment at the whole organism level (117, 119). Alternatively, depression of metabolic activity, a narcotic effect common to hydrophobic organic compounds, could be responsible (120, 121).

Induction of enzymes other than P450 (e.g. catalase, NADPH-cytochrome c reductase) has been demonstrated in mollusks (38, 117, 121), and this would also be expected to cause adverse effects arising from attenuation of normal metabolic processes.

PAHs have been shown to affect membrane structure and function, including causing the destabilization of lysosomal membranes, resulting in changes to membrane permeability (111, 122). The membrane damage may be a result of increased lipid peroxidation, attributable to PAH-induced oxidative stress (38). Impaired immune response following exposure to PAHs has been observed in *M. edulis* (123-125).

Phototoxicity of PAHs has been demonstrated in benthic invertebrates including oligochaetes and amphipods (7, 112), and may be important for some mollusks too.

1.4.7 Fate of PAHs in the environment

Important features of the cycle of PAHs in an aquatic environment are illustrated in Figure 1-7. The fate of a chemical in the environment can be conveniently modeled by using the equilibrium partitioning (EP) concept. The EP theory assumes that the distribution of a chemical between various environmental compartments (e.g. air, water, sediment, etc.), is governed by chemical equilibria, and that thermodynamic equilibrium exists between all compartments (126, 127). In the case of hydrophobic organic compounds such as PAHs, the equilibrium condition commonly used is one of equal fugacity in each environmental compartment (128, 129). However, thermodynamic equilibrium may not be achieved if, for example, there are kinetic constraints on contaminant transfer between various compartments, or if metabolism is significant (126, 127). In these cases, EP theory will fail to adequately describe chemical distribution in the environment.

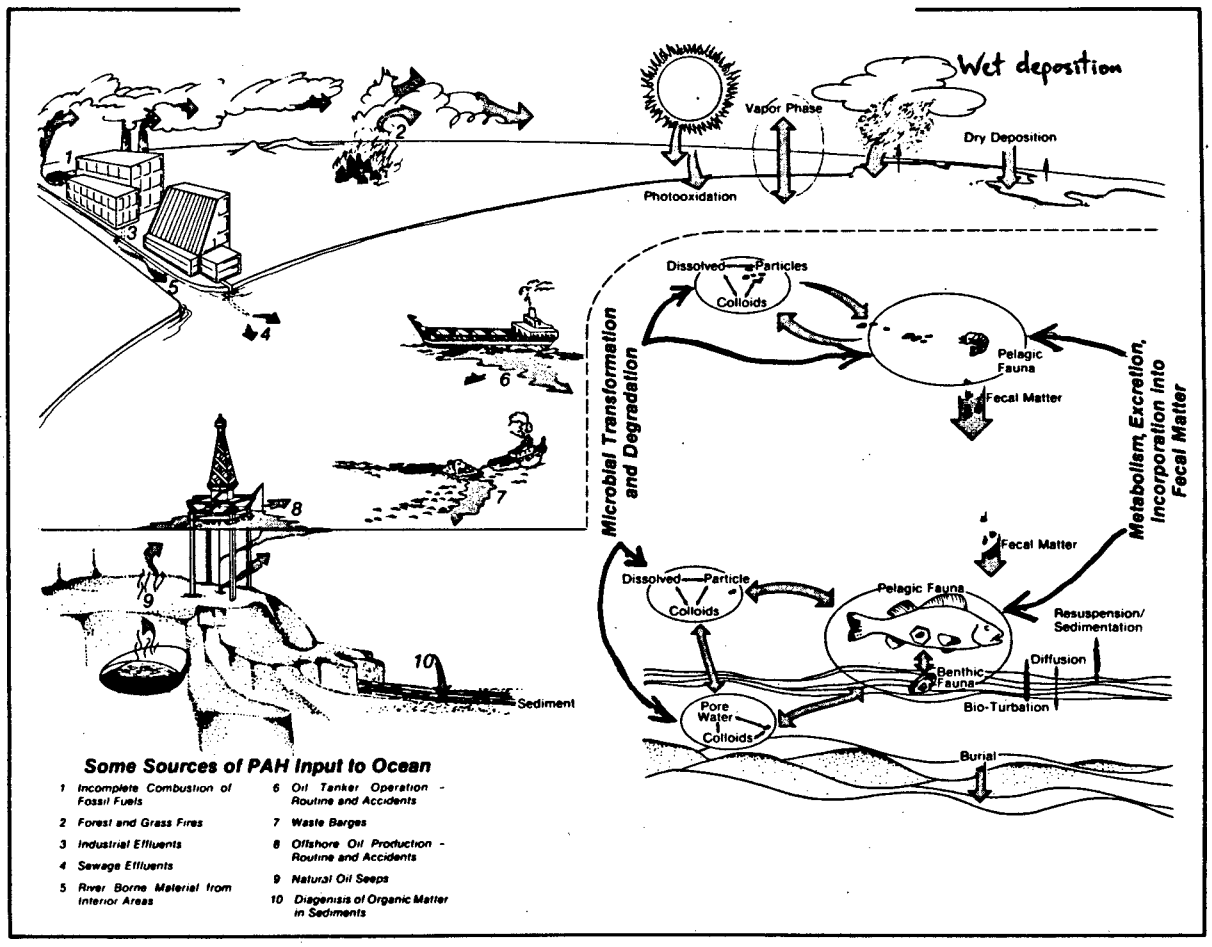

Figure 1-7 Biogeochemical cycle of PAHs in an aquatic environment. (adapted from (130)).

These limitations may be overcome in part by the use of steady-state models, which describe contaminant distribution as a balance of reaction rates (e.g. sorption/desorption, uptake/depuration, etc.) (126, 127). A major disadvantage of steady-state models is that they require measurement of a number of rate constants, and this may be difficult and time consuming.

1.4.7.1 Air

The greatest inputs of PAHs to the environment arise from combustion sources, which discharge into the atmosphere. Thus the atmosphere is a major transport medium for PAHs (8). In the elevated temperatures of combustion sources PAHs typically exist in the vapor phase, but HPAH rapidly condense onto particle surfaces at ambient temperatures (74). In the atmosphere PAH

≤ MW 202 exist predominantly in the vapor phase, while PAHs ≥ MW 202 are mainly particle associated (131-133). Partitioning of PAHs between vapor and particle phases shows a marked temperature dependence (133-135). In one study, vapor phase PAH concentrations showed a strong diurnal variation (levels were highest in the afternoon), attributed to volatilization of PAHs from plant surfaces (135). Particle associated PAH levels are highest in winter, probably due to cold-condensation of PAHs onto particles, and increased combustion for domestic heating (134). Some recent studies indicate that the gas-particle partitioning of PAHs may not be at equilibrium (74, 134, 136, 137). Wei reported that the vapor phase concentrations of PAHs in flue gas from a furnace were much lower than their respective vapor pressures (137). He proposed that once formed, PAHs are instantaneously encapsulated by the growing soot particles, thus preventing their equilibration into the vapor phase.

Processes whereby PAHs are removed from the atmosphere include wet and dry deposition and chemical reactions (8). The sunlight-activated reactions of PAHs with ozone or hydroxyl radicals are especially important (8, 74). Photo-oxidation and photolysis half lives for PAHs (excluding naphthalene) in air range from 0.4 to 68 hours (8, 74), however particle-adsorbed PAHs may be less susceptible to reaction (8, 74, 138). Pennise and Kamens (138) noted that particle-associated PAHs generated at 360-380 °C were far more susceptible to photo-degradation than were particle-associated PAHs generated at 760-800 °C.

1.4.7.2 Water

Various important sources of PAH to the aquatic environment are illustrated in Figure 1-7. Because PAHs are hydrophobic and have very low aqueous solubility, when released into an aqueous environment PAHs will rapidly partition to particles and become buried in sediments (8,

54). Thus total PAH concentrations in the water column are low, typically < 0.1 μg/L for unpolluted rivers, ground water, drinking water and seawater (54). Rivers flowing through industrialized areas, urban stormwater or surface run-off, and sewage discharges typically have elevated total PAH levels (3-5000 μg/L) associated with suspended particles (8).

Although the dissolved-phase PAH concentration is low, it has great importance. It is generally accepted that only a chemical in the dissolved phase is bioavailable (139, 140), although colloid associated PAHs may be available to some filter feeders (139), and digestive solubilization of sediment-bound chemicals has recently been shown to be important for some benthic invertebrates (141). PAHs can partition to dissolved organic matter (DOM) (e.g. humic substances). This increases the mobility and apparent solubility of the PAHs (111, 142-144), but decreases the bioavailability (111, 140). PAH levels may be enriched relative to the bulk water in sediment interstitial water (pore water) (145) and the surface microlayer (146).

Routes of removal of PAHs from the water column include volatilization, photo-oxidation, microbial metabolism, metabolism by higher organisms, and deposition to sediments (8, 54, 132, 147). Volatilization is likely to be most important for LPAHs. Hoff *et al.* recently reported that there is currently a net flux of phenanthrene and pyrene from the Great Lakes to the atmosphere via volatilization (147).

Although less sensitive to photo-oxidation in water than in air, loss of PAHs by photo-oxidation is likely to be important (10, 54). Calculated near-surface half-lives for direct photochemical transformations at 40 °N (midday, summer) ranged from 71 hours (naphthalene) to 0.5 hr (benzo(*a*)pyrene) (10). Ehrhardt *et al.* (148) and Jaquot *et al.* (92) observed that alkyl-substituted PAH derived from spilled oil undergo photochemical degradation faster than

unsubstituted PAHs. It was suggested that this was due to the presence of reactive benzylic protons in the alkylated PAHs (148). Decreased photo-reactivity was reported for PAHs associated with suspended solids (10).

1.4.7.3 Sediment

Because of their low aqueous solubility, low vapor pressure and hydrophobicity, PAHs show a strong tendency to partition from the vapor or dissolved phase onto particles (8, 54). These particles will rapidly settle through the water column and become deposited as sediments. Other sources of PAHs to surface sediments include synthesis of certain PAHs (e.g. retene) due to early diagenesis of organic material in aerobic sediments (70), and petrochemical seeps (54, 64). Total PAH levels at remote sites not impacted by human activity or other major PAH sources are typically $\leq$ 1 mg/kg (8). PAHs levels at contaminated sites are much higher, for example Vancouver Harbor (up to 330 mg/kg (149)), Hamilton Harbor (283 mg/kg (8)); Saguenay fjord (40-200 mg/kg (150)); Norwegian fjords (up to 800 mg/kg (151)).

Sediment-bound PAHs can be returned to the water column by dissolution into the aqueous phase (74) or resuspension of bulk sediment (8, 130). PAHs can be removed from the sediments via uptake into benthic invertebrates (152, 153), or via degradative processes including microbial degradation (1, 12) and chemical degradation. Partitioning to sediments has been shown to reduce availability of PAHs to biota (74, 153, 154), reduce biodegradation (1, 21), and reduce chemical degradation. Thus the ultimate fate of much of the PAHs deposited to sediments is burial. Once buried in anoxic sediments, degradation of PAHs essentially ceases (63).

The partition of hydrophobic organic chemicals (HOCs), including PAHs, between particle-associated and the dissolved phase has been well studied (155-157). It has been shown that PAHs

partition to the organic matter fractions of sediments (155, 156), and linear relationships exist between K_P (the sediment-water partition coefficient) and f_{OC} (the fractional organic carbon content of the sediment). Thus, it has proven useful to define K_{OC} (the organic carbon normalized sediment-water partition coefficient):

$$K_P = \frac{C_S}{C_W} = K_{OC} \times f_{OC} \qquad \text{eqn. (2)}$$

where C_S and C_w are concentrations of each PAH in the sediment (S) and the water (W).

K_{OC} is essentially a distribution coefficient for solute monomers between an aqueous phase and a hydrophobic organic phase. As such, it is similar to the octanol-water partition coefficient (K_{OW}), and the two quantities can be related by equations such as eqn. (3), derived by Karickhoff (155):

$$K_{OC} = \frac{Z_{OC}}{Z_O} K_{OW} = 0.411 \times K_{OW} \qquad \text{eqn. (3)}$$

where Z_{OC} and Z_O are fugacity capacities (128, 129) of the PAH in the organic carbon (OC) and octanol (O). (Note that various values of the proportionality constant Z_{OC}/Z_O have been reported by different authors (e.g. (126))

K_{OW} is readily measured in the laboratory (158, 159), or predicted from molecular properties (160). K_{OW} values have been determined for most of the environmentally important PAHs (see Table 1-1). Therefore, the relationship in eqn. (3) provides a basis whereby PAH partitioning in the environment can be estimated in the absence of actual measurements of PAH concentrations.

K_{OC} is one of the central features of the EP concept as applied to the distribution of organic chemicals in the environment. Eqn. (2) implies that f_{OC} is the only sediment property that

influences sorption of HOCs to sediment. However, in several situations the use of K_{OC} fails to adequately describe experimental and field data (161, 162), namely:

1. f_{OC} is so small that partitioning to organic matter no longer dominates over sorption to the mineral constituents of sediments.
2. levels of dissolved organic matter (DOM) are sufficiently high that partitioning to DOM is significant.
3. partition is not at thermodynamic equilibrium because of slow desorption kinetics.
4. different types of organic matter may have different affinities for HOCs (i.e. different K_{OC} values).

In the case of PAHs derived from combustion sources, there is an abundance of evidence that the K_{OC} concept is inadequate (82, 145, 161-166). The evidence includes lower-than-predicted aqueous concentrations of PAHs (82, 145, 162), reduced availability of PAHs to biota (96, 152), lack of a correlation between PAH concentrations and f_{OC} (164, 166), and seasonal and spatial variations in K_{OC} (161, 165). Recently Gustafsson *et al.* demonstrated that modifying eqn. 2 by adding a term to describe partition to soot (i.e. K_{SC} x f_{SC}; where K_{SC} is the soot-carbon-normalized sediment-water partition coefficient, and f_{SC} is the weight of soot carbon as a fraction of the total dry weight of the sediment) successfully described PAH partitioning between water and sediments (163).

1.4.7.4 Biota

Accumulation of PAHs in biota is important because of the potentially toxic effects of PAHs on indigenous species, and also the possible health risk to humans if species with PAHs in their tissues are consumed (56). Accumulation of PAHs in biota is driven by partitioning to the lipid

content of organisms, in much the same way that accumulation of PAH in sediments is driven by partitioning to f_{OC} (37, 56, 74). Accumulation of a chemical from the water is termed *bioconcentration*, and the bioconcentration factor (BCF) is defined as the ratio of the chemical concentration in the organism, divided by the chemical concentration in the water (74, 167, 168). Like K_{OC} and K_{OW}, BCF is a distribution coefficient between an aqueous phase and a hydrophobic organic phase. Hence, BCF is positively correlated with K_{OW} (167-169).

Bioaccumulation is a more general term that refers to accumulation of a chemical from all sources in the environment including air, water, sediment, and food (170, 171). When the sediment is the dominant route of PAH uptake, the biota-sediment accumulation factor (BSAF), as defined in eqn. 4, can be used to describe the partition process:

$$BSAF = \frac{C_B \times foc}{Cs \times f_L} \qquad \text{eqn. (4)}$$

where C_B is the chemical concentration in the biota and f_L is the fractional lipid content of the biota (127, 172). Because the PAH is partitioning to an organic phase in both the sediment and biota, BSAF is, according to the EP theory, independent of K_{OW} (126, 168). This prediction has not always been borne out in field studies (126, 127).

Biomagnification refers to the enrichment of a chemical in the higher trophic levels of a food chain (170, 171). This enrichment may be due to the fact that f_L often increases up the food chain. Alternatively, digestive processes in the gastrointestinal tract may create a fugacity gradient that drives uptake of the chemical into biota (173). Because higher organisms metabolize PAHs efficiently (2, 14, 22), bioaccumulation is minimal in higher organisms (74, 130) and therefore biomagnification of PAHs does not occur. Mollusks, microalgae and many other less

developed organisms do not metabolize PAHs efficiently, and bioaccumulation of PAHs by these species is significant (37, 74, 127).

In the aquatic environment, biota may accumulate HOCs, including PAHs, from water, sediments, and food (174-176). Since PAHs partition into many environmental compartments, it can be difficult to determine from which compartment an organism is accumulating its PAH burden (130). Feeding strategy can influence both uptake route and degree of accumulation (130, 153, 177). Hickey *et al.* (177) showed that the deposit feeding clam, *Macomona liliana,* accumulated higher PAH levels than did a filter feeding clam, *Austrovenus stutchburyi*, inhabiting the same sediments. Reduced bioavailability of PAHs (e.g. because of partitioning to DOM, or kinetically-limited desorption from sediments) will reduce uptake into biota (153, 154). Accumulation may also be affected by breeding status, organism health, pre-exposure to enzyme-inducing chemicals, and environmental factors including temperature, dissolved oxygen and food supply (38, 169).

Organisms which do accumulate PAHs, especially mollusks, have been widely used as biomonitors of PAH contamination in the environment (38, 56, 178). Some advantages of using biomonitors include (37, 179, 180):

1. The elevated levels of PAH accumulated in biota are simpler to analyze than trace PAH levels in seawater.

2. Biomonitors provide a time-integrating capacity that can smooth out short term temporal variations in contaminant concentrations.

3. Biomonitors provide a measure of bioavailable contaminant concentrations. This may be a more relevant measure of actual exposure and associated risk to environmental health than a measurement of total contaminant concentration would be.

Depuration of PAHs from biota may be a passive equilibrium process, or it may be an active process involving extensive metabolism of the PAHs (37, 111).

1.5 PAHs and people: Routes of exposure and toxic effects

Because of the global distribution of PAHs, the human population is exposed to trace levels of PAHs in the environment (181). Thus, the PAH metabolite 1-hydroxypyrene is found in low levels in urine from individuals without any known exposure to elevated levels of PAHs (182). The highest levels of human exposure to PAHs have been associated with certain occupations (e.g. workers in mines, coking facilities and steel or aluminum smelters), and medical treatments involving coal tars (e.g. treatment of psoriasis) (183-187). Poor air quality associated with primitive cooking and heating methods or urban environments is probably the greatest route of exposure to elevated PAH levels for the general population (188-192). Tobacco smoking, and foods are other major exposure routes for the general population (8, 181, 193).

PAHs have been detected in a number of commercial food products including vegetables, meat, smoked fish and shellfish, liquor and beer (8, 181, 194-198). The PAHs in foods may be present in the raw product, they may be transferred from contaminated packaging, or they may be introduced during the cooking process (8, 181, 198, 199). Leafy vegetables provide the greatest PAH burden in the average human diet (8, 181). It is likely that these PAHs arise from atmospheric deposition onto the leaf surfaces (181).

The effects in humans of exposure to PAHs may include various forms of cancer (e.g. lung, bladder, stomach, colo-rectal) (186, 200-202), immuno-supression (187, 203) and enzyme induction (204-206). Assessment of whether a chemical is a human carcinogen is a difficult

process. The International Agency for Research on Cancer (IARC) (207) concluded that available data were inadequate to determine whether PAHs are carcinogenic in humans. However risk assessments performed under the CEPA and by the US EPA classified several PAHs as "probable human carcinogens" (8, 208).

One of the earliest reports of cancer associated with occupational exposure to PAHs is due to the British physician Percival Pott, who in 1775 reported scrotal cancer in London chimney sweeps (209). In modern times, epidemiological evidence points to elevated lung and bladder cancer risk for workers who are occupationally exposed to PAHs through processes such as iron or steel founding, coke or aluminum production, coal gasification and diesel combustion (186, 210). For workers in these industries, exposure to PAHs is correlated with elevated urinary PAH metabolites (185, 210-212), elevated PAH-DNA or PAH-protein adducts (185, 210) and subtle immunosupressive effects (187).

PAHs are responsible for the majority of the carcinogenic effect of tobacco smoke (211). Tobacco smoke is considered an occupational lung carcinogen, and is also a risk factor for bladder and colo-rectal cancer (200-202). Smokers have elevated urinary 1-hydroxypyrene levels and elevated PAH-DNA adduct levels compared with non smokers (182, 213), and the effects of smoking can be additive with those from other sources of PAH exposure (185, 200). Smokers have also been shown to possess significantly higher aryl hydrocarbon hydroxylase activity (206).

Overlapping causes make it difficult to estimate the effects of low-level environmental exposure to PAHs (189, 201). Nevertheless, Binkova *et al.* reported a significant correlation ($r=0.71$, $p>0.001$) between PAH exposure and levels of DNA adducts for women from polluted and unpolluted areas in Bohemia (188). Mumford *et al.* studied residents of Xuan Wei county,

China, who are exposed to elevated levels of PAHs in unvented smoke from cooking and heating (190). This population was found to have elevated levels of urinary PAH metabolites, and PAH exposure may contribute to their high lung cancer mortality rate, which is five times the Chinese national average.

1.6 Regulation of PAHs

Because PAHs are both abundant and carcinogenic, many government regulations and guidelines have been written with respect to PAHs in an effort to protect human and environmental health. The first step in this process often involves placing compounds on a list that recognizes their toxicity. The US EPA lists 16 PAHs amongst their 129 priority pollutants (214), and these compounds are illustrated in Figure 1-1. CEPA lists PAHs as a class on its Priority Substance List (8), and further, identifies benzo(*a*)pyrene, benzo(*b*)fluoranthene, benzo(*k*)fluoranthene, benzo(*j*)fluoranthene and indeno(1,2,3-*cd*)pyrene as being substances that *"may constitute a danger in Canada to human life or health."* Guidelines (which are not legally enforceable) that recommend "safe" maximum levels for PAHs in soil and water have been promulgated by the Canadian Council of Ministers of the Environment (CCME), and various Canadian provincial environmental ministries. Values from CCME and the British Columbia Ministry of the Environment (BCMOE) are listed in Table 1-3. Long *et al.* (95) have published effects-based sediment quality guidelines for marine sediments. These guidelines are based on a literature review of pollutant concentrations and resulting effects on biota, and consist of effects-range-low values (ER-L; defined as that concentration of pollutant in sediments below which minimal adverse effects on biota are expected), and effects-range-median values (ER-M; that concentration of pollutant in sediments above which adverse effects on biota are expected to occur frequently). ER-L and ER-M values are listed in Table 1-3. It is worth noting that many of the 'effects endpoints' used in the studies Long *et al.* reviewed were measurements of acute toxicity arising from short-term exposures. The ER-L and ER-M values therefore may not

adequately represent chronic toxic effects (e.g. cancer) arising from long-term exposures to PAHs.

Table 1-3 Guidelines for safe levels of PAHs in sediments and water.

Compound	Long *et al.* sediment quality criteria		CCME/BCMOE† assessment criteria	
	ER-L (ng/g)	ER-M (ng/g)	Water (µg/L)	Soil (ng/g)
naphthalene	160	2100	0.2	100
acenaphthene	16	500	*6*	*100*
acenaphthylene	44	640	-	*100*
fluorene	19	540	*12*	*100*
phenanthrene	240	1500	0.2	100
anthracene	85.3	1100	-	*100*
pyrene	665	2600	0.2	100
fluoranthene	600	5100	*0.2*	*100*
benzo(*a*)anthracene	261	1600	0.01	100
chrysene	384	2800	-	*100*
benzo(*a*)pyrene	430	1600	0.01	*100*
benzofluoranthenes*	-	-	0.002	*100*
indeno(1,2,3-*cd*)pyrene	-	-	0.01	100
dibenz(*ah*)anthracene	-	-	0.01	100
benzo(*ghi*)perylene	-	-	-	-

* *sum of benzo(b)fluoranthene + benzo(j)fluoranthene + benzo(k)fluoranthene.*

† *Non-italicized figures are the CCME Interim Remediation Criteria for Soil. Italicized figures are equivalent BCMOE values from "Criteria for managing contaminated sites in British Columbia."*

1.7 Techniques for the analysis of PAHs

Specific extraction and cleanup techniques used in the analysis of PAHs from environmental samples will be discussed in subsequent sections of this chapter. This section is limited to the analytical tools used for direct identification and quantitation of PAHs as individual compounds, or as mixtures.

Because PAHs are a large and diverse class of compounds, chromatography has played an important role in the analytical chemistry of PAHs. Thin layer chromatography (TLC), gas chromatography (GC), high performance liquid chromatography (HPLC), and more recently capillary electrophoresis (CE) have been used to separate PAHs from complex environmental matrixes, and from other isomeric PAHs (6, 52, 101, 215-222). TLC is still used in some specific applications (e.g. separation of PAH-DNA adducts) (52, 101), but GC and reversed-phase HPLC are the methods of choice. GC typically provides better theoretical resolution than HPLC, but the unique shape recognition properties of some LC stationary phases (notably polymeric silica-bonded octadecylsilanes (C_{18})) provide better separation of some isomeric PAHs than can be achieved by GC (216, 219). Isomer separation is critically important because PAH toxicity can vary drastically amongst isomers. The role of temperature is critical in the HPLC separation of PAHs on polymeric C_{18} phases (222). Separation of PAHs by CE is still somewhat at the developmental stage, and has been hindered by the fact that CE typically operates with aqueous mobile phases, while PAHs are very insoluble in aqueous systems. CE does have several theoretical advantages over GC and HPLC, including greater theoretical chromatographic efficiency. Thus, CE may be expected to be widely applied to analysis of PAHs in environmental samples in the future.

Detection systems commonly used in PAH analysis include flame ionization (FID) and mass spectrometry (MS) for GC analysis (6, 216, 219), and ultra-violet/visible (UV), photodiode array (PDA), fluorescence, and (less frequently) MS for HPLC analysis (218, 219, 223, 224). Detectors such as FID and UV are relatively inexpensive and robust, but they provide limited compound specificity, and are relatively insensitive. PAHs must be identified by comparing their retention times to those of pure standards. This is a severe limitation because for many PAHs, pure standards are not commercially available. Furthermore PAHs may co-elute with other compounds, which can cause errors in quantitation or identification of PAHs in environmental samples.

When available, the GC detector of choice is MS. In addition to providing improved sensitivity compared to FID, MS provides structural information to confirm identification of the analyte. It is worth noting that because many isomeric PAHs exist, and because unsubstituted PAHs typically form molecular ions only, MS typically does not provide as high a degree of confidence in identification of PAHs as it does for many other compounds. Recently, attempts have been made to overcome this by using CI-MS and tandem-MS techniques that exploit differences in chemical reactivity between PAH isomers (225, 226).

The inherent luminescence of PAHs has meant that UV-visible spectrophotometry and fluorescence spectoscopy have been widely used in PAH analysis (6, 218, 219, 223). Single wavelength UV detection has largely been superseded by PDA detectors (which provide a higher level of specificity), and fluorescence detection. When using fluorescence detection, careful selection of the excitation-emission wavelength pairs is necessary to optimize sensitivity and compound specificity (227). Because the fluorescence signal is proportional to the incident

radiation flux, use of high irradiance UV lasers can provide exceptional sensitivity in PAH analysis.

Ultra-high resolution fluorescence spectroscopy using crystalline alkane matrixes and low temperatures (Shpol'skii spectroscopy) resolves fine structure from the broad band fluorescence emissions typically seen at room temperature (179, 228). This fine structure can be sufficiently diagnostic to allow identification of PAHs without prior chromatographic separation. While this method has been applied by some authors to the analysis of PAHs in environmental samples (179), the instrumentation is not commercially available and the technology at this stage is insufficiently robust for routine application.

Synchronous fluorescence spectroscopy (SFS) was developed by Vo-dinh (229) and Lloyd (230), and it is becoming popular for the analysis of PAH metabolites in environmental samples (231-233). SFS has been used both with and without prior chromatographic separation of the PAHs (231, 232). In SFS both the excitation and emission monochromators are scanned with a constant wavelength difference between them. The resulting spectrum, which often consists of a single peak, is simpler than a conventional fluorescence spectrum, and the wavelength corresponding to the peak maximum is used to uniquely identify the PAH metabolite.

Recently, GC coupled to isotope ratio mass spectrometry has been used in PAH analysis (234, 235). This technique facilitates determination of the $^{13}C/^{12}C$ ratio of each PAH. The $^{13}C/^{12}C$ ratio can be used to distinguish between different sources of PAHs.

1.8 Analysis of PAHs in environmental matrices

1.8.1 Analysis of PAHs in aqueous samples

It is often suggested that water is the easiest environmental matrix to analyze (236), because it is relatively homogeneous and the low levels of co-extracted material eliminate the need for further cleanup of the extract. However, the extreme insolubility of most PAHs, (especially HPAHs) causes problems including: requirements for preconcentration of the analyte from the water, highly sensitive and specific detectors, and the need to eliminate trace contamination during sample processing (possibly necessitating the use of a clean room for sample workup). In addition, PAHs will preferentially partition onto particles, DOM, or other surfaces (including glass, teflon and stainless steel), making estimation of truly dissolved PAH concentrations problematic. Lopez-Garcia *et al.* (237) monitored recovery of PAHs spiked into 1 L of water as a function of storage time and observed losses of up to 90% over periods as short as 60 hr. The losses were overcome by addition of 40% acetonitrile, or Brij-35 (a detergent) at a level above the critical micelle concentration. Addition of an organic modifier to the water sample prior to storage or analysis is often done to prevent analyte adsorption; however, this may be expected to alter the equilibrium between freely dissolved PAHs and those bound to particles or dissolved organic matter. Information on PAH phase association is often an important consideration, being critical in the development of PAH fate models. Even filtration must be undertaken with care, as dissolved-phase PAHs have been shown to adsorb to several types of filter (238).

The traditional methods used to extract organic compounds from water include partitioning the analyte between water and an organic solvent, either by shaking a flask containing both phases (146, 216), or by using a continuous liquid-liquid extractor, in which the organic phase is continually cycled though the water (239). Ultrasound has also been used to speed up

partitioning (240). Semi-permeable membrane devices (SPMDs) including dialysis membranes have been used to extract PAHs from bulk water (241-243), although extraction of HPAHs by these devices may be kinetically limited (242).

Solid phase extraction (SPE) is a promising alternative to liquid-liquid extraction that has become increasingly popular over the last decade (241, 244), and has recently been included in US EPA mandated methodologies (e.g. US EPA Method 525.1 using SPE discs). SPE involves extraction of the analyte from water by adsorption onto a solid surface (e.g. silica, teflon, styrene-divinylbenzene, polyurethane foam). The modes of SPE available include large resin-packed columns (132, 239, 242, 245) applicable to large volumes of water, membrane discs (241), small SPE cartridges which have been utilized in the analysis of body fluids such as urine and bile (232, 246), and solid phase microextraction (SPME) (241, 247). The SPE techniques described above can be applied to aqueous samples from a few milliliters up to thousands of liters. When combined with in line filtration, SPE techniques can allow freely dissolved and particle-bound PAHs to be distinguished.

1.8.2 Analysis of PAHs in sediments

Prior to extraction, soils and sediments are usually dried, either by grinding with Na_2SO_4 (64), air drying (248, 249) or freeze drying (250, 251), although some methods extract the wet sediment directly (6).

The sediment may be agitated with solvent to extract the PAHs, using either mechanical shaking, ultrasonic extraction (USE), or microwave assisted extraction (249, 252, 253). These techniques usually involve several cycles of extraction with fresh solvent to facilitate complete extraction. Alternative methods, which are less labor intensive, include soxhlet extraction, supercritical fluid

extraction (SFE) and accelerated solvent extraction (ASE) (248, 250, 251, 253). SPME has also been applied to extraction of PAHs from soils, sludges and air particles (254, 255).

Soil and sediment extracts often contain high levels of organic compounds which would interfere with the analysis of PAHs, and these must be separated from the PAHs before analysis. Adsorption chromatography is most commonly used for this purpose, utilizing sorbents such as alumina, silica and Florisil (248, 250, 251). Liquid-liquid partition (6), C_{18} cartridges (251), and size exclusion chromatography (SEC) using Sephadex LH20 have been used also (6, 248).

1.8.3 Analysis of PAHs in biological materials

Some schemes for extraction and cleanup of PAHs from biological materials are identical to schemes used for the analysis of sediments, i.e. drying the sample, extraction, adsorption chromatography (256, 257). A common alternative procedure involves saponification of the wet sample by using potassium hydroxide and methanol or ethanol, followed by liquid-liquid partition (usually several stages thereof) to recover the PAHs, and sample cleanup utilizing adsorption chromatography. Often adsorption chromatography is insufficient to deal with the high lipid content of biological samples, and a SEC cleanup step is required. Sephadex LH20 (218, 258), Biobeads SX-3 (259-261) and Biobeads SX-8 (218, 257) are commonly used. Donor-acceptor complex chromatography has also been used for lipid removal (262).

1.8.4 Analysis of PAHs in air

PAHs in the atmosphere exist in both the vapor phase and associated with particles (131-133). Therefore sample collection methods that preserve the PAH particle associations are required. Typically these methods involve a glass fibre filter to collect air particulate matter, and a sorbent train (e.g. polyurethane foam, tenax GC or XAD-2 resin) to adsorb vapor phase PAHs (132-134).

Although sample collection methods that employ only filters and no sorbent trap have been used (57, 263, 264), these methods may under-represent LPAHs due to the significant partitioning of LPAHs into the vapor phase.

The PAHs are extracted from the filter and the sorbent by using Soxhlet (132, 133, 263, 265), SFE 217, 264) or USE (57, 217). In some instances it has proven difficult to achieve quantitative extraction of PAHs from air particulate matter (264, 266). This may be because PAHs associated with combustion generated particles may be encapsulated within the particle itself (137, 138).

Clean-up of PAH containing extracts from air particulate matter can be achieved by using protocols similar to those applied to sediment extracts i.e. liquid/liquid partition, adsorption chromatography and/or SEC (6, 133, 265).

1.9 Objectives of this thesis

This thesis focuses on two related areas of the environmental chemistry of PAHs. In the first part, the distribution of PAHs in marine sediments from a contaminated fjord system near Kitimat, BC, Canada is examined. The spatial distribution of PAH contamination is explored in terms of both proximity to known sources, and bulk environmental transport processes (such as movement of air and water). Differences in the composition of the PAH burden between different sites, and with increasing depth in the sediments, are also examined. Changes in PAH composition may indicate a mixing of two different PAH sources (e.g. anthropogenic inputs vs. natural inputs, local sources vs. long range transport). Changes in PAH composition may also provide insight into the specific environmental processes that act upon the PAHs. For example, loss of PAHs from

sediment due to water washing will preferentially remove low molecular weight species, leaving a PAH profile in the sediment enriched in HPAHs. Alternatively, photo-oxidation would be expected to preferentially degrade PAHs containing the anthracene skeleton (10).

Interactions between PAHs and a sentinel bivalve, *Mya arenaria*, are described in the second part of this thesis. Studying the interactions between PAHs and biota is important because an environmental pollutant is essentially defined by its adverse effect on biota. Simply demonstrating that potentially toxic chemicals are present at elevated levels in a given ecosystem, doesn't in itself indicate an environmental problem.

Mya arenaria were collected from several beaches in the Kitimat fjord system and the PAH levels measured in them and in associated sediments. BSAFs were calculated, and correlations between BSAFs and molecular descriptors such as log K_{OW} were calculated, in order to investigate factors affecting accumulation.

The uptake and metabolism of PAHs by *Mya arenaria* and *Protothaca staminea* was investigated in laboratory studies. Two important questions were addressed: Are mollusks capable of metabolizing PAHs, and if they are, what is the identity of the metabolites formed? Quantitative aspects of metabolite formation were not studied.

2. Polycyclic Aromatic Hydrocarbon Distribution and Composition in Surface Sediments of the Kitimat Fjord System

2.1 A History of Kitimat

The town of Kitimat was incorporated in 1953 following construction of a large aluminum smelter by Alcan Smelters and Chemicals Inc. Kitimat is located at the inland end of a long fjord system on the northern Pacific coast of British Columbia, (Figure 2-1). Prior to the 1950's the area was sparsely populated by aboriginal peoples, farmers and a few ranchers, and commercial fishing was a mainstay of the local economy. With the commissioning of the smelter in 1953, immigrant labor was recruited from Europe (especially Portugal) and south-east Asia, and industry became the major regional employer. Further industrialization has seen the construction of a large Eurocan pulp mill in Kitimat, and more recently the Methanex ammonia and methanol facility. A Statistics Canada survey in 1991 showed the population of Kitimat to be 11,000, of which 1000 are aboriginal.

The Alcan smelter at Kitimat which operates eight potlines, utilizes vertical stud Söderberg electrodes (96, 267, 268). In 1992, this facility produced 272,000 tonnes of aluminum (269). Smelters of this design are known to release substantial amounts of PAHs to the receiving environment because of pyrolysis and volatilization of the pitch/tar anode binder from the Söderberg electrode, and from the handling of pitch and coke on site (60, 151). PAH emissions from the Kitimat smelter peaked at ca. 800 tonnes per annum in the mid 1970's (270).

Improvements to the smelter, including phasing out an old anode paste plant, and replacement of wet potroom scrubbers with more efficient dry scrubber technology, have drastically reduced PAH emissions from the plant. PAH emissions currently are on the order of 60 tonnes per year (269, 271).

The composition of aluminum smelter derived PAHs is characteristically dominated by four to five ring PAHs (fluoranthene, pyrene, benzo(*a*)anthracene, chrysene/triphenylene, benzofluoranthene isomers, benzopyrene isomers), and a predominance of unsubstituted PAHs over alkylated isomers (60, 151, 272).

Inevitably, increased industrialization has been accompanied by environmental problems. Kitimat is geographically isolated by surrounding mountains, that tend to trap pollutants in the head of the fjord system. Several studies have documented elevated levels of PAHs in Kitimat Arm and Douglas Channel (96, 268, 273). Detection of polychlorinated dibenzo-*p*-dioxins in Dungeness crabs from Kitimat Arm led to closure of the local crab and shrimp fishery (*Dr. W. Cretney, pers. Comm.*).

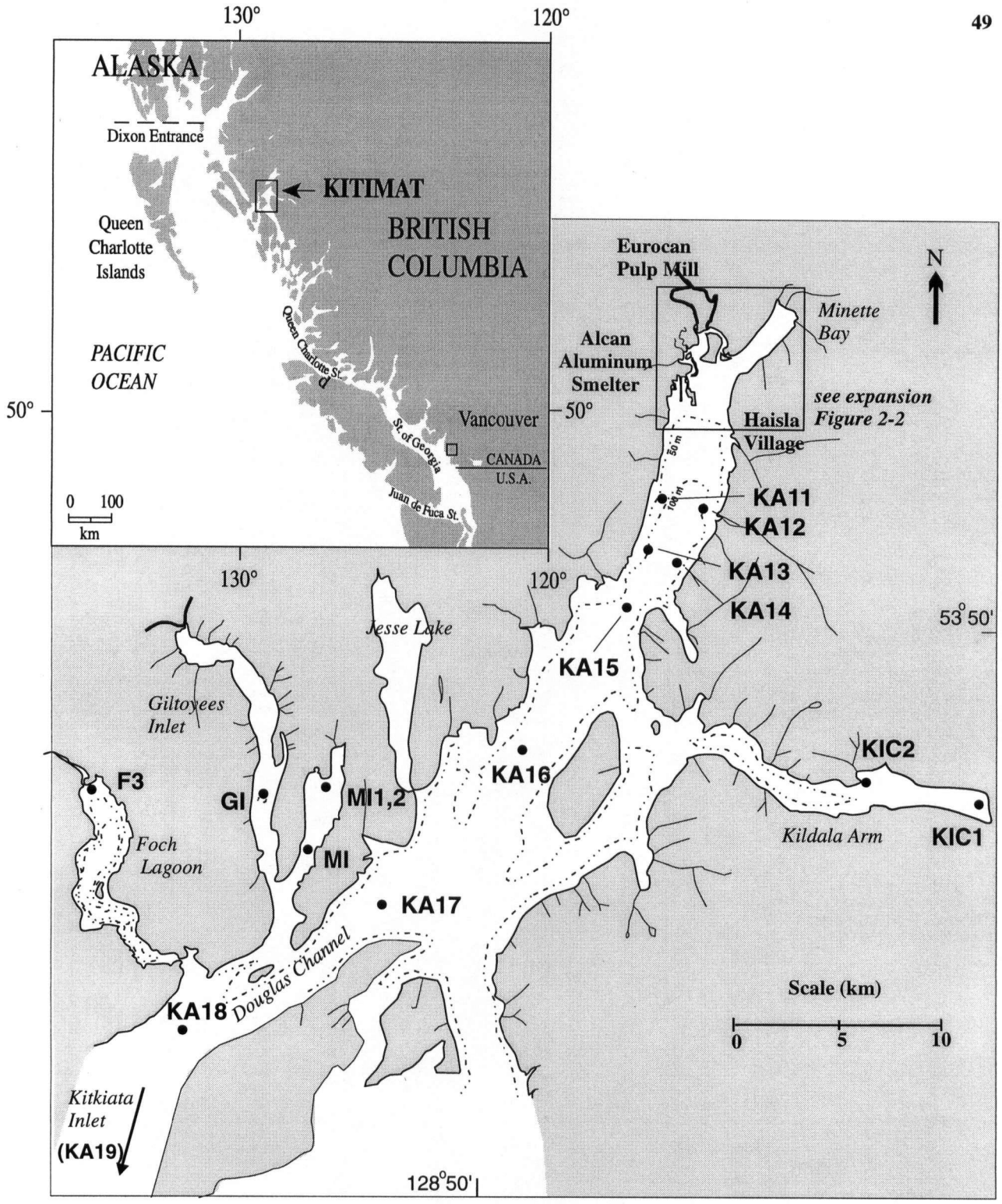

Figure 2-1 Map of Kitimat fjord system showing sampling locations

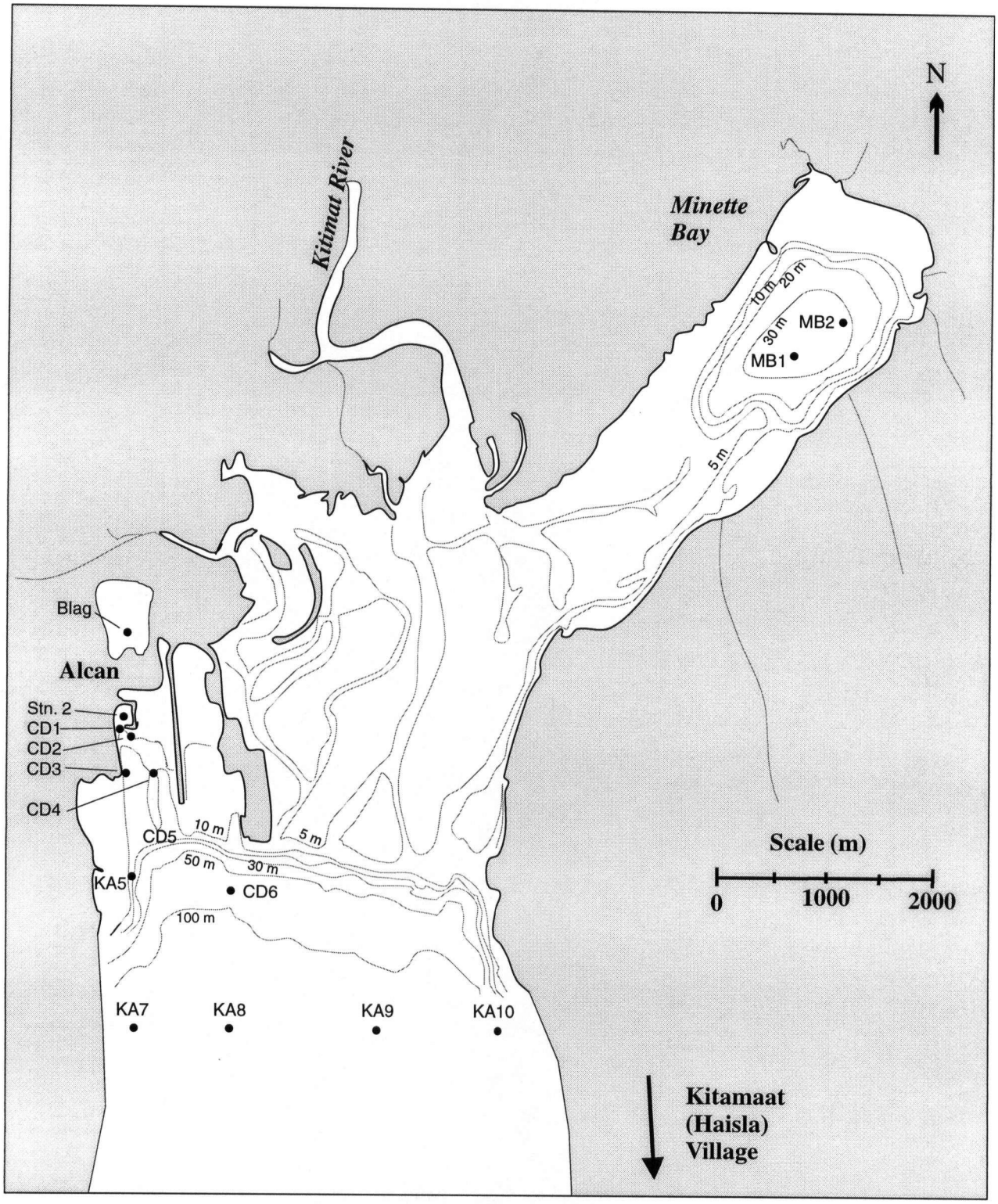

Figure 2-2 Expansion of Kitimat Arm, showing sampling locations.

2.2 Objectives

2.2.1 Analysis of priority pollutant PAHs in marine sediments from Kitimat, BC

Two previous studies, one in the Kitimat fjord system (268), and one in the vicinity of the smelter (96), revealed the presence of elevated levels of PAHs in marine sediments.

The purpose of the present work was to quantify and determine the distribution of the 16 US EPA priority pollutant PAHs within the Kitimat fjord system. In addition, data for some alkylated PAHs was collected for selected samples. A combination of graphical and multivariate techniques were applied to the data in order to provide a characteristic fingerprint of the source, and to identify changes in the PAH mixture as a result of exposure to environmental processes.

2.2.2 Method development for the determination of priority pollutant PAHs in marine sediments

In order to achieve the objectives set out in section 2.2.1, it was first necessary to develop and validate methodology suitable for the analysis of PAHs in sediment. A number of procedures for the analysis of PAHs in terrestrial soils and marine sediments, involving multiple-stage extract cleanup and GC-MS analysis have been reported (216, 219, 265, 274). These methods provide low detection limits and good reproducibility; however, they are expensive and time consuming. Simpler, more cost effective methodologies are required by industry to ensure their compliance with permissible discharge regulations, and by government agencies, academic institutions and private laboratories who are concerned with pollution monitoring and effects on the environment.

Low detection limits are not required for many sites where contaminant levels are high, and features such as high sample throughput and reduced analysis cost are more important. In the present study, analyte levels in Kitimat sediments were known to be relatively high. In addition, contaminant profiles were expected to be complicated, so GC based methodology was preferred over HPLC due to its greater separating ability (narrower peak widths). Unfortunately, for most of the present work, routine access to sensitive GC-MS instrumentation was not available, and we were limited to using GC with a flame ionization detector. Thus we set out to develop a simple cost efficient procedure for the analysis of PAHs in sediment samples, within the constraints listed above.

2.3 Experimental

2.3.1 Optimization of instrument operating conditions

GC with FID detection was used routinely for the analysis of PAHs in extracts from marine sediments during this work. GC with ion-trap MS detection was used for the sediment and clam extracts described in Chapter 4. HPLC with UV-visible and fluorescence detection was used for the analysis of PAH metabolites in extracts from seawater and biological samples. Chromatographic conditions had to be established for both HPLC and GC to ensure adequate separation of the PAHs and PAH metabolites being analyzed. This was accomplished by using solutions of authentic pure standards or standard mixtures. Detection systems were optimized while considering detection limit, precision, and detector lifetime. Instrumental detection limits and analytical figures-of-merit for analysis of pyrene on the various instruments used are listed in Table 2-1. The detection limit by GC-iontrap-MS may be improved 1-2 orders of magnitude by using selected ion monitoring, and optimizing filament current and electron multiplier voltage for

maximum sensitivity, at the expense of linear range and electron multiplier lifetime. The detection limit by HPLC-fluorescence may be improved by at least one order of magnitude by increasing the gain on the photo-multiplier. The concentration detection limit is quoted for standard injection volumes (2 μL for GC, 25 μL for HPLC), and these could be improved by about one order of magnitude in each case simply by increasing the injection volume. It should be noted that typically in environmental analysis the achievable detection limit (in ng analyte per g sample) is strongly influenced by co-extractives from the sample matrix (and hence the choice of sample pre-treatment method), and may be several orders of magnitude poorer than the instrumental detection limit.

Table 2-1 Analytical figures of merit for the analysis of pyrene, obtained on the instrumentation used in this work.

Instrument	Mass detection limit* (pg)	Concentration detection limit* (ng/mL)	Linear range (pg)	Precision**
GC-FID	1000	500	1000 - 100,000	20%
GC-MS (scan mode)	1	0.5	4 - 40,000	7%
HPLC-UV	120	5	2,400 - 40,000	12%
HPLC-fluorescence	20	0.8	20 - 40,000	6%

* *Defined as that amount of analyte which would generate a signal equal to three times the standard deviation of the signal in the absence of any analyte (noise).*

** *Determined as the relative standard deviation of three successive injections of the analyte*

Typical gas chromatograms (obtained by using GC with FID detection) for a standard mixture of PAHs, and a PAH containing sediment extract, are included as Figure 2-3.

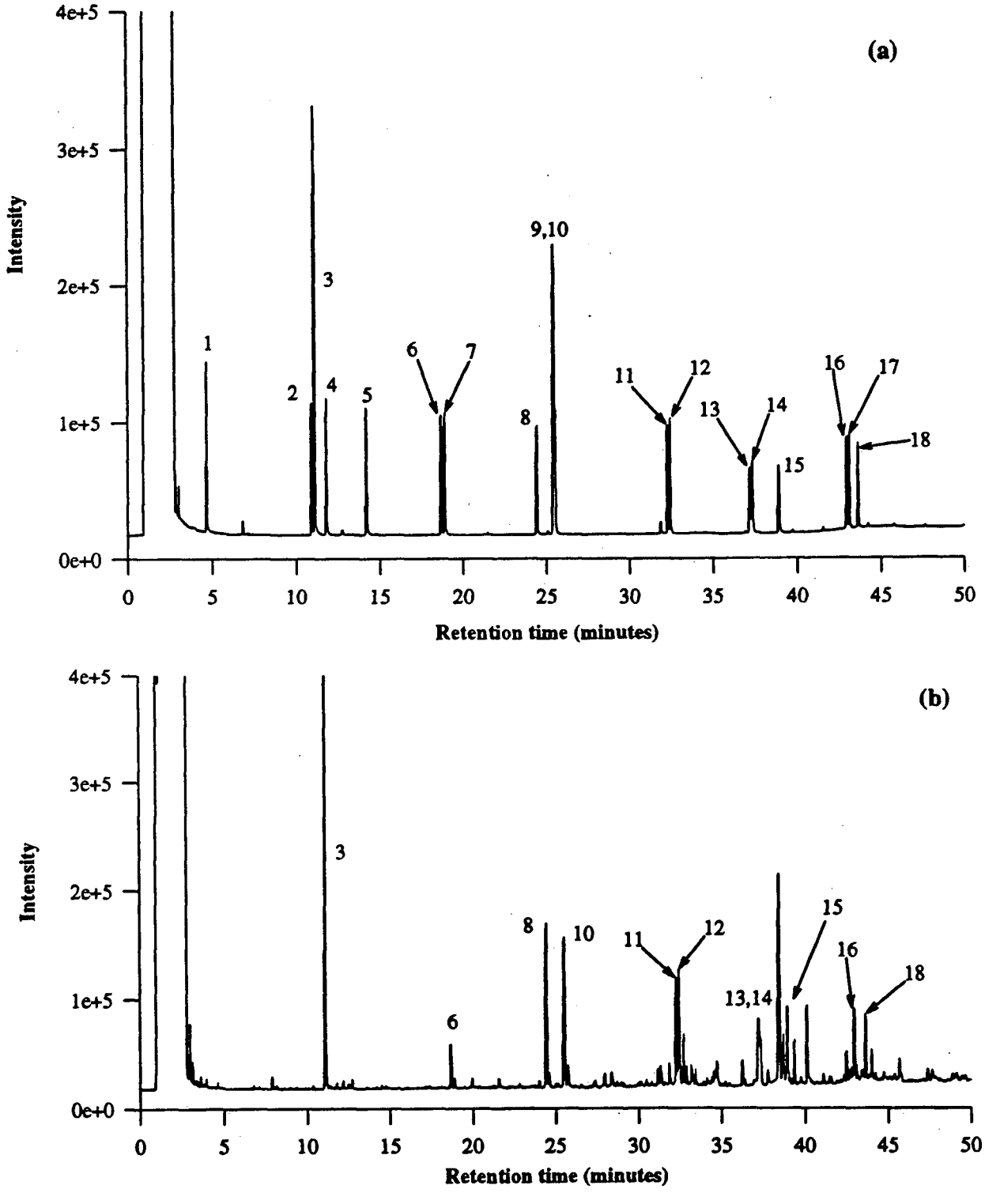

Figure 2-3 Gas chromatograms (FID detection) of (a), PAH standard mixture, and (b), PAH-containing sediment extract.

Compound identification: 1, naphthalene; 2, acenaphthylene; 3, hexamethylbenzene; 4, acenaphthene; 5, fluorene; 6, phenanthrene; 7, anthracene; 8, fluoranthene; 9, d_{10}-pyrene; 10, pyrene; 11, benzo(a)anthracene; 12, chrysene; 13, benzo(b)fluoranthene; 14, benzo(k)fluoranthene; 15, benzo(a)pyrene; 16, indeno(1,2,3-cd)pyrene; 17, dibenz(ah)anthracene; 18, benzo(ghi)perylene;.

2.3.2 Materials

Sodium sulfate (assurance grade) was obtained from BDH Chemicals Ltd. It was pre-cleaned by baking at 600 °C for 6 hours. Florisil (60-100 mesh) was obtained from Fisher Scientific, and was activated at 350°C for six hours and 2% deactivated with distilled water prior to use. Octacosane and hexamethylbenzene were obtained from Eastman-Kodak. A standard mixture containing the 16 US EPA priority pollutant PAHs (2000 μg/mL) was obtained from Supelco. This stock solution was diluted as necessary to make calibration solutions for GC analysis. Pyrene (99%), benzo(*e*)pyrene (99%), benzo(*a*)pyrene (98%) and perylene (99%) were purchased from Aldrich. Retene (98%) was purchased from ICN Biomedical. All solvents were obtained from Fisher Scientific, and were HPLC grade.

2.3.3 Sample collection and preparation

Surface sediment samples (ca. 15 cm depth) were collected from sites within the Kitimat fjord system (illustrated in Figure 2-1 and Figure 2-2) by using Smith-McIntyre or Petite Ponar grab samplers. Three grab samples from each site were mixed thoroughly, and sub-samples of the mixture were transferred to 1 L pre-cleaned and oven-baked amber glass bottles and frozen for transport back to the UBC laboratory. The mixing of three grab samples helped to minimize within-site variability, and ensured that the sediment collected was representative of each site.

The samples were freeze dried, and after removing any stones and pebbles with metal tweezers, the resulting powder was ground and re-mixed by using a mortar and pestle to ensure sample homogeneity. Sub-samples (ca. 10-20g) were then weighed out into glass extraction thimbles, covered with ca. 2g anhydrous sodium sulfate, and Soxhlet extracted with methylene chloride (130 mL) for 8 hours. Prior to extraction a quantification standard (QSTD), hexamethylbenzene,

was spiked onto the samples. The extract, in a round bottom flask, was then concentrated under reduced pressure (300 mtorr) to ca. 0.5 mL by using a rotary evaporator equipped with a dry ice/acetone condenser. The water bath was maintained at 30 °C.

In a modification of the procedure used by Brown and Maher (250), sodium sulfate (2g) was then poured onto the concentrated extract. The extract was adsorbed onto the sodium sulfate and the solvent was removed under a gentle stream of nitrogen. This step is necessary to completely remove the methylene chloride, as this solvent does not allow an adequate separation of the aliphatic fraction from the aromatic fraction on the Florisil columns. Evaporation of the methylene chloride without the presence of an adsorbent results in substantial and uncontrolled losses of the more volatile PAH. The adsorbed extract was added to a 1.2 cm diameter glass chromatography column that had been slurry packed with 3 g Florisil in hexane. To achieve quantitative transfer of the extract onto the column, two 1 mL aliquots of hexane were used to clean the round bottom flask, and these washings were used to wash the extract onto the Florisil. If the extract is not washed onto the Florisil with the washings from the round bottom flask, the PAHs desorb from the sodium sulfate into the eluent reservoir when the eluent is added, and elute in a broad band which is not resolved from the hydrocarbon fraction. The PAHs were sequentially eluted with 15 mL of hexane and 25 mL of a 1:1 (v:v) hexane:methylene chloride mixture. The first 8 mL of eluent which contained a large amount of the aliphatic material was discarded. Careful separation of the bulk of the aliphatic material from the analytes by using this procedure is critical if a non-selective GC detector such as an FID is to be used for quantification.

The eluent containing the analytes was then concentrated under reduced pressure (ca. 95 mtorr) to ca. 0.5 mL on the rotary evaporator. Toluene (2 mL) was added as a 'keeper' solvent, and the

remainder of the hexane and methylene chloride was evaporated. The final extract was pipetted into a glass vial; the round bottom flask was rinsed twice with 0.5 mL washings of toluene; the rinsings were added to the sample vial; and a recovery standard (RSTD), octacosane, was added to the vial.

2.3.4 Sample analysis

For routine analysis the sample was injected splitless into a Hewlett Packard 5890 gas chromatograph (GC) equipped with a flame ionization detector (FID). The injector was held at 300°C and purged with He after 1 minute to minimize tailing of the solvent peak. The analysis was carried out by using a 30 m FSOT PTE-5 capillary GC column (Supelco Ltd.; 0.32 mm internal diameter, 0.25 μm stationary phase), He carrier gas (45 cm/sec flow rate), and the oven was programmed as follows: initial temperature 100°C for 4 min.; 5°C/min. to 200°C, held for 3 min.; 8°C/min. to 250°C, held for 5 min.; 12°C/min. to 300°C, held for 20 min. The detector was held at 320°C. The data were collected and analyzed by using Shimadzu EZChrom™ software (version 3.1), running on a Dell™ 466/m computer. Selected samples were also analyzed by gas chromatography-mass spectrometry (GC-MS) to confirm the identification of the unsubstituted PAHs, and to identify alkylated PAHs (for which authentic standards were unavailable). These extracts were analyzed using a NERMAG R10-10 quadrupole mass spectrometer coupled to a Varian Vista 6000 gas chromatograph. A 30 m FSOT PTE-5 capillary GC column (Supelco Ltd., 0.25 mm internal diameter, 0.25 μm stationary phase) was inserted directly into the ion source. The interface was kept at 300°C, the ion source at 280°C and the injector at 310°C. The GC column and temperature program used were identical with that used for the FID analyses. The mass spectrometer was tuned to unit mass resolution and mass calibrated using a fluorinated alkane standard (FC43). The electron energy was set at 70 eV and the filament current at 0.200

mA. Data acquisition was performed in full scan mode from 100 to 300 a.m.u., scanning every 0.3 seconds. Identification of the alkylated PAHs was based upon their mass spectra. Relative amounts of the alkyl and parent PAHs present in the extracts were quantified by GC-MS for the purposes of determining the alkyl homologue distribution only. Poor sensitivity and drifting instrumental response associated with this GC-MS system meant GC-FID was preferred for all other quantitative measurements. Quantification by GC-MS was achieved by integrating ion-chromatograms of ±1 a.m.u. about the molecular ion mass. Contributions from the (M^+-15) fragment were included for quantifying C_2 and higher alkylated PAHs. Unit responses relative to the parent compound were assumed for all alkylated PAHs.

A response factor mix containing known amounts of the quantitation standard, the recovery standard and the 16 PAHs (Supelco Ltd.) was prepared daily from stock solutions, and analyzed at least three times with every batch of samples to determine retention times and response factors for the various analytes. Individual PAHs were identified on the basis of retention time matches with the standard mixture, or on the basis of mass spectra for the alkylated PAHs. Although benzo(*b*)fluoranthene and benzo(*j*)fluoranthene were adequately resolved in standard mixtures, they were often poorly resolved in sample extracts, due to the presence of a third benzofluoranthene isomer. Hence it was chosen to report a single value for total benzofluoranthene concentration in all samples.

The minimum detectable concentration was defined for each sample as that concentration of analyte which would give rise to the minimum peak area which could be reliably distinguished from the background by the integration software used. This number was typically 50-200 ng/g, and varied from sample to sample as a function of the total amount of extractable material present

in each sample. Apart from trace amounts of naphthalene (typically ca. 0.4 ng), none of the other PAHs were ever detected in blank extracts.

As a further quality control measure, selected samples were analyzed by a commercial laboratory that used standard US EPA protocols. The two sets of data showed good agreement in all cases.

The efficiency with which the QSTD is recovered in each sample can be calculated by comparing the expected concentration of the QSTD, with the concentration of the QSTD calculated relative to the RSTD. Recovery values for the QSTD were typically greater than 90%. The extraction efficiencies for the 16 PAHs were determined by spiking a standard solution of PAHs in toluene onto the surface of a freeze dried marine sediment sample known to be uncontaminated with PAHs. The final concentration was 2 μg of each PAH per g dry sediment. Quantitative recoveries were obtained for all PAHs including the QSTD, with the exception of naphthalene for which the recovery was typically ca. 30%, and no increase in recovery was observed when the extraction time was increased to 16 hours. To account for the loss of naphthalene, a correction factor was applied when the naphthalene concentration was calculated. The incomplete recovery of naphthalene was attributed to evaporative losses. These were minimized by carefully controlling the adsorption of the extract onto sodium sulfate (i.e. do not overdry), and maintaining a slow boiling rate in the rotary evaporator to minimize sample loss due to aerosol formation.

It should be noted that recoveries from a spiked sample may be substantially higher than those from a real sample because PAHs in contaminated sediments are often tightly bound or occluded within particles. This point was addressed by Burford *et al.* in a recent paper (217).

2.3.5 Sediment organic carbon (f_{OC}) analysis

Sediment total carbon was determined as CO_2 after combusting the sediment at 1050 °C by using a Carlo Erba NA-1500 NCS analyzer. Inorganic carbon (as carbonate derived CO_2) was determined by using a Coulometrics model 5010 CO_2 coulometer. Sediment percent organic carbon was therefore calculated as the difference between these two values (total carbon minus inorganic carbon).

2.3.6 Statistical analysis

Principal components analysis (PCA) was performed on the correlation matrix of normalized PAH compositional data by using the SYSTAT 5.0® software package. Prior to analysis, non-detected values in the data set were replaced with computer generated random numbers between zero and the sample-dependent minimum detectable concentration (this was done to ensure the PCA was not influenced by spurious correlations between compounds that were undetected at some sites). Then the data for individual compounds was normalized to the total PAH concentration for each sample to remove the effect of differences between sites in absolute PAH concentration.

2.4 Results and discussion

2.4.1 Florisil column chromatography

Chromatography on silica or alumina is routinely used to remove material from sediment extracts that would otherwise interfere with the analysis of PAHs, and to effect a crude separation of analytes into compound classes. However, these sorbents have been shown to catalyze photo-oxidation of PAHs (275, 276), resulting in decreased recoveries. An alternative sorbent, Florisil, has been used by some workers for cleanup of PAH contaminated extracts (172, 277, 278). Florisil has the advantage of providing good PAH separations on short columns (6), however

Altgelt and Gouw (279) noted that it strongly chemisorbed many aromatic hydrocarbons. This may be overcome by partially deactivating the Florisil with water to selectively block highly active binding sites and thus improve chromatographic performance (215).

In the present work the effect on the PAH elution profile of varying the level of Florisil deactivation was investigated. Eluent from the 3 g Florisil columns was collected in 2 mL fractions, blown to dryness under nitrogen, taken up into 4 mL of acetonitrile, and analyzed for total PAHs by using UV absorbance at 254 nm. For these experiments, the first 8 mL of eluent was not discarded. These results are presented in Figure 2-4. Each curve represents the mean of three independent determinations.

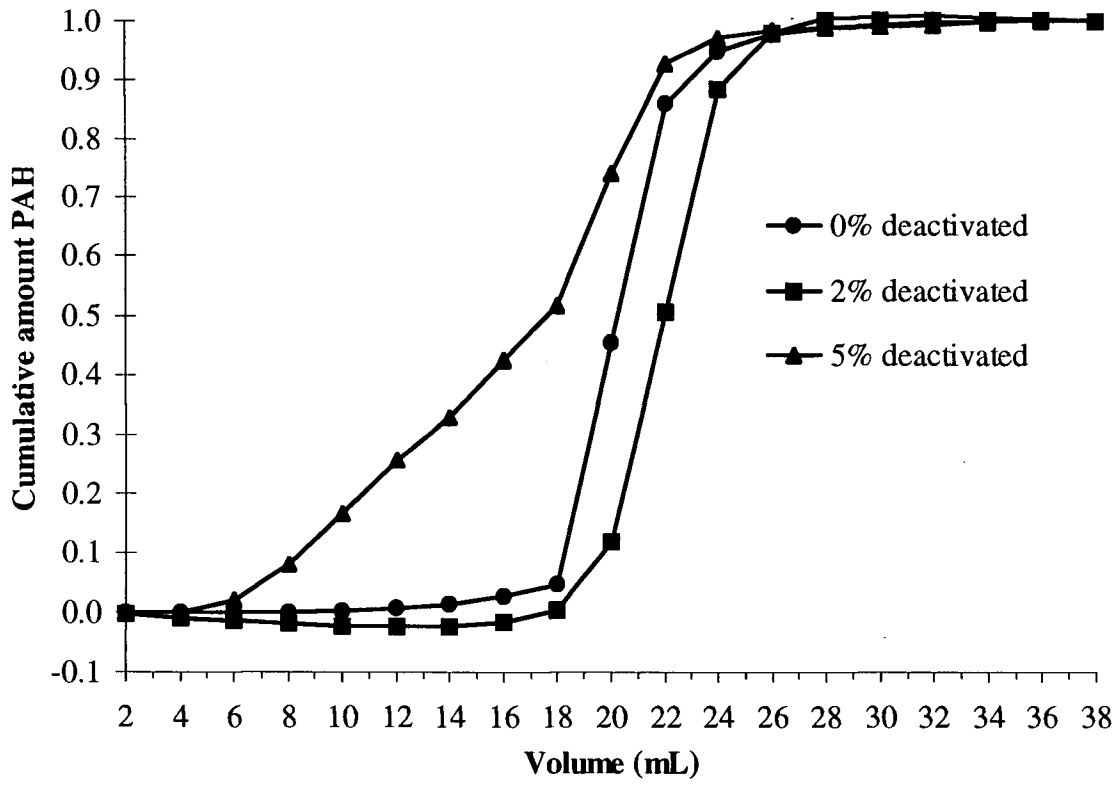

Figure 2-4 Elution of PAHs from Florisil. As the amount of water added to decativate the Florisil is increased, the retention of the PAHs decreases.

There was little difference in the PAH elution profile at 0% and 2% deactivation. However, at 5% deactivation the PAH containing band was substantially broadened and there was poor separation between the PAHs and the aliphatic compounds, most of which elute within the first 6 mL. This trend was most pronounced for 10% deactivated Florisil (data not shown). Although both the 0% and the 2% showed essentially the same elution profiles for the PAHs, the work of Dunn (215) suggested that 2% deactivated Florisil may provide a better separation of the aliphatic interferences from the PAHs. For this reason, 2% deactivated Florisil was used for the rest of this work.

2.4.2 Analysis of a standard reference material

A marine sediment standard reference material (Harbor sediment HS3, NRCC, Canada) was analyzed in triplicate to validate the analytical procedure described in this paper. Samples of the reference material were also analyzed by a local commercial laboratory by using US EPA protocols and isotope dilution GC-MS analysis to provide further validation (216). The results, presented in Table 2-2, are generally in good agreement with the certified values.

The data for the benzofluoranthenes are not directly comparable as the reference material was certified for the benzo(*b*)fluoranthene and benzo(*k*)fluoranthene isomers only, whereas both UBC and the commercial laboratory quote results for the sum of three partially resolved benzofluoranthene isomers. Complete resolution of the benzofluoranthenes is not routinely achieved on traditional capillary GC bonded phases. Values determined in this work for anthracene and fluorene are lower than those certified, as are the results reported by the commercial laboratory. It is unlikely that this represents a systematic error in our methodology, as the commercial laboratory, which also obtained low values for these compounds, routinely has

no difficulty in obtaining the certified values for anthracene and fluorene in other certified reference materials. Therefore, the problem may be specific to this batch of sediment.

Table 2-2 PAH determinations for NRCC Standard reference material HS3 (concentrations in mg/kg dry sediment).

compound	certified (± 90% CI)	This work (± 90%CI)	Commercial[a]
naphthalene	9.0±0.7	9.5±1.4	8.9, 9.1
acenaphthylene	0.3±0.1	0.3±0.03	0.33, 0.35
acenaphthene	4.5±1.5	2.6±0.1	3.7, 3.9
fluorene	13.3±3.1	7.2±0.2	8.7, 9.2
phenanthrene	85±20	73.3±2.0	85, 87
anthracene	13.4±0.5	4.8±0.1	5.9, 8.2
fluoranthene	60±9	56.3±2.5	67, 65
pyrene	39±9	33.8±1.2	39, 40
chrysene	14.1±2	10.8±0.5	14, 15
benzo(*a*)anthracene	14.6±2	14.8±0.5	12, 12
benzofluoranthenes	10.5±3.2[b]	15.1±1.9	18, 17
benzo(*a*)pyrene	7.4±3.6	6.0±0.7	7.4, 5.2
indeno(1,2,3-*cd*)pyrene	5.4±1.3	5.3±0.7	5.4, 4.9
dibenz(*ah*)anthracene	1.3±0.5	1.5±0.4	1.1, 1.0
benzo(*ghi*)perylene	5.0±2.0	4.8±0.8	3.4, 3.6

Abbreviations: CI = confidence interval.

a two independent determinations were carried out by the commercial laboratory.

b sum of benzo(b)fluoranthene and benzo(k)fluoranthene only.

It should be noted that the 90% confidence intervals for our data in Table 2-2 are a measure of the error within a single batch of samples, analyzed on the same day. Variation in instrument

performance and the laboratory environmental conditions from one day to the next contribute to a between-batch error that is substantially higher than the CI values quoted in Table 2-2 for the UBC data. Typically, the between-batch error, which is a more realistic estimate of the total error in this methodology, is ±10-20% for each analyte. Recovery of individual PAHs spiked onto previously uncontaminated marine sediment was greater than 65% for all compounds except naphthalene.

2.4.3 Spatial distribution of PAHs in the Kitimat fjord system

The analytical methodology described in the preceding sections was applied to sediments collected from Kitimat, BC. PAHs (sum of 16 US EPA priority pollutant PAHs) are present in concentrations greater than 2 mg/kg at 16 out of the 25 sites studied. The data are summarized in Table 2-3 and Figure 2-5. For comparison, PAH levels in sediments from several other polluted sites are included in Table 2-4. In contrast, typical 'background' PAH levels found at remote locations, are less than ca. 1 mg/kg, as is seen for the Kildala arm sites in the present study.

To gain some perspective on the significance of such elevated PAH levels, the data in Table 2-3 can be compared with regulatory guidelines as outlined in section 1.6. The five most contaminated sites (BLag, CD1, Stn.2, KA5, KA7) contain total PAH levels in excess of 45 mg/kg which is the effects range median (ER-M) value determined by Long *et al.* (95). In addition, all Kitimat arm sites north of KA16 contain benzo(*a*)pyrene at concentrations in excess of the ER-M for benzo(a)pyrene (1.6 mg/kg). PAH levels of this magnitude would therefore be expected to cause significant adverse effects on aquatic life. In the study by Long *et al.* (95) the incidence of (adverse) biological effects was 80% and 85% for organisms exposed to sediments with either benzo(*a*)pyrene or total PAH levels, in excess of the ER-M values. However, it

should be noted that other authors have noted lower-than-predicted toxicity associated with sediments contaminated with aluminum-smelter-derived PAHs. The CCME and BCMOE interim soil quality guidelines assessment criteria translates to ca. 1.4 mg/kg for total PAHs - a value exceeded by almost every site investigated in this study.

All of the 16 EPA PAHs, with the exception of naphthalene and acenaphthene, are present in the majority of the Kitimat Arm samples. Levels are highest in the head of Kitimat Arm - especially in the vicinity of the aluminum smelter, and decline rapidly with increasing distance from the smelter. This is illustrated in the sequence of sites down Kitimat Arm and Douglas Channel: CD1, KA7, KA13 and KA16, which have total PAH concentrations of 530, 300, 41 and 3.5 mg/kg respectively. Overall, the distribution of PAHs within the Kitimat fjord system is consistent with a major point source from the aluminum smelter. PAH levels in the sediment vary primarily as a function of distance from the smelter as can be seen from Figure 2-5. Sampling locations are illustrated on Figure 2-1 and Figure 2-2.

Exceptionally high PAH levels (10 000 mg/kg) are detected at site BLag. This sediment was collected from one of the settling ponds (the 'B' effluent lagoon) on the Alcan aluminum smelter site. The outfall of this pond flows directly into the harbor. Surface runoff from the northern part of the site and effluent from the anode plant wet scrubbers are directed into this lagoon. In the past, effluent from the potline wet scrubbers was also directed into this lagoon. (The wet scrubbers have recently been replaced by dry scrubbers, which do not generate a liquid waste stream). The lagoon outfall, therefore, is potentially a significant source of PAHs to Kitimat harbor.

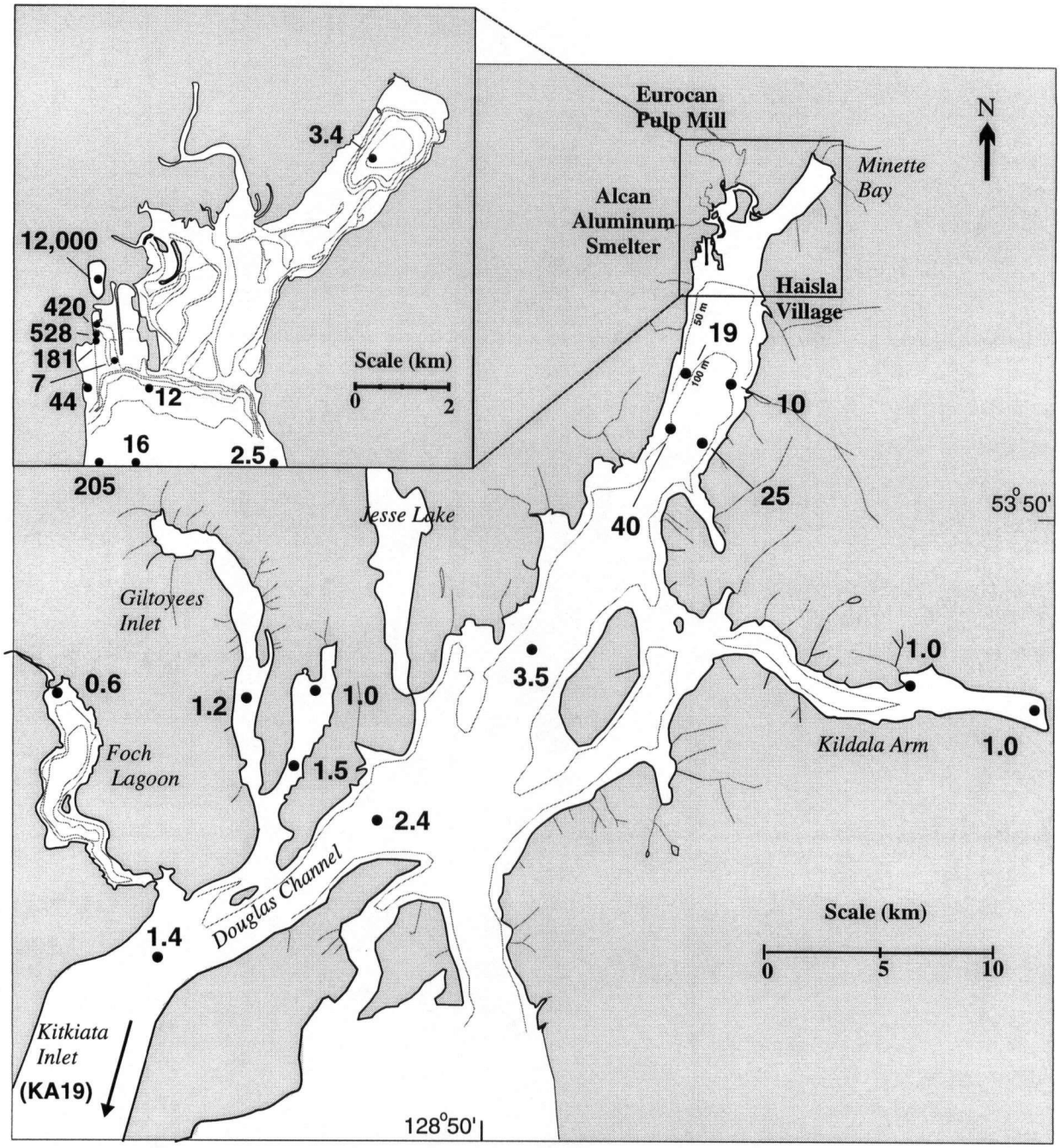

Figure 2-5 *Total PAH concentrations (sum of 16 US EPA priority pollutant PAHs, mg/kg) in sediments from the Kitimat fjord system.*

Table 2-3 PAH levels and sediment properties at sites within the Kitimat fjord system. Concentrations in mg PAH per kg of dry sediment.

site:	f_{OC}	naph	ace	flu	phen	anth	fln	pyr	chry	baa	bxf	bap	ipyr	dib	bper	Σ PAH
MB2	0.017	<0.10	<0.10	NDR	0.25	<0.10	0.29	0.34	0.14	0.55	0.13	NDR	0.53	0.44	0.48	**3.1**
MB2-b	0.018	NDR	<0.10	<0.10	0.11	<0.10	0.17	0.18	NDR	0.26	0.14	NDR	0.33	0.40	0.16	**1.7**
BLag-a	0.150	11	171	314	1475	556	1727	1411	738	616	312	736	959	217	323	**9566**
BLag-b	0.300	12	141	303	2148	734	2668	1818	844	967	614	953	1086	329	944	**13563**
CD1	0.047	0.29	2.1	1.6	17	3.6	37	34	25	34	91	56	93	25	106	**528**
CD2	0.031	0.49	1.8	0.97	9.8	2.2	18	18	11	13	34	20	23	5.7	22	**181**
STN.2	0.040	0.52	2.4	1.9	19	4.3	44	40	32	40	78	55	21	65	17	**420**
KA5-a	0.020	0.04	0.18	0.16	1.6	0.32	3.6	3.4	2.7	3.8	6.3	6.0	4.5	1.3	4.1	**38**
KA5-b	0.020	0.05	0.24	0.20	2.2	0.46	5.3	5.2	3.9	5.3	8.0	6.0	4.5	1.1	4.1	**46**
KA5-c	0.018	NDR	0.23	0.24	3.1	0.72	7.2	6.9	4.7	6.3	10.2	7.3	6.2	1.8	6.0	**61**
CD3	nd	0.07	0.05	0.03	0.25	0.03	0.61	0.58	0.52	0.60	1.4	0.60	0.56	0.44	0.90	**6.7**
CD5	nd	0.04	0.12	0.08	0.64	0.07	1.2	1.2	0.91	1.0	2.9	1.0	1.4	0.41	1.4	**12**
CD6	nd	0.09	0.26	0.18	1.7	0.39	3.2	3.0	2.4	3.2	9.0	4.2	6.8	2.0	7.5	**44**
KA7	0.021	0.22	2.4	1.7	18	4.1	35	30	21	25	50	35	34	7.6	33	**297**
KA7-b	0.022	0.10	0.80	0.58	5.5	1.2	12	11	8	10	23	13	13	3.4	12	**113**
KA8	0.018	NDR	0.11	0.13	0.76	0.18	1.7	1.9	1.7	2.4	3.4	6.5	1.7	0.40	1.5	**22**
KA8-b	0.019	NDR	NDR	0.09	0.43	0.15	0.88	1.0	0.74	1.1	1.0	2.0	0.69	0.19	0.61	**8.9**
KA10	0.014	NDR	<0.20	<0.20	NDR	<0.20	0.20	0.23	<0.20	0.58	0.25	NDR	0.49	0.44	0.27	**2.5**
KA11	0.014	NDR	0.15	NDR	0.82	0.22	1.7	2.1	1.8	2.1	2.8	2.1	2.9	1.0	2.4	**20**
KA11-b	0.015	NDR	0.13	0.12	0.90	0.32	1.7	1.9	1.4	1.8	2.9	4.1	1.5	0.33	1.5	**18**
KA12	0.015	<0.04	NDR	NDR	0.42	0.10	0.96	1.2	0.92	1.2	1.7	2.5	1.7	0.57	1.3	**13**
KA12-b	0.014	NDR	<0.04	NDR	0.12	NDR	0.27	0.37	0.44	0.56	0.73	1.3	0.83	0.37	0.95	**5.9**
KA13	0.020	NDR	0.19	0.14	1.3	0.42	3.0	3.7	3.5	4.5	7.4	6.3	4.5	1.9	4.7	**41**

Table 2-3 (continued)

site:	f_{OC}	naph	ace	flu	phen	anth	fln	pyr	chry	baa	bxf	bap	ipyr	dib	bper	Σ PAH
KA13-b	0.018	NDR	0.12	0.11	1.5	0.60	3.4	4.0	2.4	2.9	7.7	3.8	5.1	2.8	4.8	**39**
KA14	0.015	NDR	0.13	0.10	0.63	0.18	1.3	1.6	1.7	2.2	4.4	2.3	2.9	0.97	2.4	**21**
KA14-b	0.015	NDR	0.14	0.11	0.96	0.25	2.3	2.8	3.1	3.9	5.1	6.0	2.9	0.63	2.6	**31**
KA16	nd	<0.01	0.04	0.04	0.16	<0.01	0.37	0.32	0.35	0.59	0.59	0.34	0.24	0.07	0.40	**3.5**
KA17	nd	<0.01	<0.01	0.03	0.12	0.03	0.25	0.41	0.26	0.47	0.36	0.15	0.11	0.02	0.22	**2.4**
KA18	nd	<0.05	<0.05	<0.05	0.10	<0.05	0.30	0.90	0.30	<0.05	<0.05	0.10	<0.05	0.10	0.10	**1.4**
KA18-b	nd	<0.05	<0.05	<0.05	0.10	<0.05	0.20	0.70	0.20	<0.05	<0.05	0.10	<0.05	<0.05	<0.05	**1.4**
KA19	nd	0.21	<0.06	<0.06	<0.06	<0.06	0.10	0.41	0.10	<0.06	<0.06	0.50	<0.06	<0.06	0.10	**1.4**
KIC 1	nd	0.03	<0.01	0.00	0.01	<0.01	0.07	0.22	0.16	0.31	0.09	0.11	<0.01	<0.01	<0.01	**1.0**
KIC 2	nd	0.07	<0.01	<0.01	<0.01	<0.01	0.06	0.19	0.14	0.29	0.03	0.16	<0.01	<0.01	<0.01	**0.94**
GI1-a	nd	NDR	0.03	0.03	0.04	<0.01	0.16	0.46	0.15	0.02	0.11	0.08	0.08	0.06	<0.01	**1.2**
MI 1,2	0.040	0.09	<0.01	<0.01	0.03	<0.01	0.06	0.10	0.12	0.04	0.11	0.12	0.08	0.12	0.17	**1.0**
MI3,4	0.037	0.21	<0.04	<0.04	0.04	<0.04	0.55	0.09	0.09	0.02	0.11	0.09	0.07	0.08	0.14	**1.5**
F2	nd	0.03	<0.005	<0.005	0.01	<0.005	0.04	0.03	0.02	0.03	0.06	0.06	0.02	0.02	0.03	**0.37**
F3	nd	0.07	0.05	<0.005	0.01	<0.005	0.03	0.04	0.10	0.04	0.03	0.18	0.05	0.13	0.03	**0.77**

Abbreviations: nd, not determined; NDR, compound detected but failed to meet quantitation criteria

Sample replicates from a single location are designated with lower case letters. e.g. K5A-a, K5A-b

naph, naphthalene; ace, acenaphthylene; flu, fluorene; phen, phenanthrene; anth, anthracene; fln, fluoranthene; pyr, pyrene; chry, chrysene; baa, benzo(a)anthracene; bxf, benzofluoranthenes; bap, benzo(a)pyrene; ipyr, indeno(1,2,3-cd)pyrene; dib, dibenz(ah)anthracene; bper, benzo(ghi)perylene.

Table 2-4 PAH concentrations in contaminated sediments.

Location	Σ PAH concentration (mg/kg)	PAH source	Reference
Kitimat Harbor, BC	31	Aluminum Smelter	(8)
Vancouver Harbor, BC	1-330	Urban runoff and industry	(149)
Hamilton Harbor, Ontario	283	Coal Tar	(8)
Saguenay Fjord, Quebec	40-200	Aluminum Smelter	(150)
Norway	0.3-800	Aluminum Smelter	(151)
Sweden	14-200	Aluminum Smelter	(272)

The sediment geomorphology, water flows, and meteorology within this area have been extensively studied (280-282). The major water outflow in Kitimat Arm, driven by the Kitimat River, is down the western side of the arm. This would carry water-borne PAH-laden particles from the immediate vicinity of the smelter and deposit them along the western side of the arm. Similarly, prevailing winds blow essentially directly up (summer inflow) or down (winter outflow) the valley (282). Thus atmospheric emissions from the smelter will also tend to be deposited on the western side of Kitimat Arm. The sediment data are consistent with these effects and PAH levels are much higher at stations on the western side of the arm than at stations of comparable distance from the smelter on the eastern side of the arm, as demonstrated in the following series: (sites on a transect west to east, See Figure 2-2) KA7 (300 mg/kg), KA8 (17 mg/kg), KA10 (2.5 mg/kg). The sites CD3 and CD5 (see Figure 2-2) are affected by dredging operations which maintain a channel of sufficient depth to allow marine access to the Alcan dock. Removal of PAH contaminated sediment by this process may account for the anomalously low PAH levels at these two sites.

The data do not allow distinction between aeolean or fluvial inputs of PAH. However, it is highly unlikely that water-borne particles could be carried from the smelter up sidearms of Douglas Channel such as Giltoyees Inlet and Foch Lagoon, against the prevailing currents. Cretney *et al.* (268) also discounted the likelihood of fluvial transport of PAH over significant distances (>30 km) because of rapid particle removal from the water column. Processes responsible for particle removal include flocculation of particles in the estuarine mixing zone, incorporation into rapidly settling planktonic fecal pellets (283, 284), and barriers to particle transport formed by submarine sills transecting Douglas Channel (281). Cretney (268) utilized a Gaussian plume model to predict that atmospheric transport of significant amounts of particle-adsorbed PAH was feasible over distances of at least 100km. Sediment core data from Giltoyees Inlet (see Chapter 3) show substantial increases in PAH contamination concomitant with the commencement of operations at the Kitimat smelter. This result strongly suggests that the PAHs in Giltoyees Inlet arise from atmospheric emissions from the smelter. Air monitoring data, in conjunction with sediment data, is required at remote sites in the Kitimat fjord system to test this hypothesis, and to allow calculation of PAH fluxes from both atmospheric and water-borne routes.

2.4.4 PAH composition

The relative proportions of the PAHs detected in these samples are similar, especially amongst sites in Kitimat Arm itself (KA5-KA15, CD sites, Stn. 2), in spite of the fact that absolute PAH levels in these samples vary by over two orders of magnitude. PAH compositions for a representative selection of sites are shown in Figure 2-6.

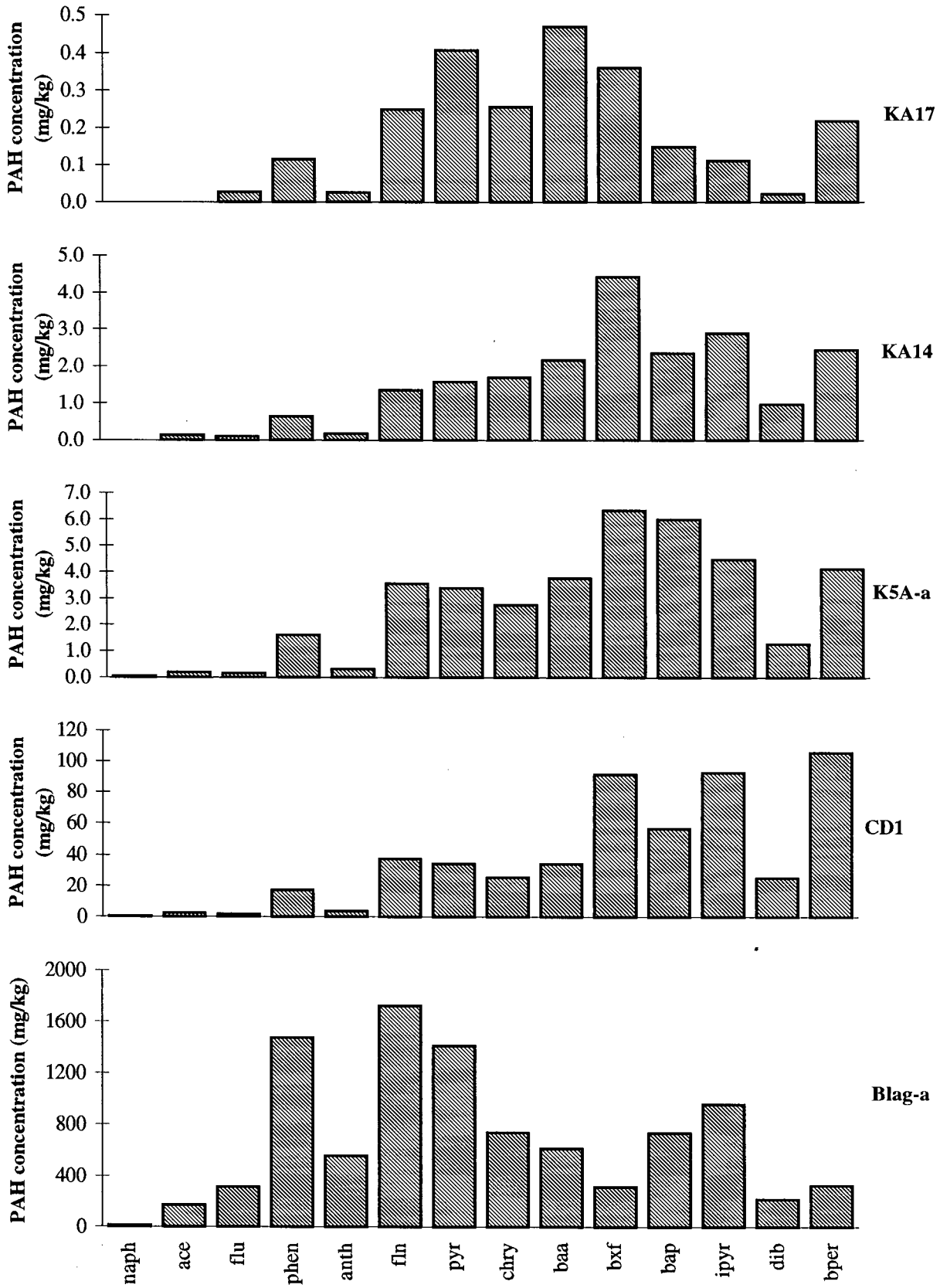

Figure 2-6 PAH composition in sediments from selected sample locations within the Kitimat fjord system. Refer to Table 2-3 for definitions of PAH abbreviations.

The PAH composition in Kitimat Arm sites is dominated by high molecular weight PAHs (HPAHs; defined as *m/z* ≥202). The PAH profile for sediment samples from the smelter settling ponds (BLag) is similar to the Kitimat Arm sites, however the pond samples show higher proportions of low molecular weight PAHs (LPAHs *m/z* <202). This observation is confirmed by the principle components analysis (Figure 2-9), which is described later in this chapter. PAH compositions from the more distant sites are less similar, nevertheless these also are dominated by HPAH, especially the fluoranthene, pyrene (*m/z* 202) and benzofluoranthene isomers, benzo(*a*)pyrene, benzo(*e*)pyrene (*m/z* 252) series. For all sites, the total amounts of 4 and 5-ring PAHs are greater than the amounts of 2 and 3-ring PAHs. This pattern is considered typical of combustion generated PAH mixtures (62, 64-66). The BLag-a sample does have a higher proportion of LPAHs than the other samples shown in Figure 2-6, nevertheless the PAH composition in this sample is still typical of a combustion generated PAH mixture. No consistent trend is evident in the differences between the PAH profiles at the distant sites, and the PAH profile for the sites near the smelter. However, it should be noted that concentrations of many PAHs at the distant sites are near or below the quantification limits, consequently high uncertainties are associated with PAH levels at the distant sites and interpretation of trends in the data is difficult.

The mixture of PAHs present in a particular sample reflects, to some extent, the sources that produced the PAHs, as described in section 1.4.1 (55, 62, 64, 65). The PAH profile for the Kitimat Arm sites is consistent with contamination from a local high temperature source. Specifically, the dominance of unsubstituted PAHs, the elevated levels of fluoranthene and pyrene (*m/z* 202) and benzofluoranthenes and benzopyrenes (*m/z* 252), and the phenanthrene/anthracene and pyrene/fluoranthene isomer ratios, are all typical of combustion generated PAHs (62-64, 84,

94). The mean phenanthrene/anthracene ratio of 4.0 is substantially closer to the value for urban (i.e. combustion generated) particles (ca. 3) than it is to the value for remote sites (ca. 30) (84).

A few studies have shown that, with increasing exposure to environmental processes, the concentration ratios of isomeric PAHs change systematically in favor of the thermodynamically more stable isomers (84, 285). However the present data show no significant changes between sites in the following PAH ratios: phenanthrene to anthracene, pyrene to fluoranthene, (chrysene + triphenylene) to benzo(*a*)anthracene and benzo(*ghi*)perylene to indeno(1,2,3-*cd*)pyrene).

2.4.5 Alkyl homologue distribution

Four of the sediment samples (BLag-a, KA7, KA12-b, KA16) have been analyzed for parent and alkyl PAHs by using GC-MS (267). All of these samples have alkyl homologue distributions (AHD) dominated by the non-alkylated PAHs, and with progressively lower proportions of the higher alkylated species, as shown in Figure 2-7. The decreasing AHD is typical of combustion or pyrolytically derived PAHs, as demonstrated by previous work in this field (55, 65, 268). The similarity in the relative proportions in each AHD among these sites (BLag<1>, KA7, KA12(b), KA16), and the progressively lower PAH contamination along Douglas Channel, indicate the lack of any major secondary inputs of PAHs as well as the lack of selective degradation towards a particular homologue. The relatively higher proportion of the C1 and C2 homologues found for the lower molecular weight PAHs could be due to either an increase in formation of alkylated species for the lower molecular weight PAHs or possibly to a lower extraction efficiency for the more highly alkylated, higher molecular weight compounds.

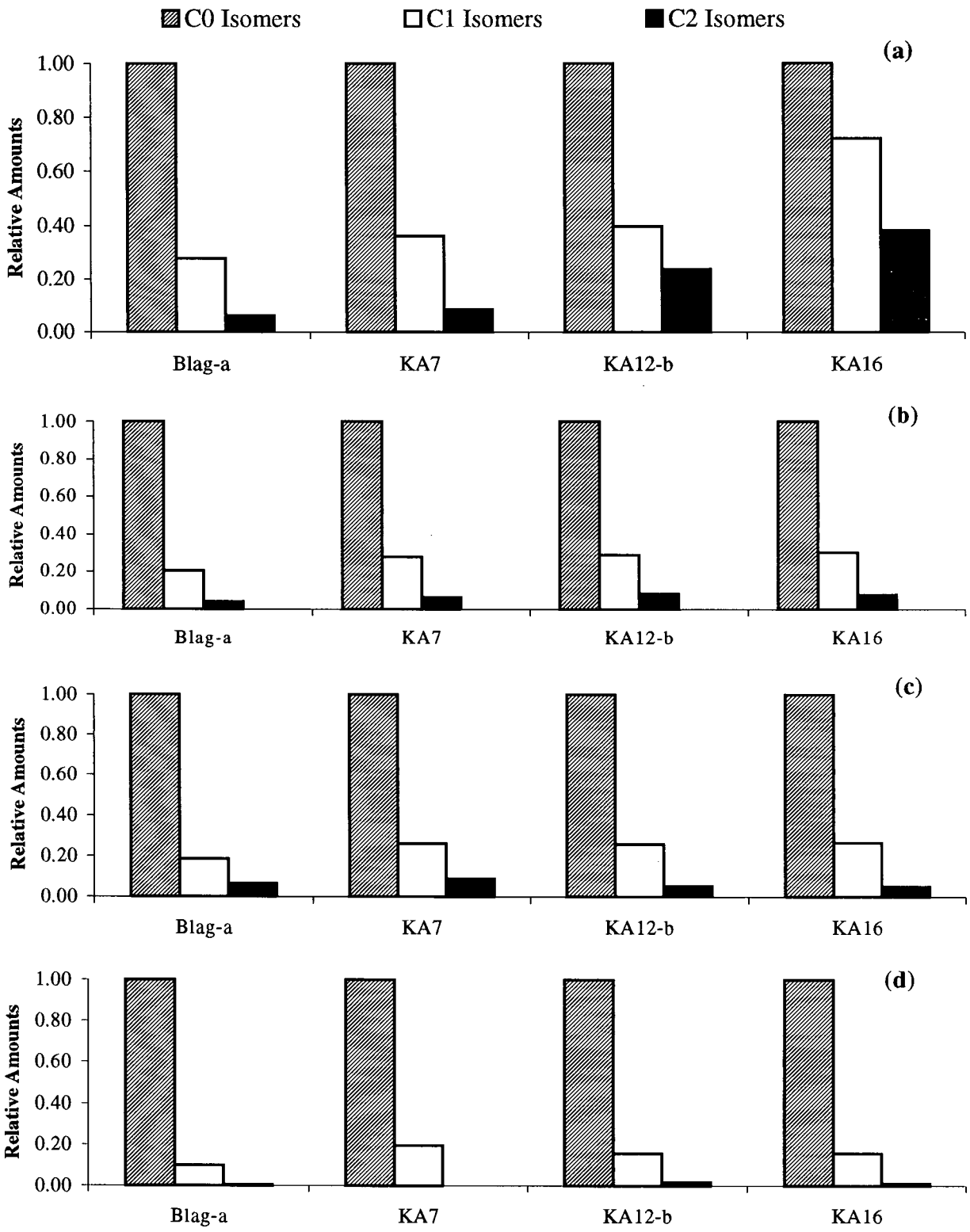

Figure 2-7 Relative alkyl-PAH homologue distribution (normalized to unsubstituted isomer). (a), m/z 178 alkyl homologues; (b), m/z 202 alkyl homologues; (c), m/z 228 alkyl homologues; (d) m/z 252 alkyl homologues. Figure adapted from reference (267).

2.4.6 Principal components analysis

Principal components analysis (PCA) is one of a group of related data transformation techniques, which includes factor analysis (FA). In PCA the original data is described in terms of new variables (principal components, PCs), which are linear combinations of the original variables. The PCs are developed such that the first principal component (PC1) accounts for the maximum variance in the data set; PC2 is uncorrelated with (orthogonal to) PC1 and accounts for the maximum residual variance; and subsequent PCs are developed similarly (286). PCA has been applied to chemical data including organochlorine (287, 288) and PAH residues (64, 87, 88, 289) in environmental samples, in which PCA has been used to differentiate sources of chemical contamination and provide insights into the fate of chemical contaminants in the environment. In the present study PCA was used to highlight inter-site differences in the PAH profile, and to help determine which variables (i.e. PAH isomers) showed the greatest variability between sites.

The correlation matrix of the normalized sediment data was subjected to principal component analysis, as described in section 2.3.6. Most of the total variance in the data set (73%) was accounted for by two principal components (PC1, 52%; PC2, 21%). From the loadings plot (Figure 2-8) it can be seen that LPAHs plot negative with respect to the major component (PC1), whereas HPAHs plot positive. This indicates that PC1 is driven by chemical differences between individual PAHs that are related to the molecular size or weight of each compound. To demonstrate this, a linear regression of compound loading on PC1 against log K_{OW} was performed. log K_{OW} values from the literature (160) were used. The linear regression showed a strong positive correlation (r=0.84) that was significant at the 98% level (t-test). This relationship is not surprising given that log K_{OW} is strongly correlated with molecular size (160), as are vapor

pressure, solubility and biodegradability. All these processes influence the fate and distribution of PAHs in the environment.

The minor component (PC2) is less easy to interpret. Only benzo(*a*)anthracene and chrysene/triphenylene are distinguished from the other PAHs on this component. No plausible explanation for this is apparent, although it should be noted that the minor component is more strongly influenced by random differences (noise) in the data, and is substantially less significant than PC1.

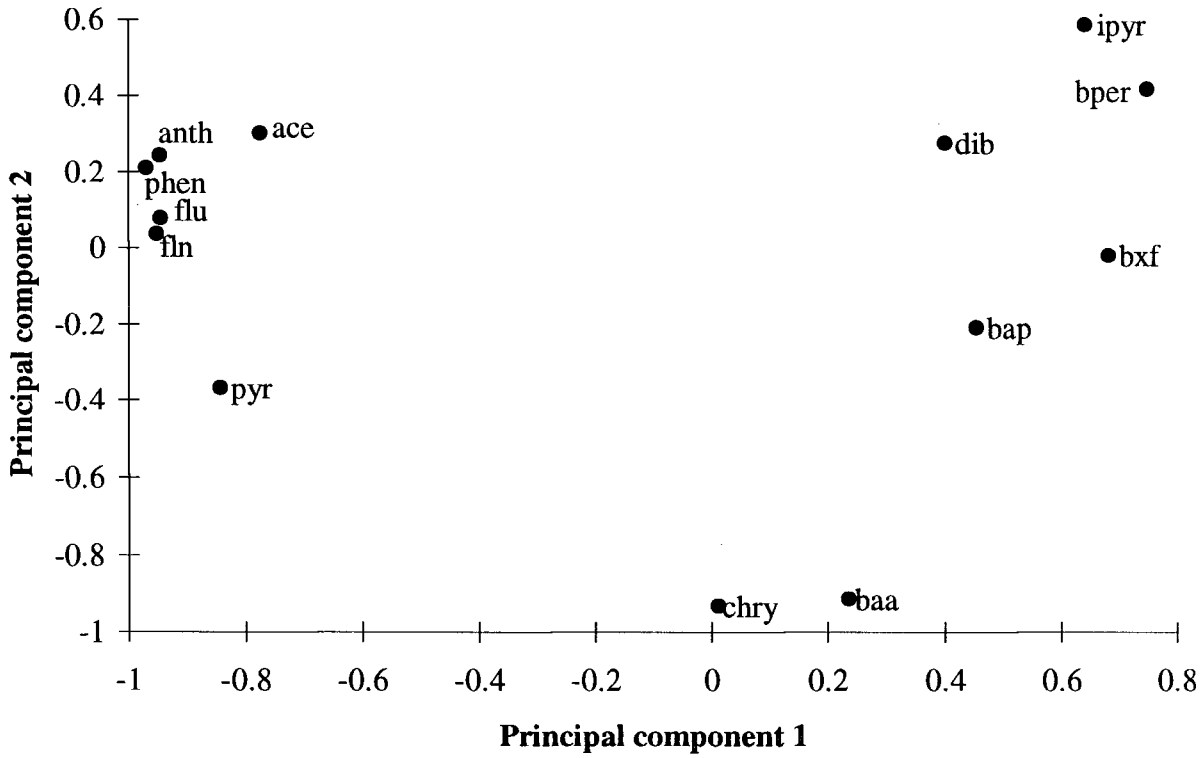

Figure 2-8 Loading plot for PCA of Kitimat sites, illustrating the influences of the 13 original variables (individual PAHs) on the two major principal components.

The sampling locations fall into three distinct clusters when projected onto PC1 and PC2 as shown in Figure 2-9. The three BLag samples plot as one cluster in the upper left quadrant —

negative with respect to PC1. This reflects the higher proportion of LPAHs in these samples, as mentioned earlier.

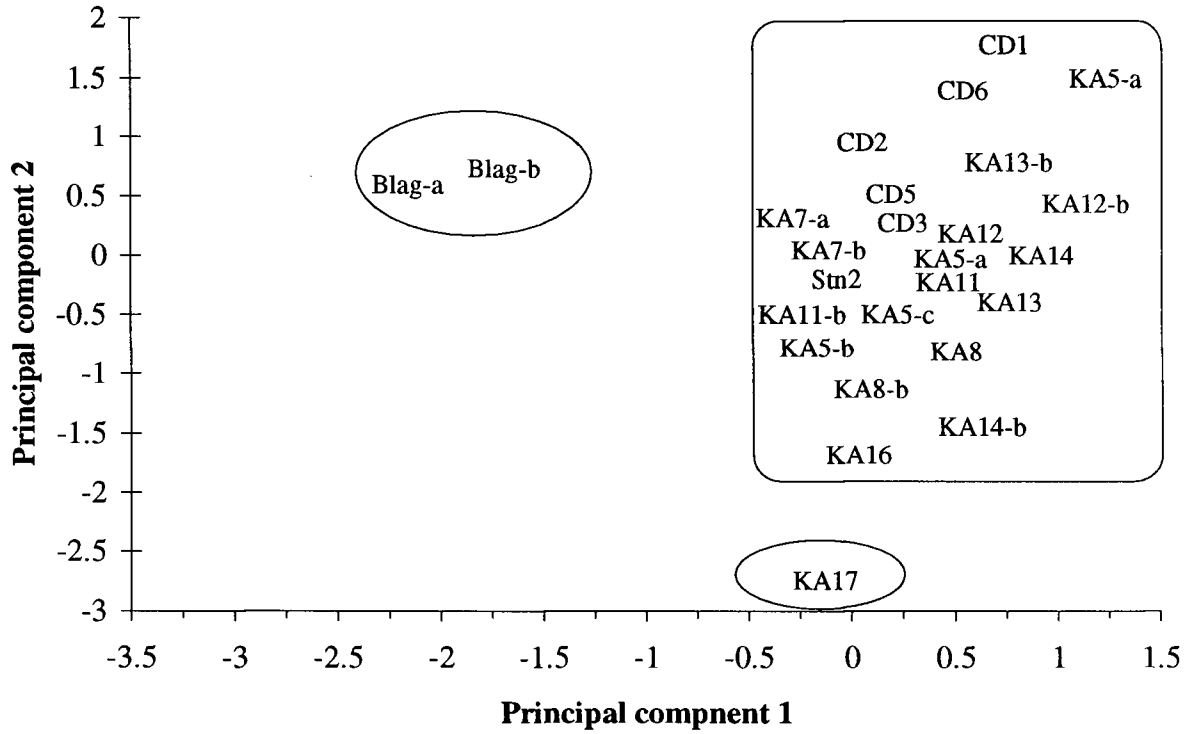

Figure 2-9 Projection of Kitimat sample sites onto principal components 1 and 2. Note the separation of sites into 3 clusters.

Most of the other sites form a large cluster on the right side of Figure 2-9. The scatter of the KA5 replicates throughout this cluster implies that: (i) there are no important differences in the PAH profile at the sites in this cluster, and (ii) spreading of the cluster with respect to PC2 is not significant. The remaining site, KA17, plots strongly negative on PC2. An inspection of the corresponding graph in Figure 2-6 reveals that this is undoubtedly due to an anomalously high proportion of benzo(*a*)anthracene detected in the PAH profile from this site. Given the consistency in the PAH profile at the other sites, it seems highly unlikely that this result is genuine. A possible explanation for this anomaly is the presence of an interfering compound in

the extract from this site which co-elutes with benzo(*a*)anthracene under the GC-FID conditions we were using, thus inflating the peak attributed to benzo(*a*)anthracene.

The only important differences in the PCA, therefore, are between the three BLag samples and all other sites. Two explanations for this difference may be postulated. Firstly, it is possible that PAHs from the lagoon do contribute significantly, via the lagoon outfall, to the contamination in the harbor. It is conceivable that the reduced abundance of LPAHs in the harbor sediments arises from rapid loss within the lagoon of a readily available fraction of, specifically, the LPAHs. Biodegradation, photolysis or volatilization are examples of processes that may preferentially degrade the LPAHs. In addition, it is likely that biodegradation proceeds more rapidly in the shallow, freshwater lagoon than it does in the saltwater environment of the harbor. Indeed, bacteria isolated from Kitimat harbor sediments and which have the ability to metabolize PAHs, were found to be more active in freshwater media (290). Certainly, the PCA indicates that little (if any) selective loss of individual PAHs occurs once the PAHs are deposited into the receiving environment.

Alternatively, the PAH profile in the lagoon may arise from a subtly different mixture of sources from those that contribute most of the contamination to the harbor. For example, volatile and particle emissions from the smelter potroom that arise from the volatilization of the non-baked section of the Söderberg anode are probably not important contributors to the PAH load in the lagoon, as they are not redirected into the lagoon by the potroom scrubbers. However, they may be significant inputs with respect to the total PAH load in the harbor.

The present data do not allow these two possibilities to be distinguished. The presence of a "readily available PAH fraction", as suggested above, could be determined by laboratory based

experiments addressing bioavailability of PAHs in the lagoon sediments. In addition, a comparison of the PAH profile in the air downwind from the smelter, with the PAH composition we have determined in the harbor sediments would indicate whether water-borne and atmospheric inputs have different PAH compositions.

2.4.7 Effect of organic carbon on PAH distribution

According to the equilibrium partioning (EP) theory, under steady state conditions (i.e where contaminant inputs are uniform), the distribution of hydrophobic organic compounds such as PAHs in marine sediments is expected to be driven by equilibrium partitioning of the PAHs to sediment organic carbon (f_{OC}) (155, 156, 291). A number of workers have noted a correlation between PAH levels in the sediment and f_{OC} (150, 268, 292). A positive correlation is found between these two parameters in the present study (ρ=0.974 n=25, P=0.95) (Figure 2-10), however the correlation is strongly influenced by inner harbor sites with very high PAH levels. There is no significant correlation between f_{OC} and PAHs at sites where the total PAH concentration was less than 2 mg/kg.

Based on these findings, it is unlikely that the observed positive correlation represents preferential partitioning of PAHs onto sediment with a high f_{OC} for two reasons. Firstly, the correlation does not hold for remote sites, and secondly, the assumption that PAH inputs are uniform across the sites studied is obviously incorrect. The data in Table 2-3 clearly indicate a strong dependence of PAH levels on proximity to the aluminum smelter. It is suggested that the correlation in Figure 2-10 is an artifact associated with emissions from the smelter. Particle emissions from the smelter comprise mainly soot, coal dust, tar balls, and accidental spillage of pitch during unloading of the raw materials (273). All of these particles are very high in both PAHs and f_{OC}, as demonstrated

by the exceptionally high f_{OC} values for the BLag sediments. Because of their chemical properties and mode of release, PAHs entering the receiving environment from the smelter are likely to be associated with atmospheric or sediment particles, rather than existing free in the gas or dissolved phase (8, 132, 166). Because the particles emitted from the smelter have a high f_{OC} themselves, the correlation in Figure 2-10 may simply indicate that PAHs in Kitimat harbor remain adsorbed onto or occluded within the particles with which they were released into the environment. This low mobility of PAHs in sediments has been established by a number of studies (63) (and references therein), (166) which suggest that combustion produced PAHs are strongly adsorbed and not bioavailable.

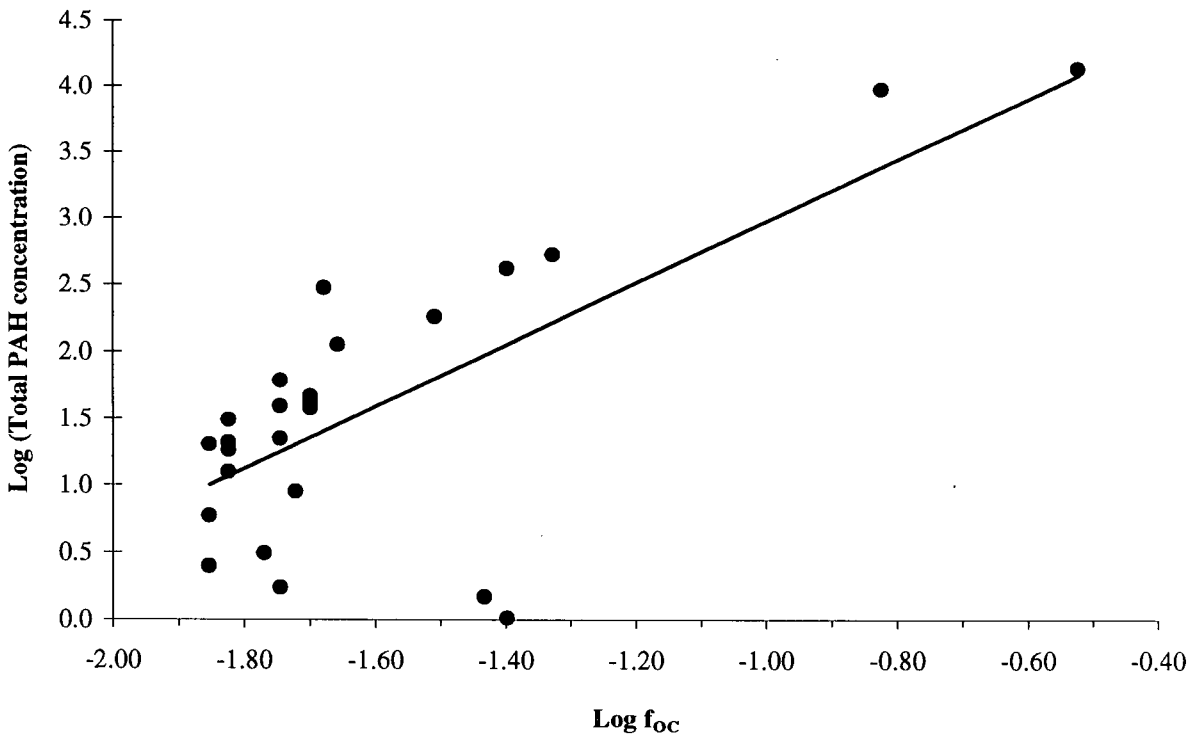

Figure 2-10 Correlation between total PAH levels and f_{OC} in marine sediments from the Kitimat fjord system. Both data sets were log-transformed to allow better visualization of the full range in PAH concentrations.

In Chapter 3 it is shown that *in the vicinity of the smelter*, PAHs are preferentially associated with a larger particle size sediment fraction; however, at remote sites the PAHs were evenly distributed across all particle size fractions analyzed. This observation may be interpreted as further evidence for the contention that smelter particulates continue to influence PAH disposition in sediments after their release into the environment.

In contrast to the present work, data from a previous study in this area by Cretney *et al.* (268) show a positive correlation between f_{OC} and PAH concentrations for remote sites (Total PAHs <0.4 mg/kg), but no correlation for the contaminated sites. The remote sites in Cretney's study are sufficiently distant from the aluminum smelter that the assumption that PAH inputs are uniform across these sites is most likely valid. Hence the correlation in his data probably does reflect thermodynamically driven partitioning of PAHs onto sediment organic carbon. In contrast, Cretney did not sample extensively in the vicinity of the smelter itself, and his "contaminated sites" are some distance from the smelter discharges. Thus the correlation between f_{OC} and PAH concentration at sites proximate to the smelter which we have observed, was not seen in his work.

In summary, the present data reveal a complex relationship between PAH levels and sediment f_{OC}. Although the two parameters correlated well for contaminated sites, it is likely that this reflects PAHs remaining associated with the highly carbonized soot, coke and pitch fragments released from the smelter, rather than active thermodynamically driven partitioning of PAHs into biogenic sediment organic carbon. Overall, the PAH contamination in surface sediments within the Kitimat system appears to be very persistent, showing little evidence of degradation even after transport over significant distances.

3. Polycyclic aromatic hydrocarbon composition in marine sediments near Kitimat, BC: The influence of sediment particle size and early diagenesis

3.1 Introduction

The Kitimat fjord system has a number of features that make it useful for studying the transport and fate of PAHs in a marine system. In Chapter 2 it was shown that marine sediments in the Kitimat fjord system are contaminated with PAHs. The majority of these PAHs are generated by a single well-defined point source - namely the Alcan aluminum smelter. The isolation of Kitimat provides a closed system where the environmental chemistry of PAHs can be investigated without many of the complications associated with multiple PAH sources in urban environments.

The PAH composition at a given point in the environment reflects the source from which the PAHs were derived. This 'source signature' can be altered by environmental processes that act selectively or differentially on individual PAHs. These changes will depend upon the nature of the chemical (e.g. volatility, hydrophobicity, chemical stability), its initial form (e.g. liquid phase, particle occluded or adsorbed on surface), and dominant environmental processes at or en-route to the receptor (e.g. microbial degradation, photolysis). Thus the change in composition of PAH burden with depth in sediment cores has been explained in terms of changing source inputs over time (70, 150), or long term diagenesis (71, 93). Changes in PAH composition as a function of sediment particle size have been attributed to different source inputs (166), or differential partitioning amongst particle size classes (164, 165).

The objective of this study was to evaluate the distribution of individual PAHs among five different sediment size-fractions. In addition, changes in PAH composition with depth in sediments associated with both diagenesis and the onset of anthropogenic activities in Kitimat Arm was investigated.

Kitimat Arm (Figure 3-1) and its history has been described in some detail in Chapter 2. The studies reported in Chapter 2 confirmed earlier reports documenting elevated levels of PAHs in Kitimat Arm and Douglas Channel which are due to inputs from the aluminum smelter (96, 268). Recently, there has been speculation that in spite of the greatly elevated levels of PAHs in sediments close to the smelter, these PAHs have only limited bioavailability (96). PAHs produced/released during combustion may be occluded or otherwise trapped inside particles in a manner that might limit redistribution and uptake through biological membranes (138). But even if the form of particle-bound PAHs produced during combustion limits bioavailability, PAHs in surface sediments might become more bioavailable over time due to microbial leaching or break-down of particles, coupled with bioturbation and uptake into burrowing fauna. Any changes in bioavailability, or in chemical composition of the PAHs, will affect the risk assessment for biota.

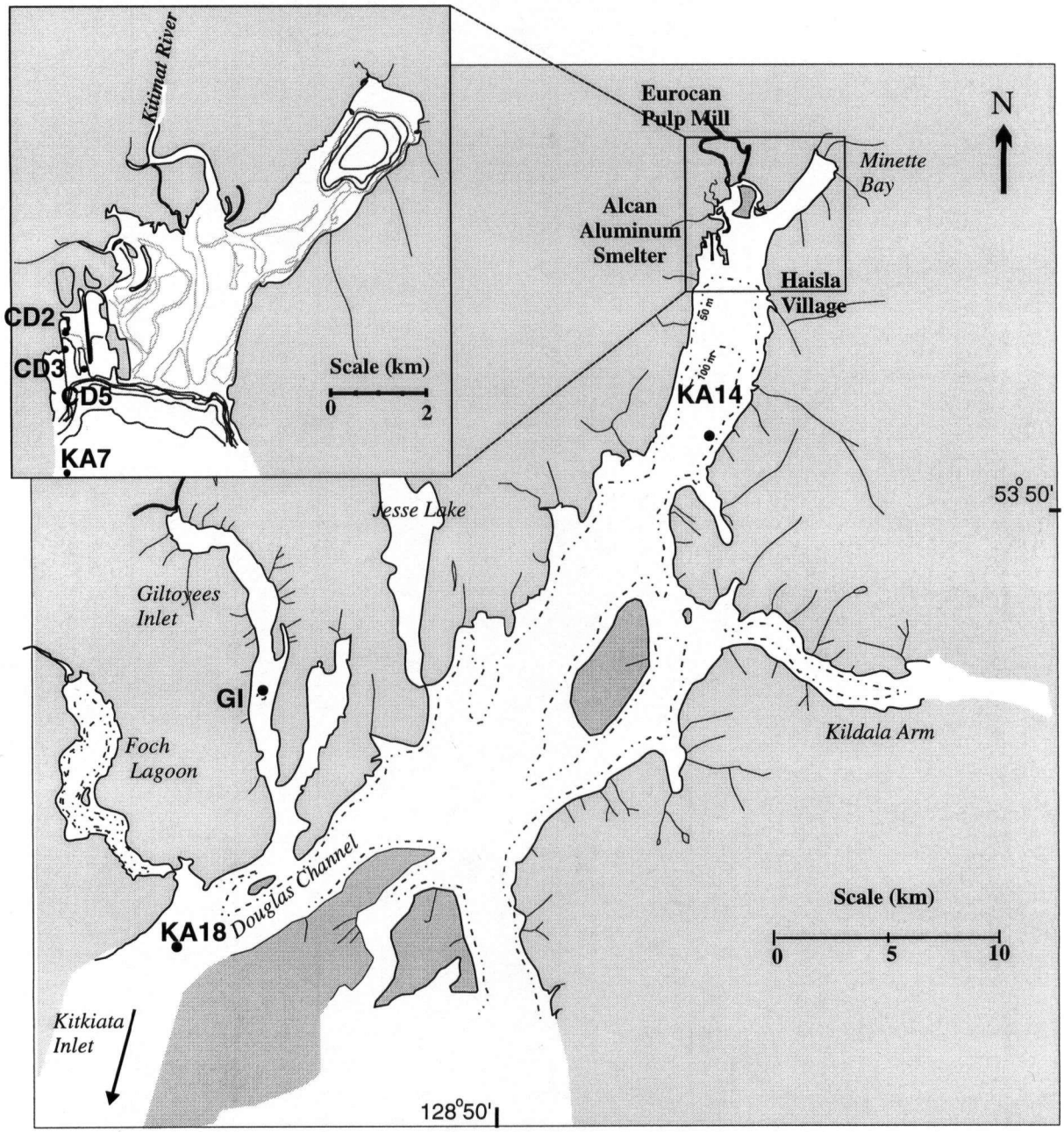

Figure 3-1 Map of Kitimat fjord system showing sampling locations

3.2 Experimental

3.2.1 Sample collection

Surface sediment samples (approximately 15 cm depth) were collected from seven sites in Kitimat Arm, Douglas Channel, British Columbia (Figure 3-1), as described in section 2.3.3.

A sediment core was collected in Giltoyees Inlet (see Figure 3-1). The 9.0 cm diameter gravity corer consisted of a 122 cm long polyacrylic tube mounted at one end in a weighted aluminium-alloy head and fitted with a stainless steel cutter/catcher at the other. The core was sub-sectioned vertically into 5 cm slices, which were wrapped in baked aluminum foil, frozen at -20° C and transported back to the laboratory.

3.2.2 Analysis of surface sediments

All sediment samples (except core segments) were freeze dried and then dry sieved through brass sieves into the following size fractions: >1180 μm, 1180-300 μm, 300-180 μm, 180-38 μm, <38 μm. Sediment samples were analyzed for PAHs by using the procedure described in section 2.3.3. Routine analysis was performed by using capillary gas chromatography on a Hewlett Packard 5890 GC with FID detection as described in section 2.3.4. The identification of the unsubstituted and alkylated PAHs in selected samples was confirmed by gas chromatography-mass spectrometry (GC-MS) analysis, using a Varian Star 3400 CX gas chromatograph interfaced to a Saturn 4D quadrupole ion-trap mass spectrometer.

3.2.3 Analysis of sediment core samples

The sediment core samples were analyzed at Axys Analytical Services Ltd., Sidney, BC, for sediment organic carbon, as well as for a suite of unsubstituted and alkylated PAH (Table 3-2).

The analytical methods used were very similar to those described by Yunker *et al.* (64) as follows. For PAH analysis, sediment samples were thoroughly homogenized, and spiked prior to analysis with an aliquot of perdeuterated surrogate standards (acenaphthene, chrysene, naphthalene, perylene, phenanthrene, pyrene, dibenz(*ah*)anthracene, and benzo(*ghi*)perylene). A portion of the sediment sample (10-15 g wet weight) was ground with anhydrous sodium sulfate to a free flowing powder. This powder was transferred to a glass chromatographic column containing methanol and eluted with additional methanol followed by dichloromethane. Iso-octane was added to the eluate which was back-washed with potassium hydroxide and solvent extracted water. The resulting solution was dried over anhydrous sodium sulfate, concentrated in a Kuderna-Danish flask and cleaned on a silica gel column.

The loaded silica gel column was eluted with pentane (discarded) followed by dichloromethane. The dichloromethane fraction was concentrated in a Kuderna-Danish flask and an aliquot of recovery standard (containing d_{12}-benzo(*b*)fluoranthene, d_{10}-fluoranthene, and d_8-acenapthylene) was added. The extract was then transferred to a microvial, concentrated under a stream of nitrogen and analyzed for PAHs by using GCMS.

The GC-MS system consisted of a Finnigan Incos 50 mass spectrometer equipped with a Varian 3400 gas chromatograph which was fitted with a CTC autosampler and a DG 10 data system. Chromatographic separation was carried out using a DB-5 column (30 m, 0.25 mm i.d., 0.25 μm film thickness). The mass spectrometer was operated in the electron impact (EI) mode (70 Ev) using Multiple Ion Detection (MID) to enhance sensitivity, acquiring two characteristic ions for each target analyte and surrogate standard. A split/splitless injection sequence was used.

The unsubstituted PAHs were quantified with reference to the deuterated spikes and authentic standards by using relative retention times and mass chromatogram peak maxima. Individual alkyl-substituted PAHs and alkyl- homologue groups, as listed in Table 3-2, were also analyzed. Authentic standards were available for the individual alkylated PAHs listed. Homologue series for alkyl PAHs were determined by integrating the parent ion profiles within the expected retention time range. Peaks were not included, however, if their mass spectra did not correspond to the compounds of interest or if the appropriate confirming ion was absent.

3.2.4 Statistical analysis

Principal Components Analysis (PCA) was performed on the correlation matrix of the PAH compositional data for samples from seven sites x five size fractions (n=35) by using the SYSTAT 5.0® software package. Prior to analysis, non-detected values in the data set were replaced with computer generated random numbers between zero and the sample-dependent minimum detectable concentration. This was done to ensure the PCA was not influenced by spurious correlations between compounds that were undetected at some sites. Then the data for individual compounds was normalized to the total PAH concentration for each sample to remove the effect of differences between sites in absolute PAH concentration.

3.3 Results and discussion

3.3.1 Distribution of PAHs amongst particle size classes in marine sediments

PAH concentrations for each sediment size fraction from the seven sites are listed in Table 3-1. The size distribution of sediment particles at each site is illustrated in Figure 3-2. An examination of the absolute PAH concentration in each sediment size fraction (Table 3-1) suggests obvious differences between size fractions only for the inner harbor sites CD2 and CD3, where individual

PAHs (except perylene at CD3) were enriched in the larger particle size fractions. Correlations between increasing median particle size and higher PAH levels were statistically significant for site CD2 ($n=5$; $r=0.98$; $P=0.0023$), but not for CD3 ($r=0.42$; $P=0.44$) or any other site ($P \geq 0.22$ for all). For sites other than CD2 and CD3, individual and total PAH concentrations were similar in all size fractions, or exhibited only slight variation with no apparent pattern. Enrichment of PAHs in specific particle size classes has been reported previously in marine sediments (165, 166), suspended particles (82) and forest soils (293). Prahl and Carpenter (166) determined that PAHs in coastal marine sediments near Washington State were selectively associated with a low density, large particle size sediment fraction (>64 μm) which they suggested comprised mainly vascular plant remains and pieces of charcoal. Maruya *et al.* (165) noted a correlation between PAH content and the abundance of silt and clay in San Francisco Bay sediments, but the correlation between PAH and organic carbon content of the sediments was poor. They ascribed these observations to a heterogeneity of organic carbon matrices, and specifically, to aromatic-rich soot particles which strongly bind PAHs in the silt/clay fraction.

Table 3-1 PAH concentrations (mg/kg) in marine sediments from the Kitimat fjord system, BC, Canada.

Site	Fraction	Wt. %	naph	acen	acny	flu	phen	anth	fln	pyr	chry	Baa	Bxf	Bep	Bap	Pery	ipyr	dib	bper	Σ PAH
CD2	>1180μm	3	16	<0.01	27	16	165	39	367	342	244	291	327	331	450	118	372	112	360	**3577**
	1180-300μm	8	16	<0.01	15	8.9	85	19	163	147	102	111	269	122	159	42	147	41	145	**1593**
	300-180μm	22	3.1	0.02	3.5	2.2	21	4.7	41	37	26	30	75	35	47	13	58	15	54	**465**
	180-38μm	49	1.3	<0.01	1.3	0.8	8.0	1.6	16	15	11	13	28	11	17	5.3	18	5.3	18	**171**
	<38μm	18	0.32	<0.01	0.35	0.22	2.4	0.45	5.5	5.0	3.4	4.6	11	5.6	6.0	2.3	7.8	2.2	7.2	**65**
																			Weighted Total [PAH]:	**423**
CD3	>1180μm	5	0.04	<0.01	0.02	<0.01	0.12	0.03	0.63	0.66	0.49	0.62	1.3	0.77	1.1	0.56	1.1	0.23	1.0	**8.7**
	1180-300μm	8	0.51	<0.01	0.32	0.17	1.3	0.27	2.5	2.2	1.6	2.2	4.1	2.3	3.1	2.0	2.9	0.90	2.7	**29**
	300-180μm	16	0.17	<0.01	0.12	0.06	0.49	0.11	1.0	0.92	0.61	0.80	1.3	0.80	1.1	2.4	1.2	0.46	1.3	**13**
	180-38μm	50	0.08	<0.01	0.02	0.01	0.10	0.02	0.22	0.20	0.15	0.21	0.32	0.20	0.28	1.3	0.21	0.07	0.23	**3.7**
	<38μm	23	0.07	<0.01	0.01	0.01	0.04	0.01	0.08	0.07	0.09	0.12	0.16	0.10	0.21	2.4	0.13	0.07	0.20	**3.7**
																			Weighted Total [PAH]:	**7.3**
CD5	>1180μm	14	0.04	<0.01	0.02	0.02	0.07	0.01	0.16	0.18	0.17	0.14	0.20	0.16	0.12	0.04	0.11	0.05	0.17	**1.7**
	1180-300μm	32	0.04	<0.01	0.02	0.02	0.07	0.01	0.14	0.15	0.17	0.13	0.18	0.17	0.13	0.05	0.13	0.12	0.12	**1.7**
	300-180μm	26	0.08	<0.01	0.03	0.02	0.08	0.01	0.17	0.17	0.17	0.15	0.18	0.17	0.17	0.05	0.05	0.06	0.14	**1.7**
	180-38μm	17	0.04	<0.01	0.01	0.02	0.09	0.01	0.19	0.19	0.17	0.16	0.25	0.16	0.15	0.05	0.12	0.05	0.17	**1.8**
	<38μm	11	0.04	<0.01	0.01	0.01	0.05	0.01	0.09	0.12	0.12	0.10	0.15	0.11	0.10	0.03	0.08	0.05	0.10	**1.2**
																			Weighted Total [PAH]:	**1.6**

Table 3-1 (continued)

Site	Fraction	Wt. %	naph	acen	acny	flu	phen	anth	fln	pyr	chry	Baa	Bxf	Bep	Bap	Pery	ipyr	dib	bper	Σ PAH
KA7	>1180µm	5	0.21	<0.01	0.18	0.11	1.1	0.25	2.2	2.2	1.5	2.0	2.2	2.0	2.4	0.73	2.1	0.59	2.0	**22**
	1180-300µm	47	0.89	<0.01	0.28	0.33	2.1	0.40	4.3	4.1	3.0	4.0	2.0	2.2	3.3	0.99	2.7	0.47	2.5	**34**
	300-180µm	0.4	1.1	<0.01	0.03	0.05	0.37	0.06	0.79	0.83	0.67	1.1	1.8	0.84	1.5	0.12	0.83	0.45	0.95	**12**
	180-38µm	26	0.19	<0.01	0.15	0.10	1.01	0.20	2.1	2.0	1.3	1.8	2.0	1.2	1.8	0.58	1.7	0.50	1.4	**18**
	<38µm	22	0.13	<0.01	0.03	0.04	0.27	0.06	0.60	0.59	0.50	0.70	0.48	0.49	0.62	0.23	0.50	0.09	0.49	**5.8**
																			Weighted Total [PAH]:	**23**
KA14	>1180µm	36	0.05	<0.01	0.03	0.01	0.14	0.03	0.29	0.29	0.28	0.25	0.53	0.26	0.29	0.14	0.32	0.13	0.40	**3.4**
	1180-300µm	31	0.06	<0.01	0.04	0.01	0.15	0.04	0.31	0.32	0.28	0.26	0.54	0.26	0.29	0.13	0.27	0.10	0.31	**3.4**
	300-180µm	8	0.07	<0.01	0.02	0.02	0.14	0.03	0.27	0.30	0.26	0.27	0.52	0.26	0.30	0.13	0.26	0.11	0.34	**3.3**
	180-38µm	15	0.06	<0.01	0.03	0.03	0.17	0.04	0.33	0.33	0.27	0.30	0.56	0.27	0.33	0.14	0.28	0.10	0.33	**3.6**
	<38µm	10	0.08	<0.01	0.02	0.01	0.13	0.02	0.28	0.31	0.23	0.24	0.54	0.27	0.33	0.13	0.29	0.11	0.29	**3.3**
																			Weighted Total [PAH]:	**3.4**
KA18	>1180µm	42	0.09	<0.01	0.01	0.03	0.09	<0.01	0.12	0.16	0.27	0.21	0.19	0.13	0.17	0.11	0.21	0.13	0.15	**2.1**
	1180-300µm	42	0.09	<0.01	<0.01	0.03	0.08	<0.01	0.12	0.18	0.30	0.26	0.23	0.15	0.14	0.17	0.13	0.07	0.19	**2.1**
	300-180µm	6	0.17	<0.01	0.03	0.03	0.10	<0.01	0.16	0.23	0.28	0.21	0.26	0.17	0.21	0.10	0.16	0.10	0.18	**2.4**
	180-38µm	8	0.13	<0.01	0.02	0.02	0.10	<0.01	0.14	0.18	0.26	0.16	0.20	0.14	0.18	0.08	0.14	0.11	0.16	**2.0**
	<38µm	2	0.43	<0.01	0.02	0.03	0.11	<0.01	0.14	0.17	0.26	0.09	0.26	0.17	0.64	0.06	0.13	0.12	0.16	**2.8**
																			Weighted Total [PAH]:	**2.1**

Table 3-1 (continued)

Site	Fraction	Wt. %	naph	acen	acny	flu	phen	anth	fln	pyr	chry	Baa	Bxf	Bep	Bap	Pery	ipyr	dib	bper	Σ PAH
GI	>1180μm	7	0.11	<0.01	0.01	0.03	0.05	0.03	0.14	0.26	0.31	0.13	0.23	0.24	0.20	0.15	0.21	0.17	0.16	**2.4**
	1180-300μm	40	0.08	<0.01	<0.01	0.02	0.03	0.01	0.08	0.12	0.22	0.05	0.11	0.13	0.08	0.09	0.06	0.07	0.11	**1.3**
	300-180μm	26	0.09	<0.01	<0.01	0.02	0.02	0.01	0.07	0.11	0.19	0.05	0.11	0.11	0.07	0.08	0.10	0.17	0.13	**1.3**
	180-38μm	21	0.09	<0.01	<0.01	0.02	0.03	0.01	0.08	0.11	0.21	0.05	0.13	0.12	0.11	0.10	0.30	0.45	0.19	**2.0**
	<38μm	7	0.12	<0.01	<0.01	0.01	0.04	0.01	0.08	0.13	0.16	0.05	0.12	0.11	0.10	0.06	0.16	0.18	0.13	**1.5**
																			Weighted Total [PAH]:	**1.5**

PAH concentrations (mg/kg) in raw materials from the Alcan aluminum smelter.

Sample Type	naph	acen	acny	flu	phen	anth	fln	pyr	chry	Baa	Bxf	Bep	Bap	Pery	ipyr	dib	bper	Σ PAH
Coke Briquettes	347	<0.5	606	330	3963	822	8674	8640	6508	7703	17810	8407	11552	3275	9078	1975	7440	97130
Pencil pitch	1302	<0.5	2711	1278	11892	2398	25264	25384	19540	23252	56700	25217	34593	8703	26473	6308	21579	292593

Abbreviations: naph, napthalene; ace, acenaphthylene; flu, fluorene; phen, phenanthrene; anth, anthracene; fln, fluoranthrene; pyr, pyrene; chry, chrysene; baa, benzo(a)anthracene; bxf, benzofluoranthenes; bap, benzo(a)pyrene; ipyr, indeno(1,2,3-cd)pyrene; dib, dibenz(ah)anthracene; bper, benzo(ghi)perylene.

Weighted total [PAH] equals the total PAH concentration in each particle-size fraction (PSF), multiplied by the fraction of the total sediment dry weight contributed by that PSF.

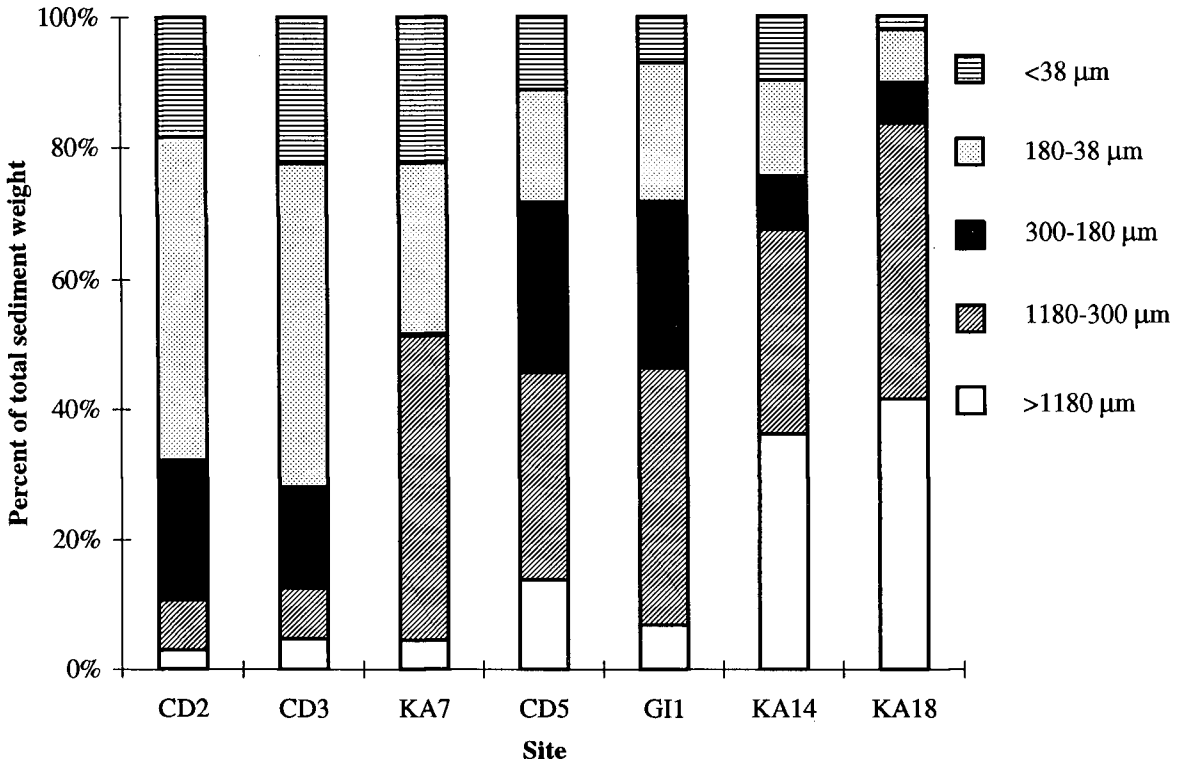

Figure 3-2 Sediment particle size distribution in Kitimat Arm surficial sediments.

The major sources of PAHs to Kitimat Arm are expected to be atmospheric particulate emissions, aqueous effluents, and spillage of raw materials (coke briquettes, pencil pitch) from the aluminum smelter. PAHs released at elevated temperatures in the vapor phase rapidly become particle-associated at ambient temperature due to the low vapor pressure of PAHs. Inputs of dissolved-phase PAHs into Kitimat Arm from smelter effluents are insignificant because of the low aqueous solubility of PAHs, and the high suspended sediment load in smelter effluents which favors sorption of PAHs to particles. The preferential association of PAH with larger particle sizes at the inner harbor sites (CD2, CD3), the very high absolute PAH concentrations (especially at CD2), and the striking similarity in PAH composition between smelter feedstocks and harbor sediments (Table 3-1) strongly suggest that raw material spillage is the dominant PAH input affecting the inner harbor sites.

The PAH composition at CD3 is sharply different from all other sites - especially in the smaller size fractions where perylene becomes the dominant PAH. If perylene is ignored, however, the composition in all size fractions at CD3 is almost identical with CD2. Furthermore, perylene concentrations tend to be highest in the smaller particle size fractions - an opposite trend to the other PAHs. These differences in the distribution of perylene compared to the other PAHs, amongst the various sediment particle size classes, cannot be explained in terms of different partitioning behavior of perylene. The most likely explanation for these differences is that the perylene at CD3 (at least in the smaller size fractions) was generated from a different source than are the other PAHs. In the light of the unusual distribution of perylene at CD3, the original GC-MS data from the CD3 extracts was re-examined in search of other naturally derived PAHs. Retene (1-methyl, 7-isopropyl phenanthrene) was detected in all extracts from CD3 and its distribution correlated significantly with perylene ($n=5$, $r=0.963$, $P<0.05$), and poorly with all other PAHs ($r<0.45$). Retene was not detected in coke briquettes or pencil pitch from the aluminum smelter, and combustion or pyrolysis of these fossil fuels would not be expected to form retene.

Retene is thought to be formed through early diagenesis of abietic acid (70, 75), and is often present in sediments impacted by runoff from coniferous forests (conifers are the dominant flora in the Kitimat catchment.) Retene has been detected in effluent streams from pulp mills (294), so the retene in Kitimat fjord sediments may also be derived from the Eurocan pulp mill which discharges effluent into the Kitimat River. For both of these sources the retene is derived from (recent) breakdown of terrestrial organic matter. High perylene concentrations (in the absence of other PAHs) are also usually associated with anoxic sediments and decaying organic matter (53).

Therefore the close coupling between retene and perylene at CD3 (and the accompanying poor correlation with other PAHs) indicates a recent terrestrial origin for these compounds.

Thus we conclude that the PAH composition at CD3 is the result of mixing of smelter derived inputs which dominated the large particle size fractions, and PAHs derived from terrestrial organic matter (retene, perylene) which dominate the small particle size fractions.

Differential partitioning of PAHs amongst sediment particle size classes could also affect the composition of individual PAHs within complex mixtures. The composition of PAHs in individual samples representing five different size fractions and six different sites was examined by using principal components analysis (PCA). PCA allows the exploration of similarities or differences between samples based on complex compositional data. The inter-sample variation in concentrations of the 16 individual PAHs is 'captured' onto a reduced set of principal components, which are linear combinations of the original variables.

The PCA analysis was run initially with all data shown in Table 3-1, but PAH data from site CD3 were subsequently excluded. The perylene-rich PAH composition of all size fractions of the sample collected from CD3, especially the finer fractions, set them apart from all other samples. Figure 3-3 shows that the first two principal components captured 34.7% and 20.2% of the between-sample variation in the original data set. The third and fourth principal components accounted for an additional 16.4% and 8.0% of the variation.

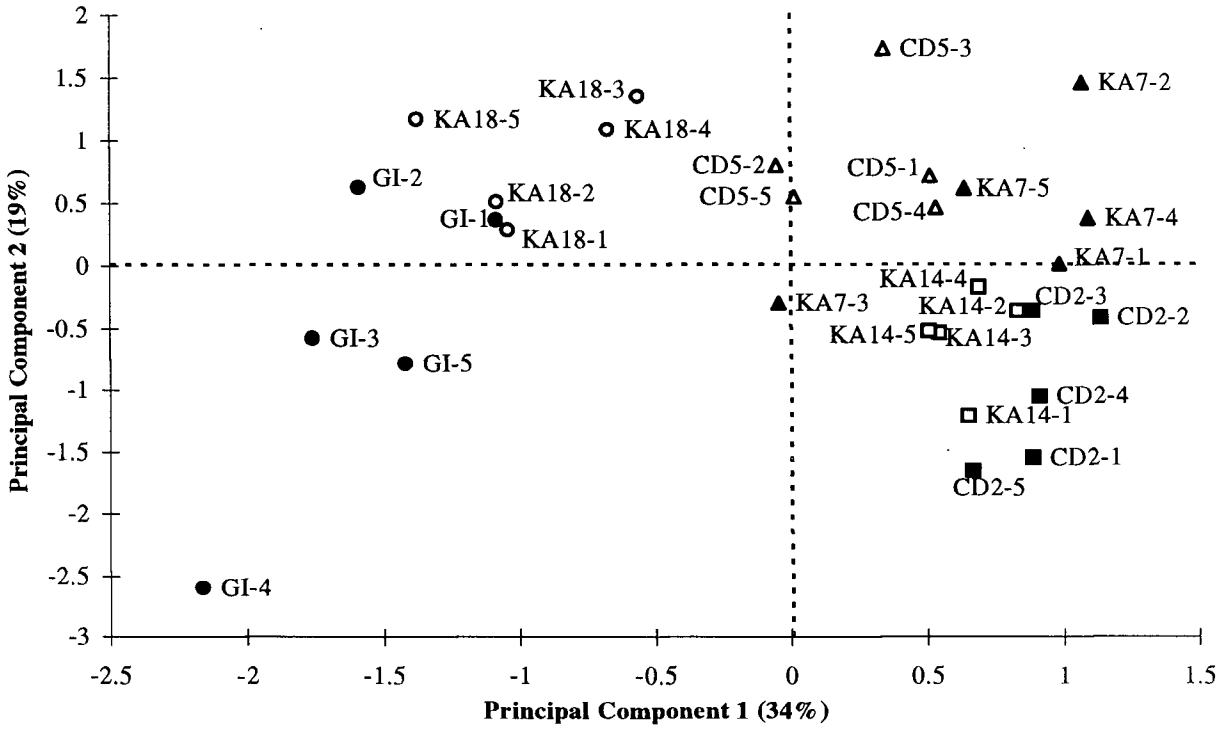

Figure 3-3 Principal components analysis of PAH composition across sites and different particle size fractions (legend: -1: > 1180 μm; -2: 300-1180 μm; -3: 180-300 μm; -4: 38-180 μm; -5: < 38 μm; e.g. CD5-3 is the 300-1180 μm sediment particle size fraction from site CD5). Note the separation of the distant sites (KA18, GI) from the other sites, on principal component 1.

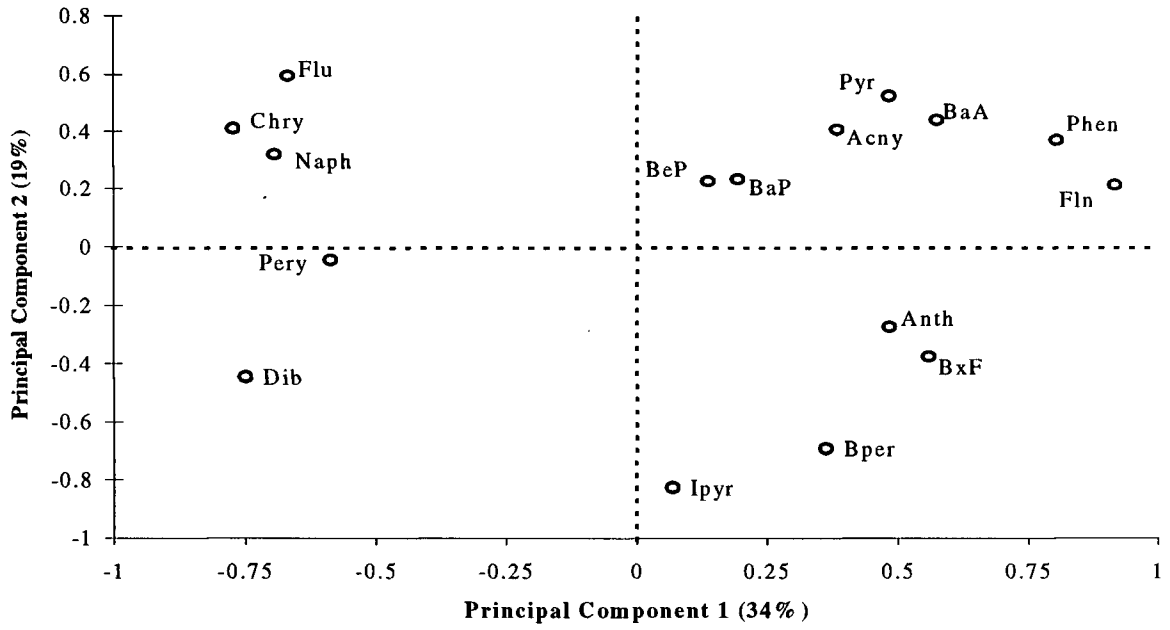

Figure 3-4 Principal component loading plot, showing influence of individual PAHs on the PCA. See footnote to Table 3-1 for abbreviations.

The proximity of individual samples to each other in Figure 3-3 reflects their compositional similarity. The five particle size classes are coded in the figure as 1 to 5 (e.g., CD5-5), from the largest to the smallest size fraction. There was no apparent grouping of the samples based on similarities in particle size for any of the first four principal components. The PAH composition instead reflects the geographic location of the collection sites. The sites are distributed along the first principal component according to their proximity to the head of Kitimat Arm, with samples (all size fractions) from Giltoyees Inlet (site GI) and KA18 plotting to the left of the origin. Some separation between different sites is also evident on the second principal component: Site CD2 is distinguishable from CD5 based on the PAH composition, with sites KA7 and KA14 forming an intermediate, semi-discrete group. Similar site groupings were evident when the dataset was subjected to cluster analysis.

The influence of specific PAHs on multivariate similarities or differences between samples is evident from the loading plot (Figure 3-4). Samples from sites with negative scores on the first principal component in Figure 3-3 (GI and KA18) were influenced primarily by higher relative concentrations of perylene, dibenz(*a*)anthracene, chrysene, naphthalene and fluorene (compounds with negative scores on the first principle component in Figure 3-4). The separation of samples from Giltoyees Inlet in the lower left quadrant of Figure 3-3 from other sites resulted from higher relative concentrations of dibenz(*a*)anthracene and perylene, and low levels of phenanthrene in particular. The positions in Figure 3-3 of samples from sites CD2, KA7 and KA14 reflected elevated levels of fluoranthene and benzofluoranthenes. The probable source of this latter set of PAHs is through combustion (pyrogenesis), whereas perylene - which increases in relative concentration down the inlet - is attributable to both combustion and natural plant sources.

The PCA reflects, above all, a different PAH composition at sites proximate to the smelter compared to sites further removed from it. This may be explained by a decline in the proportion of aluminum-smelter-derived PAHs at the distant sites, relative to naturally occurring PAHs.

As was the case for the other Kitimat Arm sites not in the immediate vicinity of the smelter (KA7, KA14, KA18), no consistent relationship was observed between PAH concentration and particle size fractions at the GI site. The Giltoyees Inlet site (GI), in a side arm to the main channel, is substantially isolated geographically from water-borne particles carried down Kitimat Arm and Douglas Channel. Atmospheric transport of particles is probably the only major mechanism by which anthropogenic PAHs inputs can occur at site GI. It should be noted, however, that the water surface in Giltoyees Inlet comprises a much smaller area than the surrounding terrestrial environment within the Giltoyees Inlet catchment area. The composition of atmospheric PAH inputs could potentially be modified during deposition of PAH-laden particles onto terrestrial surfaces and soils, followed by water-borne transport into the inlet and subsequent sedimentation.

Equilibrium models of hydrophobic organic compound partitioning to particles predict that compounds with higher K_{OW} should be progressively enriched on small particles with high organic matter content, as has been observed with polychlorinated biphenyls (295). We see little variation in PAH composition amongst the various sediment particle size factions in Kitimat sediments. This may suggest that PAH partitioning in Kitimat sediments is controlled by the rate of desorption.

3.3.2 Influence of sediment diagenesis on PAH composition in Giltoyees Inlet

The concentrations of unsubstituted and alkylated PAHs, and sediment f_{OC}, in the Giltoyees Inlet core are listed in Table 3-2.

Table 3-2 PAH concentrations (ng/g, dry weight) in 5 cm sections from a Giltoyees Inlet core.

Depth in Sediment (cm)	**0-5**	**5-10**	**10-15**	**15-20**	**45-50**	**50-55**	**55-60**	**60-65**	**65-70**
f_{OC}	0.013	0.010	0.0084	0.0082	0.0081	0.0083	0.0084	0.0080	0.0078
Compounds									
Naphthalene	25	16	4.5	5.2	3.6	7[1]	7.6	13[1]	6.4
Acenaphthylene	0.4[1]	0.3	0.28[1]	0.16[1]	<0.12	<0.14	<0.16	<0.19	<0.15
Acenaphthene	3.0	3.0	0.38[1]	<0.17	<0.26	<0.18	<0.19	<0.2	<0.33
Fluorene	4.0	2.0	0.67	0.25	0.27[1]	<0.25	0.35[1]	<0.28	<0.33
Phenanthrene	24	20	5.1	1.7	1.3	1.4	1.3	1.2	1.2
Anthracene	5.0	5.0	0.93	0.17[1]	<0.15	<0.17	<0.18	<0.17	<0.18
Fluoranthene	66	54	12	2.5	0.22[1]	0.36[1]	0.41[1]	0.24	0.43
Pyrene	59	54	14	4.1	1.0[1]	0.97[1]	0.8[1]	0.73	0.88
Benzo(a)anthracene	30	28	6.4	1.2	<0.21	<0.23	<0.24	<0.23	<0.21
Chrysene	50	39	8.4	1.6	0.64	0.36[1]	0.64[1]	0.53	0.5
Benzofluoranthenes	170	170	35	7.6	0.65[1]	0.75[1]	<0.28	<0.26	<0.23
Benzo(e)pyrene	69	68	16	3.1	<0.26	<0.29	<.3	<0.28	<0.25
Benzo(a)pyrene	55	50	9.5	1.8	<0.31	<0.34	<0.35	<0.33	<0.29
Perylene	140	62	30	26	23	22	22	22	22
Dibenz(ah)anthracene	13[1]	13	2.1[1]	<0.47	<0.66	<0.44	<0.45	<0.46	<0.55
Indeno(1,2,3-cd)pyrene	76	72	13	3.5	0.49[1]	0.4[1]	<0.4	<0.38	<0.34
Benzo(ghi)perylene	66	65	16	4.2	<0.34	0.69	0.56	0.65[1]	0.65[1]
Total unsubstituted PAHs	**855**	**721**	**174**	**63**	**31**	**34**	**34**	**38**	**32**
C1 naphthalenes	5.0	4.0	1.1	1.3	1.5	1.6	1.0	1.6	1.4
C2 naphthalenes	7.0	4.0	<1.6	<1.0	<0.86	<1.1	<1.2	<1.4	<1.5
C3 naphthalenes	4.0	3.0	<0.55	<0.28	<0.21	<0.28	<0.5	<0.32	<0.49
C4 naphthalenes	<0.02	<0.02	<0.58	<0.37	<0.31	<0.41	<0.44	<0.48	<0.55
C5 naphthalenes	0.6	0.3[1]	<0.49	<0.29	<0.21	<0.3	<0.33	<0.46	<0.4

Table 3-2 (continued)

Depth in Sediment (cm)	0-5	5-10	10-15	15-20	45-50	50-55	55-60	60-65	65-70
C1 phenanthrenes/anthracenes	14	13	2.7	0.98	1.2	1.4	1.1	1.0	1.2
C2 phenanthrenes/anthracenes	23	14	<0.21	<0.17	<0.17	<0.19	<0.2	<0.33	<0.18
C3 phenanthrenes/anthracenes	<0.05	8.0	<0.34	<0.27	<0.28	<0.18	<0.25	<0.3	<0.19
C4 phenanthrenes/anthracenes	3.0	8.0	1.7	1.2	0.94	0.89	0.9	1.1	0.94
Retene	3.0	8.0	1.7	1.2	0.94	0.89	0.9	1.1	0.94
C5 phenanthrenes/anthracenes	<0.05	<0.05	<0.34	<0.27	<0.23	<0.33	<0.23	<0.48	<1.3
C1 fluoranthenes/pyrenes	48	34	6.2	2.2	0.81	<0.14	0.85	0.56	0.26
C2 fluoranthenes/pyrenes	40	21	6.3	<0.33	<0.3	<0.26	<0.35	<0.31	<0.4
C3 fluoranthenes/pyrenes	<0.07	<0.07	<0.66	<0.3	<0.42	<0.4	<0.34	<0.26	<0.48
C4 fluoranthenes/pyrenes	<0.08	<0.08	<0.72	<0.57	<0.37	<0.56	<0.53	<0.36	<0.53
C5 fluoranthenes/pyrenes	<0.2	<0.2	<0.86	<0.62	<0.66	<0.83	<0.69	<0.85	<0.49
Dibenzothiophene	2.0	2.0	<0.18	<0.15	<0.14	<0.16	<0.16	<0.16	<0.16
C1 dibenzothiophenes	1.0	0.9	<0.19	<0.1	<0.09	<0.09	<0.12	<0.16	<0.19
C2 dibenzothiophenes	1.0	1.0	<0.1	<0.08	<0.06	<0.1	<0.12	<0.11	<0.08
2-methyl naphthalene	4.0	2.0	1.0	0.9	1.0	1.0	1.0	1.0	0.9
1-methyl naphthalene	2.0	1.0	<0.9	0.4	0.4	0.5	<0.5	<0.5	<0.4
2,6/2,7-dimethyl naphthalene	3.0	1.0	<1.0	<0.9	<0.7	<1.0	<1.0	<1.0	<1.0
1,2-dimethyl naphthalene	<0.06	<0.08	<2.0	<1.0	<1.0	<1.0	<1.0	<2.0	<2.0
1,4,6/1,3,5/2,3,6-trimethyl naphthalene	1.0	0.7	<0.6	<0.3	<0.2	<0.3	<0.5	<0.3	<0.5
1,2,7/1,6,7/1,2,6/2,3,5-trimethyl naphthalene	0.8	0.6	<0.5	<0.3	<0.2	<0.3	<0.5	<0.3	<0.5
3-methyl phenanthrene	3.0	3.0	0.6	<0.2	0.3	0.3	0.2	<0.2	0.2
2-methyl phenanthrene	4.0	3.0	1.0	0.3	0.4	0.5	0.4	0.4	0.4
2-methyl anthracene	1.0	1.0	<0.3	<0.2	<0.2	<0.2	<0.2	<0.2	<0.2
9-methyl/4-methyl phenanthrene + 1-Methyl Anthracene	2.0	3.0	0.6	<0.2	0.2	0.3	0.2	<0.2	0.3
1-methyl phenanthrene	2.0	2.0	0.4	<0.2	0.2	0.2	0.2	<0.2	0.2
3,6-dimethyl phenanthrene	0.6	0.6	<0.1	<0.09	<0.09	<0.1	<0.1	<0.1	<0.09
9,10-dimethyl anthracene	<0.01	<0.01	<0.1	<0.09	<0.09	<0.1	<0.1	<0.1	<0.09
2-methyl fluoranthene	9.0	8.0	0.7	0.5	0.2	0.2	0.3	0.1	0.2

[1]*Peak detected, but did not meet quantification criteria.*

Organic carbon content (f_{OC})was highest in the surface sediments, with minimal changes-with-depth below approximately 15 cm. The elevated f_{OC} in sediments from the upper part of the core may reflect increased organic matter inputs in recent times because of logging activity in the Giltoyees watershed.

Total PAH concentrations were highest in the top segments of the core, and declined dramatically with depth over the top 20 cm. Below a depth of 40 cm, total PAH levels remained relatively constant. This trend is illustrated in Figure 3-5. The PAH composition also changed dramatically with depth. The upper 20 cm was dominated by unsubstituted PAHs of intermediate and high molecular weight. The profile is very similar to the contaminated surface sediments discussed earlier in this chapter, and is attributed to anthropogenic combustion inputs - arising primarily from the aluminum smelter at Kitimat. The core sediments were not dated; however, if it is assumed that the increase in PAH concentrations at a depth between 20 and 45 cm coincides with the commencement of operations at the aluminum smelter in 1954, and at the same time the effects of sediment compaction and biological mixing are ignored, an approximate sedimentation rate of 0.25-0.5 cm per year is estimated. This is well within the range of values calculated for recent uncompacted sediments in the Kitimat fjord system (281). Other workers have reported sub-surface maxima in PAH concentrations, coincident with a worldwide reduction in coal combustion and improved emission control technology (85, 296, 297). The lack of a sub-surface maxima in the present data supports our contention that the PAH flux at this site is dominated by ongoing local inputs.

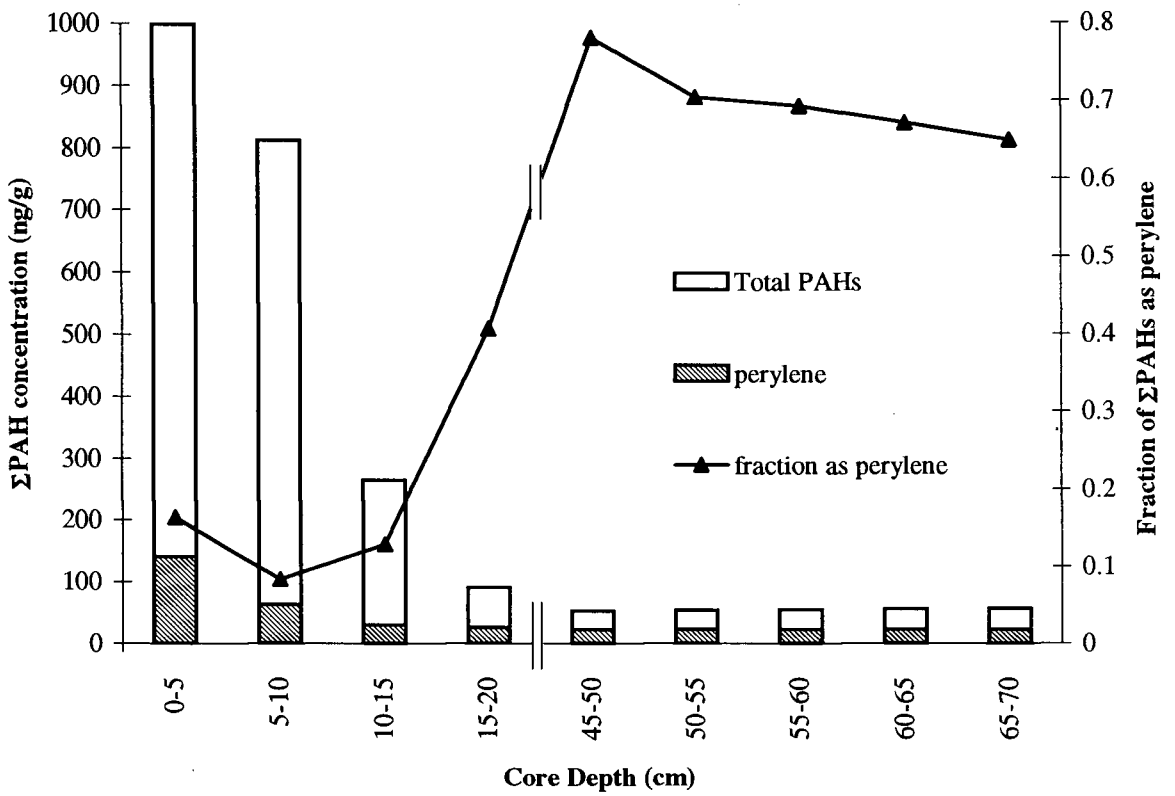

Figure 3-5 Trends in total PAH concentration and perylene concentration versus sediment depth in a sediment core from Giltoyees Inlet.

The PAH composition in core segments below 45 cm is accounted for almost entirely by unsubstituted and alkylated forms of naphthalene, phenanthrene and pyrene, and unsubstituted chrysene and perylene. Many of these compounds have been previously reported in PAH assemblages arising from early diagenesis of plant material (70, 75, 150, 166). The major downward trend in the upper core is progressive dilution of the smelter PAH composition by the natural PAH signature. This is especially evident in the higher relative amounts of naphthalene, phenanthrene and perylene, as well as diminution of anthracene at 15-20 cm compared with 0-5 cm (Table 3-2, Figure 3-6).

In the Giltoyees Core, the proportion of perylene changes independently of the other PAHs as a function of depth (Figure 3-5). Perylene has been reported by several researchers as a minor component of combustion particles (53, 55), and in the present study it was detected in raw

materials from the Alcan smelter (Table 3-1). Perylene has also been found in significant concentrations where other combustion derived PAHs are absent, in some instances comprising up to 80% of the total PAHs present (53). In these instances perylene is thought to be formed as a result of the early diagenesis of plant material, and its production seems to be favored by suboxic conditions in the sediments (298). As can be seen from Figure 3-5, the trend in the absolute concentration of perylene follows the trend in total PAHs very closely (i.e. concentrations were highest at the top of the core, declining to stable background levels by the 15-20 cm segment). However, the fraction of total PAHs accounted for by perylene changes dramatically with sediment depth. Perylene contributed 3-5% of total PAHs in smelter feedstock and surface sediments at sites CD2, CD5, KA7 and KA14 (Table 3-1), and 9-17% of the total PAHs in the top 15 cm of the core, but accounted for approximately 70% of the total PAHs in core sections below 45 cm, where most of the other combustion generated PAHs were below the detection limits. This trend, which clearly illustrates the dual sources of perylene, was also observed by Wilcock et al. (299) in a long (approximately 2 m) sediment core collected in New Zealand, and by Wakeham (300) in the top 10 cm of a sediment core from the Black Sea. The major inputs of perylene may be either natural or anthropogenic, and the dominant source for a given site may change over time.

Recent studies have suggested that rates of PAH removal from aerobic environments are influenced by the degree of alkylation (89, 301): More highly alkylated forms tend to be more recalcitrant to both weathering and biodegradation, resulting in preferential loss of lower alkylated and unsubstituted forms. In contrast, photo-oxidation of crude oil results in preferential loss of higher alkylated species (92, 148). These processes, and others that act differentially upon individual PAHs, will alter the PAH composition in the environment. The data in Table 3-2 were

examined for evidence of post depositional changes in PAH composition. In addition, in order to explore post-depositional changes in the *anthropogenically-enhanced PAHs specifically,* we attempted to remove the contribution of natural inputs from anthropogenically-enhanced PAHs. This was done by calculating the average concentration for each PAH in samples below 45 cm depth, and subtracting these average concentrations from PAH levels in more recent sediments. The (non-subtracted) profiles of various alkyl- or unsubstituted homologue groups are illustrated in Figure 3-6.

Levels of C2- and C3-naphthalenes are highest in recent sediments (upper 10 cm, Figure 3-6), indicating that C2 and C3 naphthalenes are derived from anthropogenic inputs. Their absence in older sediments (deeper than 10 cm) simply reflects decreasing anthropogenic inputs with increasing sediment depth. (C1, C2 and C3 alkyl homologues of naphthalene, phenanthrene/anthracene and fluoranthene/pyrene are present in pencil pitch and coke briquettes used at the aluminum smelter) (data not shown). For sediment depths greater than 10 cm, any changes seen in the ratios of alkyl-substituted naphthalenes to unsubstituted naphthalenes, C1 naphthalenes to C2 naphthalenes, or 1-methylnaphthalene to 2-methylnaphthalene, based on either data corrected for natural inputs or the original data, are primarily an artifact of the data being at or below the detection limit in core samples below 10 cm depth.

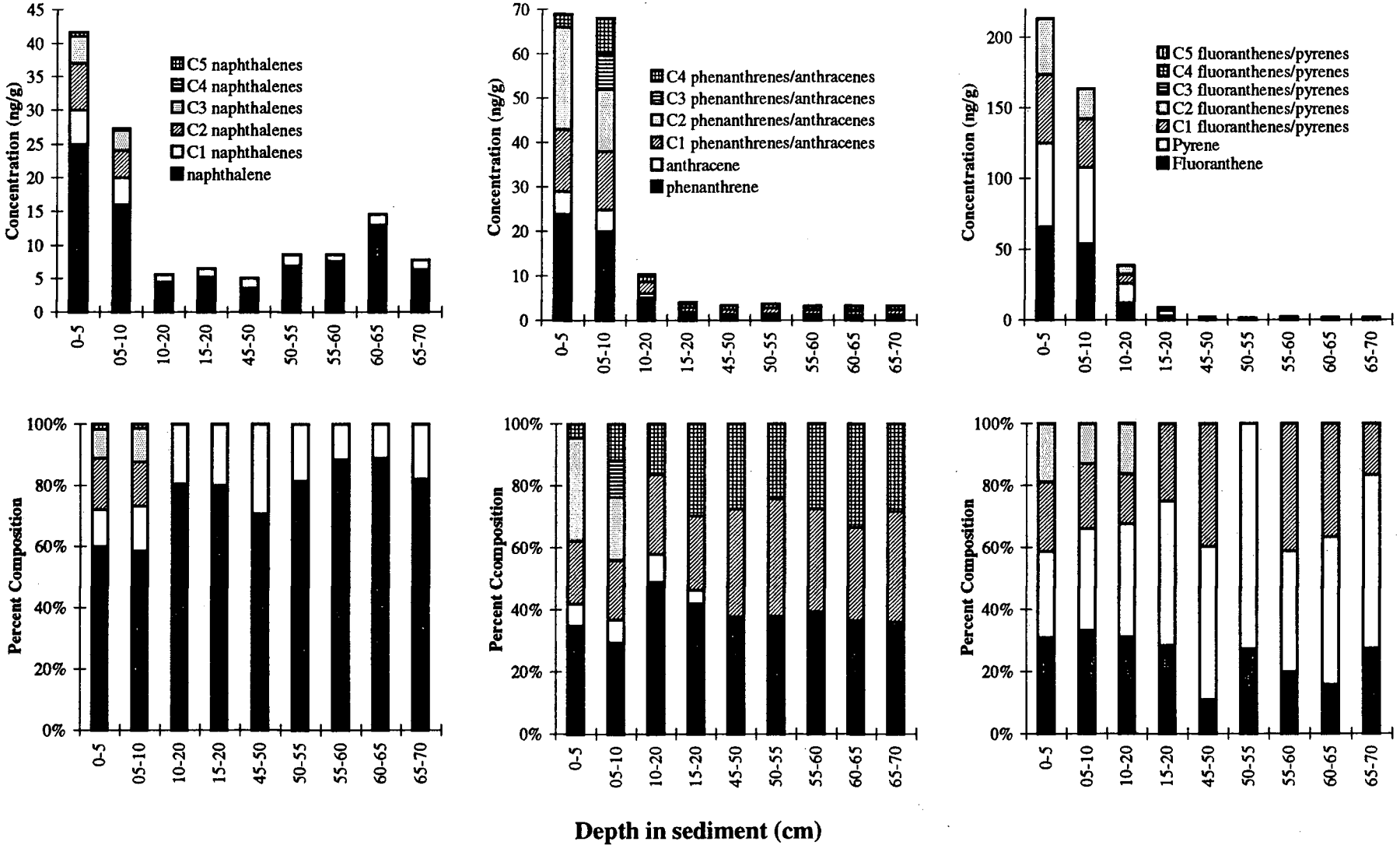

Figure 3-6 Vertical trends in alkyl- vs. unsubstituted PAH composition in a sediment core from Giltoyees Inlet.

The absolute concentrations of all phenanthrene alkyl homologue groups are highest in the top 20 cm (Figure 3-6), indicating significant anthropogenic inputs of these compounds. As was observed for the naphthalene series, there is a general decline in the proportion of C2-phenanthrenes and anthracenes below 10 cm depth, and this trend parallels the decline in anthracene, which is contributed by anthropogenic inputs from the aluminum smelter. Retene accounts for the entire C4-anthracenes/phenanthrenes concentration at all depths. The *proportion* of retene increases with increasing depth over the first 20 cm, coincident with decreasing levels of anthropogenic PAHs. However, absolute amounts of retene decrease with depth in the top portion of the core, and are constant below 45 cm. The constant retene concentration in the lower core implies that there is no net post-depositional production or degradation of retene in deep sediments, whereas the trend of higher retene concentrations in the upper core suggest an increased flux of retene to recent Giltoyees Inlet sediments, probably related to logging activities in the watershed.

Long term diagenesis - as in coal or oil maturation, for example - is often characterized by an initial increase in the ratio of alkylated phenanthrenes to phenanthrene, accompanied by a progressive enrichment of the more thermodynamically stable alkyl- isomers. (71, 93, 302). This has led to the development of maturation indices based upon C1-phenathrene ratios, in particular. Early diagenesis of anthropogenic PAH in Giltoyees Inlet (top 20 cm) was not accompanied by any consistent trend in the relative proportions (before or after correcting for average natural inputs) of any of the individually analyzed alkylated phenanthrenes or anthracenes (Figure 3-7). However, in the lower core (45-70 cm) the proportion of C1-phenathrenes:phenanthrene exhibited a slight increase with increasing depth which may indicate net production of C1-phenanthrenes due to early diagenesis of detrital organic material.

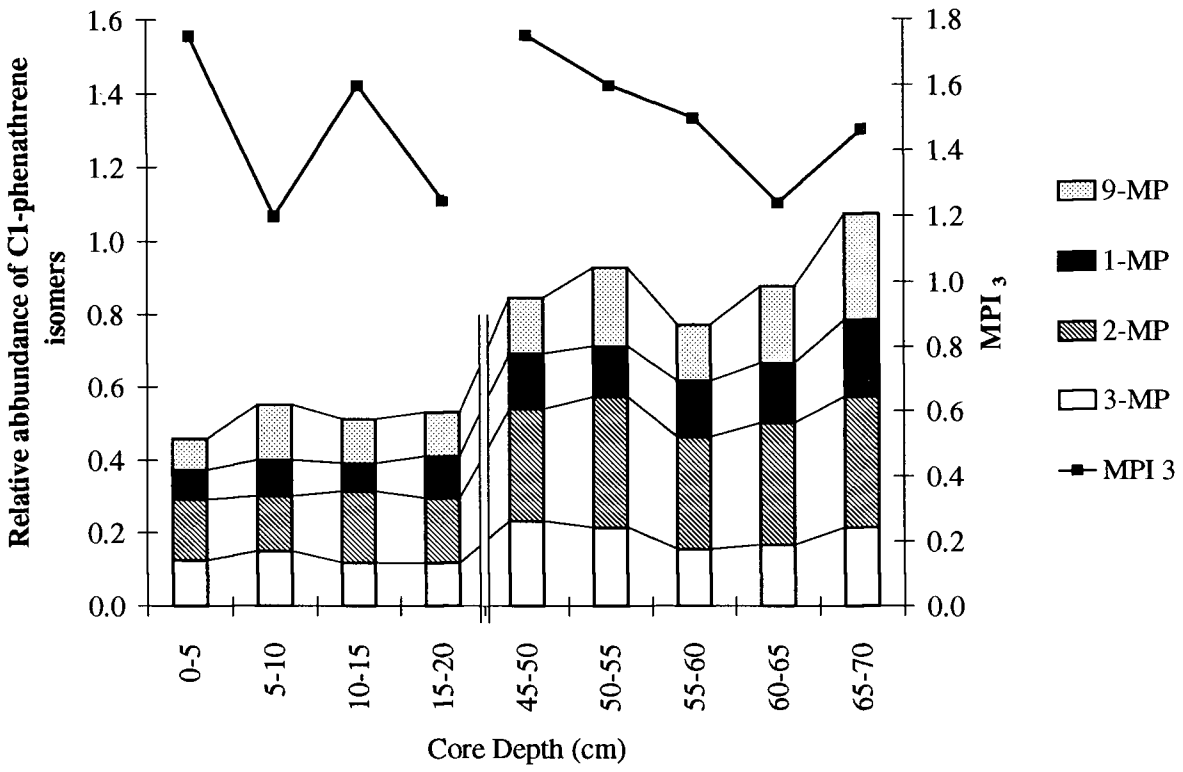

Figure 3-7 Vertical trends in relative abundance of individual monomethyl phenanthrene isomers (abundance of each compound expressed as a fraction of the phenanthrene concentration in each sample), and in the methyl phenanthrene index MPI_3 versus depth in the Giltoyees Inlet sediment core. (Legend: 9-MP : 9-methyl phenanthrene; 1-MP : 1-methyl phenanthrene; 2-MP : 2-methyl phenanthrene; 3-MP : 3-methyl phenanthrene).

The methyl phenanthrene index MPI_3 is defined by Garrigues *et al.* (93) as the sum of 3-methyl + 2-methyl phenanthrene divided by the sum of 1-methyl + 9-methyl + 4-methyl phenanthrene, and has often been used as an index of oil maturation. The value of MPI_3 increases as the oil matures due to enrichment of the 2-methyl and 3-methyl phenanthrenes, which have greater thermodynamic stability than the other isomers. In the present study, MPI_3 showed a significant decrease in the lower core ($n=5$, $r=-0.996$, $P<0.05$) due to increasing proportions of 9-methyl phenanthrene (Figure 3-7). This trend is opposite to that defined by the thermodynamic stability of the C1-phenathrenes, but it is consistent with 9-methyl phenanthrene being especially resistant to microbial degradation, as observed by Bayona et al. (68). These authors suggested that oxidation of the 9-10 double bond is the favored site of microbial attack for the phenanthrene

homologues, and this pathway is effectively blocked by the presence of a methyl group at the 9 position in 9-methyl phenanthrene.

The only obvious change in the fluoranthene/pyrene distribution with depth is the dramatic disappearance of the C2-fluoranthene/pyrene compounds below 15 cm depth (Figure 3-6), indicating an anthropogenic origin for these compounds. (None of the corresponding individual isomers were analyzed). Detailed interpretation of the alkyl-substituted fluoranthene:pyrene ratios in the Giltoyees Inlet core was not attempted, since levels were near or below the detection limits in most cases.

Because of the absence of most unsubstituted PAHs below 45 cm in the sediment core, possible diagenetic changes in unsubstituted PAHs could be investigated in the upper core segments only. As described earlier, the data set was first corrected (where necessary) for natural inputs by subtracting the average concentration of each compound in the lower core (which was zero in many cases) from its concentration in each segment in the upper core. In general, the concentrations of low molecular weight unsubstituted PAHs declined more rapidly with depth than did high molecular weight unsubstituted PAHs. This suggests loss of the low molecular weight compounds due to either greater ease of biodegradation, or higher water solubility relative to the other PAHs.

Various workers have demonstrated changes in ratios of specific PAH isomers as a result of weathering by environmental processes, including enrichment of the thermodynamically-most-stable isomers (84, 285). In the present work the following ratios increased with increasing sediment depth; (thermodynamic isomer in numerator) Bper/Ipyr, Pyr/Fln, Bep/Bap; although these changes are not statistically significant ($P>0.05$). Phen/Anth and Chry/Baa ratios showed no

discernible trend. These results, therefore, show only limited evidence of enrichment of the thermodynamic isomers with increasing sediment depth. The absence of a discernible trend in these isomer ratios with depth is consistent with data from other sediment cores (63, 297), and further demonstrates the recalcitrance of PAHs in sediments. This recalcitrance may be due to; (i) limited chemical and biological availability of the anthropogenic PAHs in these samples which may be particle occluded, having been generated by combustion processes (145, 166), and, (ii) increased resistance to biodegradation of PAHs in these samples due to rapid onset of anoxia in the sediments.

In summary, changes in the ratios of alkylated to unsubstituted PAH homologues, and ratios of thermodynamic to kinetic PAH isomers in the present data set largely reflect changes in the proportion of anthropogenic versus natural PAH inputs. The data do not permit a complete analysis, however, since detailed PAH assignments have not been confirmed for the major portion of the homologue groups. The only evidence for biodegradation of PAHs is seen in the data for the phenanthrene homologue group in the form of a decrease in MPI_3, and an increase in the proportion of C1-phenanthrenes with depth, in the lower core. It is possible to speculate that these naturally derived PAHs would be more bioavailable than the anthropogenic PAHs in the upper core (and hence more amenable to biodegradation). This is because the natural PAHs are less likely to be particle occluded than the combustion generated anthropogenic PAHs, and the natural PAHs are also less likely to be associated with soot carbon, which binds PAHs especially strongly (163). The present data, however, are insufficient to provide conclusive evidence of biodegradation *in situ*.

4. Partitioning of Polycyclic Aromatic Hydrocarbons between sediments and the Soft-Shelled Clam, *Mya arenaria*

4.1 Introduction

It is well known that aquatic organisms accumulate significant quantities of organic contaminants in their tissues - often to levels well in excess of the surrounding water. It is partly for this reason that the analysis of aquatic biota has become an important tool for monitoring chemical contamination of the environment. Bivalves are particularly favored for this purpose as they are sedentary, abundant, and possess limited ability to metabolize PAHs (38, 56, 116, 180).

However, accumulation of toxic chemicals by mollusks may lead to problems for human health if they are eaten. If the contaminated mollusks are eaten by other organisms, they will provide a route of re-entry for PAHs into the food chain.

4.2 Objectives

Mya arenaria were collected from four beaches in the Kitimat fjord system as shown in Figure 4-1. Three sites (Hospital Beach (HB), Eurocan Beach (EU), Kitimaat Beach (KV)) were expected to be impacted by PAHs discharged from the Alcan aluminum smelter. The fourth site, Kildala Beach (KB), was chosen as a reference site, because the analysis of marine sediments collected from Kildala Inlet (Chapter 2), showed minimal contamination by PAHs. Beach sediments were also collected from the same locations as the clam specimens, and both clams and sediments were analyzed for PAHs.

The first objective of this experiment was to determine the extent of PAH accumulation in *Mya arenaria* i.e. measure biota-sediment accumulation factors (BSAFs). By relating the measured BSAFs to theoretical predictions it should be possible to test the validity of the equilibrium partitioning (EP) theory in these samples, and to gain insight into the processes affecting PAH accumulation at these sites. The EP model was chosen because it is widely used by regulators. It is also more readily tested that dynamic accumulation models. The PAH composition in *Mya arenaria* and sediments can also be compared to determine whether any differential accumulation of PAHs takes place.

4.3 Theories of hydrophobic organic contaminant accumulation in biota

Theories developed to describe contaminant accumulation by biota fall into two classes: equilibrium models and kinetic models (126, 127, 176).

The EP theory assumes that chemical uptake into an organism is an equilibrium process, as described in Chapter 1. Partition of the chemical between an organism and its environment is governed by differences in the fugacity of the contaminant in different environmental compartments (126, 127, 303). Hydrophobic organic compounds (HOCs) partition to the organic matter content of the sediment (155, 156), and to the lipid phase of biota (37, 56). Thus, when uptake of the chemical is primarily from contaminated sediment, the BSAF can be defined as in eqn. (1) (see section 1.4.7.3 for definition of abbreviations).

$$BSAF = \frac{C_B \times foc}{C_S \times f_L} \qquad \text{eqn. (1)}$$

Eqn. (1) implies that there is no correlation between BSAF and hydrophobicity and that BSAFs should be identical for all organisms (i.e. for any given PAH in any species the ratio C_B/C_S at

equilibrium should be constant, the value of which is suggested to be about 1.7) (170). An attractive feature of the EP model is that it allows the prediction of contaminant concentrations in water, or in biota, based on measurement of contaminant concentrations in the sediment, measurement of f_{OC}, and realistic estimates of f_L and/or DOM. The EP model treats the organism as a single homogeneous phase which is in thermodynamic equilibrium with the sediments. It ignores the physiological processes responsible for contaminant transfer between the various compartments. If the assumption of thermodynamic equilibrium does not hold, the EP theory is an inappropriate model to use.

Alternative models view bioaccumulation as a dynamic balance between rates of contaminant uptake and rates of contaminant release (126, 127, 176). The simplest expression of this type of model, which assumes first order kinetics, is shown in eqn. (2):

$$\frac{d}{dt}C_B = k_1 C_S - k_2 C_B \qquad \text{eqn. (2)}$$

where k_1 and k_2 are the rate constants for uptake and depuration respectively. The steady-state solution for eqn. (2) is shown in eqn. (3):

$$\frac{C_B}{C_S} = \frac{k_1}{k_2} \qquad \text{eqn. (3)}$$

Steady-state models such as eqn. (3) are not constrained by the necessity for thermodynamic equilibrium. Steady-state models also allow for differences in BSAFs between individual PAHs, and between different organisms (126, 127).

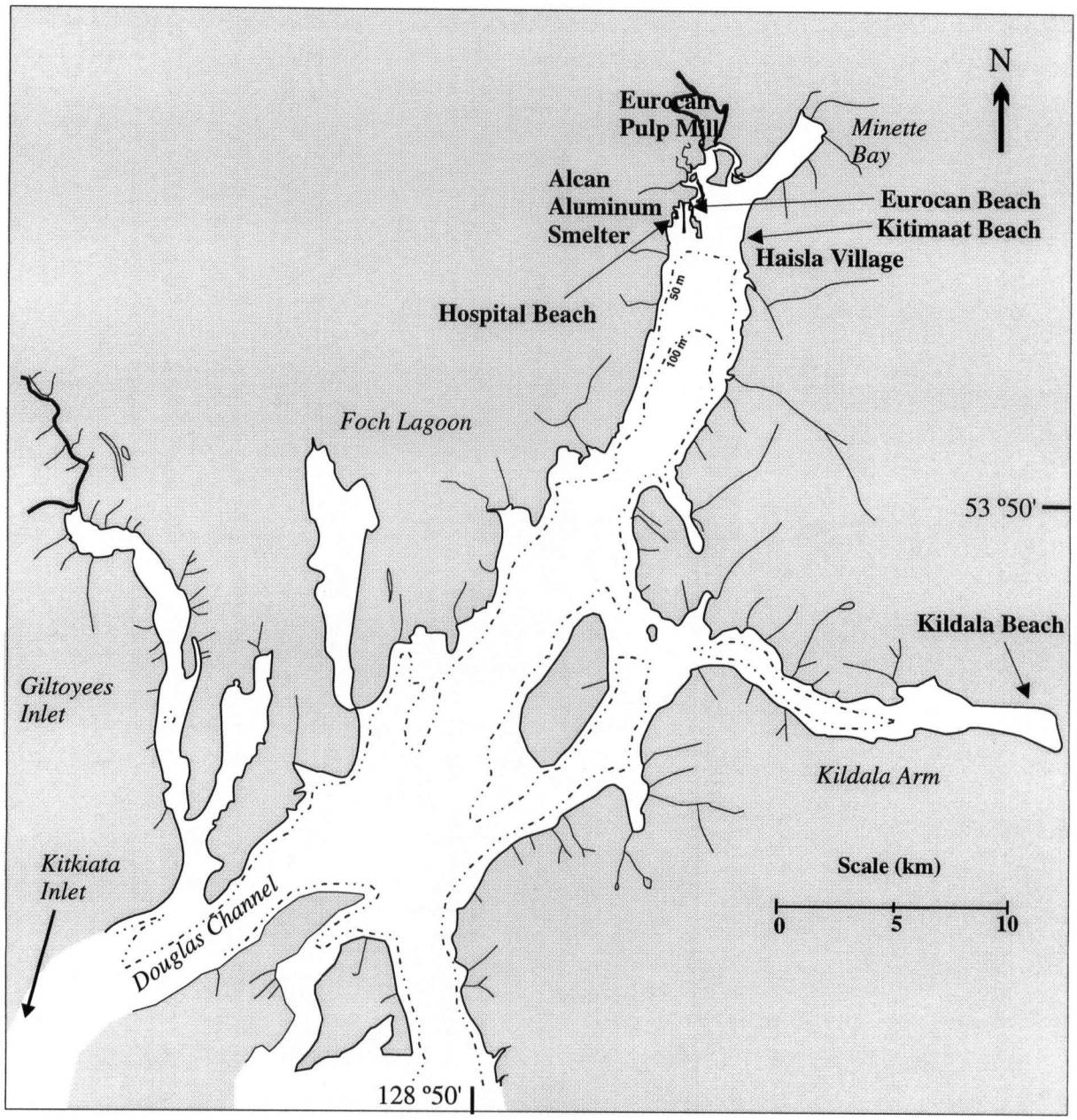

Figure 4-1 *Map of Kitimat fjord system, showing beaches where clams and sediments were collected*

4.4 Experimental

4.4.1 Sample collection

Mya arenaria were collected at four beaches in the Kitimat fjord system, as shown in Figure 4-1. All *Mya arenaria* were collected from colonies located near small stream or river channels. A drain from the Alcan property, believed to be the effluent lagoon D discharge, and containing a high load of black suspended particles, fed into the Hospital Beach stream. *Mya arenaria* were buried at a depth of between 20-50 cm, and extreme care was required when digging them out of the sand to prevent fracturing the shells. After collection *Mya arenaria* were placed in flowing seawater for 6 to 12 hours to allow depuration of gut content. They were then placed in plastic ziplock bags and frozen for subsequent analysis.

Beach sediments were also collected from the same location as *Mya arenaria.* Sediments were sampled with methylene chloride rinsed stainless-steel scoopulas and collected into pre-cleaned 1 L amber glass bottles (two bottles per site). The bottles were immediately frozen for subsequent analysis.

4.4.2 Validation of Biobeads SX-3 size exclusion chromatography (SEC)

Because of the high lipid content of biota, an extra sample cleanup step must be incorporated to separate the PAHs from the lipids. In the present work this was accomplished by using SEC, with Biobeads SX-3 as the stationary phase. A stainless steel column (32 cm x 2.5 cm) was slurry packed with Biobeads SX-3 which had been pre-equilibrated in 50:50 chloroform:hexane. The column was connected to an HPLC system consisting of a Waters 600E system controller, Waters U6K injector and Waters model 470 scanning fluorescence detector. A new solvent mixture, 75:25 chloroform: hexane, was then pumped through the column at 0.2 mL/min. This new mobile

phase causes swelling of the Biobeads. There was also the possibility that swelling the Biobeads to their final volume inside the stainless-steel column would minimize channeling in the stationary phase. The flow rate through the column was 2 mL/min. and the eluent composition was 75:25 chloroform:hexane. The elution of both lipids and PAHs was monitored on line by fluorescence detection (excitation λ 340 nm, emission λ 380 nm).

The SEC column was calibrated by injecting 2 mL of a solution of canola oil in chloroform (0.125 g/mL), that had been spiked with a standard mixture of the US EPA 16 priority pollutant PAHs. The eluent was collected into test-tubes by using a Gilson FC203 fraction collector. A portion was taken from each test-tube for analysis of the PAHs by GC-MS, and the remainder was used for gravimetric determination of the lipid.

4.4.3 Determination of PAHs in clam tissue

Mya arenaria were allowed to partially thaw, and then were measured across the longest axis of the shell, and weighed. They were then shucked, and the periostracum and the tip of the siphon, which were contaminated with sediment, were removed. The soft parts were rinsed with deionized water to remove any sediment and were patted dry with lint-free paper towels. Three individuals (137 g - 187 g total wet weight) were pooled for each sample and then homogenized in a blender for ca. 5 min. Three replicates were prepared for each site. The homogenates were transferred to pre-weighed clean glass beakers and freeze dried.

The freeze dried, homogenized clam tissue was further ground with a mortar and pestle, and then an aliquot was extracted with methylene chloride (210 mL) for 8 hours, as described previously (see Chapter 2) for sediment samples. An internal standard (d_{10}-pyrene, 258 ng), was added to each sample prior to extraction.

The methylene chloride extract was reduced in volume to ca. 2 mL by using a rotary evaporator, and transferred quantitatively with two methylene chloride rinses to 15 mL cleaned, pre-weighed conical test tubes. The extract was evaporated to dryness at 40 °C, and the lipid determined gravimetrically.

Chloroform (2 mL) was added to each test-tube to dissolve the extract. The extract was then filtered through 0.22 μm PTFE syringe filters. Between 0.6-1.0 mL of filtered extract was injected onto a SEC column to separate the PAHs from the lipids, as described in section 4.4.2. The PAH containing fraction (40 min. - 70 min.) from the SEC system was collected, then reduced in volume on a rotary evaporator, and then subjected to Florisil column chromatography as described in section 2.3.3. The cleaned sample extracts were then analyzed by ion-trap GC-MS. Because sample size was limited for the clam extracts, and because two of the beaches investigated were expected to have low absolute levels of PAHs, it was decided to analyze the clam samples by using GC-MS, using a (newly-purchased) ion trap GC-MS, as this provides enhanced sensitivity compared with GC with FID detection (Table 2-1). The use of GC-MS also allowed an isotopically labeled internal standard (d_{10}-pyrene) to be used in place of hexamethylbenzene. d_{10}-Pyrene was expected to be a more suitable internal standard because its physical-chemical properties are more similar to the analytes than are those of hexamethylbenzene. The GC-MS system used consisted of a Star 3400Cx gas chromtograph equipped with a 1078 temperature programmable injector and interfaced to a Saturn 4D ion-trap mass spectrometer (Varian Ltd.). A capillary column (DB5-MS, 30 m length, 0.25 mm i.d., 0.25 μm coating, from J&W Scientific) was used. The GC parameters used (injection routine, column temperature program) were identical to those described for GC-FID in Chapter 2. The transfer line between the gas chromatograph and the mass spectrometer was maintained at 290 °C. The ion trap was maintained at 270 °C and was operated in selected ion storage mode.

To improve sensitivity, different mass ranges were stored for each group of PAH isomers, as shown in Table 4-1. The GC-MS system was controlled by an STD 486 personal computer.

Table 4-1 MS acquisition parameters.

acquisition segment	target compounds	Retention time (minutes)	masses stored	quantitation masses
1	acenaphthylene	7-14	149-160	150-155
	acenaphthene	7-14	149-160	150-155
2	fluorene	15-18	160-170	163-167
3	phenanthrene	18-23	170-185	176-179
	anthracene	18-23	170-185	176-179
4	fluoranthene	23-31	99-220	200-203
	d_{10}-pyrene	23-31	99-220	211-213
	pyrene	23-31	99-220	200-203
5	benzo(*a*)anthracene	31-37	110-235	227-229
	chrysene	31-37	110-235	227-229
6	benzo(*b*)fluoranthene	37-44	120-260	251-253
	benzo(*k*)fluoranthene	37-44	120-260	251-253
	benzo(*e*)pyrene	37-44	120-260	251-253
	benzo(*a*)pyrene	37-44	120-260	251-253
	perylene	37-44	120-260	251-253
7	indeno(1,2,3-*cd*)pyrene	44-54	130-280	130-280
	dibenz(*ah*)anthracene	44-54	130-280	274-297
	benzo(*ghi*)perylene	44-54	130-280	130-280

Compound identification for each PAH was based upon comparison of both retention time and mass spectrum with those of authentic standards. For most compounds quantitation was based on the sum of the mass-intensities of the parent ion cluster (see Table 4-1). However, for indeno(1,2,3-*cd*)pyrene and benzo(*ghi*)perylene, the relative intensities of the M^+ and M^{2+} clusters were variable, and it was decided to quantify these compounds on the basis of the total ion current. A standard mixture containing the 16 US EPA priority pollutant PAHs plus d_{10}-pyrene was analyzed to determine reference spectra and retention times for the PAHs. Standard solutions of perylene and benzo(*e*)pyrene were analyzed in order to determine retention times for these two compounds. Response factors for the 16 PAHs were calculated relative to the response of d_{10}-pyrene, which was added to all the environmental samples as an internal standard. Perylene and benzo(*e*)pyrene were assigned the same response factor as benzo(*a*)pyrene. The use of selected ion storage, and selected ion quantitation eliminated most of the 'chromatographic noise', thus limits of detection were not affected by co-extractives to the same degree that the GC-FID analyses were (Chapter 2 and Chapter 3). The only PAH detected in method blanks was naphthalene, which was present at ~ 120 ng/mL. This was significant in comparison to the naphthalene levels in the samples, and we were unable to identify the source of the naphthalene contamination or eliminate it. This contamination prevented any meaningful analysis of naphthalene in the environmental samples.

4.4.4 Determination of PAHs in intertidal marine sediments

The sediments were thawed, removed from the glass bottles, mixed thoroughly on a stainless-steel tray, then freeze dried in cleaned glass beakers. The freeze dried sediments were Soxhlet extracted with methylene chloride, the extracts were cleaned up on Florisil columns and then analyzed for PAHs as described in Chapter 2. One major change to the sediment analysis was the

use of GC-MS instead of GC-FID. This was done to facilitate direct comparison between PAH levels in the clams and the associated sediments, as was required for calculation of biota-sediment accumulation factors. The GC-MS analysis is described in the preceding section.

4.4.5 Sediment organic carbon (f_{OC}) determination

The carbonate analysis described in section 2.3.5 revealed that carbonate formed an insignificant fraction of the sediment carbon in Kitimat sediments. Therefore for the beach sediments, organic carbon was determined as CO_2 after ignition at 1050°C by using a Carlo Erba NA-1500 NCS analyzer. A co-oxidant (CuO) was used to ensure complete oxidation of the sediment carbon.

4.5 Results

4.5.1 Calibration of Biobeads SX-3 SEC columns

The removal of lipids from the sample extract by using SEC on Biobeads SX-3 was based on published methods (259, 304). The results of the analysis of one of the PAH spiked-canola oil samples used to calibrate the biobeads column are shown in Figure 4-2. The curve generated from the GC-MS data represents the sum of the peak areas of 15 of the US EPA priority pollutant PAHs (naphthalene excluded) in each fraction collected. Using this column and solvent system the PAHs all showed similar elution profiles. The separation between the lipid fraction and the PAH fraction using this technique was adequate for the present work.

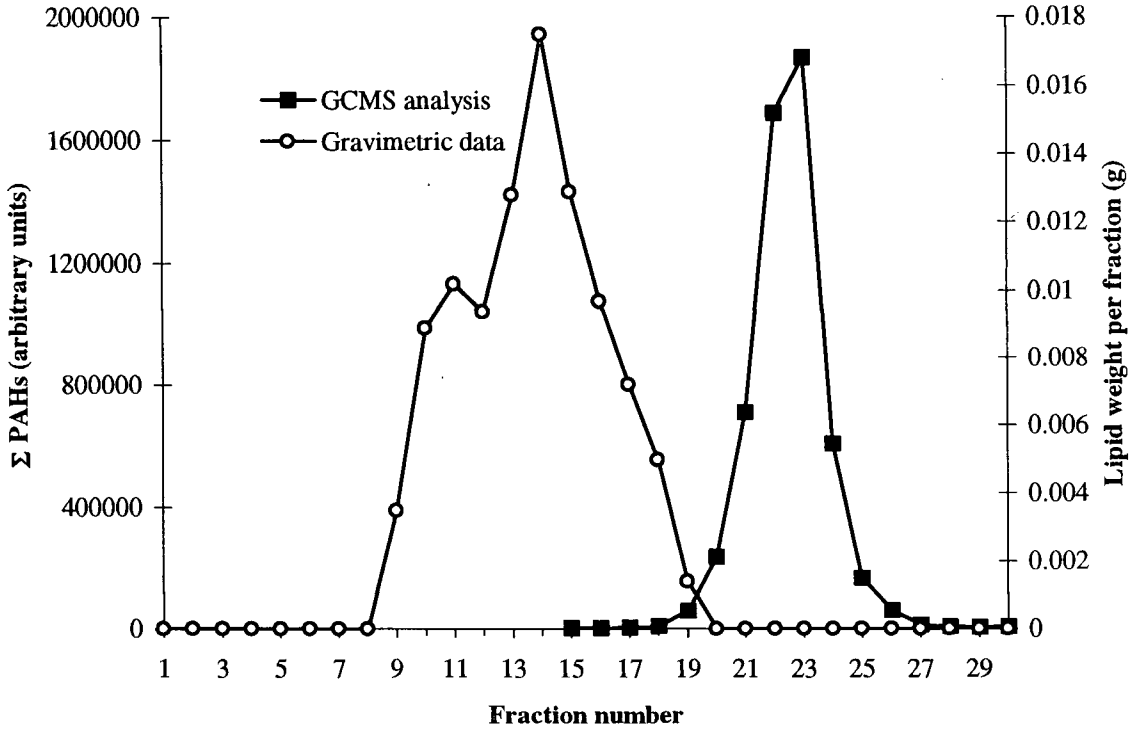

Figure 4-2 Elution profile of lipids and PAHs from Biobeads SX3 SEC columns.

The separation of lipids from PAHs was also examined in extracts of clam tissue that had been spiked with the standard PAH mixture. The elution profiles of lipids and PAHs, which were monitored by using on-line fluorescence detection, were identical to those for the spiked canola oil sample illustrated in Figure 4-2.

4.5.2 PAHs in *Mya arenaria* and intertidal marine sediments

Beach sediments collected from areas colonized by *Mya arenaria* were analyzed for PAHs, and the results are included as Table 4-2. Values of f_{OC} for the four sites are: 0.0054 (Kildala beach); 0.0121 (Kitimaat Beach); 0.0621 (Eurocan Beach); 0.0263 (Hospital Beach).

Table 4-2 PAH concentrations (ng/g, dry weight) in intertidal beach sediments associated with Mya arenaria in the Kitimat fjord system.

Site	Kildala Beach		Kitimaat Beach		Eurocan Beach		Hospital Beach	
compound	SKB-a	SKB-b	SKV-a	SKV-b	SEU-a	SEU-b	SHB-a	SHB-b
acenaphthylene	0.01	0.02	1.3	1.6	0.41	0.59	16	18
acenaphthene	0.11	0.11	1.2	1.5	3.8	3.8	924	1023
fluorene	1.7	1.5	3.7	15	3.2	4.2	487	548
phenanthrene	6.8	8.0	29	72	16	18	5264	5642
anthracene	0.34	0.61	25	19	4.5	7.3	1031	1083
fluoranthene	1.9	2.8	105	111	53	60	14077	13202
pyrene	2.3	4.2	69	65	39	40	11896	12521
benzo(*a*)anthracene	0.32	0.53	45	34	19	42	11397	8882
chrysene	0.43	0.49	56	53	22	55	11986	9466
benzo(*b*)fluoranthene	0.46	0.90	48	49	31	54	18549	13852
benzo(*k*)fluoranthene	0.17	0.28	18	18	10	19	6728	4841
benzo(*a*)pyrene	0.20	0.15	21	21	16	28	16479	7220
indeno(1,2,3-*cd*)pyrene	0.20	0.15	16	16	9.2	13	15287	8683
dibenz(*ah*)anthracene	0.04	0.05	1.0	1.5	0.94	1.4	1410	785
benzo(*ghi*)perylene	0.21	0.18	10	13	7.7	9.9	9478	6344
benzo(*e*)pyrene	0.37	0.52	24	26	16	27	11306	9657
perylene	0.76	0.48	3.7	4.0	400	460	4722	6280
Σ 15 PAH*	15	20	449	490	235	356	125010	94111

* *sum of 15 of the US EPA priority pollutant PAHs (does not include perylene and benzo(e)pyrene or naphthalene).*

All of the 16 US EPA priority pollutant PAHs were detected in all sediment samples, including sediments from the reference site (Kildala Beach). Benzo(*e*)pyrene and perylene were detected in all sediment samples also. Total PAH concentrations were lowest at Kildala Beach (~15-20

ng/g). This value is typical for remote locations not directly influenced by major sources of PAHs (see section 1.4.7.3). PAH concentrations at the three other locations are all elevated with respect to Kildala Beach; however, the PAHs present at Kitimaat Beach and Eurocan Beach are well below government sediment quality guidelines or levels considered likely to cause adverse effects (see Table 1-3). At Hospital Beach the levels of most PAHs are in excess of CCME/BCMOE assessment criteria, and in excess of the ER-M values published by Long *et al.* (95). The high PAH concentrations at Hospital Beach can be attributed to the fact that this site received direct effluent discharges from the aluminum smelter, in addition to atmospheric emissions from the smelter and airborne dust from unloading of raw materials at the smelter.

The physical attributes of the *Mya* analyzed from each site are listed in Table 4-3, and the results of the analysis of PAHs in *Mya* collected from beaches in the Kitimat fjord system are included as Table 4-4. For comparison, PAH levels in mollusks from other contaminated sites are included in Table 4-5.

Table 4-3 Physical attributes of Mya arenaria specimens analyzed in this study.

Site	number of specimens	length range (cm)	mean length (cm)	weight range (g)	mean weight (g)
Hospital Beach (HB)	9	5.5-9.6	7.7	17.35-73.28	44.52
Eurocan Beach (EU)	9	6.9-8.8	7.9	30.06-68.26	48.16
Kitimaat Beach (KV)	9	6.5-9.1	8.0	23.28-75.75	55.00
Kildala Beach (KB)	8	7.4-8.6	8.1	43.07-68.55	56.99

Table 4-4 PAH concentrations (ng/g, dry weight) in Mya arenaria collected from beaches in the Kitimat fjord system.

Site	Kildala Beach		Kitimaat Beach		Eurocan Beach		Hospital Beach	
compound	mean	*SD*	mean	*SD*	mean	*SD*	mean	*SD*
% lipid	**9.2**	***1.9***	**9.1**	***2.4***	**6.5**	***1.2***	**6.6**	***0.2***
acenaphthylene	0.23	*0.16*	7.0	*3.0*	0.99	*0.38*	1.3	*0.3*
acenaphthene	0.60	*0.22*	2.6	*1.3*	0.85	*0.37*	7.6	*2*
fluorene	1.6	*0.27*	6.1	*3.0*	6.5	*3.1*	14	*2*
phenanthrene	20	*0.58*	88	*27*	71	*27*	170	*35*
anthracene	4.7	*2.3*	16	*9.0*	3.4	*1.4*	9.1	*3*
fluoranthene	20	*1.9*	382	*149*	250	*108*	727	*173*
pyrene	16	*3.7*	224	*64*	207	*86*	576	*137*
benzo(*a*)anthracene	2.5	*0.93*	79	*42*	88	*39*	483	*120*
chrysene	11	*4.2*	145	*62*	167	*73*	803	*179*
benzo(*b*)fluoranthene	4.0	*2.2*	73	*35*	142	*67*	1005	*269*
benzo(*k*)fluoranthene	1.5	*0.77*	22	*13*	40	*16*	306	*77*
benzo(*a*)pyrene	1.5	*2.3*	17	*15*	49	*24*	604	*156*
indeno(1,2,3-*cd*)pyrene	<0.2	-	17	*5.3*	31	*10*	507	*153*
dibenz(*ah*)anthracene	<0.2	-	2.1	*0.59*	3.9	*1.4*	83	*32*
benzo(*ghi*)perylene	<0.2	-	28	*9.3*	39	*8.7*	363	*107*
benzo(*e*)pyrene	4.4	*1.9*	83	*32*	130	*51*	769	*170*
perylene	<0.2	-	<0.2	-	63	*69*	165	*27*
Σ 15 PAH*	83	*13*	1110	*417*	1100	*460*	5657	*1439*

* *sum of 15 of the US EPA priority pollutant PAHs (does not include perylene and benzo(e)pyrene or naphthalene). Mean and standard deviation (SD) determined from three independent analyses for each site.*

Most of the PAHs analyzed for were detected at all sites (some of the HPAHs were not detected at Kildala Beach, and perylene was not detected at Kitimaat Beach). Total PAH levels in *Mya arenaria* at the four sites show the same trend as was seen for the sediment data, i.e. levels are lowest at the reference site (Kildala Beach), and elevated at the other three locations. Of particular interest is the fact that the PAH levels in *Mya arenaria* from Hospital Beach are only five times greater than in the samples from Eurocan Beach and Kitimaat Beach. In comparison, the PAH levels in sediments at Hospital Beach are ~200-300 times greater than at the other contaminated beaches.

Table 4-5 PAH concentrations (ng/g, dry weight) in mollusks collected from various contaminated sites.

Location	species	Σ PAH concentration	PAH source	Reference
Hamilton Harbor, Ontario	*Dreissina polymorpha* (Zebra mussel)	350-10,000*	Coal tar, Steel smelters	(258)
Kitimat	*Mya arenaria* (soft-shelled clam)	1530	Aluminum Smelter	D. Goyette, unpublished data
Norwegian fjords	*Mytilus edulis* (Blue mussel)	8,300-1,730,000	Aluminum Smelter	(151)
Norwegian fjords	*Modiolis modiolis* (Horse mussel)	33,000-523,000	Aluminum Smelter	(151)
Swedish Baltic Coast	*Mytilus edulis* (Blue mussel)	6,000	Aluminum Smelter	(272)
Swedish Baltic Coast	*Macoma balthica* (Baltic tellins)	170,000	Aluminum Smelter	(272)

* *Concentrations in ng/g wet mussel homogenate*

As shown in Table 4-3, the clams sampled from each site were all of similar size. The average clam wet-weight was lowest for the two sites with highest PAH concentrations (Hospital Beach, Eurocan Beach), but the differences are not statistically significant (ANOVA, P=0.05). Similarly

f_L values (expressed in Table 4-4 as a percent of the clam dry weight), were lowest at the two sites with highest levels of PAH contamination. Again, this difference was not significant (P=0.05).

The total PAH concentrations in *Mya arenaria* at the three contaminated beaches are similar to data from Goyette for northwest Kitimat Arm (D. Goyette, Environment Canada- *unpublished results*). When compared with data for mollusks at other contaminated sites, the present data fall towards the low end of the values listed in Table 4-5.

4.5.3 Comparison of PAH composition in sediments and clams

Figure 4-3 illustrates the PAH composition in clams and sediments from the four beaches investigated in the present study. The data for each PAH has been normalized to the sum of all PAHs (except perylene) to allow direct comparison of PAH composition in samples with different absolute concentrations of PAHs. The perylene data, which is anomalous, was excluded from the analysis in Figure 4-3 and is discussed in a subsequent paragraph.

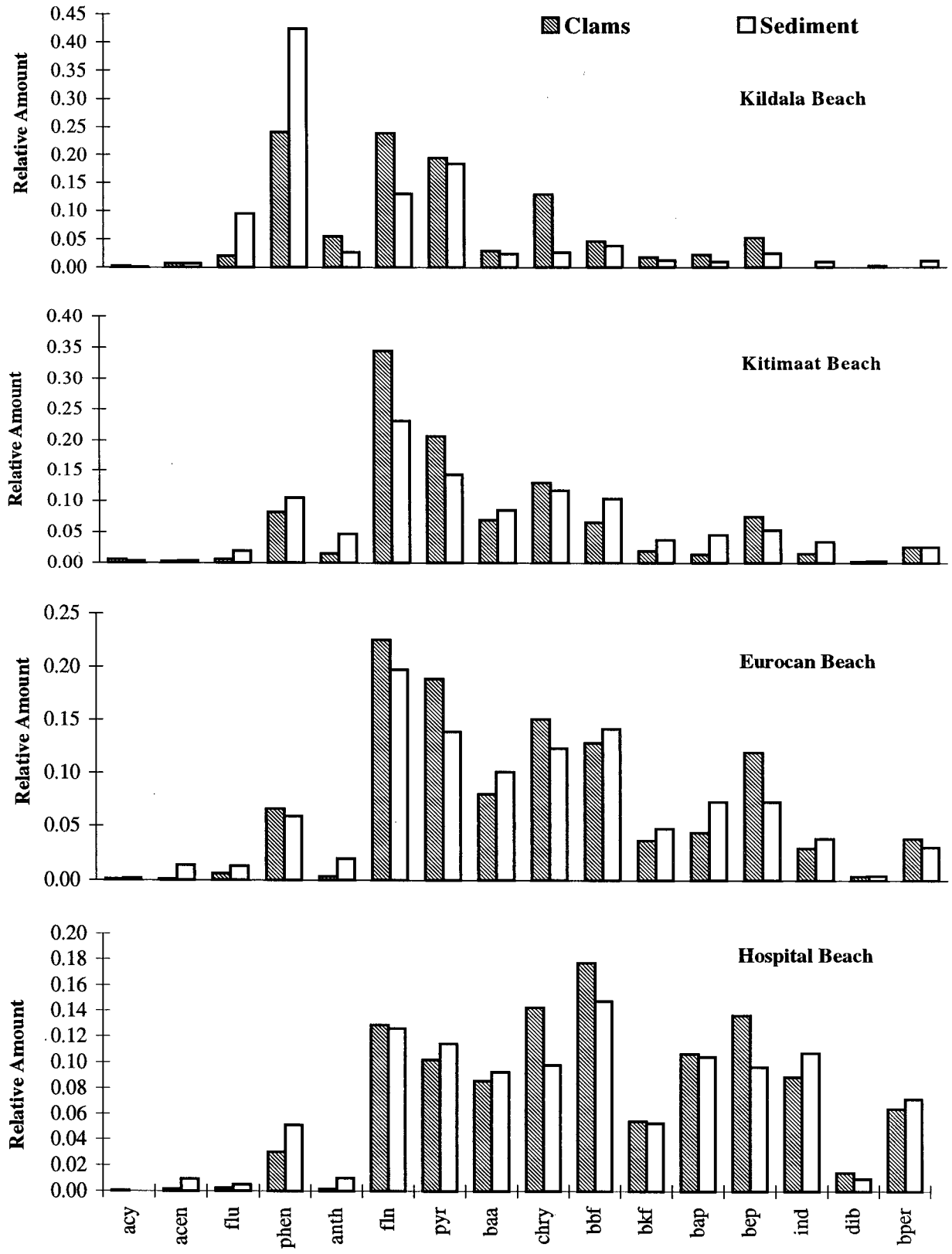

Figure 4-3 PAH composition in sediments and clams from beaches in the Kitimat fjord system. PAH concentrations for each compound have been normalized to the total PAH concentration at each site.

For the three sites with elevated levels of PAHs, the PAH composition is similar in both clams and sediment. Four and five-ring PAHs are present in greater abundance than two and three-ring PAHs, which is typical of PAHs generated by combustion sources (See section 1.4.1.1). The proportion of HPAHs is somewhat higher in the Hospital Beach samples compared to the other two sites. The PAH composition at the reference site (Kildala Beach) has some similarities to the other three sites, especially in the relative amounts of the HPAHs. An important difference, however, is the high relative amount of phenanthrene at this site, especially in the sediment samples. Wakeham *et al.* detected phenanthrene (~40-50 ng/g) in Lake Lucerne sediment from core sections pre-dating the industrial revolution (70). They concluded that the phenanthrene probably originated from diagenesis of steroid precursors. Phenanthrene was also detected in sections of the Giltoyees Inlet sediment core pre-dating operation of the Alcan smelter at Kitimat (Chapter 3, this thesis). The high relative levels of phenanthrene at Kildala Beach probably arise from diagenic sources, and the overall PAH composition at Kildala Beach is consistent with a mixture of diagenic and combustion sources. Diagenic sources no doubt contribute to the PAH load at the three contaminated sites also. However the levels of combustion-generated PAHs at the contaminated sites are sufficiently high that the contribution from diagenic inputs is obscured.

The data in Table 4-2 and Table 4-4 illustrate differences between perylene and the other PAHs. Most notably, the absolute perylene concentration in sediments at Eurocan Beach (~400-460 ng/g) is higher than the combined concentrations of the 16 other PAHs. At the three other beaches, the perylene concentration is less than 10% of the sum of the other PAHs. Perylene also dominated the PAH composition for sections from the Giltoyees Inlet sediment core pre-dating the operation of the Alcan smelter at Kitimat, and in specific particle-size-fractions of sediment from site CD3 (as described in Chapter 3 of this thesis). It was suggested that the perylene may

be generated diagenically, from plant precursors. This may take place either *in situ* in the marine sediments, or in terrestrial soils that are subsequently eroded, then deposited as fjord sediments.

Another unusual feature of the perylene data is the fact that perylene was not detected in *Mya* from Kildala Beach or Kitimat Beach, whereas it was detected in the sediment at these locations. In fact, the levels of perylene detected in the sediments were comparable with the levels of the other MW 252 PAH isomers. Because the other MW 252 PAH isomers were detected in the clam tissue at both sites, perylene should also have been detected in the clam tissue if it was accumulated to the same degree as the other MW 252 PAH isomers. Thus it seems that perylene accumulates to a lesser degree than the other MW 252 PAH isomers.

The data in Figure 4-3 show some differences between the PAH composition in sediments and the PAH composition in clams. For example, the proportions of fluorene and phenanthrene are generally higher in the sediments, whereas the proportions of fluoranthene, benzo(*e*)pyrene and chrysene are higher in the clams. Generally, these differences are small, however, and simple visual inspection of Figure 4-3 does not provide convincing evidence of an overall trend in PAH pattern between *Mya arenaria* and sediments.

PCA was used to further investigate differences in PAH composition between sites, and also between sediments and *Mya arenaria*. PCA was performed on the normalized data-set (perylene excluded) as described previously in Chapter 2 and Chapter 3. Perylene was excluded because its anomalous concentrations at Eurocan Beach would dominate the PCA and obscure the influences of other variables. Figure 4-4 illustrates the projection of the various samples onto the two major principal components. Principal component 1 (PC1) accounted for 57.3% of the total variance in the data set, and principal component 2 (PC2) accounted for a further 20.4% of the total variance.

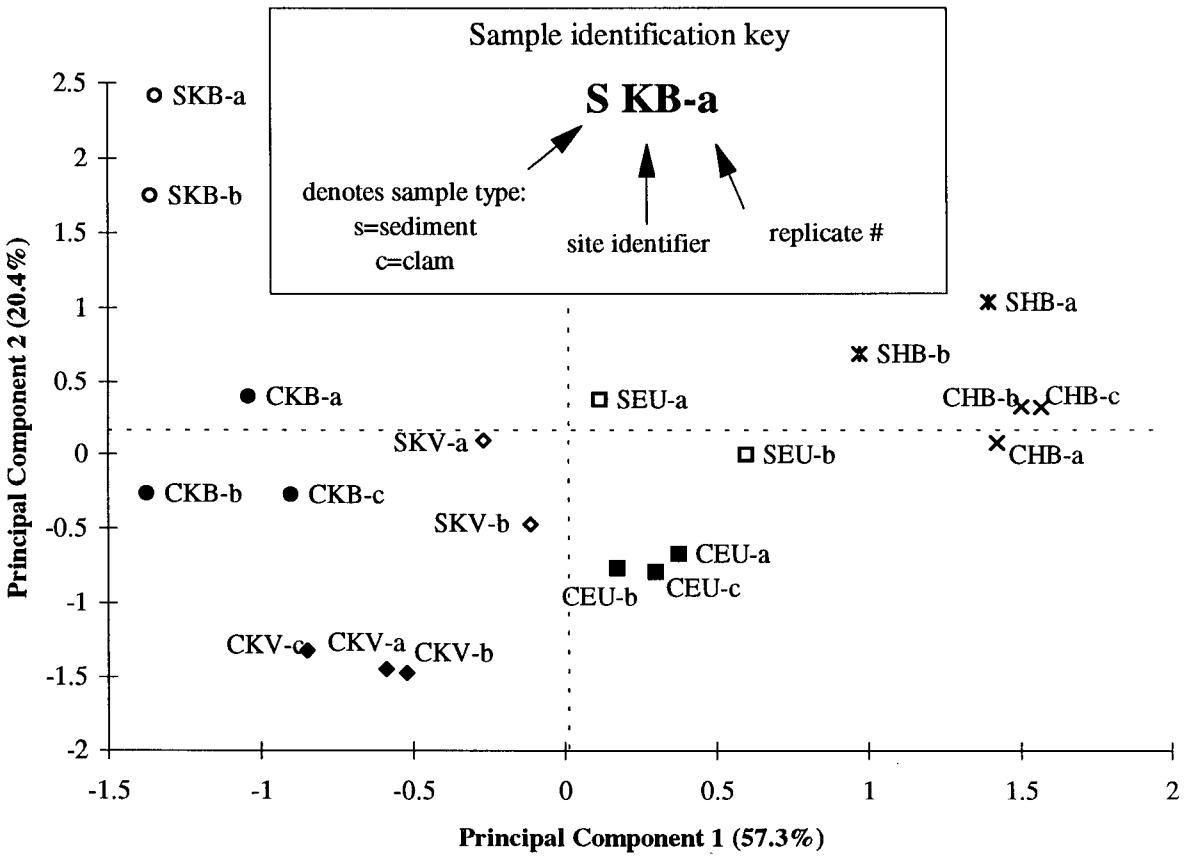

Figure 4-4 PCA of PAH composition in sediments and Mya arenaria from beaches in the Kitimat fjord system. Note separation of sites along PC1, and that sediment and clam samples from each site are differentiated on PC2.

The four beaches are differentiated on PC1, with Hospital Beach samples plotting on the far right in Figure 4-4, and samples from the other three beaches plotting in sequence from right to left across the figure. This trend reflects the proximity of the four sites to the aluminum smelter.

For each site, sediment samples are differentiated from the clam samples on PC2 (i.e. the sediment samples from a given site always plot positive on PC2, relative to the clam samples from the same site).

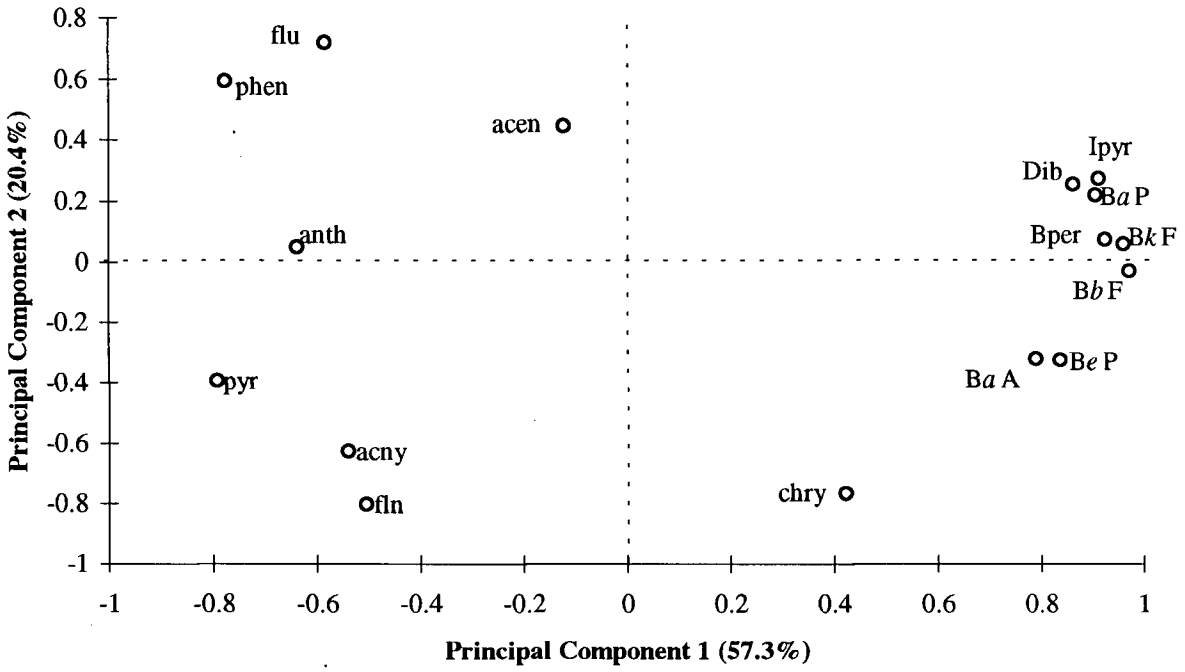

Figure 4-5 Principal Component loading plot, showing influence of individual PAHs on the PCA. See Table 3.1 for compound abbreviations.

The loadings of the 16 PAHs on the two major principal components are illustrated in Figure 4-5. Variable loadings on PC1 are statistically significant (p=0.05) for all compounds except fluoranthene, chrysene and acenaphthene. There is a clear delineation between LPAHs and HPAHs on PC1, with LPAHs plotting on the left of the figure and HPAHs plotting on the right. The variable loadings on PC1 in Figure 4-5 suggest that sites which plot positive on PC1 in Figure 4-4 have a greater proportion of HPAHs than do sites which plot negative on PC1. This prediction is borne out by inspection of the PAH composition at these sites (Figure 4-3), in which it can be seen that sediments from Kildala Beach do indeed have the highest proportion of LPAHs, and sediments from Hospital Beach have the highest proportion of HPAHs. The PAH composition in sediments at the other two sites is intermediate between these extremes.

The differences in PAH composition at the four sites can be attributed to different sources of PAH inputs to each site. Hospital Beach receives smelter-derived PAH inputs both in the form of smelter effluent, and atmospheric deposition, and absolute PAH levels in sediments at Hospital Beach are much higher than at the other locations. Given the high amounts of black particles observed in the effluent stream flowing through Hospital Beach, it is reasonable to assume that most of the PAH burden at Hospital Beach is due to the effluent. The outflow of the Kitimat river creates a south flowing current in Kitimat Arm, that would almost certainly prevent aqueous effluent discharges from the Alcan smelter from reaching Kitimaat Beach on the east side of Kitimat Arm. Kitimaat Beach, therefore, would only receive smelter-derived PAHs from atmospheric inputs. Eurocan Beach is located 'upstream' of the Alcan discharges, but eddy currents in the north west corner of Kitimat Arm may bring a small fraction of the aqueous smelter effluents ashore at this site. Most of the smelter-derived PAH inputs at Eurocan Beach are likely to be via atmospheric inputs, however. As mentioned previously, anthropogenic PAH inputs to Kildala Beach are sufficiently low, that diagenic PAHs make a significant contribution to the PAH burden (and hence PAH composition) at this site. PAH levels at the two intermediate sites (Kitimaat Beach, Eurocan Beach) are sufficiently high that diagenic inputs are unlikely to be significant, but other anthropogenic PAH sources (e.g. a marina at Kitimaat Village, municipal wastewater discharges) may provide a significant contribution to the PAH load at these sites.

Only five PAHs (fluoranthene, chrysene, acenaphthylene, fluorene and phenanthrene) have statistically significant loadings on PC2 (P=0.05), and it is these compounds which discriminate clam samples from sediment samples on PC2. This result is consistent with the graphical data in Figure 4-3 which show higher proportions of fluoranthene, chrysene, acenaphthylene in the clams, but higher proportions of fluorene and phenanthrene in the sediments. The discrimination

between clam and sediment samples on PC2 indicates that all PAHs are not accumulated to the same degree. Differential accumulation of PAHs from sediment by clams has been reported, but the results are somewhat inconsistent (154, 170, 172, 176, 305). In a recent review, Meador *et al.* noted that some authors reported preferential accumulation of 4-ring PAHs, or 4-ring + 5-ring PAHs, while other authors reported preferential accumulation of 2-ring and 3-ring PAHs (170). In another study, differential accumulation of PAHs was observed in *Macoma balthica*, but the pattern of PAH accumulation varied between sample locations (172).

4.5.4 Biota-sediment accumulation factors (BSAFs)

BSAFs (lipid and organic-carbon-normalized) have been calculated for clams from the four beaches, and are tabulated in Table 4-6. The BSAFs for individual PAHs at a given site are similar; however statistically significant differences in BSAFs exist between sites (ANOVA, P=0.05).

Absolute values of the BSAFs at three out of four sites: Kildala Beach, Kitimaat Beach and Eurocan Beach, are within the range of values reported in other studies. For example BSAFs for *Macoma balthica* were 0.5-2.2 in one study (170), and 0.1-10 in another (172). BSAF values of 0.2-4 have been reported for various clam species, as reviewed by Meador *et al.* (170). The BSAFs at Kildala Beach and Kitimaat Beach are slightly less than the theoretical equilibrium value of 1.7, whereas the BSAFs at Eurocan Beach are slightly higher than this value. The higher BSAFs for Eurocan Beach may be related to the high f_{OC} value determined for this site, and used in the BSAF calculation. This value (0.062) may not be realistic. If a more typical f_{OC} value is substituted (e.g. f_{OC}=0.01), the Eurocan data falls into line with the other two sites.

Table 4-6 Lipid and organic-carbon-normalized BSAFs for Mya arenaria collected from four beaches in the Kitimat fjord system.

Site	Kildala Beach		Kitimaat Beach		Eurocan Beach		Hospital Beach	
	BSAF	*SD*	BSAF	*SD*	BSAF	*SD*	BSAF	*SD*
acenaphthylene	0.85	*0.53*	0.64	*0.15*	1.86	*0.82*	0.039	*0.023*
acenaphthene	0.31	*0.10*	0.24	*0.09*	0.20	*0.04*	0.004	*0.002*
fluorene	0.06	*0.01*	0.09	*0.11*	1.61	*0.62*	0.014	*0.007*
phenanthrene	0.16	*0.03*	0.23	*0.18*	3.91	*0.70*	0.016	*0.008*
anthracene	0.55	*0.35*	0.10	*0.06*	0.53	*0.27*	0.005	*0.002*
fluoranthene	0.51	*0.17*	0.46	*0.10*	4.08	*0.86*	0.028	*0.014*
pyrene	0.29	*0.14*	0.45	*0.03*	4.89	*0.79*	0.025	*0.012*
benzo(*a*)anthracene	0.34	*0.19*	0.26	*0.13*	2.65	*1.85*	0.025	*0.017*
chrysene	1.38	*0.45*	0.35	*0.09*	4.06	*3.13*	0.039	*0.024*
benzo(*b*)fluoranthene	0.33	*0.30*	0.20	*0.05*	3.11	*1.97*	0.033	*0.023*
benzo(*k*)fluoranthene	0.40	*0.31*	0.16	*0.05*	2.59	*1.52*	0.027	*0.018*
benzo(*a*)pyrene	0.65	*0.49*	0.10	*0.06*	2.07	*1.28*	0.027	*0.027*
indeno(1,2,3-*cd*)pyrene	<0.06*	-	0.14	*0.01*	2.62	*1.03*	0.022	*0.019*
dibenz(*ah*)anthracene	<0.23*	-	0.22	*0.09*	3.19	*1.37*	0.040	*0.038*
benzo(*ghi*)perylene	<0.06*	-	0.32	*0.07*	4.27	*0.98*	0.024	*0.018*
benzo(*e*)pyrene	0.56	*0.24*	0.44	*0.10*	5.59	*2.74*	0.038	*0.022*
perylene	<0.02*	-	<0.01*	-	0.13	*0.13*	0.015	*0.009*
mean BSAF	0.49	*0.17*	0.27	*0.04*	2.79	*0.85*	0.02	*0.01*

* *BSAF determined by substituting the approximate LOD (2ng/g, lipid) for non-detected compounds in clams*

The BSAF data for Hospital Beach is lower than the other three sites by an order of magnitude. Similar low BSAF values have been reported by some authors (154, 177), and these were attributed to reduced bioavailability of PAHs or, possibly, significant metabolism of the PAHs. In the present case it is likely that reduced bioavailablity of the PAHs is responsible for the low

BSAFs at Hospital Beach. Previously in this thesis it was suggested that limited bioavailability of smelter-derived PAHs may be responsible for the lack of major changes in the PAH profile in marine sediments in Kitimat Arm (Chapter 2), and in sections from the Giltoyees Inlet sediment core (Chapter 3). Paine *et al.* also suggested that limited bioavailability of smelter-derived PAHs was responsible for the lower-than-expected toxicity of sediments adjacent to the Alcan smelter (96).

PAH metabolism is often higher at contaminated sites than at reference sites (177). Therefore it might be expected that clams from Hospital Beach would have higher metabolic capacity towards PAHs than do clams from the other sites, and this would lead to lower BSAFs. However, in view of the fact that mollusks appear to have very limited capacity to metabolize PAHs (38, 43), it seems unlikely that metabolism is responsible for the low BSAFs observed at Hospital Beach.

The EP theory predicts that BSAFs should be identical for all PAHs. In the present study BSAFs for individual PAH do show some consistent differences. However, the differences in BSAFs were small. For example, chrysene, fluoranthene and benzo(*e*)pyrene typically have the highest BSAFs at each site, whereas the BSAFs for fluorene, indeno(1,2,3-*cd*)pyrene and perylene are consistently amongst the lowest at each site. Correlation coefficients were calculated between the BSAFs determined in this study and molecular properties including K_{OW} and solubility. These correlation coefficients were not significant (t-test, p=0.05). In contrast, Pruell *et al.* found that BSAFs for *Mytilus edulis* exposed to contaminated suspended sediments increased over 16-fold with increasing K_{OW} (305). In studies with other benthic invertebrates, Meador *et al.* found that BSAFs decreased with increasing K_{OW} for a polychaete, but no trend in BSAFs was observed for an amphipod (154).

In summary, the differential accumulation of PAHs observed in the present study is not anticipated by the EP theory. However, these differences are small, and the absolute BSAF values of most of the PAHs at three of the sites investigated (Kildala Beach, Kitimaat Beach, Hospital Beach) are within an order of magnitude of the EP prediction. The EP theory also cannot account for differences in BSAFs between sites. The BSAF values determined for Hospital Beach are up to one hundred times lower than predicted. The EP theory, therefore, does not adequately describe PAH partitioning between sediments and biota at Hospital Beach.

5. Metabolism of Pyrene by two Clam Species, *Mya arenaria* and *Protothaca staminea*

5.1 Introduction

Many bivalve mollusk species live buried in marine sediments and feed by filtering suspended particles from water just above the sediment surface, or by grazing on the organic film coating the sediment particles. Because PAHs in esturine systems rapidly adsorb onto particles and are deposited into sediments, sediment dwelling organisms including mollusks may be particularly exposed to PAHs in polluted environments. It is commonly assumed that mollusks possess little or no capacity to metabolize PAHs (31, 56, 111, 306), and ingested PAHs are accumulated within the fatty tissues of the mollusks.

However, as detailed in Chapter 1, mollusks possess the same enzyme systems utilized by higher organisms to metabolize PAHs. This apparent capacity for PAH metabolism in mollusks is at odds with the frequent failure to detect PAH metabolites from mollusks - either in feeding studies, or in the environment (31, 33, 43). In order to investigate this incongruity some studies of PAH metabolism in representative mollusks were conducted.

An experiment was designed with two objectives in mind, firstly, to determine if a target mollusk, the soft-shelled clam *(Mya arenaria)*, was capable of metabolizing a typical PAH (pyrene), and secondly, to identify any metabolites produced. It was recognized that a quantitative determination of the amounts of any metabolites formed might not feasible, due to the lack of authentic standards of pyrene metabolites.

Mya arenaria was selected as an appropriate target mollusk for several reasons. Firstly, *Mya arenaria* is relatively abundant at beaches throughout the Kitimat fjord system, including highly contaminated beaches near the Alcan smelter. These *Mya arenaria* populations have recently been studied by Brand *et al.* (*pers comm.*), who showed that *Mya arenaria* collected at Hospital Beach, adjacent to the Alcan smelter, reacted with an antibody specific to leukemia cells. This assay is used to detect disseminated neoplasia - a leukemia-like condition that has been detected previously in *Mya arenaria* and other clam species (114, 307), including populations of *Mya arenaria* exposed to PCBs (308). The initial work of Brand *et al.* has prompted further studies, funded by Alcan, to determine whether PAHs are responsible (either directly, or due to an immunosupressive effect) for the neoplasia in *Mya arenaria.* It is generally accepted that PAHs are not direct acting carcinogens because they require metabolic activation to reactive metabolites which are the ultimate carcinogens. Therefore, if PAHs are responsible for the leukemia-like condition observed in the Hospital Beach *Mya arenaria* population, this may suggest that mollusks are capable of metabolism of PAHs. The converse of this argument has been used by other workers (111), who suggested that the absence of PAH-metabolizing ability in mollusks might protect them against PAH-induced carcinogenesis.

Mya arenaria is not in fact native to the west coast of North America, having arrived here sometime last century (309). The native littleneck *(Protothaca staminea)* is native to this coast, and inhabits a similar ecological niche to *Mya arenaria.* Therefore it was decided to investigate pyrene metabolism in *Protothaca staminea* also, to facilitate comparison between the two species, and to broaden the generality of any findings concerning PAH metabolism in mollusks.

Pyrene was chosen as a representative PAH for several reasons. Firstly, many of its physical-chemical properties (solubility, vapor pressure, molecular weight) are intermediate in the range

exhibited by PAHs. Secondly, pyrene is a major component of many PAH mixtures, including those in Kitimat sediments. Finally, the metabolic pathways of pyrene in higher organisms tend to be simpler than those for other PAHs. This is largely because the C1 carbon atom in pyrene is substantially more reactive towards substitution than any of the other positions. Therefore pyrene metabolites formed by higher organisms are almost exclusively the C1-substituted isomers.

5.2 Experimental

5.2.1 Materials

Mya arenaria were collected from an intertidal site at Boundary Bay Marine Reserve, south of Vancouver, British Columbia. *Protothaca staminea* were purchased from local wholesalers (The Lobster Man and Albion Fisheries). All were stored in sea water at 4°C for 36 hours to allow depuration of gut contents. Only clams that appeared to be actively siphoning were selected for the exposure experiments.

Pyrene (purity 99%), 1-hydroxypyrene (purity 98%) and pyrene-1-carboxyaldehyde (purity 98%) were purchased from Aldrich. 4,5,9,10-^{14}C pyrene (55 μCi), uridine 5'-diphosphoglucuronic acid trisodium salt (purity 98-100%), uridine 5'-diphosphoglucuronyl-transferase (type III, from bovine liver), β-glucosidase (from almonds) and sulfatase (type VI, from *Aerobacter aerogenes*) were purchased from Sigma. Antibiotic/antimycotic solution, containing 10,000 units per mL penicillin G sodium, 10,000 μg/mL streptomycin sulfate and 25 μg/mL amphotericin B in 0.85% saline, was obtained from Gibco. C_{18} solid phase extraction disks (47 mm) were purchased from Varian Ltd. All solvents used were HPLC grade or better, and were purchased from Fisher Scientific.

5.2.2 HPLC Analysis

Extracts of clam tissue and sea water were analyzed by using HPLC with fluorescence detection. The HPLC system consisted of the following: Waters model 600E four channel solvent delivery system, Waters model U6K injector with 2 mL sample loop, 5 μm in-line filter, 2 cm guard column with C_{18} stationary phase (Supelco Ltd.), Waters Lambda-Max model 481 UV/visible detector set to 254 nm and a Waters model 470 programmable fluorescence detector (excitation 340 nm, emission 380 nm, bandpass 18 nm). The detector output was collected by using a Dell 486 personal computer running Shimadzu EZ-Chrom™ chromatography software. The guard and analytical columns were housed inside a column heater operated at 50 °C. Sample injection volume was typically 10 or 25 μL, except when fractions were to be collected for subsequent analysis and injection volumes of 100 to 750 μL were used. Initially, the HPLC analytical column used was a 25cm x 4.6mm LC-PAH column packed with 5 μm particles of octadecylsilica (Supelco Ltd.). This column was subsequently replaced by a 25cm x 4.6mm Inertsil ODS analytical column packed with 5 μm particles of octadecylsilica (GL Sciences, Japan). Retention times differed somewhat between the two systems. The HPLC conditions are listed in Table 5-1.

Table 5-1 HPLC conditions used for the analysis of pyrene metabolites.

time (min)	flow rate (mL/min)	% acetonitrile	% water
Initial	1.2	10	90
15	1.2	100	0
25	1.5	100	0
35	1.2	10	90

5.2.3 Analysis using GC-MS and ESI-MS/MS

Mass spectrometry was used to aid identification of pyrene metabolites. GC-MS using electron ionization (EI) is a highly sensitive technique appropriate for non-polar metabolites, but it is not suitable for polar conjugated metabolites which are thermally labile. The method of choice for analysis of conjugated metabolites is electrospray ionization (ESI-MS). The GC-MS system used consisted of a Star 3400 Cx gas chromatograph equipped with a 1078 temperature programmable injector and interfaced to a Saturn 4D ion trap mass spectrometer (Varian Ltd.). A capillary column (DB5-MS, 30 m length, 0.25 mm i.d., 0.25 μm coating, from J&W Scientific) was used. The GC injection conditions and column temperature program are described in Chapter 2. The transfer line between the gas chromatograph and the mass spectrometer was maintained at 290 °C. The ion trap was maintained at 270 °C and operated in scan mode over a range from m/z 100 to m/z 450. The GC-MS system was controlled by an STD 486 personal computer.

ESI-MS and ESI-MS/MS analyses were carried out on a VG Quattro triple stage quadrupole mass spectrometer, equipped with an electrospray ionization (ESI) source. The instrument was operated in negative ionization mode with the following operating conditions: source temperature 80 °C, capillary voltage 2.52 kV, cone voltage 24 kV, skimmer offset 0 V. The ions were accelerated towards the first quadrupole (MS1) (which was used to mass-select the parent ion) by a potential difference of 1.4 V. Fragmentation was achieved by collision-induced dissociation (CID) in a collision cell containing 0.0003 mBar Argon, and ions were subsequently analyzed in the third quadrupole (MS2) which was floated at a potential of 11.4 V relative to MS1. In flow injection mode, sample was introduced at 20 μL/minute by using a Beckmann System Gold HPLC pump. The eluent was 80:20 acetonitrile:water containing 0.1% ammonium acetate. In HPLC mode the sample was first separated on a C_{18} analytical HPLC column, as described in

section 5.2.2. The eluent flow was then split post-column between the mass spectrometer and a fluorescence detector, such that the flow through the mass spectrometer was ca. 20 μL/minute. The gradient composition was as described in Table 5-1, 0.1% ammonium acetate added to both solvent reservoirs.

5.2.4 ^{1}H-NMR analysis

^{1}H-NMR spectroscopy was used to provide isomer specific identification of metabolite 2. The samples were dissolved in d_6-acetone or d_4-methanol, and spectra were acquired on a Bruker 400 MHz NMR spectrometer.

5.2.5 Fluorescence spectroscopy

Fluorescence spectroscopy was also used to characterize the PAH metabolites. Metabolite extracts were dissolved in acetonitrile or methanol, and pipetted into a 1 cm quartz cuvette. Fluorescence measurements were made by using an Aminco-Bowman Series 2 luminescence spectrometer. The bandpass was set to 4 nm, and the monochromators were scanned at 1 nm/second. Excitation spectra were obtained while monitoring emission at 380 nm, and emission spectra were obtained by using an excitation wavelength of 340 nm. In addition to excitation and emission spectra, synchronous scan fluorescent spectra were acquired, in which the excitation and emission monochromators were scanned with a constant wavelength difference of 37 nm.

5.2.6 Metabolic studies with *Mya arenaria*

The metabolic studies were conducted in glass beakers containing 800 mL aerated seawater at 15°C, and covered with parafilm. Pyrene was added to three beakers (1 mL of a 5 mg/mL solution of pyrene in acetone), and 1-hydroxypyrene was added to three other beakers (1 mL of a

12 mg/mL solution of 1-hydroxypyrene in acetone). *Mya arenaria* (2 specimens/beaker) were placed in two of the beakers containing pyrene and two of the beakers containing 1-hydroxypyrene. The other two beakers in which no clams were placed served as a positive control, to ensure that any metabolites detected were due to the clams, and not the action of some other agent. A negative control in which clams were kept in seawater with no added pyrene or 1-hydroxypyrene was set up concurrently. In addition, antibiotic/antimycotic solution (1 mL) was added to each beaker to inhibit growth and metabolism of micro-organisms. After 5-10 days, the experiment was terminated and both clams and water were analyzed for pyrene and possible metabolites. The exposure was carried out in the dark, and subsequent sample manipulations were performed under UV shielded fluorescent lighting to prevent photo-degradation of the analytes.

5.2.7 Metabolic studies with *Protothaca staminea*

The experimental design for studying pyrene and 1-hydroxypyrene metabolism in *Protothaca staminea* was identical with that described for the experiments with *Mya arenaria*, in the previous section.

5.2.8 Metabolic studies using ^{14}C-labeled pyrene

The primary method used for detection of clam metabolites was the observation of new fluorescent peaks by using HPLC with fluorescence detection at wavelengths appropriate for the analysis of pyrene (excitation 340 nm, emission 380 nm). It is possible that any metabolites formed which do not retain the intact pyrene aromatic ring system (e.g. ring cleavage products or dihydrodiols) may not exhibit fluorescence under these conditions. Furthermore, it is possible, although unlikely, that non-pyrene derived metabolites may exhibit fluorescence under these

conditions, and thus be erroneously attributed as pyrene metabolites. In order to address these concerns both clam species were exposed to ^{14}C-labeled pyrene. The experimental design was identical to that described in section 5.2.6, with the following exceptions: Disposable 2 L polyethylene containers were used instead of glass beakers, and 1800 mL of sea water was used instead of 800 mL. Exposures were not carried out in duplicate. ^{14}C-labelled pyrene (4.15 μCi) and unlabeled pyrene (5.14 mg) was added (in 1 mL acetone) to two containers. *Mya arenaria* (1 specimen) was placed in one of these containers and *Protothaca staminea* (3 specimens) were placed in the other. A positive control containing 4.15 μCi ^{14}C-pyrene, 5.14 mg unlabeled pyrene, 1800 mL seawater and no clams was set up also. The experiments were terminated after 10 days exposure. Clam tissue and seawater was extracted and analyzed as described in sections 5.2.9 and 5.2.10. In addition, fractions from the HPLC column were collected at 0.5 minute or 1 minute intervals into liquid scintallation vials containing 3 mL of scintillator (Scintisafe™ 30%, Fisher Scientific) and counted in a Packard TR1900 liquid scintillation counter for 20 minutes.

5.2.9 Analysis of clam tissue

Clam tissue was homogenized for 5 minutes with 50 mL water by using an Ultra-Turrax homogenizer. The solid was separated by centrifugation at 4500 rpm for 30 min. The supernatent was decanted, and the solid pellet homogenized for 5 minutes with 50 mL of 50:50 acetonitile:water. The homogenate was again centrifuged, the supernatent decanted and the solid pellet re-homogenized for 5 minutes in 50 mL acetonitrile. The supernatants were combined and were analyzed by HPLC using the conditions described in section 5.2.2 and Table 5-1.

5.2.10 Analysis of seawater

Pyrene and metabolites were extracted from seawater by using C18 solid phase extraction (SPE) disks (Varian Ltd.). The extraction procedure, described below, was adapted from Singh *et al.* (246). The apparatus consisted of a 1L filter flask connected to a rotary vacuum pump. A cold finger immersed in liquid nitrogen was placed between the pump and the flask to freeze out solvent vapors. A fritted glass support was connected to the top of the Erlenmeyer flask via a ground glass joint, and a 300 mL glass solvent reservoir was clamped on top of the glass support. A C18 SPE disk (47 mm dia.) and a glass fiber filter (Whatman GF/F, 47 mm dia., 0.7 μm porosity) were placed between the reservoir and the glass support.

The system was cleaned by drawing 20 mL methanol through the disks under vacuum, followed by 30 mL of acetonitrile. The SPE disk was then conditioned by soaking in 30 mL of methanol for 3 minutes. The methanol was drawn through the disk under vacuum, followed by 100 mL of distilled water, taking care not to allow the disk to dry out. The conditioning process wets the C18 bed, and orientates the C18 chains to maximize their interaction with the water. Next the sample was applied to the SPE disk and drawn through under vacuum. The sample container was rinsed with 100 mL deionized water which is also drawn through the SPE disk.

After extraction was completed, the liquid was removed from the Erlenmeyer flask, and a boiling tube placed in the Erlenmeyer flask, under the glass support, to collect eluent from the SPE disk. The sample container was rinsed with 30 mL of 40:60 acetonitrile:water, which was then used to elute the SPE disk. The sample container was further rinsed with 50 mL of acetonitrile which was also used to elute the SPE disk. The eluent was then concentrated to ca. 2 mL on a rotary evaporator. The concentrated extracts were analyzed by HPLC using the conditions described in

section 5.2.2 and Table 5-1. To confirm that complete recovery of metabolites was achieved using the conditions described above, the SPE disk was occasionally eluted with a further 50 mL of acetonitrile. No significant amounts of metabolites were ever recovered from this extra amount of eluent.

5.2.11 Synthesis of pyrene-1-β-D-glucopyranosiduronic acid (pyrene-1-glucuronide)

No standard compounds exist for pyrene metabolites conjugated to polar moieties such as glucose, sulfate, or glucuronic acid. However inspection of the enzyme activity data in Chapter 1, Table 1.2, shows that the transferase enzymes that generate these conjugates are far more active in mollusks than the mixed function oxidase enzymes responsible for initial oxidation of PAHs. This suggests that the phenols formed from initial oxidation of pyrene are likely to be rapidly converted to polar conjugates, and these could well be the major metabolites of pyrene.

A standard pyrene-conjugate compound would be useful for optimizing extraction and analysis methodology for the determination of pyrene metabolites formed by mollusks. Pyrene-1-β-D-glucopyranosiduronic acid was selected for synthesis because the necessary transferase enzymes and cofactors required to achieve the enzyme mediated synthesis of this compound were commercially available. Pyrene-1-β-D-glucopyranosiduronic acid was synthesized enzymatically according to Singh *et al.* (246). 1-hydroxypyrene (6 mg), uridine 5'-diphosphoglucuronyl-transferase (1 unit), uridine 5'-diphosphoglucuronic acid (15 mg) and $MgCl_2$ (500mg) were dissolved in 20 mL of 50 mM tris buffer (pH 7.5), and allowed to react at 37 °C for 3.5 hours, after which time the reaction was stopped by the addition of ethanol. The solvents were removed by freeze drying and the residue was redissolved in 50:50 acetonitrile:water (10 mL). The product was separated from excess reagents by HPLC, and analyzed by ESI-MS/MS.

The pseudomolecular ion ([M-H]$^-$, m/z 393) was mass selected, fragmented by CID with argon in a collision cell, and the resulting fragment ions were analyzed. The resulting mass chromatogram is included as Figure 5-1, along with proposed structures for the major ions. The base peak is the pseudomolecular ion ([M-H]$^-$, m/z 393). Fragment ions are generated via cleavage of the β-glycosidic bond to release the hydroxypyrene anion (m/z 217), and a rearrangement product of glucuronic acid (m/z 175). This mass spectrum matches that published by Law *et al.* (22) for the glucuronic acid conjugate of 1-hydroxypyrene.

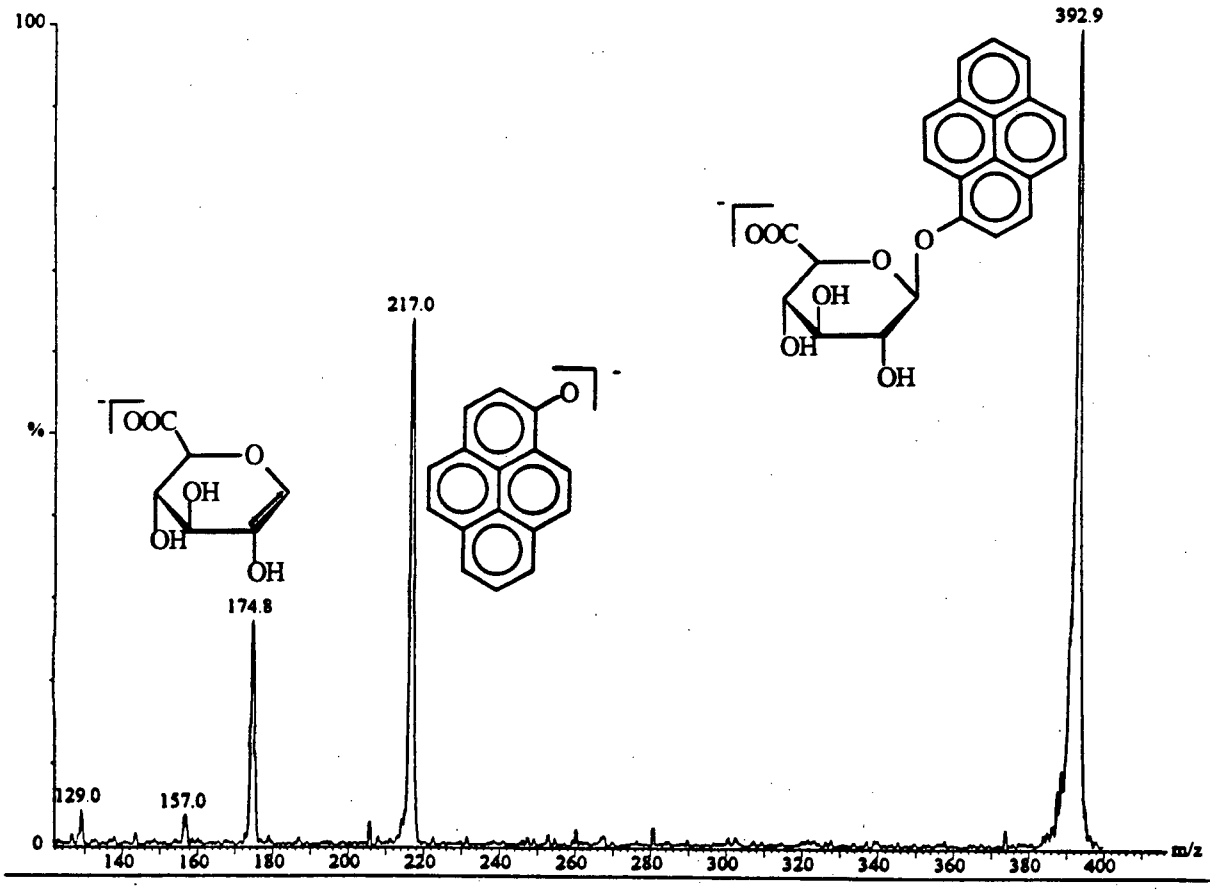

Figure 5-1 Mass spectrum of pyrene-1-β-D-glucopyranosiduronic acid. This mass spectrum was obtained by CID fragmentation of the pseudomolecular ion (m/z 393).

The synthetic pyrene-1-β-D-glucopyranosiduronic acid was also analyzed by fluorescence spectroscopy. The resulting spectra has peaks at 242 nm, 276 nm and 346 nm (excitation spectrum), and 383 nm, 403 nm and 425 nm (emission spectrum), which is in agreement with published data for this compound (246).

5.2.12 Hydrolysis of putatative pyrene-conjugate metabolites

Treatment of pyrene conjugates with specific hydrolases such as β-glycosidase, β-glucuronidase or aryl-sulfatase, will selectively cleave β-glucose, β-glucuronic acid and sulfate respectively to produce hydroxypyrene (22, 246, 310). These reactions can be utilized to indicate what type of conjugate an unknown pyrene metabolite is, although cross-reactivity of some hydrolases with several classes of conjugate can confound the identification.

Metabolite containing fractions collected from the HPLC were treated with β-glucosidase or sulfatase. The HPLC fractions were first dried under a stream of nitrogen, then redissolved in 600 μL of 0.1 M sodium acetate buffer (pH 5.0). β-glucosidase (140 units) or sulfatase (5 units) were added, and the mixture was incubated at 37 °C for 24 hours. A control, consisting of sample plus buffer but no enzyme, was run concurrrently. After hydrolysis the reaction was stopped by the addition of acetonitrile, and the solutions were analyzed for hydroxypyrene by using HPLC with fluorescence detection, as described in section 5.2.2.

5.3 Results and Discussion

5.3.1 Aqueous phase metabolites of pyrene

In extracts from the experiments where *Mya arenaria* and *Protothaca staminea* were exposed to pyrene, two major metabolites (retention times: metabolite 1, ca. 2 min; metabolite 2, ca. 10 min),

and one minor metabolite (metabolite 3, ca. 18 min) were detected. Representative chromatograms of seawater extracts are shown in Figure 5-2. The apparent absence of metabolite 3 in Figure 5-2 (c) is an artifact of the low efficiency of metabolism of pyrene in this particular experiment. In other experiments where *Protothaca staminea* was exposed to pyrene, metabolite 3 was detected. As will be shown in section 5.3.5, the extent of metabolite formation was highly variable between experiments.

In the positive control, only a single peak (retention time ca. 21 min) corresponding to pyrene was detected. Thus no metabolism of pyrene by seawater microorganisms, or other agents, was detected. In the negative control, no peaks were detected under the fluorescence conditions used. This implies that the seawater and clam specimens used were substantially uncontaminated with pyrene or other fluorescent compounds. Thus the fluorescent compounds detected in the exposure experiment are probably metabolites of pyrene.

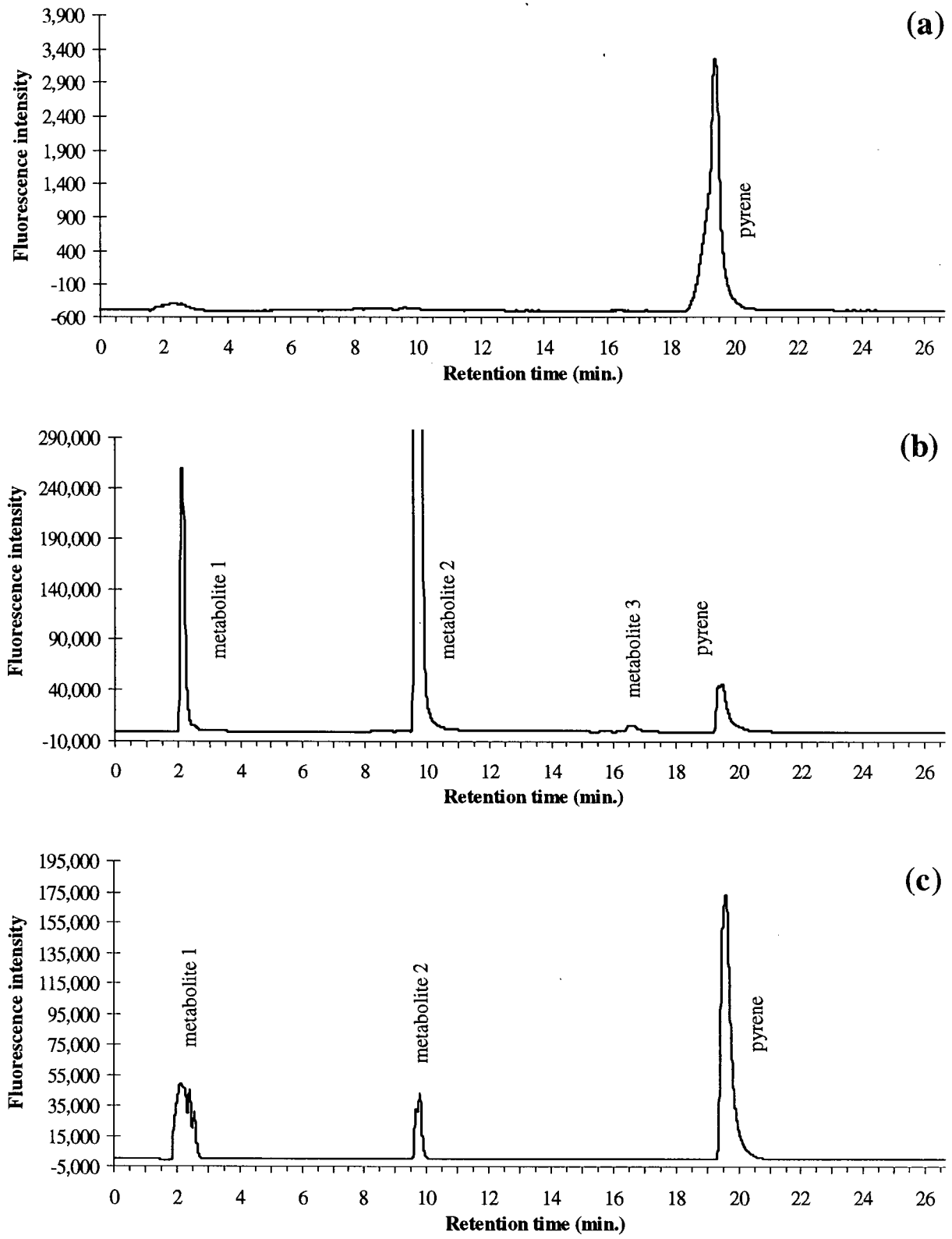

Figure 5-2 HPLC-fluorescence chromatograms showing metabolites in seawater extracts from experiments where clams were dosed with pyrene: (a) Control; (b) Mya arenaria; (c) Protothaca staminea.

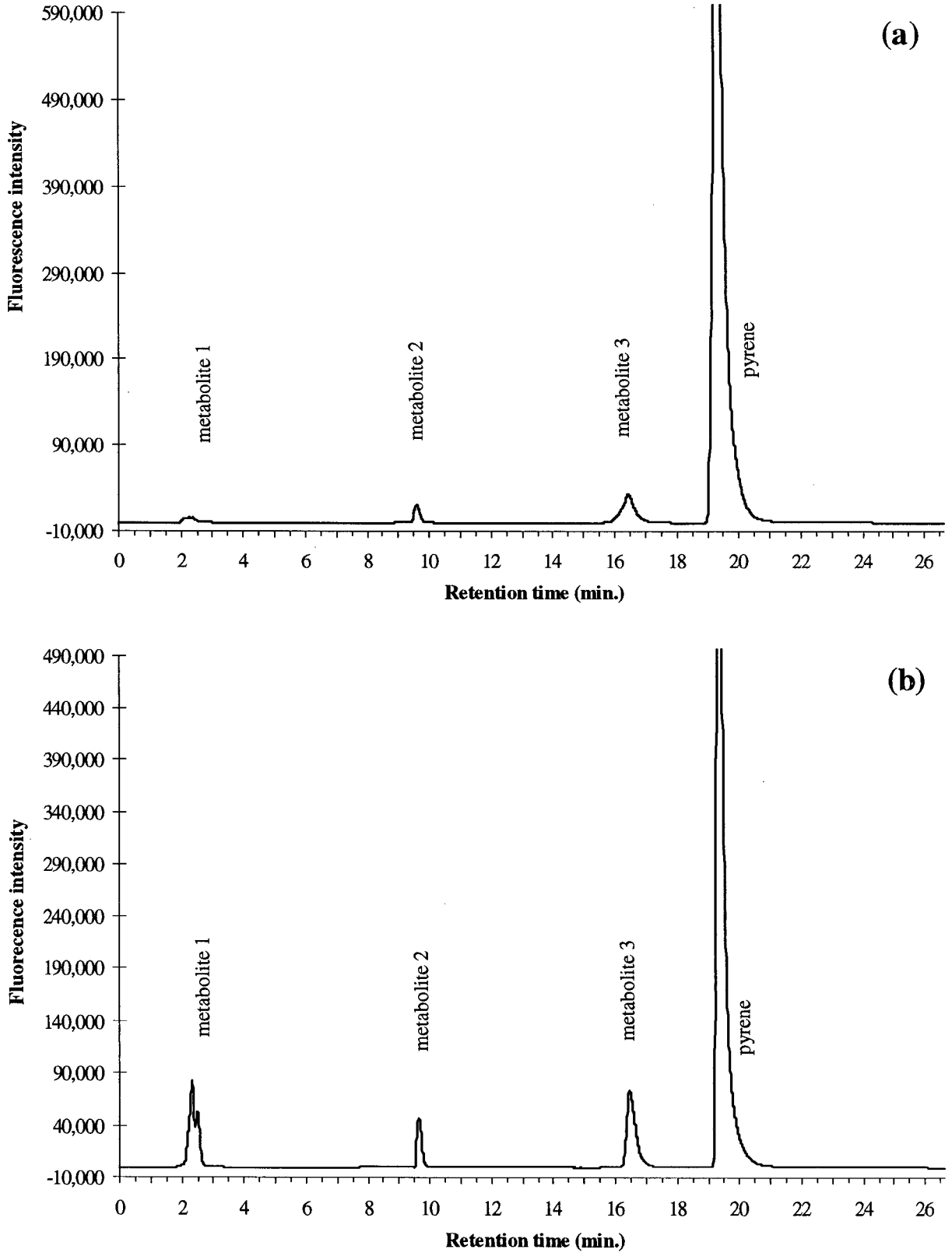

Figure 5-3 HPLC-fluorescence chromatograms showing metabolites in tissue extracts from experiments where clams were exposed to pyrene: (a) Mya arenaria; (b) Protothaca staminea.

5.3.2 Metabolites of pyrene in clam tissue

The clam tissue was also analyzed for pyrene metabolites. The resulting HPLC chromatograms for *Mya arenaria* and *Protothaca staminea* are included as Figure 5-3.

By comparing Figure 5-2 and Figure 5-3 it is apparent that the same metabolites are present in both the aqueous phase and the tissue extracts. However the relative proportions of the metabolites differ. The tissue extract contains a higher proportion of pyrene, and metabolite 3, which co-elutes with an authentic standard for 1-hydroxypyrene. Both these compounds are lipophilic and rather insoluble in water. In contrast the seawater extract is enriched in metabolites 1 and 2. Since they elute from the HPLC earlier than pyrene and hydroxypyrene under reversed phase conditions, it may be concluded that these metabolites are more polar. In fact, metabolite 2 has a similar retention time to the synthetic pyrene-1-β-D-glucopyranosiduronic acid, indicating that metabolite 2 could be a pyrene conjugate.

5.3.3 Metabolism of ^{14}C-labeled pyrene

Mya arenaria and *Protothaca staminea* were exposed to a mixture of ^{14}C-labelled pyrene and unlabeled pyrene, in order to confirm that the fluorescent compounds observed upon exposing these clams to pyrene were indeed derived from pyrene. Figure 5-4 shows the chromatograms obtained from this experiment, using both fluorescence detection, and liquid scintillation counting to detect the ^{14}C label.

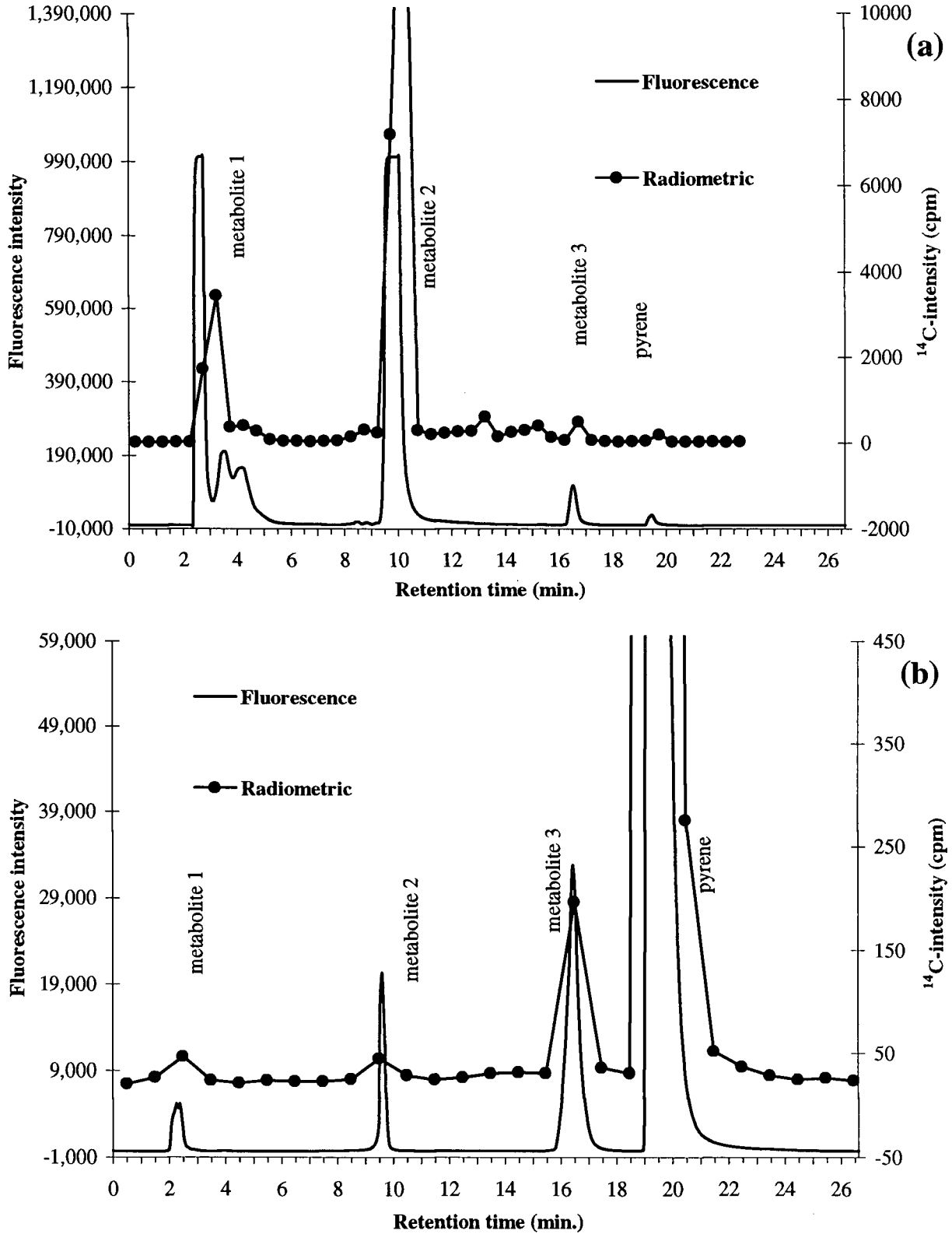

Figure 5-4 HPLC chromatograms showing metabolites in seawater extracts from experiments where clams were dosed with pyrene and ^{14}C-pyrene: (a) Mya arenaria; (b) Protothaca staminea.

As can be seen from Figure 5-4, the three metabolites indicated in the previous sections are shown to be ^{14}C containing, thus confirming that they are indeed derived from pyrene. In addition, several extra (small) peaks are present between 12 and 16 minutes, in the radio-chromatogram for Figure 5-4 (a), which are not present in the fluorescence chromatogram. These peaks may be due to metabolites in which the pyrene aromatic nucleus has been disrupted (e.g. ring cleavage products or dihydrodiols). Although these 'extra metabolites' are not seen in Figure 5-4 (b), this may be because they are below the detection limit in this case. In this example, the conversion of pyrene to metabolites was much better by *Mya arenaria* (Figure 5-4 (a)) than it was by *Protothaca staminea.*

Another feature that is apparent from Figure 5-4 (a), is that the peak that was previously labeled as 'metabolite 1' is in fact a cluster containing at least three separate compounds.

5.3.4 Aqueous phase metabolites of 1-hydroxypyrene

In extracts from the experiments where *Mya arenaria* and *Protothaca staminea* were exposed to 1-hydroxypyrene, two major metabolites (retention times: metabolite 1, ca. 2 min; metabolite 2, ca. 10 min.) were detected. Representative chromatograms of seawater extracts are shown in Figure 5-5. The metabolites eluting at ca. 2 min and ca. 10 min had retention times identical to those of metabolites 1 and 2, detected when clams were exposed to pyrene. In the positive control, only a single peak (retention time ca. 17 min) corresponding to 1-hydroxypyrene was detected. Thus no metabolism of 1-hydroxypyrene by seawater microorganisms, or other agents, was detected.

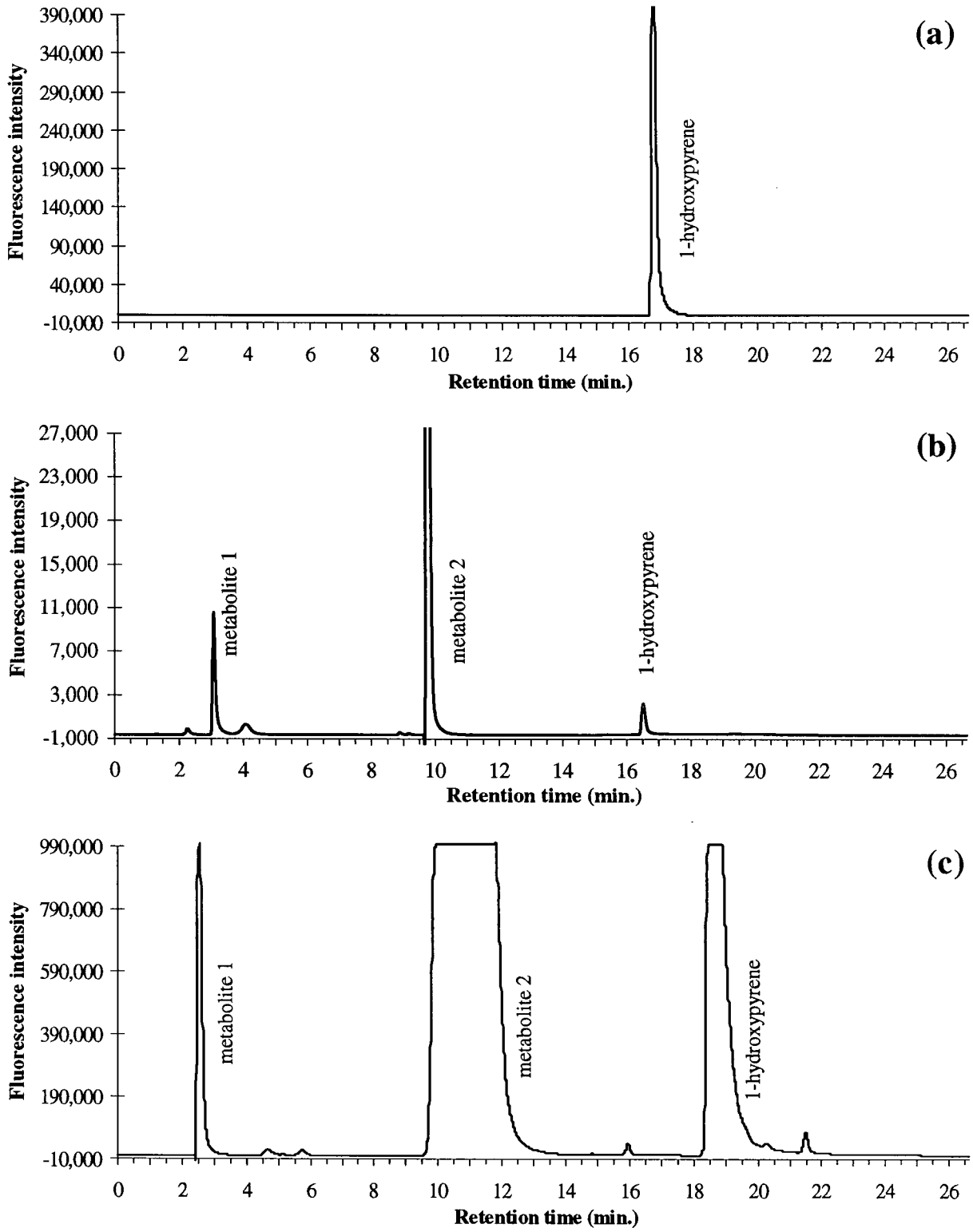

Figure 5-5 HPLC-fluorescence chromatograms showing metabolites in seawater extracts from experiments where clams were dosed with 1-hydroxypyrene: (a) Control; (b) Mya arenaria; (c) Protothaca staminea.

In the negative control, no peaks were detected under the fluorescence conditions used. This implies that the seawater and clam specimens used were substantially uncontaminated with 1-hydroxypyrene or other fluorescent compounds and, thus, the fluorescent compounds detected in the exposure experiment are probably metabolites of 1-hydroxypyrene.

5.3.5 Semi-quantitative analysis of pyrene and 1-hydroxypyrene metabolite formation

As mentioned in section 5.1, this experiment was not designed to provide a thorough quantitative analysis of metabolite formation. However, the data obtained in these experiments can be analyzed to provide at least semi-quantitative information on the extent of metabolite formation.

Peak areas obtained from the HPLC-fluorescence chromatograms can not be directly compared because the metabolites will certainly have different response factors. For example Singh *et al.* (246) determined that (under a specific set of conditions) the fluorescence intensity of pyrene-1-β-D-glucopyranosiduronic acid is 3-fold higher than that of 1-hydroxypyrene, and the fluorescence intensity of pyrene-1-sulfate is 4-fold higher than that of 1-hydroxypyrene. Strickland *et al.* compared fluorescence intensities of 1-hydroxypyrene and pyrene-1-β-D-glucopyranosiduronic acid by using SFS, and determined that the fluorescence intensity of the conjugate was 5-fold higher than that of 1-hydroxypyrene (232).

In contrast, the *molar* radioactivity of each of the metabolites formed from ^{14}C-pyrene would be identical, assuming that any quenching of the radioactivity is similar for each metabolite. Quenching, due to inter- or intra-molecular absorption of β-radiation, causes the average energy of the β-radiation to shift to lower values. In fact, the degree to which the energy distribution for

a particular isotope in a quenched sample differs from the energy distribution in an (unquenched) standard can be used to correct the observed activity for any quenching.

In the present work, no significant quenching of the ^{14}C-radiation was observed. Thus the ratio of the ^{14}C-derived radioactivity associated with each metabolite containing fraction collected from the HPLC, and the peak area of the corresponding metabolite as determined by fluorescence detection, can be used to generate fluorescence response factors (relative to pyrene) for each metabolite. These relative response factors (RRFs) were determined to be 1.0 (pyrene), 1.3 (1-hydroxypyrene), 2.3 (metabolite 2), and 3.0 (metabolite 1). Based on the RRFs, the metabolites are detected by the fluorescence detector with greater sensitivity than are the parent compounds (under the anlysis conditions used). Dividing the fluorescence signal for each compound by its RRF compensates for differences between the metabolites in molar response to the fluorescence detector, and provides an appropriate basis for calculating the relative amounts of each metabolite formed. The results are shown in Table 5-2.

As can be seen from Table 5-2, there is a lot of variability in the extent of metabolism of pyrene by the two clam species. For example, in separate experiments where *Mya arenaria* was exposed to pyrene, the fraction of metabolites generated ranged from 1.5% to 86% of the total fluorescence signal. This variability is of sufficient magnitude to obscure any differences between the two clam species in the extent of pyrene metabolism. Major factors contributing to the variability in Table 5-2 include differences in clam biomass between the various experiments, and differences in health and metabolism between the individual clams used in these experiments. Evidently in order to obtain useful quantitative data, it would be necessary to use a larger population of clams in each experiment.

Table 5-2 Amounts of pyrene and 1-hydroxypyrene metabolites formed by Mya arenaria and Protothaca staminea (expressed as percent of the total fluorescence peak areas in each extract).

Experiment	phase analyzed	metabolite 1	metabolite 2	hydroxypyrene	pyrene
Mya arenaria and pyrene	aqueous	16	9.1	0.1	74.6
	aqueous	0.5	0.8	0.1	98.6
	aqueous	10	75	1.3	13.4
	tissue	0.9	13	0.1	86
	tissue	3.4	1.7	9.2	86
Protothaca staminea and pyrene	aqueous	0.9	6.1	0.2	93
	aqueous	1.7	17	1.5	80
	tissue	1.2	11	8.8	79
	tissue	0.2	0.5	3.2	96
Mya arenaria and 1-hydroxypyrene	aqueous	4.9	91	4.0	0
	aqueous	2.3	81	17	0
Protothaca staminea and 1-hydroxypyrene	aqueous	0.5	64	36	0

5.3.6 Identification of metabolite 3 as an hydroxypyrene isomer ($C_{16}H_9$-OH)

The minor peak at ca. 18 minutes in tissue and sea water extracts from both clam species exposed to pyrene, co-elutes with an authentic standard of 1-hydroxypyrene. To facilitate identification of this metabolite a large volume (750 µL) of the seawater extract from experiments where *Mya arenaria* was exposed to pyrene was injected onto the HPLC and the fraction containing metabolite 3 was collected for subsequent analysis. This fraction was reduced to dryness under a stream of nitrogen, and then the residue was taken up in methylene chloride and analyzed by GC-

MS. The resulting chromatogram contained a peak at retention time 34.2 min. (Figure 5-6) This peak had the same retention time and mass spectrum as an authentic standard of 1-hydroxypyrene.

The mass spectrum of metabolite 3 (Figure 5-6 (b)) contains a molecular ion at m/z 218 and one major fragment ion at m/z 189, resulting from H• migration and loss of CO and H• with subsequent rearrangement. This fragmentation pattern is characteristic of phenols.

The mass spectrum, however, cannot indicate at which position the OH group is attached to the aromatic ring system. Gas chromatography using standard polydimethylsiloxane phases probably does not resolve the mono-hydroxypyrene isomers (1-hydroxypyrene, 2-hydroxypyrene and 4-hydroxypyrene) (310). Krahn *et al.* claim that the three mono-hydroxypyrene isomers are resolved on C18 HPLC columns (310), but this observation remains unconfirmed. In the present work, the absence of authentic standards for the three mono-hydroxypyrene isomers precludes the unique identification of metabolite 3 based on GC or HPLC retention times alone, and this metabolite was not isolated in quantities sufficient for analysis by ^{1}H-NMR.

However, the preponderance of evidence from other studies indicates that 1-hydroxypyrene is formed almost to the exclusion of the other isomers by organisms utilizing mono-oxygenase mediated metabolic pathways (15, 22, 311, 312). Furthermore, in the present work metabolite 2 is uniquely identified as a C1-substituted hydroxypyrene conjugate (section 5.3.7). Since metabolite 2 appears to be formed from metabolite 3, it may be concluded that metabolite 3 is the 1-hydroxypyrene isomer.

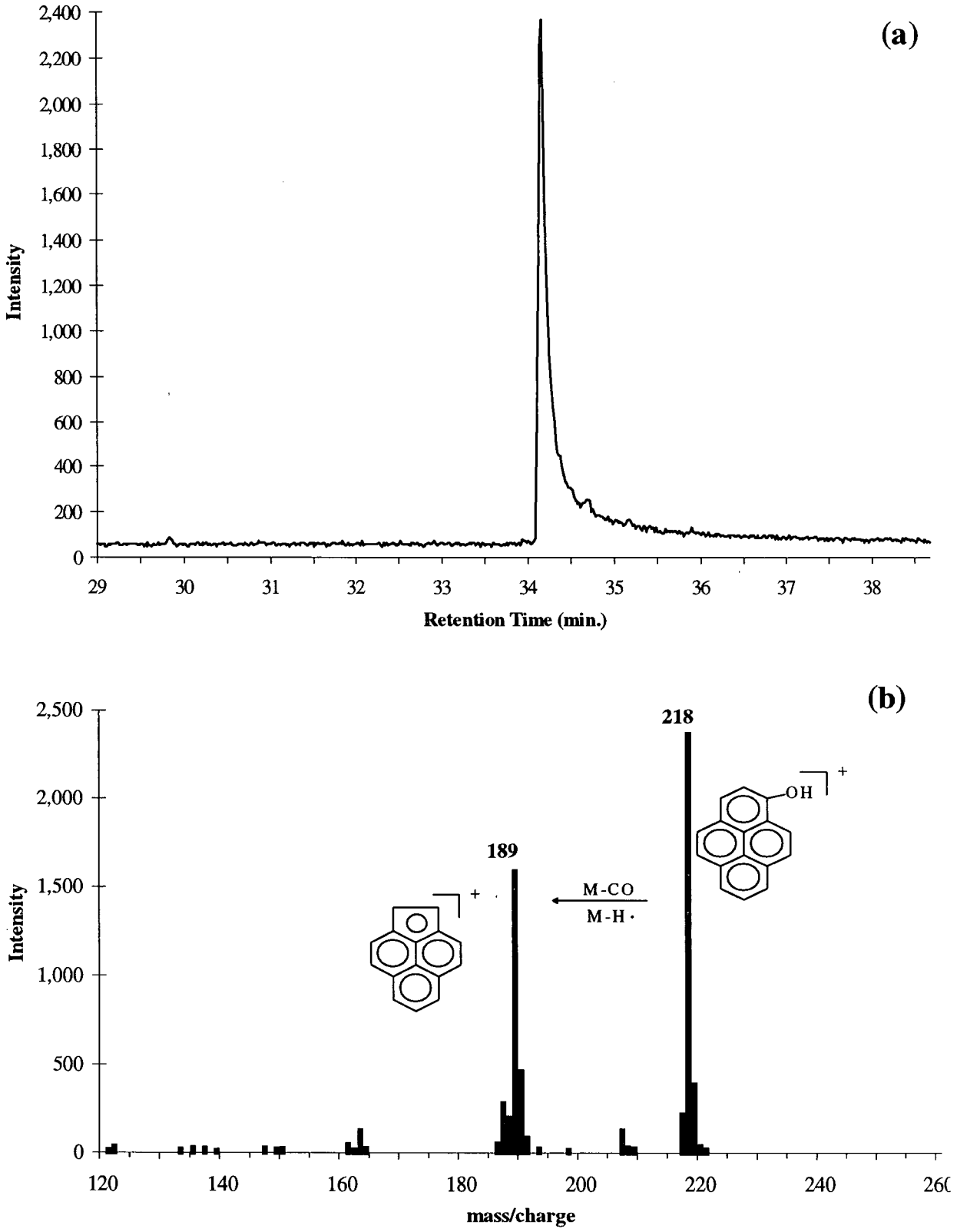

Figure 5-6 Total ion chromatogram of (a) HPLC fraction containing metabolite three; and (b) corresponding mass spectrum of peak at retention time 34.2 min.

5.3.7 Identification of metabolite 2 as 1-pyrenol-1-hydrogensulfate (pyrene-1-sulfate)

The major peak at ca 10 minutes (metabolite 2) in tissue and sea water extracts from both clam species exposed to pyrene and 1-hydroxypyrene has a retention time similar to the synthetic standard of pyrene-1-β-D-glucopyranosiduronic acid. This suggested that metabolite 2 may be a pyrene conjugate. To facilitate identification of this metabolite a large volume (750 µL) of the seawater extract from *Mya arenaria* exposed to pyrene was injected onto the HPLC and the metabolite 2 containing fraction collected for subsequent analysis. A portion of these fractions was reduced to dryness under a stream of nitrogen, and then the residues were taken up in 50:50 acetonitrile:water, containing 0.1% ammonium acetate and analyzed by ESI-MS/MS, in both flow injection mode and with in line HPLC. The resulting mass spectrum is shown in Figure 5-7.

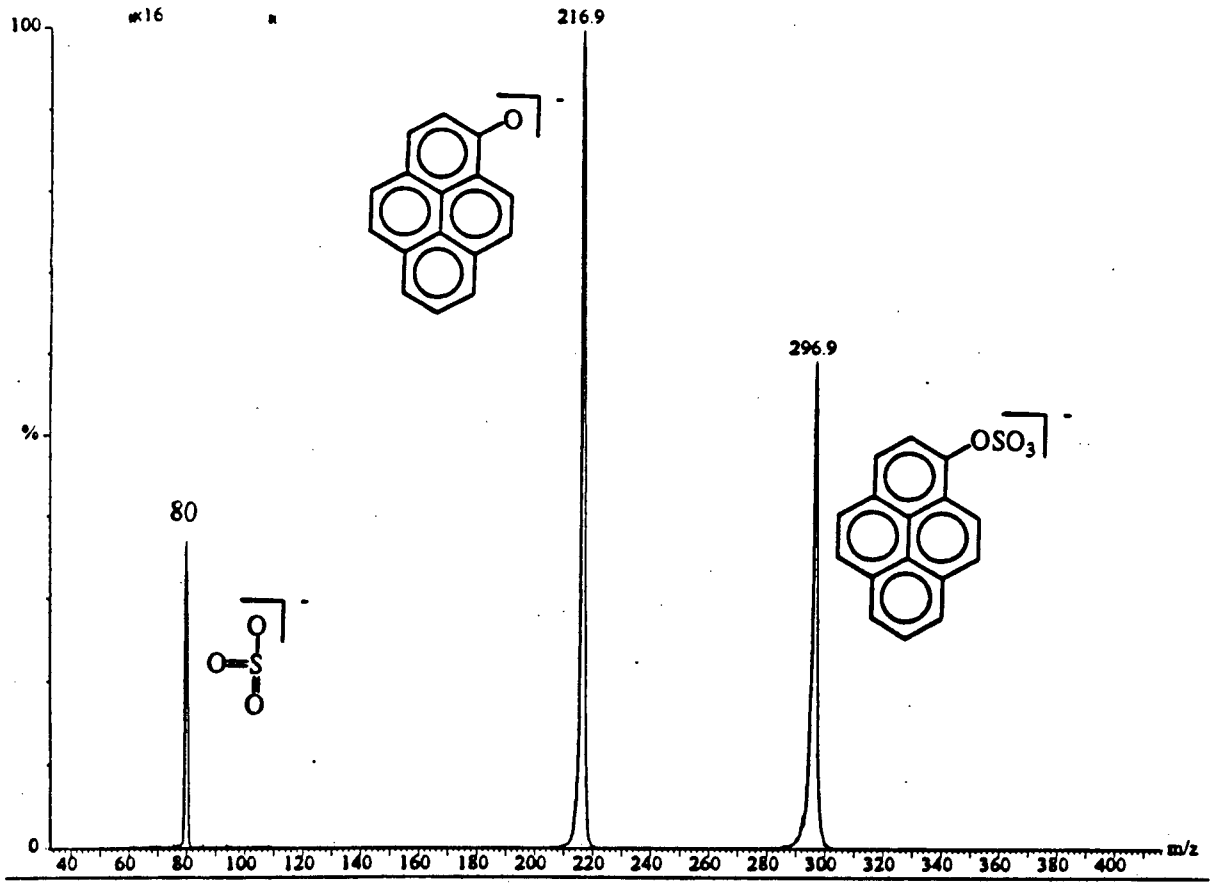

Figure 5-7 Mass spectrum of Metabolite 2, obtained by CID fragmentation of pseudomolecular ion (m/z 297). Note that the intensities of m/z 60-110 are multiplied by a factor of 16 relative to the other masses.

The mass spectrum in Figure 5-7 was generated by selecting the pseudomolecular ion at m/z 297, fragmenting it by CID, and analyzing the resulting fragment ions. Residual pseudomolecular ion is evident at m/z 297, together with fragment ions at m/z 217 and m/z 80. This spectrum is consistent with the compound pyrene sulfate, and proposed structures for the fragment ion, generated by cleavage of the sulfate-ester bond, are illustrated on Figure 5-7. This fragmentation pattern was also observed when the same sample was analyzed by using an ion-trap mass spectrometer (Finnigan LCQ), but the fragment ion at m/z 80 was not seen, because ions less than 25% of the molecular weight of the parent ion are not stable in the ion-trap (under the standard operating conditions for this instrument).

The seawater extracts from experiments where *Protothaca staminea* was exposed to pyrene and hydroxypyrene (2 extracts) were also analyzed by ESI-MS/MS without prior HPLC fractionation. The major compound in both these extracts gave a mass spectrum identical to Figure 5-7.

The metabolite 2 containing fraction was further analyzed by fluorescence spectroscopy. The excitation and emission spectra are included as Figure 5-8. Excitation maxima occur at 240 nm, 274 nm, 324 nm and 339 nm. Emission maxima occur at 379 nm, 399 nm and 421 nm. The spectral data are in agreement with fluorescence spectra published by Singh (246) for pyrene-1-sulfate isolated from mouse urine.

The combined results of sulfatase hydrolysis, ESI-MS/MS and fluorescence spectroscopy confirmed that metabolite 2 is an isomer of pyrene sulfate, but none of these techniques can uniquely identify which isomer is present. Therefore the metabolite 2 containing fraction was dissolved in d_6-acetone and further analyzed by ^{1}H-NMR spectroscopy. The results are listed in Table 5-3.

Table 5-3 1H-NMR data for metabolite 2.

proton #	signal	multiplicity	$J_{(H,H)}$
2	8.15	d	8.4 (2,3)
3	8.33	d	8.4 (2,3)
4	8.07	d	8.9 (4,5)
5	8.00	d	8.9 (4,5)
6	8.17	d	7.6 (6,7)
7	7.98	t	7.6 (6,7) (7,8)
8	8.16	d	7.6 (7,8)
9	8.06	d	9.2 (9,10)
10	8.55	d	9.2 (9,10)

The chemical shifts and mutiplicity of the NMR signals are in agreement with data from Lange *et al.* (311) for the pyrene sulfate isomer with the sulfate group attached to C1 of pyrene. In particular, the multiplicity of the signals in Table 5-3 can only be consistent with pyrene-1-sulfate, as the other two possible isomers (sulfate attached to C2 or C4) would generate signals of different multiplicity. Thus, metabolite 2 is uniquely identified as pyrene-1-sulfate. This result is as expected, given the greater reactivity of C1 in pyrene, compared to C2 and C4. It is also consistent with the observation that the vast majority of pyrene metabolites involving mono-substitution carry the substituent at C1 (15, 22, 311, 312).

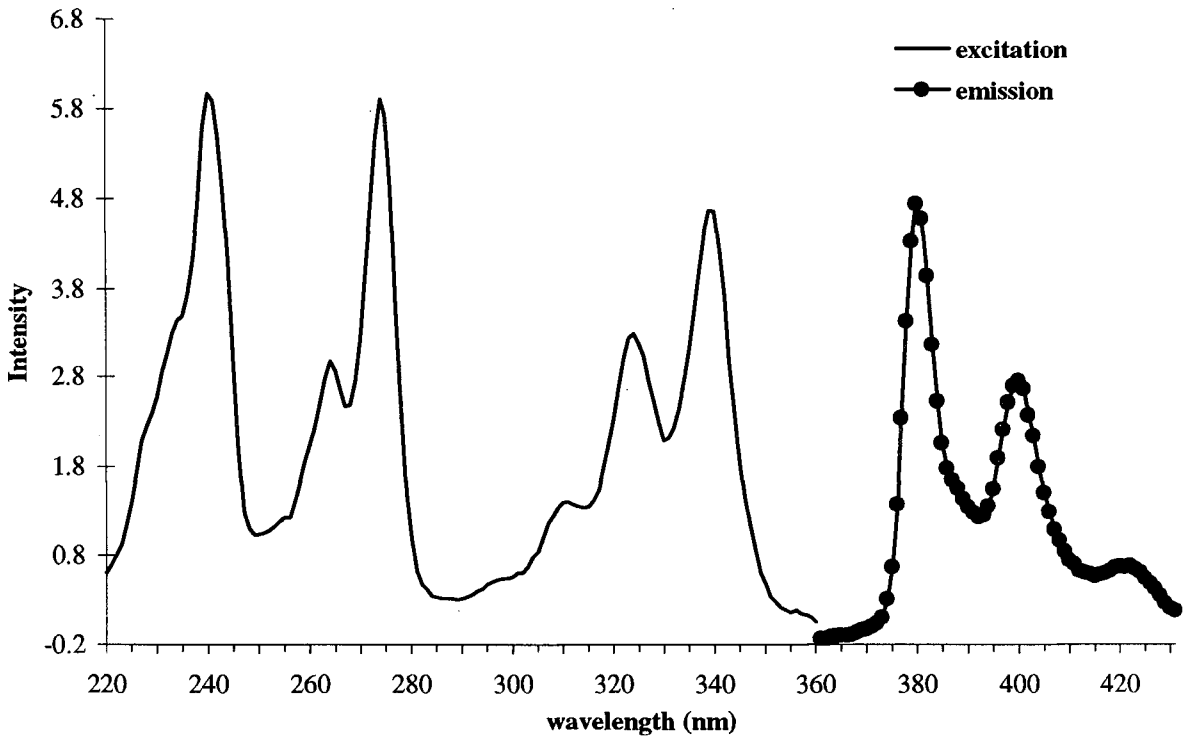

Figure 5-8 Excitation and emission spectra of metabolite 2 (run in methanol).

5.3.8 Synchronous fluorescence spectroscopy of pyrene-1-sulfate ($C_{16}H_9$-OSO_3H)

Synchronous fluorescence spectroscopy (SFS), developed by Vo-dinh (229) and Lloyd (230), is becoming popular for the analysis of PAH metabolites in environmental samples (231-233). In SFS both the excitation and emission monochromators are scanned with a constant wavelength difference between them. The resulting spectrum, which often consists of a single peak, is simpler than a conventional fluorescence spectrum. The wavelength corresponding to the peak maximum is used to uniquely identify the PAH metabolite. SFS spectra (in 50:50 ethanol:water, $\Delta\lambda$=37 nm) have been published for 1-hydroxypyrene and pyrene-1-β-D-glucopyranosiduronic acid (231), and Eickhoff has determined values of SFS maxima (emission wavelengths) for pyrene (372 nm), 1-hydroxypyrene (387 nm), pyrene-1-β-D-glucopyranosiduronic acid (384 nm), and pyrene-1-β-D-glucose (379 nm) (313). However, no value has been published for pyrene-1-sulfate. Therefore,

SFS spectra were recorded for pyrene-1-sulfate, and are included as Figure 5-9. It is important to note the significant effect of solvent choice in SFS. Changing from acetonitrile to methanol as solvent caused a blue shift in the SFS maximum, from 381 nm to 378 nm. Such a shift could lead to mis-identification of metabolites if the solvent used is different from that in which the standard compounds were analyzed.

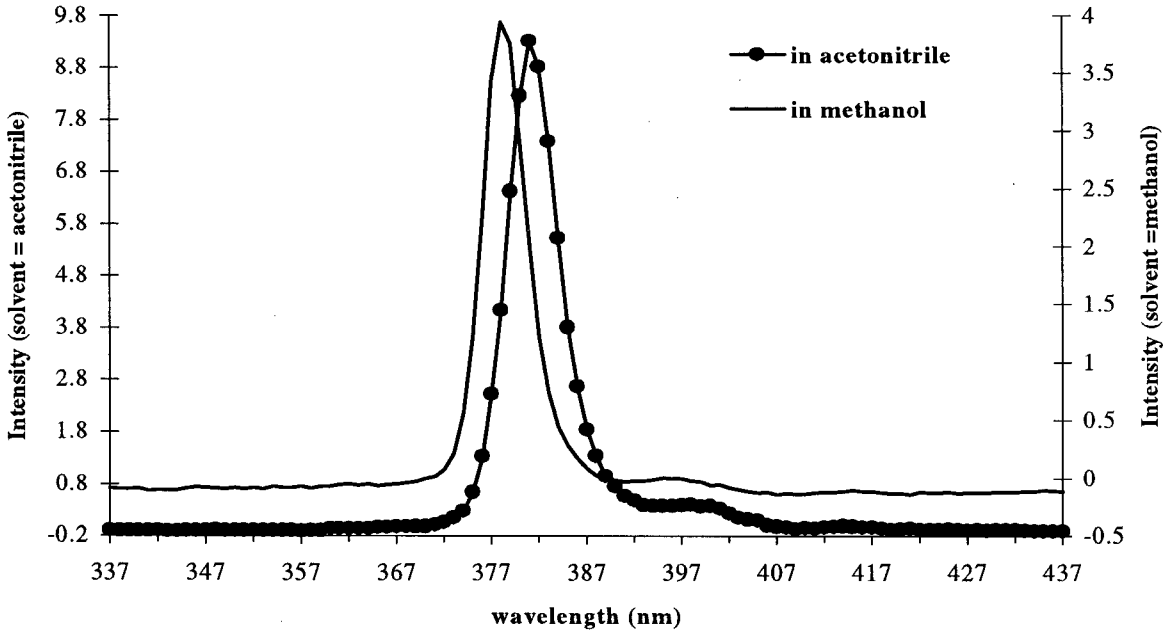

Figure 5-9 SFS spectra of pyrene-1-sulfate, obtained by using a constant wavelength difference of 37 nm between the excitation and emission monochromators.

5.3.9 Identification of pyrenediol-hydrogen sulfate (hydroxypyrene sulfate) in the metabolite 1 fraction

Early eluting metabolites, identified as metabolite 1, were present in sea water extracts from both clam species exposed to both pyrene and 1-hydroxypyrene. The HPLC retention behaviour of these compounds suggests that they are fairly polar, and may well be pyrene conjugates. To facilitate identification of these metabolites, a large volume (750 μL) of the seawater extract from

Mya arenaria exposed to 1-hydroxypyrene was injected onto the HPLC and the metabolite containing fraction (ca. 2-4 min.) was collected for subsequent analysis. A portion of this fraction was reduced to dryness under a stream of nitrogen, and then the residue was taken up in 50:50 acetonitrile:water, containing 0.1% ammonium acetate and analyzed by ESI-MS/MS, in both flow injection mode and with in line HPLC. The resulting mass spectrum is shown in Figure 5-10.

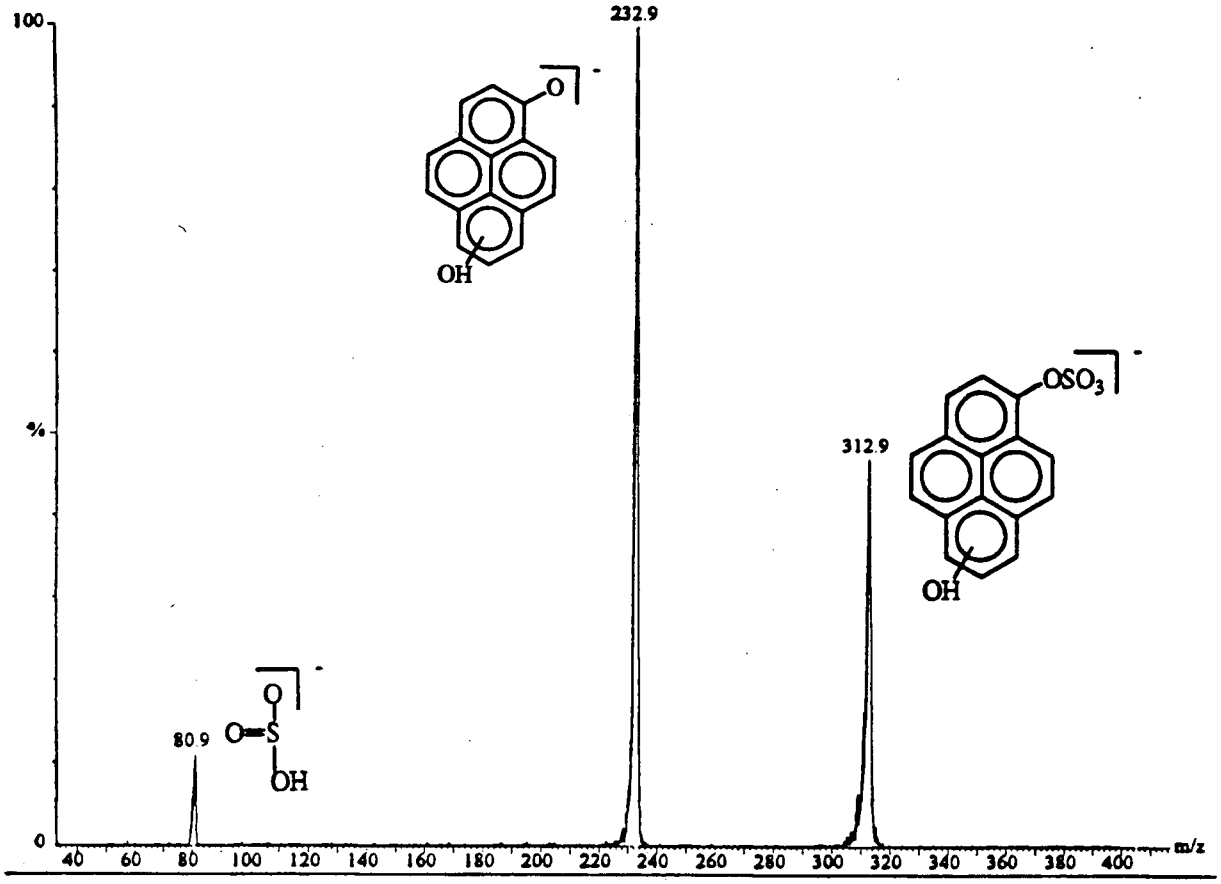

Figure 5-10 Mass spectrum, from metabolite 1 fraction, collected from Mya arenaria exposed to 1-hydroxypyrene. Mass spectrum obtained by CID fragmentation of the pseudomolecular ion (m/z 313).

The mass spectrum in Figure 5-10 was generated by selecting the pseudomolecular ion at m/z 313, fragmenting it by CID, and analyzing the resulting fragment ions. Residual pseudomolecular ion $[M-H]^-$ is evident at m/z 313, together with daughter ions at m/z 233 and

m/z 81. This spectrum is consistent with the compound hydroxypyrene sulfate, and proposed structures for the fragment ions, generated by cleavage of the sulfate-ester bond, are illustrated on Figure 5-10.

The seawater extract from experiments where *Protothaca staminea* was exposed to 1-hydroxypyrene was also analyzed by ESI-MS/MS without prior HPLC fractionation. Hydroxypyrene sulfate was also identified in this extract based upon a mass spectrum identical to that shown in Figure 5-10.

However, when the corresponding HPLC fraction from seawater extracts of experiments where *Mya arenaria* was exposed to pyrene was analyzed, hydroxypyrene sulfate was not detected. Similarly, hydroxypyrene sulfate was not detected when an unfractionated seawater extract from the *Protothaca staminea* + pyrene was analyzed by ESI-MS/MS. This may be because in the case of pyrene, insufficient amounts of metabolite 3 (1-hydroxypyrene) accumulate to cycle through the oxidation step a second time, as required to form hydroxypyrene sulfate. Alternatively, hydroxypyrene sulfate may have been formed from pyrene in the present experiments, but not in sufficient quantities to be detected by ESI-MS/MS.

There is an unusual contrast in the mass spectra shown in Figure 5-7 and Figure 5-10. In Figure 5-7 the sulfate-derived fragment appears at m/z 80, corresponding to SO_3^-, whereas in Figure 5-10 the sulfate-derived fragment appears at m/z 81, corresponding to HSO_3^-. This observation has not been investigated in detail, and the possibility cannot be ruled out that the difference is simply due to a mass assignment error by the mass spectrometer. However, since the other masses are correctly assigned, this difference is probably real.

5.3.10 Results of metabolite hydrolysis

As part of the process of attempting to identify the unknown pyrene metabolites 1 and 2, as shown in Figure 5-2, HPLC fractions containing the metabolites 1 and 2 were collected and subjected to enzymatic hydrolysis by β-glucosidase and sulfatase.

Treatment of metabolite 2 with sulfatase caused complete hydrolysis, as evidenced by the disappearance of the metabolite 2 peak, and the appearance of a peak with a retention time corresponding to 1-hydroxypyrene. This is as expected for a sulfate conjugate of hydroxypyrene, and is consistent with the results from ^{1}H-NMR, ESI-MS/MS and fluorescence spectroscopy that identified metabolite 2 is pyrene-1-sulfate.

Treatment of metabolite 2 with β-glucosidase caused incomplete hydrolysis after 24 hours, as seen by a reduction in the metabolite 2 peak-height and the appearance of a peak with a retention time corresponding to 1-hydroxypyrene. This is not expected, as pyrene sulfate should not react with a β-glucosidase. The most likely explanation is that the β-glucosidase enzyme preparation, which is impure, may possess some general hydrolysis activity. It is not uncommon for impure enzyme preparations to exhibit cross-reactivity of this sort.

Treatment of the metabolite 1 containing fraction with sulfatase caused partial hydrolysis, as seen in the ca. 75% diminution of the metabolite 1 peak height, however no new fluorescent metabolite peaks (e.g. corresponding to hydroxylated pyrenes) were detected. Partial hydrolysis of the metabolite 1 fraction is expected, as this fraction contains several fluorescent metabolites, of which only one was identified as a sulfate conjugate. The expected hydrolysis product - a dihydroxypyrene isomer - should exhibit some fluorescence at the wavelengths used in this

experiment. Because only a small amount of metabolite 1 was available for hydrolysis, it is possible that insufficient dihydroxypyrene was formed to be detected under the present conditions. A second possibility is that the dihydroxypyrene formed was auto-oxidized by air to a pyrene quinone - a process that occurs readily (15, 314). The UV absorption spectra of the pyrene quinones are very different from hydroxylated or conjugated pyrene metabolites that maintain the aromaticity of the pyrene nucleus (15). Because of the similar absorption processes involved in UV and fluorescence spectroscopy, the fluorescence absorption and emission properties of pyrene quinones would also be expected to differ from other pyrene metabolites. Therefore the pyrene quinones may not exhibit fluorescence under the conditions used in this experiment.

5.3.11 Detection of pyrene metabolites in *Mya arenaria* from Kitimat

Having determined under laboratory conditions that clams are capable of metabolism of pyrene, pyrene metabolites were sought in *Mya arenaria* inhabiting sediments contaminated with PAHs at Kitimat, BC. *Mya arenaria* were collected from Kitimat, the tissue was extracted with ethyl acetate, and the extract was analyzed by HPLC, after exchanging the solvent for 40:60 acetonitrile:water. A section of the resulting chromatogram is illustrated in Figure 5-11 (solid line). The peak at 12.0 min. has a retention time corresponding to pyrene-1-sulfate. The extract was spiked with the pyrene-1-sulfate metabolite extract and reanalyzed (dashed line in Figure 5-11). The increase in height of the peak at 12 min. indicates that the peak in the clam extract is due to pyrene-1-sulfate.

To provide confirmatory evidence of the existence of pyrene-1-sulfate in extracts of from Hospital Beach clams, a large volume of the extract was separated by HPLC, the pyrene-1-sulfate containing fraction was collected, and it was analyzed by ESI-MS/MS. Unfortunately, this extract

contained high levels of co-extracted material that were not removed by the HPLC clean-up. These co-extractives prevented meaningful analysis of this extract by using ESI-MS.

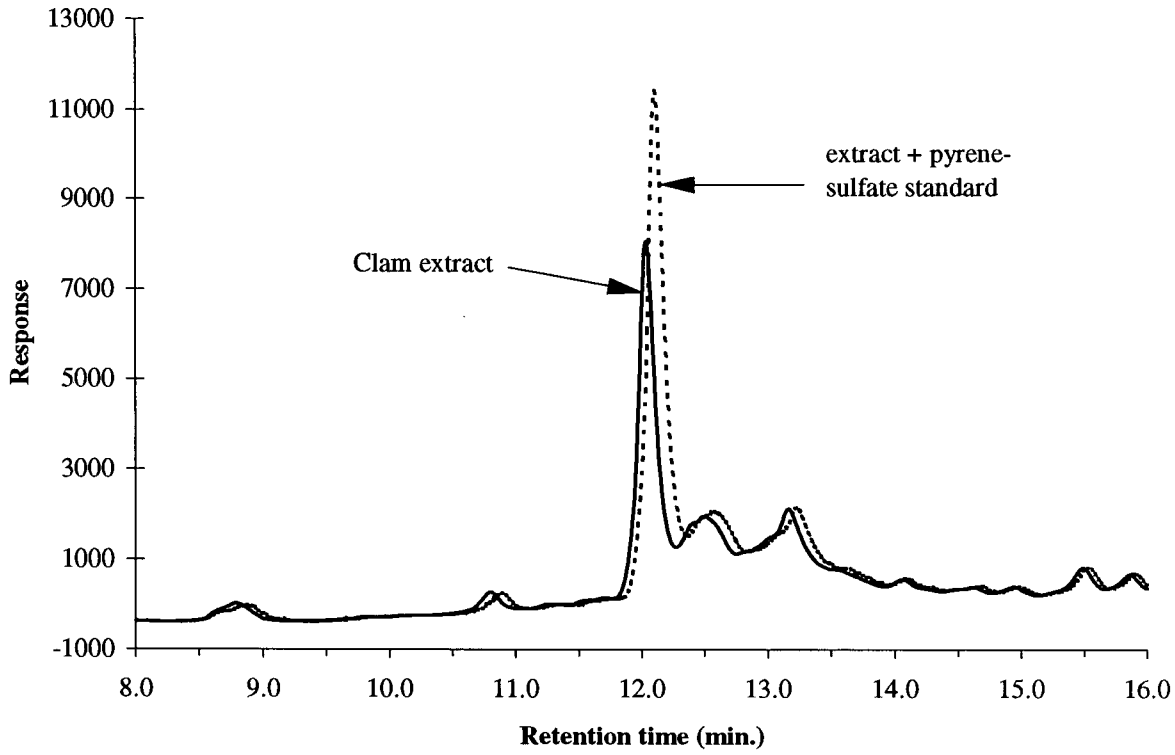

Figure 5-11 HPLC chromatogram showing putative pyrene metabolites in Mya arenaria collected from Hospital Beach, Kitimat, BC.

5.3.12 Discussion

The results from the preceding sections are consistent with the established mono-oxygenase mediated metabolic pathways of pyrene. Namely, metabolism proceeds initially through mono-oxygenation of the aromatic moiety. In pyrene, the resulting epoxide is unstable and readily converts non-enzymatically to a phenol. The phenol is then conjugated with simple hydrophilic molecules to facilitate excretion. This is the dominant pathway of PAH metabolism in vertebrates and crustacea, and is important for some fungi (14, 15, 306).

In the present study, the only conjugates detected are sulfate esters. To the best of the author's knowledge, this study is the first to report conjugated metabolites of unsubstituted PAHs from the phylum *Molluska.* Because of this, no direct comparison can be made with other findings. However, in studies with related compounds 1-naphthol and pentachlorophenol, sulfate metabolites were the major water-soluble metabolites formed (315, 316). Glucoside and glucuronide conjugates of PAHs are often found together with sulfate conjugates as major water soluble PAH metabolites. ESI-MS with selected ion monitoring was used specifically to look for the presence of glucoside and glucuronide conjugates of pyrene in seawater extracts where *Mya arenaria* had been exposed to pyrene and hydroxypyrene, but these compounds were not found to be present.

Sulfation of phenols, including PAH-phenols, is a well established metabolic pathway, as summarized below (39, 317, 318):

$$\text{R-OH} + \text{PAPS} \xrightarrow{\text{ST}} \text{R-O-SO3H} + \text{ADP}$$

A phenol (R-OH) is converted to its sulfuric acid ester (R-O-SO_3H) in the presence of a sulfotransferase enzyme (ST) and a sulfate donor (adenosine 3'-phosphate 5'-sulfatophosphate, PAPS). Sulfate-conjugates of many PAHs, including pyrene, have been identified in crustacea, echinoderms, fungi and vertebrates (1, 2, 22, 317). Pyrene sulfate has been isolated from fungi (311, 319, 320) and rats (246). 6-hydroxypyrene-1-sulfate and pyrene-1,6-disulfate have also been isolated from fungi (319).

The results in the present work are also consistent with the enzyme activity data in mollusks, presented in Chapter 1, Table 1.2. The rate limiting step in the metabolic pathway appears to be the initial oxidation of pyrene. This conclusion is based on the observation that the initial oxidation product, hydroxypyrene, is only present as a minor metabolite, whereas pyrene-sulfate, formed as the sulfate ester of hydroxypyrene, is the major metabolite. In addition, when the slow oxidation step is circumvented by exposing the clams to hydroxypyrene instead of pyrene, the pyrene-sulfate metabolite rapidly accumulates in the water to much higher levels than if pyrene is used as the starting compound.

It should be noted that a different series of metabolites, dominated by *cis*-dihydrodiols and ring cleavage products, would have been expected if significant microbial metabolism of PAHs had occurred in the experiments described in the present study. This is because procaryotes typically utilize dioxygenase mediated oxidation pathways for PAH metabolism (12). Because metabolites of this type were not detected, it may be concluded that microbial metabolism did not contribute significantly to the formation of the metabolites detected in this study.

While the time course of hydroxypyrene metabolism was not specifically studied, it was observed that conversion of hydroxpyrene to pyrene-sulfate plateaued after several days, and did not go to completion. This is also consistent with the enzyme activity data in Chapter 1, Table 1.2, from which it is apparent that, in addition to the ability to synthesize sulfate conjugates, mollusks also posses substantial sulfatase capacity, which would hydrolyze a portion of the pyrene-sulfate back to hydroxypyrene. This process is an example of futile cycling. Futile cycling of endogenous and xenobiotic metabolites is a process in which conjugation takes place in the liver, and deconjugation occurs primarily in the gut, followed by reabsorption of the phenol to complete the

cycle. This process has been well established in higher organisms and is termed *entero-hepatic cycling* (23). This cycling may well be associated with the production of reactive metabolites capable of binding to DNA or proteins and initiating carcinogenesis (23).

It is generally claimed that formation of PAH-conjugates is a detoxification step because it facilitates excretion of the PAHs, thereby preventing their accumulation. In the case of sulfate-conjugate formation, however, the metabolites may in fact have greater toxicity than the parent compound. Sulfuric acid esters of benzylic hydroxy, benzylic hydroxymethyl or N-hydroxy derivatives of PAHs can yield extremely reactive electrophilic carbocations or nitrenium ions respectively, which are capable of binding to DNA and proteins (321-323). 1-methylpyrene-1-hydrogen sulfate ($HO_3SO\text{-}CH_2\text{-}C_{16}H_9$) has been shown to be an ultimate carcinogen formed from methyl pyrene or hydroxymethyl pyrene (321).

In view of the results from this study, it is worthwhile to pose the question, why have metabolites of unsubstituted PAHs heretofore been detected infrequently in mollusks, and PAH conjugates not at all (33, 38, 43)? In many cases the answer may be that researchers were looking in the wrong place. The studies by Payne (32) and Vandermeulen and Penrose (33), which failed to detect PAH metabolites in clams, utilized an assay developed by Nebert and Gelboin (324) which was optimized for the detection of phenolic benzo(*a*)pyrene metabolites. This assay would not have detected water soluble conjugated PAH metabolites, that were found to be the major PAH metabolites in the present study. Similarly, the techniques used by Lee *et al.* (31), and Varanasi *et al.* (43) would probably not have detected polar PAH conjugates.

The absence of PAH-quinones as major metabolites in the present study is in contrast to several studies in which the major products of benzo(*a*)pyrene metabolism in *Mytilus edulis* and

Cryptochiton stelleri were quinones (42, 44, 45). However, Cavalieri and Rogan (25) in studies of PAH metabolism by various *in vitro* systems concluded that only PAHs with an ionization potential lower than approximately 7.35 eV would be appreciably metabolized to quinone metabolites by biological systems. The ionization potential of benzo(*a*)pyrene is 7.23 eV whereas the ionization potential of pyrene is 7.50 eV (25); therefore based on the observations of Cavalieri and Rogan, the formation of pyrene-quinone metabolites would not be expected.

The quantitative aspects of metabolite formation were not expressly studied in the present work, so no firm conclusions can be drawn as to the importance of PAH metabolism, relative to PAH accumulation, by mollusks. Nevertheless, it is possible to speculate on some of the implications of the results from these studies.

As mentioned earlier, hydrolysis or decomposition of PAH conjugates can release potentially reactive metabolites (23, 325, 326). These may be toxic not only to mollusks, but also to other marine organisms which may be exposed to PAH-conjugates excreted by mollusks.

It has been speculated that the toxicity of PAHs may be partially mitigated by reduced bioavailability associated with low water solubility and high sediment-water partition coefficients (111). This argument has been used by some researchers studying the Kitimat system to explain the lower-than-expected acute toxicity of contaminated Kitimat sediments (96). However, since the PAH-conjugates have much greater aqueous solubility than the parent compound, formation of PAH-conjugate metabolites, as demonstrated in this study, may provide a route for making sediment-associated PAHs more bioavailable.

6. Conclusions and Future Work

The emphasis in this thesis is on the determination of PAHs in environmental samples, and also on the accumulation and metabolism of PAHs by mollusks. The Kitimat Fjord system, BC, Canada was chosen as the focus of the environmental studies in this thesis because this location is known to be contaminated with PAHs.

A method was developed and validated for the analysis of priority pollutant PAHs in marine sediments. The method involved Soxhlet extraction of the freeze dried sediments, clean-up of the sediment extract by using Florisil column chromatography, and analysis by using GC with FID detection. This method was applied to marine sediments collected from the Kitimat fjord system. Total PAH concentrations (sum of 16 US EPA priority pollutant PAHs) in these samples were 1-500 mg/kg. Total PAH levels of ca. 10, 000 mg/kg were detected in sediment from an effluent lagoon located on the property of the Alcan aluminum smelter. PAH levels were highest at locations in close proximity to the Alcan smelter, and declined with increasing distance from the smelter.

The PAH composition of all the samples analyzed was typical of PAH mixtures produced from combustion sources. Specifically, 4- and 5-ring PAHs were present in greater proportions than 2 and 3-ring PAHs, and unsusbstituted PAHs predominated over alkylated PAHs. The PAH composition in the harbor sediments was similar to the PAH composition in coke and pitch from the Alcan smelter, as was the PAH composition in sediment samples collected from the Alcan B effluent lagoon.

The equilibrium partitioning (EP) theory predicts that hydrophobic organic compounds, including PAHs, will partition preferentially to sediment particles with high area-to-volume ratios and high organic matter content (f_{OC}). In the present work, a correlation between PAH levels and f_{OC} was only significant for highly contaminated sites proximate to the Alcan smelter. Contrary to the EP predictions, PAH levels were not correlated with f_{OC} at the less contaminated sites. It has been suggested that at highly contaminated sites, the PAHs may be associated with particles of soot, coke and pitch. These particles also have high values of f_{OC}. Therefore the correlation between PAH levels and f_{OC} at the contaminated sites may indicate that the PAHs remain associated with the particles with which they were deposited into the sediments (rather than partitioning into the sediment organic matter).

Distribution of PAHs among different sediment particle size fractions (PSFs) was investigated in sediments collected from seven locations. Only two sites (CD2, CD3), both located in close proximity to the aluminum smelter, exhibited differential distribution of PAHs among PSFs. At all other sites, PAHs were uniformly distributed among sediment PSFs. At site CD3 the distribution of perylene and retene among sediment PSFs was opposite to the trend observed for all the other PAHs. Perylene and retene were enriched on smaller sediment particles, whereas levels of the other PAHs were highest in the larger PSFs. This observation indicates that the source of perylene and retene to CD3 is different from the source of the other PAHs. Both perylene and retene may be formed from diagenesis of organic material, although for both compounds the formation reactions are not well understood. Retene has also been associated with effluent discharges from pulp mills.

Alkylated and unsubstituted PAHs were determined in sections from a sediment core collected from Giltoyees Inlet. Concentrations of the unsubstituted PAHs are highest in the top part of the core, and declined to a constant low level below 45 cm. The PAH composition in the upper part of the core is typical of combustion generated PAHs, and is similar to the PAH composition in other harbor sediments in the Kitimat fjord system. The sediment core was not dated. However, if it is assumed that the increase in PAH concentrations at depths between 20 and 45 cm coincides with the commencement of operations at the Alcan smelter in 1954, an approximate sedimentation rate of 0.25-0.5 cm per year is estimated. This estimate is well within the range of values calculated for recent uncompacted sediments in the Kitimat fjord system.

In the lower portion of the core, below a depth of 45 cm, perylene levels remain fairly constant and account for ca. 70% of the total unsubstituted PAHs. Most of the PAHs typical of combustion mixtures are absent below depth 45 cm, therefore, it must be concluded that perylene in the lower core arises from diagenesis. However, perylene levels in the upper sections of the core co-vary with the other (combustion generated) PAHs. Therefore, most of the perylene in the upper core is associated with combustion generated inputs.

Accumulation of PAHs was investigated in the soft-shelled clam *Mya arenaria*, collected from four beaches within the Kitimat Fjord system. PAHs were detected in the clams (0.8-5.7 mg/kg) and the sediments (0.02-125 mg/kg) from all four beaches. The PAH composition was similar in clams and sediments, and was characteristic of combustion generated PAH inputs. However by using principal components analysis (PCA) it was shown that samples from the four sites could be differentiated based on PAH composition. Specifically, sites in close proximity to the Alcan smelter have a greater proportion of HPAHs than do the other sites. Furthermore, the PCA

showed that sediment samples and clam samples from a given location have different PAH compositions. The proportions of fluoranthene, chrysene and benzo(*e*)pyrene are enriched in clam samples compared to sediments, whereas phenanthrene and fluorene are depleted. Lipid and organic-carbon-normalized biota sediment accumulation factors (BSAFs) were calculated for the four beaches. At three of the four beaches, mean BSAFs were between 0.3-2.8, which is close to the theoretical equilibrium value of 1.7 predicted by the EP theory. However, at Hospital Beach the mean BSAF was only 0.02. The EP theory, therefore, does not adequately describe partitioning of PAHs between sediments and biota at Hospital Beach. Hospital Beach sediments have very high absolute levels of PAHs, deposited from smelter effluents, atmospheric emissions, and spillage of raw materials. It was suggested that PAHs from thse sources may have limited bioavailability. Additionally, the high levels of PAHs at this site may stimulate PAH metabolism in *Mya arenaria.*

In general, the environmental studies at Kitimat supported the hypothesis that PAHs in this system have limited bioavailability. This was evident in the failure of the EP theory to predict PAH partitioning at highly contaminated sites, and also in the lack of discernible changes in the PAH profile that would be expected due to biodegradation or weathering. It was suggested that the differences in PAH composition between samples that were observed, were the result of the mixing of various PAH sources, each with a different PAH composition. There was only limited evidence for alteration of the PAH composition from any given source by environmental processes including weathering or biodegradation.

In terms of future studies, it may be useful to investigate a marine environment contaminated with oil derived PAHs which are expected to be more bioavailable than combustion generated PAHs.

Results could be compared with the present study, to determined whether the oil derived PAHs are indeed more susceptible to biodegradation and weathering. In the Kitimat system, it would be useful to obtain an improved inventory of PAH inputs, including atmospheric emissions from the Alcan smelter and from the Kitimat township itself. Inputs of PAHs from other industries may be important also. For example, it would be expected that the Eurocan pulp mill would discharge substantial amounts of non-regulated PAHs such as retene. It would also be interesting to investigate the fate of PAHs in the terrestrial environment.

Metabolism of pyrene and 1-hydroxypyrene was investigated in two species of mollusk, *Mya arenaria* and *Protothaca staminea.* The metabolites hydroxypyrene, pyrene-1-sulfate, and hydroxypyrene-sulfate were identified. This study is the first to report the identification of PAH-conjugates as PAH metabolites from members of the phylum *Molluska.* The particular metabolites identified suggest that mollusks metabolize PAHs by using similar biochemical pathways to those used by vertebrates for PAH metabolism. Pyrene-1-sulfate was also tentatively identified (on the basis of HPLC retention time) in extracts of *Mya arenaria* collected from Hospital Beach.

An obvious extension of these studies would be to investigate the ability of mollusks to metabolize PAHs other than pyrene. It would be particularly interesting to investigate whether mollusks metabolize PAHs with low ionization potentials by different metabolic pathways (e.g. 1 electron oxidations), as has been speculated by other authors (37). Quantitative aspects of PAH metabolism in mollusks could be investigated also, and this would be facilitated by the use of radio-labeled compounds.

The methodology used in the present work for analysis of PAH metabolites needs to be improved, especially with a view to detection of PAH metabolites in real world samples. The SPE methodology worked well for recovering metabolites from seawater, but it needs to be validated for environmental samples with high levels of suspended solids and dissolved organic matter. In addition, there is an expectation that any metabolites more polar than, for example, the pyrene-sulfate conjugate, may not be quantitatively extracted by using this system. Synthesis of appropriate metabolite standards (e.g. pyrene-sulfate, or pyrene di-sulfate) would assist in the optimization of techniques for recovery of metabolites from environmental samples, and chromatographic clean-up of metabolite containing extracts.

References

(1) Cerniglia, C. E. *Biodegradation* **1992,** *3*, 351-368.

(2) Varanasi, U.; Nishimoto, M.; Stein, J. E. In *Metabolism of Polycyclic Aromatic Hydrocarbons in the Aquatic Environment*; Varanasi, U., Ed.; CRC Press: Boca Raton, Florida, 1989, pp 203-252.

(3) Blumer, M. *Sci. Am.* **1976,** *234*, 34-45.

(4) Stein, S. *Acc. Chem. Res.* **1991,** *24*, 350-356.

(5) Aihara, J. *Sci. Am.* **1992,** *266*, 62-68.

(6) Lee, M. L.; Novotny, M. V.; Bartle, K. D. *Analytical Chemistry of Polycyclic Aromatic Compounds*; Academic Press: New York, USA, 1981.

(7) Ankley, G. T.; Collyard, S. A.; Monson, P. D.; Koslan, P. A. *Environ. Toxicol. Chem.* **1994,** *13*, 1791-1796.

(8) Canadian Environmental Protection Act (CEPA), *Priority substances list assessment report, Polycyclic aromatic hydrocarbons*, 1994.

(9) Huang, X.-D.; Dixon, D. G.; Greenberg, B. M. *Ecotoxicol. Environ. Saf.* **1995,** *32*, 194-200.

(10) Payne, J. R.; Phillips, C. R. *Environ. Sci. Technol.* **1985,** *19*, 569-579.

(11) Mackay, D.; Shiu, W. Y.; Ma, K. C. *Illustrated Handbook of Physical-Chemical Properties and Environmental Fate for Organic Chemicals. Volume 2. Polynuclear Aromatic Hydrocarbons, Polychlorinated Dioxins and Dibenzofurans*; Lewis Publishers Inc.: Chelsea, Michigan, USA, 1992.

(12) Cerniglia, C. E.; Heitcamp, M. A. In *Metabolism of Polycyclic Aromatic Hydrocarbons in the Aquatic Environment*; Varanasi, U., Ed.; CRC Press: Boca Raton, Florida, 1989, pp 41-68.

(13) Wilson, S. C.; Jones, K. C. *Environ. Poll.* **1993,** *81*, 229-249.

(14) Gelboin, H. V. *Physiol. Rev.* **1980,** *60*, 1107-1166.

(15) Cerniglia, C. E.; Kelly, D. W.; Freeman, J. P.; Miller, D. W. *Chem.-Biol. Interact.* **1986,** *57*, 203-216.

(16) Hammel, K. E.; Kalyanaraman, B.; Kirk, T. K. *J. Biol. Chem.* **1986,** *261*, 16948-16952.

(17) Li, X.-F.; Cullen, W. R.; Reimer, K. J.; Le, X.-C. *Sci. Total Environ.* **1996,** *177*, 17-29.

(18) Heitkamp, M. A.; Freeman, J. P.; Cerniglia, C. E. *Appl. Environ. Microbiol.* **1987,** *53*, 129-136.

(19) Bossert, I. D.; Bartha, R. *Bull. Environ. Contam. Toxicol.* **1986,** *37*, 490-495.

(20) Genthner, B. R. S.; Townsend, G. T.; Lantz, S. E.; Mueller, J. G. *Arch. Environ. Contam. Toxicol.* **1997,** *32*, 99-105.

(21) Singleton, I. *J. Chem. Technol. Biotechnol.* **1994,** *59*, 9-23.

(22) Law, F. C. P.; Meng, J. X.; He, Y. T.; Chui, Y. C. *Xenobiotica* **1994,** *24*, 221-229.

(23) Smith, R. L. *The Excretory Function of Bile*; Chapman and Hall: London, 1973.

(24) Dipple, A. In *DNA Adducts: Identification and Biological Significance*; Hemminki, K., Dipple, A., Shuker, D. E. G., Kadlubar, F. F., Segerback, D., Bartsch, H., Eds.; International Agency for Research on Cancer: Lyon, 1994.

(25) Cavalieri, E. L.; Rogan, E. G. In *Polycyclic Hydrocarbons and Carcinogenesis*; Harvey, R. G., Ed.; American Chemical Society: Washington, DC, 1985, pp 289-305.

(26) Cavalieri, E. L.; Rogan, E. G. *Xenobiotica* **1995,** *25*, 677-688.

(27) Stansbury, K. H.; Flesher, J. W.; Gupta, R. C. *Chem. Res. Toxicol.* **1994,** *7*, 254-259.

(28) Smith, M. T. *Environ. Health Perspect.* **1996,** *104*, 1219-1225.

(29) Pothuluri, J. V.; Heflich, R. H.; Fu, P. P.; Cerniglia, C. E. *Appl. Environ. Microbiol.* **1992,** *58*, 937-941.

(30) Launen, L.; Pinto, L.; Wiebe, C.; Kiehlmann, E.; Moore, M. *Can. J. Microbiol.* **1995,** *41*, 477-488.

(31) Lee, R. F.; Sauerheber, R.; Benson, A. A. *Science* **1972,** *177*, 344-346.

(32) Payne, J. F. *Mar. Poll. Bull.* **1977,** *8*, 112-116.

(33) Vandermeulen, J. H.; Penrose, W. R. *J. Fish. Res. Bd. Can.* **1978,** *35*, 643-647.

(34) Suteau, P. M.; Narbonne, J. F. *Mar. Biol.* **1988,** *98*, 421-425.

(35) Suteau, P. M.; Daubeze, M.; Migaud, M. L.; Narbonne, J. F. *Mar. Ecol. Prog. Ser.* **1988,** *46*, 45-49.

(36) Stegeman, J. J.; Lech, J. J. *Environ. Health Perspect.* **1991,** *90*, 101-109.

(37) Livingstone, D. R. In *Persistant Pollutants in Marine Ecosystems*; Walker, C. H., Livingstone, D. R., Eds.; Pergamon Press: Oxford, 1992, pp3-34.

(38) Livingstone, D. R. In *Advances in Comparative and Environmental Physiology*; Gilles, R., Ed.; Springer-Verlag Devon, United Kingdom, 1991; Vol. 7, pp 46-188.

(39) Foureman, G. L. In *Metabolism of Polycyclic Aromatic Hydrocarbons in the Aquatic Environment*; Varanasi, U., Ed.; CRC Press: Boca Raton, Florida, 1989, pp 185-202.

(40) Sole, M.; Porte, C.; Biosca, X.; Mitchelmore, C. L.; Chipman, J. K.; Livingstone, D.; Albaiges, J. *Comp. Biochem. Physiol. C:* **1996,** *113*, 257-265.

(41) Sole, M.; Porte, C.; Albaiges, J. *Environ. Toxicol. Chem.* **1995,** *14*, 157-164.

(42) Stegeman, J. J. *Mar. Biol.* **1985,** *89*, 21-30.

(43) Varanasi, U.; Reichert, W. L.; Stein, J. E.; Brown, D. W.; Sanborn, H. R. *Environ. Sci. Technol.* **1985,** *19*, 836-841.

(44) Schlenk, D.; Buhler, D. R. *Aquat. Toxicol.* **1988,** *13*, 1765-182.

(45) Livingstone, D. R.; Garcia-Martinez, P.; Stegeman, J. J.; Winston, G. W. *Biochem. Soc. Trans.* **1988,** *16*, 779.

(46) Anderson, R. S. *Mar. Environ. Res.* **1985,** *17*, 137-140.

(47) Augenfeld, J. M.; Anderson, J. W.; Riley, R. G.; Thomas, B. L. *Mar. Environ. Res.* **1982,** *7*, 31-50.

(48) Riley, R. T.; Mix, M. C.; Schaffer, R. L.; Bunting, D. L. *Mar. Biol.* **1981,** *61*, 267-276.

(49) Lu, P.-Y.; Metcalf, R. L.; Mandel, N. P. *Arch. Environ. Contam. Toxicol.* **1977,** *6*, 129-142.

(50) Venier, P.; Canova, S. *Aquat. Toxicol.* **1996,** *34*, 119-133.

(51) Marsh, J. W.; Chipman, J. K.; Livingstone, D. R. *Aquat. Toxicol.* **1992,** *22*, 115-128.

(52) Kurelec, B. *Mar. Environ. Res.* **1988,** *24*, 317-320.

(53) Venkatesan, M. I. *Mar. Chem.* **1988,** *25*, 1-27.

(54) Neff, J. M. In *Fundamentals of Aquatic Toxicology*; Rand, G. M., Petrocelli, S. R., Eds.; Hemisphere Publishing Corp.: Washington, 1985, pp 416-454.

(55) Laflamme, R. E.; Hites, R. A. *Geochim. Cosmochim. Acta* **1978,** *42*, 289-303.

(56) Mix, M. C. *Rev. Environ. Toxicol.* **1984,** *50*, 51-102.

(57) Simoneit, B. R. T. *Int. J. Environ. Anal. Chem.* **1985,** *22*, 203-233.

(58) Youngblood, W. W.; Blumer, M. *Geochim. Cosmochim. Acta* **1975,** *39*, 1303-1314.

(59) Bjorseth, A.; Ramdahl, T. In *Handbook of Polyaromatic Hydrocarbons*; Bjorseth, A., Ramdahl, T., Eds.; Marcel Dekker Inc: New York, USA, 1983; Volumes 2, pp 1-20.

(60) Thrane, K. E. *Water, Air, Soil Poll.* **1987,** *33*, 385-393.

(61) Radke, M.; Willsch, H.; Leythauser, D.; Teichmuller, M. *Geochim. Cosmochim. Acta* **1982,** *46*, 1831-1848.

(62) Lipiatou, E.; Saliot, A. *Mar. Chem.* **1991,** *32*, 51-71.

(63) Eganhouse, R. P.; Gosset, R. W. In *Organic Substances in Sediments and Water, Volume 2: Processes and Analytical*; Baker, R. A., Ed.; Lewis Publishers: Michigan, USA, 1991.

(64) Yunker, M. B.; Macdonald, R. W.; Cretney, W. J.; Fowler, B. R.; McLaughlin, F. A. *Geochim. Cosmochim. Acta* **1993,** *57*, 3041-3061.

(65) Sporstol, S.; Gjos, N. *Environ. Sci. Technol.* **1983,** *17*, 282-286.

(66) Jones, D. M.; Rowland, S. J.; Douglas, A. G. *Int. J. Environ. Anal. Chem.* **1986,** *24*, 227-247.

(67) Canton, L.; Grimalt, O. *J. Chromatogr.* **1992,** *607*, 279-286.

(68) Bayona, J. M.; Albaiges, J.; Solanas, A. M.; Pares, R.; Garrigues, P.; Ewald, M. *Int. J. Environ. Anal. Chem.* **1986,** *23*, 289-303.

(69) Volkman, J. K.; O'Leary, T.; Summons, R. E.; Bendall, M. R. *Org. Geochem.* **1992,** *18*, 669-682.

(70) Wakeham, S. G.; Schaffner, C.; Giger, W. *Geochim. Cosmochim. Acta* **1980,** *44*, 415-429.

(71) Radke, M.; Welte, D. H.; Willsch, H. *Geochim. Cosmochim. Acta* **1982,** *46*, 1-10.

(72) Voigtmann, M. F.; Yang, K.; Batts, B. D.; Smith, J. W. *Fuel* **1994,** *73*, 1899-1903.

(73) Schobert, H. H. *The Chemistry of Hydrocarbon Fuels*; Butterworths and Co Ltd.: London, 1990.

(74) National Research Council of Canada, Ottawa, Canada, 1983, Polycyclic aromatic hydrocarbons. *Environmental Health Criteria Document.*

(75) Tan, Y. L.; Heit, M. *Geochim. Cosmochim. Acta* **1981,** *45*, 2267-2279.

(76) Peters, A. J.; Gregor, D. J.; Teixeira, C. F.; Jones, N. P.; Spencer, C. *Sci. Total Environ.* **1995,** *161*, 167-179.

(77) Bicego, M. C.; Weber, R. R.; Ito, R. G. *Mar. Poll. Bull.* **1996,** *32*, 549-553.

(78) Kennicutt, M. C.; McDonald, S. J.; Sericano, J. L.; Boothe, P.; Oliver, J.; Safe, S.; Presley, B. J.; Liu, H.; Wolfe, D.; Wade, T. L.; Crockett, A.; Bockus, D. *Environ. Sci. Technol.* **1995,** *29*, 1279-1287.

(79) Wing, M. R.; Bada, J. L. *Origins Life Evol. Biosphere* **1992,** *21*, 375-383.

(80) Wall, W. F.; Reach, W. T.; Hauser, M. G.; Arendt, R. G.; Weiland, R. G.; Weiland, J. L.; Berriman, G. B.; Bennett, C. L.; Dwek, E.; Leisawitz, D.; Mitra, P. M.; Odenwald, S. F.; Sodroski, T. J.; Toller, G. N. *Astrophys. J.* **1996,** *456*, 566-597.

(81) Bohme, D. K. *Chem. Rev.* **1992,** *92*, 1487-1508.

(82) Readman, J. W.; Mantoura, R. F. C.; Rhead, M. M. *Fresenius' J. Anal. Chem.* **1984,** *319*, 126-121.

(83) Wakeham, S. G.; Schaffner, C.; Giger, W. *Geochim. Cosmochim. Acta* **1980,** *44*, 403-413.

(84) Gschwend, P. M.; Hites, R. A. *Geochim. Cosmochim. Acta* **1981,** *45*, 2359-2367.

(85) Venkatesan, M. I. *Mar. Chem.* **1987,** *21*, 267-299.

(86) Ramdahl, T. *Nature* **1983,** *306*, 580-582.

(87) Naes, K.; Oug, E. *Environ. Sci. Technol.* **1997,** *31*, 1253-1258.

(88) Grimalt, J. O.; Canton, L.; Olive, J. *Chemom. Intell. Lab. Syst.* **1993,** *18*, 93-109.

(89) Roques, D. E.; Overton, E. B.; Henry, C. B. *J. Environ. Qual.* **1994,** *23*, 851-855.

(90) Douglas, G. S.; Bence, A. E.; Price, R. C.; McMillan, S. J.; Butler, E. L. *Environ. Sci. Technol.* **1996,** *30*, 2332-2339.

(91) Bence, A. E.; Kvenvolden, K. A.; Kennicutt, M. C. *Org. Geochem.* **1996,** *24*, 7-42.

(92) Jacquot, F.; Guiliano, M.; Doumenq, P.; Munoz, D.; Mille, G. *Chemosphere* **1996,** *33*, 671-681.

(93) Garrigues, P.; Connan, J.; Parlanti, E.; Bellocq, J.; Ewald, M. *Adv. Org. Geochem.* **1988,** *13*, 1115-1121.

(94) Kvalheim, O. M.; Christy, A. A.; Telnaes, N.; Bjorseth, A. *Geochim. Cosmochim. Acta* **1987,** *51*, 1883-1888.

(95) Long, E. R.; Macdonald, D. A.; Smith, S. L.; Calder, F. D. *Environ. Manage.* **1995,** *19*, 81-97.

(96) Paine, M. D.; Chapman, P. M.; Allard, P. J.; Murdoch, M. H.; Minife, D. *Environ. Toxicol. Chem.* **1996,** *15*, 2003-2018.

(97) Bailey, G. S.; Goeger, D. E.; Hendricks, J. D. In *Metabolism of Polycyclic Aromatic Hydrocarbons in the Aquatic Environment*; Varanasi, U., Ed.; CRC Press: Boca Raton, Florida, 1989, pp 253-268.

(98) Malins, D. C.; Haimanot, R. *Biochem. Biophys. Res. Comm.* **1990,** *173*, 614-619.

(99) Krahn, M. M.; Rhodes, L. D.; Myers, M. S.; Moore, L. K.; McLeod, W. D.; Malins, D. C. *Arch. Environ. Contam. Toxicol.* **1986,** *15*, 61-67.

(100) Goyette, D.; Brand, D.; Thomas, M. ; Environment Canada, Conservation and Protection, Pacific and Yukon region,: Vancouver, B.C., 1988.

(101) Ericson, G.; Liewenborg, B.; Balk, L. *Mar. Environ. Res.* **1995,** *39*, 303-307.

(102) Burgeot, T.; Bocquene, G.; Porte, C.; Dimeet, J.; Santella, R. M. *Mar. Ecol. Prog. Ser.* **1996,** *131*, 125-141.

(103) Bucheli, T. D.; Fent, K. *Crit. Rev. Environ. Sci. Technol.* **1995,** *25*, 201-268.

(104) Dipple, A. In *Polycyclic Hydrocarbons and Carcinogenesis*; Harvey, R. G., Ed.; American Chemical Society: Washington DC, 1985; Vol. 283, pp 1-17.

(105) Jerina, D. M.; Yagi, H.; Lehr, R. E.; Thakker, D. R.; Schaefer-ridder, M.; Karle, J. M.; Levin, W.; Wood In *Polycyclic Hydrocarbons and Cancer*; Gelboin, H. V., Ts'o, P. O. P., Eds.; Academic Press: New York, USA, 1978; Vol. 1, pp 173-185.

(106) Silkworth, J. B.; Lipinskas, T.; Stoner, C. R. *Toxicology* **1995,** *105*, 375-386.

(107) Kim, K. B.; Lee, B. M. *Cancer Lett.* **1997,** *113*, 205-212.

(108) Prough, R. A.; Linder, M. W.; Pinaire, J. A.; Xiao, G. H.; Falkner, K. C. *FASEB J.* **1996,** *10*, 1369-1377.

(109) Saas, P.; Bohuon, C.; Pallardy, M. *J. Toxicol. Environ. Health* **1996,** *49*, 371-387.

(110) Santodonato J *Chemosphere* **1997,** *34*, 835-848.

(111) Knutzen, J. *Sci. Total Environ.* **1985,** *163,* 107-122.

(112) Ankley, G. T.; Erickson, R. J.; Sheedy, B. R.; Kosian, P. A.; Mattson, V. R.; Cox, J. S. *Aquat. Toxicol.* **1997,** *37*, 37-50.

(113) Veith, G. D.; Mekeyan, O. G.; Ankley, G. T.; Call, D. J. *Chemosphere* **1995,** *30*, 2129-2142.

(114) Elston, R. A.; Moore, J. D.; Brooks, K. *Rev. Aquat. Sci.* **1992,** *6*, 405-466.

(115) Harper, D. M.; Flessas, D. A.; Reinisch, C. L. *J. Invert. Pathol.* **1994,** *64*, 234-237.

(116) Mix, M. C. *Mar. Environ. Res.* **1986,** *20*, 1-141.

(117) Moore, M. N.; Livingstone, D. R.; Widdows, J. In *Metabolism of Polycyclic Aromatic Hydrocarbons in the Aquatic Environment*; Varanasi, U., Ed.; CRC Press: Boca Raton, Florida, 1989, pp 291-328.

(118) Park, J.-Y. K.; Shigenaga, M. K.; Ames, B. N. *Proc. Natl. Acad. Sci. USA* **1996,** *93*, 2322-2327.

(119) Magnusson, K.; Ekelund, R.; Dave, G.; Granmo, A.; Forlin, L.; Wennberg, L.; Samuelsson, M.; Berggren, M.; Brorstromlunden, E. *J. Sea Res.* **1996,** *35*, 223-234.

(120) Jaworska, J. S.; Hallam, T. B.; Schultz, T. W. *Environ. Toxicol. Chem.* **1996,** *15*, 1049-1056.

(121) Eertman, R. H. M.; Groenink, C. L. F. M. G.; Sandee, B.; Hummel, H. *Mar. Environ. Res.* **1995,** *39*, 169-173.

(122) Moore, M. N.; Farrar, S. V. *Mar. Environ. Res.* **1985,** *17*, 222-225.

(123) Dyrynda, E. A.; Law, R. J.; Dyrynda, P. E. J.; Kelly, C. A.; Pipe, R. K.; Graham, K. L.; Ratcliffe, N. A. *J. Mar. Biol. Assoc. UK* **1997,** *77*, 281-284.

(124) Grundy, M. M.; Moore, M. N.; Howell, S. M.; Ratcliffe, N. A. *Aquat. Toxicol.* **1996,** *34*, 273-290.

(125) Grundy, M. M.; Ratcliffe, N. A.; N, M. M. *Mar. Environ. Res.* **1996,** *42*, 187-190.

(126) Gobas, F. A. P. C.; Bedard, D. C.; Ciborowski, J. J. H.; Haffner, G. D. *J. Great Lakes Res.* **1989,** *15*, 581-588.

(127) Morrison, H. R.; Gobas, F. A. P. C.; Lazar, R.; Haffner, G. D. *Environ. Sci. Technol.* **1996,** *30*.

(128) Mackay, D.; Di Guardo, A.; Paterson, S.; Cowan, C. *Environ. Toxicol. Chem.* **1996,** *15*, 1627-1637.

(129) Mackay, D.; Diamond, M.; Stiver, W. In *Organic Substances in Sediments and Water*; Baker, R. A., Ed.; Lewis Publishers: Chelsea, Michigan, USA, 1991; Vol. 3: Biological.

(130) McElroy, A. E.; Farrington, J. W.; Teal, J. M. In *Metabolism of Polycyclic Aromatic Hydrocarbons in the Aquatic Environment*; Varanasi, U., Ed.; CRC Press: Boca Raton, Florida, 1989, pp 2-39.

(131) Atlas, E. L.; Schauffler, S. In *Long Range Transport of Pesticides*; Kurtz, D. A., Ed.; Lewis Publishers Inc.: Chelsea, Michigan, USA, 1988, pp 161-184.

(132) Baker, J. E.; Eisenreich, S. J. *Environ. Sci. Technol.* **1990,** *24*, 342-352.

(133) Smith, D. J. T.; Harrison, R. M. *Atmos. Environ.* **1996,** *30*, 2513-2525.

(134) Gustafson, K. E.; Dickhut, R. M. *Environ. Sci. Technol.* **1997,** *31*, 140-147.

(135) Hornbuckle, K. C.; Eisenreich, S. J. *Atmos. Environ.* **1996,** *30*, 3935-3945.

(136) Bevan, D. R.; Ruggio, D. M. In *11th International Symposium on Polynuclear Aromatic Hydrocarbons - Measurement, Means and Metabolism*; Cooke, M., Loening, K., Merritt, J. Eds.; Batelle Press, Columbus, Ohio, USA.

(137) Wei, Y. L. *J. Hazard. Mater.* **1996,** *49*, 267-280.

(138) Pennise, D. M.; Karmens, R. M. *Environ. Sci. Technol.* **1996,** *30*, 2832-2842.

(139) Harkley, G. A.; Landrum, P. F.; Klaine, S. J. *Chemosphere* **1994,** *28*, 583-596.

(140) Landrum, P. F.; Reinhold, M. D.; Nihart, S. R.; Eadie, B. J. *Environ. Toxicol. Chem.* **1985,** *4*, 459-467.

(141) Mayer, L. M.; Chen, Z.; Findlay, R. H.; Fang, J. S.; Sampson, S.; Self, R. F. L.; Jumars, P. A.; Quetel, C.; Donard, O. F. X. *Environ. Sci. Technol* .**1996,** *30*, 2641-2645.

(142) Johnson, W.; Amy, G. *Environ. Sci. Technol.* **1995,** *29*, 807-817.

(143) Landrum, P. E.; Nihart, S. R.; Eadie, B. J.; Gardner, W. S. *Environ. Sci. Technol.* **1984,** *18*, 187-192.

(144) Chin, Y. P.; Gschwend, P. M. *Environ. Sci. Technol.* **1992,** *26*, 1621-1626.

(145) McGroddy, S. E.; Farrington, J. W. *Environ. Sci. Technol.* **1995,** *29*, 1542-1550.

(146) Hardy, J. T.; Crecelius, E. A.; Antrim, L. D.; Kiessser, S. L.; Broadhurst, V. L.; Boem, P. D.; Steinhauer, W. G.; Coogan, T. H. *Mar. Chem.* **1990,** *28*, 333-351.

(147) Hoff, R. M.; Strachan, W. M. J.; Sweet, C. W.; Chan, C. H.; Shackleton, M.; Bidleman, T. F.; Brice, K. A.; Burniston, D. A.; Cussion, S.; Gatz, D. F.; Harlin, K.; Schroeder, W. H. *Atmos. Environ.* **1996,** *30*, 3505-3527.

(148) Ehrhardt, M. G.; Burns, K. A.; Bicego, M. C. *Mar. Chem.* **1992,** *37*, 53-64.

(149) Goyette, D. *Point Source Profiles of PAHs in Sediments and Biota.* Presentation at conference: Polycyclic Aromatic Hydrocarbons in British Columbia, Vancouver, BC, Canada, 1995.

(150) Smith, J. N.; Levy, E. M. *Environ. Sci. Technol.* **1990,** *24*, 874-879.

(151) Naes, K.; Knutzen, J.; Berglind, L. *Sci. Total Environ.* **1995,** *163*, 93-106.

(152) Harkey, G. A.; Van Hoof, P. L.; Landrum, P. F. *Environ. Toxicol. Chem.* **1995,** *14*, 1551-1560.

(153) Lee, H. E. In *Organic Substances and Sediments in Water*; Baker, R. A., Ed.; Lewis Publisher Inc.: Michigan, USA, 1991; Volume 3: Biological.

(154) Meador, J. P.; Casillas, E.; Sloan, C. A.; Varanasi, U. *Mar. Ecol. Prog. Ser.* **1995,** *123*, 107-124.

(155) Karickhoff, S. W. *Chemosphere* **1981,** *10*, 833-846.

(156) Di Toro, D. M. *Chemosphere* **1985,** *14*, 1503-1538.

(157) Sun, S.; Boyd, S. A. *Environ. Sci. Technol.* **1993,** *27*, 1340-1346.

(158) De Bruijn, J.; Busser, F.; Seinen, W.; Hermans, J. *Environ. Toxicol. Chem.* **1989,** *8*, 49-512.

(159) Simpson, C. D.; Wilcock, R. J.; Smith, T. J.; Wilkins, A. L.; Langdon, A. G. *Bull. Environ. Contam. Toxicol.* **1995,** *55*, 149-153.

(160) Gusten, H.; Horvatic, D.; Sabljic, A. *Chemosphere* **1991,** *23*, 199-213.

(161) Koelmans, A. A.; Gillissen, F.; Makatita, W.; Van den Berg, M. *Water Res.* **1997,** *31*, 461-470.

(162) Socha, S. B.; Carpenter, R. *Geochim. Cosmochim. Acta* **1987,** *51*, 1273-1284.

(163) Gustafsson, O.; Haghseta, F.; Chan, C.; Macfarlane, J.; Gschwend, P. M. *Environ. Sci. Technol.* **1997,** *31*, 203-209.

(164) Kukkonen, J.; Landrum, P. F. *Chemosphere* **1996,** *32*, 1063-1076.

(165) Maruya, K. A.; Risebrough, R. W.; Horne, A. J. *Environ. Sci. Technol.* **1996,** *30*, 2942-2947.

(166) Prahl, F. G.; Carpenter, R. *Geochim. Cosmochim. Acta* **1983,** *47*, 1013-1023.

(167) Veith, G. D.; DeFoe, D. L.; Bergstedt, B. V. *J. Fish. Res. Bd. Can.* **1979,** *36*, 1040-1048.

(168) Hellou, J.; Mackay, D.; Fowler, B. *Environ. Sci. Technol.* **1995,** *29*, 2555-2560.

(169) Bruner, K. A.; Fisher, S. W.; Landrum, P. F. *J. Great Lakes Res.* **1994,** *20*, 725-734.

(170) Meador, J. P.; Stein, J. E.; Reichert, W. L.; Varanasi, U. *Rev. Environ. Contam. Toxicol.* **1995,** *143*, 79-165.

(171) Schnoor, J. L. In *Fate of Pesticides and Chemicals in the Environment*; Schnoor, J. L., Ed.; John Wiley and Sons, Inc.: New York, 1992, pp 1-24.

(172) Foster, G. D.; Wright, G. A. *Mar. Poll. Bull.* **1988,** *19*, 459-465.

(173) Gobas, F. A. P. C.; Zhang, X.; Wells, R. *Environ. Sci. Technol.* **1993,** *27*, 2855-2863.

(174) Obana, H.; Hori, S.; Nakamura, A.; Kashnoto, T. *Water Res.* **1983,** *17*, 1183-1187.

(175) Frank, A. P.; Landrum, P. F.; Eadie, B. J. *Chemosphere* **1986,** *15*, 317-330.

(176) Landrum, P. F. *Environ. Sci. Technol.* **1989,** *23*, 588-595.

(177) Hickey, C. W.; Roper, D. S.; Holland, P. T.; Trower, T. M. *Arch. Environ. Contam. Toxicol.* **1995,** *29*, 221-231.

(178) Pereira, W. E.; Domagalski, J. L.; Hostettler, F. D.; Brown, L. R.; Rapp, J. B. *Environ. Toxicol. Chem.* **1996,** *15*, 172-180.

(179) Ariese, F.; Kok, S. J.; Verkaik, M.; Hoornweg, G.; Goojier, C.; Velthorst, N.; Hofstraat, J. W. *Anal. Chem.* **1993,** *65*, 1100-1106.

(180) Phillips, D. J. H. *Rev. Environ. Contam. Toxicol.* **1991,** *120*, 105-129.

(181) Menzie, C. A.; Potocki, B. B.; Santodonato, J. *Environ. Sci. Technol.* **1992,** *26*, 1278-1284.

(182) Strickland, P.; Kang, D.; Sithisaranku, l. P. *Environ. Health Perspect.* **1996,** *104*, 927-932.

(183) Santella, R.; Perera, F.; young, T.; Zhang, Y.; Chiamprasert, S.; Tang, D.; Wang, L.; Beachman, A.; Lin, J.; Deleo, V. *Mutation research: Environmental Mutagenesis and Related Subjects* **1995,** *334*, 117-124.

(184) Vanschooten, F. J.; Godschalk, R. *Drug Safety* **1996,** *15*, 374-377.

(185) Tas, S.; Buchet, J. P.; Lauwerys, R. *Int. Arch. Occ. Environ. Health* **1994,** *66*, 343-348.

(186) Mastrangelo, G.; Fadda, E.; Marzia, V. *Environ. Health Perspect.* **1996,** *104*, 1166-1170.

(187) Winker, N.; Tuschl, H.; Kovac , R.; Weber, E. *J. Appl. Toxicol.* **1997,** *17*, 23-29.

(188) Binkova, B.; Lewtas, J.; Miskova, I.; Rossner, P.; Cerna, M.; Mrackova, G.; Peterkova, K.; Mumford, J.; Meyer, S.; Sram, R. *Environ. Health Perspect.* **1996,** *104*, 591-597.

(189) Gundel, J.; Mannschreck, C.; Buttner, K.; Ewers, U.; Angerer, J. *Arch. Environ. Contam. Toxicol.* **1996,** *31*, 585-590.

(190) Mumford, J. L.; Li, X. M.; Hu, F. D.; Lu, X. B.; Chiang, J. C. *Carcinogenesis* **1995,** *16*, 3031-3036.

(191) Raiyani, C. V.; Shah, S. H.; Desai, N. M.; Venkaiah, J. S.; Patel, J. S.; Parikh, D. J.; Kashyap, S. K. *Atmos. Environ.* **1993,** *27A*, 1643-1655.

(192) Moller, L.; Grzybowska, E.; Zeisig, M.; Cimander, B.; Hemminki, K.; Chorazy, M. *Carcinogenesis* **1996,** *17*, 61-66.

(193) Lawrence, J. *Human Expoure to PAHs through the Food Supply.* Presentation at conference: Polycyclic Aromatic Hydrocarbons in British Columbia, Vancouver, BC, Canada, 1995.

(194) Moret, S.; Amici, S.; Bortolomeazzi, R.; Lercker, G. *Z. Lebensm. Unters. Forsch.* **1995,** *201*, 322-326.

(195) Kleinjans, J. C. S.; Moonen, E. J. C.; Dallinga, J. W.; Albering, H. J.; Vandenbogaard, A. E. J. M.; Vanschooten, F. J. *Lancet* **1996,** *348*, 1731.

(196) Chen, B. H.; Wang, C. Y.; Chiu, C. P. *J. Ag. Food Chem.* **1996,** *44*, 2244-2251.

(197) Karl, H.; Leinemann, M. *Z. Lebensm. Unters. Forsch.* **1996,** *202*, 458-464.

(198) Lawrence, J. F.; Das, B. S. *Int. J. Environ. Anal. Chem.* **1986,** *24*, 113-131.

(199) Simko, P.; Khunova, V.; Simon, P.; Hruba, M. *Int. J. Food Sci. Technol.* **1995,** *30*, 807-812.

(200) Gabbani, G.; Hou, S. M.; Nardini, B.; Marchioro, M.; Lambert, B.; Clonfero, E. *Carcinogenesis* **1996,** *17*, 1677-1681.

(201) Talaska, G.; Underwood, P.; Maier, A.; Lewtas, J.; Rothman, N.; Jaeger, M. *Environ. Health Perspect.* **1996,** *104*, 901-906.

(202) Alexandrov, K.; Rojas, M.; Kadlubar, F. F.; Lang, N. P.; Bartsch, H. *Carcinogenesis* **1996,** *17*, 2081-2083.

(203) Davila, D. R.; Romero, D. L.; Burchiel, S. W. *Toxicol. Appl. Pharmacol.* **1996,** *139*, 333-341.

(204) Arnott, M. S.; Yamauchi, T.; Johnston, D. A. In *Polynuclear Aromatic Hydrocarbons: Third International Symposium on Chemistry and Biology - Carcinogenesis and Mutagenesis*; Jones, P. W., Leber, P., Eds.; Ann Arbor Science Publishers Inc.: AnnArbor, Michigan, USA, 1976.

(205) Pelkonen, O.; Karki, N. T.; Korhonen, P.; Koivisto, M.; Tuimala, R.; Kauppila, A. In *Polynuclear Aromatic Hydrocarbons: Third International Symposium on Chemistry and Biology - Carcinogenesis and Mutagenesis*; Jones, P. W., Leber, P., Eds.; Ann Arbor Science Publishers Inc.: AnnArbor, Michigan, USA, 1976.

(206) Pelkonen, O. *Metabolism of benzo(a)pyrene in human adult and fetal tissues*; Raven Press: New York, USA, 1975.

(207) International Agency for Research on Cancer (IARC). *IARC Monographs on the Evaluation of the Carcinogenic Risk of Chemicals to Humans* **1983,** *32*, 33-91.

(208) United States Environmental Protection Agency (US EPA): *Evaluation and Estimation of Potential Carcinogenic Risks of Polynuclear Aromatic Hydrocarbons.* Washington DC, USA, 1985.

(209) Pott, P. *Reprinted In: Natl. Cancer Inst. Monogr., 1963* **1775,** *10*, 7-13.

(210) Nielsen, P. S.; Andreassen, A.; Farmer, P. B.; Ovrebo, S.; Autrup, H. *Toxicol. Lett.* **1996,** *86*, 27-37.

(211) Grimmer, G.; Jacob, J.; Dettbarn, G.; Naujack, K. W.; Heinrich, U. *Exp. Toxic. Pathol.* **1995,** *47*, 421-427.

(212) Petry, T.; Schmid, P.; Schlatter, C. *Ann. Occ. Hyg.* **1996,** *40*, 345-357.

(213) Mumford, J. L.; Williams, K.; Wilcosky, T. C.; Everson, R. B.; Young, T. L.; Santella, R. M. *Mutation Res.* **1996,** *359*, 171-177.

(214) Keith, L. H.; Telliard, W. A. *Environ. Sci. Technol.* **1979,** *13*, 416-423.

(215) Dunn, B. *Environ. Sci. Technol.* **1976,** *10*, 1018-1021.

(216) United States Environmental Protection Agency. *Federal Register* **1979,** *44*.

(217) Burford, M. D.; Hawthorne, S. B.; Miller, D. J. *Anal. Chem.* **1993,** *65*, 1497-1505.

(218) Thompson, D.; Jolley, D.; Maher, W. *Microchem. J.* **1993,** *47*, 351-362.

(219) Wise, S. *J. Chromatogr.* **1993,** *642*.

(220) Yan, C.; Dadoo, R.; Zare, R. N.; Rakestraw, D. J.; Anex, D. S. *Anal. Chem.* **1996,** *68*, 2726-2730.

(221) Miller, J. L.; Khaledi, M. G.; Shea, D. *Anal. Chem.* **1997,** *69*, 1223-1229.

(222) Makela, M.; Pyy, L. *J. Chromatogr. A* **1995,** *699*, 49-57.

(223) Bruggemánn, O.; Freitag, R. *J. Chromatogr. A* **1995,** *717*, 309-324.

(224) Galceran, M. T.; Moyano, E. *J. Chromatogr. A* **1996,** *731*, 75-84.

(225) Burrows, E. P. *J. Mass Spectr.* **1995,** *30*, 312-318.

(226) Shusham, B.; Boyd, R. K. *Org. Mass Spectr.* **1980,** *15*, 445.

(227) Marriott, P. J.; Carpenter, P. D.; Brady, P. H.; McCormick, M. J.; Griffiths, A. J.; Hatvani, T. S. G.; Rasdell, S. G. *J. Liquid Chromatogr.* **1993,** *16*, 3229-3247.

(228) Garrigues, P. P.; Budzinski, H. *Trends. Anal. Chem.* **1995,** *14*, 231-239.

(229) Vo-Dinh, T. *Anal. Chem.* **1978,** *50*, 396-401.

(230) Lloyd, J. B. F. *Nature* **1971,** *231*, 64-65.

(231) Ariese, F.; Kok, S. J.; Verkaik, M.; Gooijer, C.; Velthorst, N. H.; Hofstraat, J. W. *Aquat. Toxicol.* **1993,** *26*, 273-286.

(232) Strickland, P. T.; Kang, D.; Bowman, E. D.; Fitzwilliam, A.; Downing, T. E.; Rothman, N.; Groopman, J. D.; Weston, A. *Carcinogenesis* **1994,** *15*, 483-487.

(233) Vahangas, K.; Haugen, A.; Harris, C. C. *Carcinogenesis* **1985,** *6*, 1109-1115.

(234) McRae, C.; Love, G. D.; Murray, I. P.; Snape, C. E.; Fallick, A. E. *Anal. Comm.* **1996,** *33*, 331-333.

(235) O'Malley, V. P.; Abrajano, T. A.; Hellou, J. *Org. Geochem.* **1994,** *21*, 809-822.

(236) Law, R. J.; Biscaya, J. L. *Mar. Poll. Bull.* **1994,** *29*, 235-241.

(237) Lopez-Garcia, A.; Blanco Gonzalez, E.; Garcia Alonso, J. I.; Sanz-Medel, A. *Analytica Chimica Acta* **1992,** *264*, 241-248.

(238) Capangpangan, M. B.; Noblet, J. A.; Suffet, I. H. *J. Chromatogr.* **1996,** *753*, 279-290.

(239) Gomez-Belinchon, J. I.; Grimalt, J. O.; Albiges, J. *Environ. Sci. Technol.* **1988,** *22*, 677-685.

(240) Kubinec, R.; Kuran, P.; Ostrovsky, I.; Sojak, L. *J. Chromatogr. A* **1993,** *653*, 363-368.

(241) de Voogt, P. *Trends Anal. Chem.* **1994,** *13*, 389-397.

(242) Gustafson, K. E.; Dickhut, R. M. *Environ. Toxicol. Chem.* **1997,** *16*, 452-461.

(243) Bennett, E. R.; Metcalfe, T. L.; Metcalfe, C. D. *Chemosphere* **1996,** *33*, 363-375.

(244) Junk, G. A. In *Organic pollutants in water*; Suffet, I. H., Malaiyandi, M., Eds.; Americal Chemical Society: Washington DC, USA, 1987; Vol. 214.

(245) Ehrhardt, M.; Petrick, G. *Mar. Chem.* **1993,** *42*, 57-70.

(246) Singh, R.; Tuek, M.; Maxa, K.; Tenglerova, J.; Weyland, E. H. *Carcinogenesis* **1995,** *16*, 2909-2915.

(247) Langenfeld, J. J.; Hawthorne, S. B.; Miller, D. J. *Anal. Chem.* **1996,** *68*, 144-155.

(248) Wenclawiak, B.; Rathmann, C.; Teuber, A. *Fresenius' J. Anal. Chem.* **1992,** *344*, 497-500.

(249) Marvin, C. H.; Allan, L.; McCarry, B. E.; Bryant, D. W. *Int. J. Environ. Anal. Chem.* **1992,** *49*, 221-230.

(250) Brown, G.; Maher, W. *Org. Geochem.* **1992,** *18*, 657-668.

(251) Leeming, R.; Maher, W. *Org. Geochem.* **1992,** *15*, 469-476.

(252) Barnabas, I. J.; Dean, J. R.; Fowlis, I. A.; Owen, S. P. *Analyst* **1995,** *120*, 1897-1904.

(253) Heemken, O. P.; Theobald, N.; Wenclawiak, B. W. *Anal. Chem.* **1997,** *69*, 2171-2180.

(254) Yang, Y.; Hawthorne, S. B.; Miller, D. J. *Environ. Sci. Technol.* **1997,** *31*, 430-437.

(255) Hageman, K. J.; Mazeas, L.; Grabanski, C. B.; Miller, D. J.; Hawthorne, S. B. *Anal. Chem.* **1996,** *68*, 3892-3898.

(256) Hale, R. C. *Estuaries* **1988,** *11*, 255-263.

(257) Mothershead, R. F.; Hale, R. C.; Greaves, J. *Environ. Toxicol. Chem.* **1991,** *10*, 1341-1349.

(258) Marvin, C. H.; McCarry, B. E.; Bryant, D. W. *J. Great Lakes Res.* **1994,** *20*, 523-530.

(259) Cejpek, K.; Hajsova, J.; Jehlickova, Z.; Merhaut, J. *Int. J. Environ Anal. Chem.* **1995,** *61*, 65-80.

(260) Uthe, J. F.; Musial, C. J. *Bull. Environ. Contam. Toxicol.* **1986,** *37*, 730-738.

(261) Speer, -. K.; Steeg, E.; Horstmann, P.; Kuhn, T.; Montag, A. *J. High Res. Chromatogr.* **1990,** *13*, 104-111.

(262) Vanstijn, F.; Kerkhoff, M. A. T.; Vandeginste, B. G. M. *J. Chromatogr.* **1996,** *750*, 263-273.

(263) Benner, B. A.; Wise, S. A.; Currie, L. A.; Klouda, G. A.; Klinedinst, D. B.; Zweidinger, R. B.; Stevens, R. K.; Lewis, C. W. *Environ. Sci. Technol.* **1995,** *29*, 2382-2389.

(264) Langenfeld, J. J.; Hawthorne, S. B.; Miller, D. J.; Pawliszyn, J. *Anal. Chem.* **1993,** *65*, 338-344.

(265) Cretney, J. R.; Gee, H. K.; Wright, G. J.; Swallow, W. H.; Taylor, M. C. *Environ. Sci. Technol.* **1985,** *19*, 397-404.

(266) Hawthorne, S. B.; Miller, D. J. *Anal. Chem.* **1994,** *66*, 4005-4012.

(267) Simpson, C. D.; Mosi, A. A.; Cullen, W. R.; Reimer, K. J. *Sci. Total Environ.* **1996,** *181*, 265-278.

(268) Cretney, W. J.; Wong, C. S.; Macdonald, R. W.; Erickson, P. E.; Fowler, B. R. *Can. Tech. Rpt. Hydrogr. Ocean Sci.* **1983,** *18*, 162-195.

(269) Ayres, J. *PAH releases from Primary Aluminum Smelters in Canada.* Presentation at conference: Polycyclic Aromatic Hydrocarbons in British Columbia, Vancouver, BC, Canada, 1995.

(270) Reid, A. D. *Report to Kitimat Multistakeholders Committee.* June 12, 1992.

(271) Carrier, R. , *Regulatory Approaches Applicable to PAH Discharges and Emissions at Primary Aluminum Smelters.* Presentation at conference: Polycyclic Aromatic Hydrocarbons in British Columbia, Vancouver, BC, Canada, 1995.

(272) Naf, C.; Broman, D.; Axelman, J. *Sci. Total Environ.* **1994,** *156*, 109-118.

(273) EVS Consultants Ltd., *Integrated Review: Alcan Marine Impact Studies, Volume 2: Polycyclic Aromatic Hydrocarbons (PAHs).* 1991

(274) National Oceanic and Atmospheric Administration (NOAA). *Sampling and Analytical Methods of the National Status and Trends Program: Volume IV: Comprehensive Descriptions of Trace Organic Analytical Methods.* 1993, NOS ORCA71

(275) Inscoe; N, M. *Anal. Chem.* **1964,** *36*, 2505-2506.

(276) Katz, M.; Chan, C.; Tosine, H.; Sakuma, T. In *Polycyclic Aromatic Hydrocarbons: 3rd International symposium onchemistry and biology - carcinogenesis and mutagenesis;* Jones, P., Leber, P., Eds., Ann Arbor

(277) Howard, J. W.; Teague, R. T.; White, R. H. *J. Assoc. Off. Anal. Chem.* **1966,** *49*, 595-611.

(278) Bagg, J.; Smith, J. D. In *11th International Symposium on Polynuclear Aromatic Hydrocarbons - Measurement, Means and Metabolism*; Cooke, M., Loening, K., Merritt, J. Eds.; Batelle Press, Columbus, Ohio, USA.

(279) Altgelt, K. H.; Gouw, T. H. In *Advances in chromatography*; Giddings, J. C., Grushka, E., Keller, R. A., Cazes, J., Eds.; Marcel Dekker Inc.: New York, USA, 1975; Vol. 13.

(280) Macdonald, R. W.; Bornhold, B. D.; Webster, I. *Can. Tech. Rpt. Hydrogr. Ocean Sci.* **1983,** *18*, 2-13.

(281) Bornhold, B. D. *Can. Tech. Rpt. Hydrogr. Ocean Sci.* **1983,** *18*, 88-115.

(282) Bell, L. M.; Kallman, R. J. *The Kitimat River Estuary, Environmental Knowledge to 1976,* Department of the Environment, Regional Board Pacific Region, Environment Canada, 1976.

(283) Prahl, F. G.; Carpenter, R. *Geochim. Cosmochim. Acta* **1979,** *43*, 1959-1972.

(284) Lipiatou, E.; Marty, J.-C.; Saliot, A. *Mar. Chem.* **1993,** *44*, 43-54.

(285) Aceves, M.; Grimalt, J. O. *Atmos. Environ.* **1993,** *27B*, 251-263.

(286) Daultry, S. *Principal Components Analysis*; Geo Abstracts Ltd.: Norwich, 1976.

(287) Bright, D. A.; Dushenko, W. T.; Grundy, S. L.; Reimer, K. J. *Sci. Total. Environ.* **1995,** *160/161*, 251-263.

(288) Muir; G, D. C.; *Environ. Sci. Technol.* **1993,** *27.*

(289) Pettersen, H.; Naf, C.; Broman, D. *Mar. Poll. Bull.* **1997,** *34*, 85-95.

(290) Cullen, W. R.; Li, X. F.; Reimer, K. J. *Sci. Total Environ.* **1994,** *156*, 27-37.

(291) Oliver, B. G. *Chemosphere* **1985,** *14*, 1087-1106.

(292) Johnson, A. C.; Larsen, P. F.; Gadbois, D. F.; Humason, A. W. *Mar. Environ. Res.* **1985,** *15*, 1-16.

(293) Pichler, M.; Guggenburger, G.; Hartmann, R.; Zech, W. *Environ. Sci. Poll. Res.* **1996,** *3*, 24-31.

(294) Garcia, K. L.; Delfino, J. J.; Powell, D. H. *Water Res.* **1993,** *27*, 1601-1613.

(295) Pierard, C.; Budzinski, H.; Garrigues, P. *Environ. Sci. Technol.* **1996,** *30*, 2776-2783.

(296) Sanders, G.; Jones, K. C.; Hamilton-Taylor, S.; Dorr, H. *Environ. Poll.* **1995,** *89*, 17-25.

(297) Van Zoest, R.; Van Eck, G. T. M. *Mar. Chem.* **1993,** *44*, 95-103.

(298) Meyers, P. A.; Ishiwatari, R. *Org. Geochem.* **1993,** *20*, 867-900.

(299) Wilcock, R.; Northcott, G. *NZ J. Mar. Fresh. Res.* **1995,** *29*, 107-116.

(300) Wakeham, S. G. *Mar. Chem.* **1996,** *53*, 187-205.

(301) Venosa, A. D.; Suidan, M. T.; Wrenn, B. A.; Strohmeier, K. L.; Haines, J. R.; Eberhart, B. L.; King, D.; Holder, E. *Environ. Sci. Technol.* **1996,** *30*, 1764-1775.

(302) Kawaka, O. E.; Simoneit, B. R. T. *Org. Geochem.* **1994,** *22*, 947-978.

(303) Mackay, D. *Environ. Sci. Technol.* **1982,** *16*, 274-278.

(304) Smith, T. J. D. Phil Thesis, University of Waikato, Hamilton, 1991.

(305) Pruell, R. J.; Lake, J. L.; Davis, W. R.; Quinn, J. G. *Mar. Biol.* **1986,** *91*, 497-507.

(306) James, M. O. In *Metabolism of Polycyclic Aromatic Hydrocarbons in the Aquatic Environment*; Varanasi, U., Ed.; CRC Press: Boca Raton, Florida, 1989, pp 69-92.

(307) Brousseau, D. J.; Baglivo, J. A. *Mar. Biol.* **1991,** *110*, 249-252.

(308) Harper, D. M.; Flessas, D. A.; Reinisch, C. L. *J. Invert. Pathol.* **1994,** *64*, 234-237.

(309) Quayle, D. B. *The Intertidal Bivalves of British Columbia*: Victoria, BC, 1960.

(310) Krahn, M. M.; Burrows, D. G.; Jr., W. D. M.; Malins, D. C. *Arch. Environ. Contam. Toxicol.* **1987,** *16*, 511-522.

(311) Lange, B.; Kremer, S.; Sterner, O.; Anke, H. *Appl. Environ. Microbiol.* **1994,** *60*, 3602-3607.

(312) Jacob, J.; Grimmer, G.; Raab, G.; Schmoldt, A. *Xenobiotica* **1982,** *12*, 45-53.

(313) Eickhoff, C. V.; Law, F. C. P.; Cretney, W. **1995,** Poster presented at the 2nd SETAC World Conference, Vancouver, Canada; #PW230.

(314) Lambert, M.; Kremer, S.; Sterner, O.; Anke, H. *Appl. Environ. Microbiol.* **1994,** *60*, 3597-3601.

(315) Kobayashi, K.; Akitake, H.; Tomiyama, T. *Bull. Jpn. Soc. Sci. Fish.* **1970,** *36*, 103-108.

(316) Ernst, W. *Veroff. Inst. Meeresforsch. Bremerh.* **1979,** *17*, 233-240.

(317) Nemoto, N.; Takayama, S.; Gelboin, H. V. *Chem.-Biol. Interact.* **1978,** *23*, 19-30.

(318) Mulder, G. J. In *Sulfation of Drugs and Related Compounds*; Mulder, G. J., Ed.; CRC Press: Boca Raton, Florida, 1981, pp1-3.

(319) Lange, B.; Kremer, S.; Sterner, O.; Anke, H. *Can. J. Microbiol.* **1996,** *42*, 1179-1183.

(320) Wunder, T; Kremer, S; Sterner, O; Anke, H. *Appl. Microbial Biotech.* **1994,** *42,* 636-641.

(321) Horn, J.; Flesher, J. W.; Lehner, A. F. *Biochem. Biophys. Res. Comm.* **1996,** *228*, 105-109.

(322) Mulder, G. J. In *Sulfation of Drugs and Related Compounds*; Mulder, G. J., Ed.; CRC Press: Boca Raton, Florida, 1981, pp213-226.

(323) Surh, Y.-J.; Tannenbaum, S. R. *Chem. Res. Toxicol.* **1995,** *8*, 693-698.

(324) Nebert, D. W.; Gelboin, H. V. *J. Biol. Chem.* **1968,** *243*, 6242-6243.

(325) Mulder, G. J. In *Sulfation of Drugs and Related Compounds*; Mulder, G. J., Ed.; CRC Press: Boca Raton, Florida, 1981, pp131-185.

(326) Kinoshita, N.; Gelboin, H. V. *Science* **1978,** *199*, 307-309.